1-1-2006

A systematic design recovery framework for mechanical components.

R. Jill Urbanic
University of Windsor

A SYSTEMATIC DESIGN RECOVERY FRAMEWORK FOR MECHANICAL COMPONENTS

by

R. Jill Urbanic

A Dissertation

Submitted to the Faculty of Graduate Studies and Research

through Mechanical, Automotive and Materials Engineering

in Partial Fulfillment of the Requirements for

the Degree of Doctor of Philosophy at the

University of Windsor

Windsor, Ontario, Canada

2006

Your file Votre référence
ISBN: 978-0-494-42385-1
Our file Notre référence
ISBN: 978-0-494-42385-1

ABSTRACT

Reverse engineering aims at reproducing an existing object by analysing its dimensions, features, form, and properties. The collected data and information must be transformed into pertinent product knowledge at various levels of detail. In reverse engineering research, emphasis has been placed on recovering the general form or the product functions. For the form recovery tasks, existing techniques focus on creating computer aided design (CAD) surface models from point cloud data collected from scanning systems. This model is mathematically 'exact', but may be inaccurate due to noise contained in the model. As well, the surfaces and edges in the resulting CAD model have no functional meaning, which is inappropriate for mechanical components. The functional related tasks focus on establishing the component's functional requirements and its relationship within the product. For effective design recovery, these aspects must be combined and expanded upon at various levels of granularity. To meet these challenges, a systematic approach is adopted in a comprehensive manner to extract the relevant information and transform it into pertinent design knowledge. A modular design recovery framework is presented that captures the component's structure, function and feature information at varying perspectives. An integrated approach that assesses the component from different perspectives in an innovative manner leads to a more complete model, as no one perspective or set of tools can provide a complete, comprehensive engineering representation. The design recovery framework can be leveraged to assess or improve the product design using other design methodologies and tools.

To complement the framework, form recovery algorithms have been developed to transform point cloud data into wire frame geometry consisting of standard line and arc elements. Once the points are converted into curve primitives, adjustments are made to capture the design intent using heuristics, and common shapes and 2D patterns are detected. From this geometry, a surface or solid model can be constructed using established geometry creation tools. Several practical case studies are presented that illustrate the application of the design recovery framework and highlight its merits.

ACKNOWLEDGMENTS

Funny things happen in life – sometimes you have to be at the right place at the right time for opportunities to occur. Years ago I was in an accident, and doubted my abilities, endurance, and capacity to think. During the rehabilitation period, I decided to pursue my Masters at the University of Windsor. The research endeavours pursued by Dr. Waguih and Dr. Hoda ElMaraghy are very similar to the project challenges I pursued in industry, and I wanted to expand my horizons in the realm of manufacturing systems. It was a perfect match. It had been years since I have had so much fun. Obviously the work was challenging, but I have been exposed to so many new ideas, intelligent people, and interesting research. There is so much to learn, and so much to do. My industrial experience gave me a solid appreciation for the research being conducted at the IMS Centre, and for Dr. Waguih's management style. His knowledge, his sense of humour, and his respect and support of his research students is truly special. I enjoyed working on my Masters research so much, I decided to pursue my Ph.D. I sincerely thank my supervisors, Dr. Waguih ElMaraghy and Dr. Robert Gaspar, for the opportunity to do so. Without the support and encouragement presented by these two gentlemen, this research would have never been conducted. I also wish to thank Dr. Zamani, Dr. Minaker and Dr. Wu, my committee members, for their guidance and encouragement.

Thanks are also due to the staff of the Mechanical, Automotive, and Materials Engineering and the Industrial and Manufacturing Systems Engineering Departments for their friendly assistance and support, and to the IMS Centre group, especially Dr. Hoda ElMaraghy and Ms. Zaina Batal.

Finally, I must convey my deep gratitude to my husband, Bob Hedrick, who has supported me unconditionally in this endeavour, and has helped me in so many ways. He has patiently helped me with several computer problems and my software development. However, this is the most telling example of his endorsement of my research, which would definitely be understood by any car buff. Bob has a 1977 Corvette, which he loves to drive and race. He enters it into car shows and enjoys the yearly "Windsor Weekend"™ drag race competition. I have been involved in troubleshooting when problems occur in the vehicle, and when something pops up that could lend itself to my research, the car has stayed on its jacks in order for me to complete my work. If that is not support, I do not know what is.

TABLE OF CONTENTS

LIST OF TABLES

LIST OF FIGURES

GLOSSARY

2D.	Two Dimensional
3D.	Three Dimensional
3D-2D parts.	Stamped components consisting of a thin sheet with a free form shape
3D-3D parts.	Castings or weldments consisting of engineered and free form shapes
AD.	Axiomatic Design
AF.	Algebraic Fit
CAD.	Computer Aided Design
CAM.	Computer Aided Manufacturing
CAPP.	Computer Aided Process Planning
CCD.	Charge Couple Device
CMM.	Coordinate Measuring Machine
CNC.	Computer Numerically Controlled
CT.	Computer Tomography
Circumcircle.	Circle created from three points
DFX.	Design for X (Machining, Casting, Assembly, and so forth)
DoDAF.	U.S. Department of Defense Architecture Framework
DP.	Design Parameter
DSM.	Design Structure Matrix
E2AF.	Extended Enterprise Architecture Framework
FE.	Forward Engineering
FEA.	Federal Enterprise Architecture
FEM.	Finite Element Modelling

FR.	Functional Requirements
ICP.	Iterative Closest Point
IDEF.	Integrated DEFinition
IGES.	Initial Graphic Exchange Standard
GD&T.	Geometric Dimensioning and Tolerancing
G0 continuity.	End point continuity
G1 continuity.	Tangency continuity
MA.	Morphological Analysis
MRI.	Magnetic Resonance Imaging
NIST.	National Institute of Standards and Technology
Point cloud data.	Spatial coordinates representing the surface
Polyline.	Point-to-point line segments
PV.	Process Variable
QFD.	Quality Function Deployment
RE.	Reverse Engineering
SAE.	Society of Automotive Engineers
STEP.	STandard Exchange of Product data
STL.	Standard Triangulation Language
TRIZ.	Theory of Inventive Problem Solving
VE.	Value Engineering

Chapter 1

INTRODUCTION

1 INTRODUCTION

Reverse engineering techniques are applied to generate a part model where there is no existing documentation or it is no longer up to date. Formal reverse engineering (RE) generally refers to the process of reproducing an existing object (component or product), without the aid of formal specifications such as drawings or a computer model by analysing the object's physical dimensions, features, and material properties. In the general sense, ground-up reverse engineering is challenging as it may require engineers in different disciplines to capture all of the ideas related to the components and their interrelationships within a given system. The goal of reverse engineering is to construct a characterization of the product by accumulating all of the technical data and knowledge of how a product works.

A product consists of a system of components, and it is designed to address a specific need using forward engineering techniques. Forward engineering is a top-down hierarchical process where general principles are methodically applied to synthesize solutions that satisfy the need. Rules are established based on constraints, experience and preferences, limiting the design degrees of freedom. Interrelationships between the components within a product and the various manufacturing stages are rigorously assessed to ensure that no unexpected behaviours could emerge during usage. Several engineering design methodologies such as Value Engineering (VE) [Miles, 1989], Axiomatic Design [Suh, 2001], and the Theory of Inventive Problem Solving (TRIZ) [Altshuller, 1997] assist the designer in creating a robust design that meets the necessary functional requirements (FRs) based on logical and rational thought processes. Along with the product's physical form, there are functional requirements for the overall product, for its individual components, and the features within a component. These functional requirements drive the design parameters at the system level and at the detail level. Knowledge gained throughout the design cycle is used to refine and finalize the design details. The final design 'colour' results from blending the various essential elements (Figure 1-1).

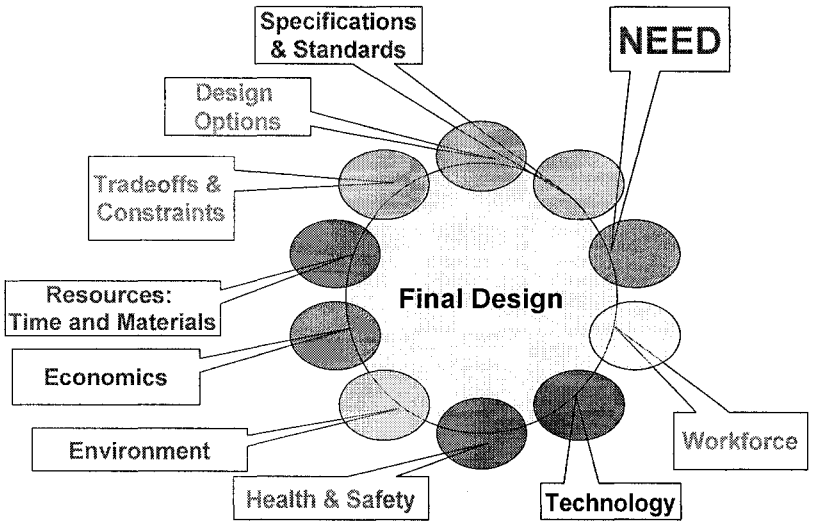

Figure 1-1: Elements that Influence the Final Design

Consequently, when reverse engineering an engineered component there must be a methodology for recognizing the design intent of the features, and systems of features in both the physical (form) and logical (FR) domains.

The classical definition of reverse engineering has negative connotations. Reverse engineering meant making a copy of an existing competitors product. However, reverse engineering is useful as a benchmarking tool for design recovery, product redesign or for a new product introduction [Otto and Wood, 1996]. Presently, reverse engineering refers to the process of creating a three dimensional (3D) geometric model from a physical object. This in essence is not reverse engineering, but reverse surface modelling, which is a fundamental building block of the reverse engineering process. Developments in data collection devices (3D scanning and digitizing instruments) and processing techniques (converting the acquired data to a surface model) have lead to efficient part – to – CAD model processes [Langbein, 2003], [Krause et al, 2003], [Fischer and Park, 1998], [Fischer and Smolin, 1997], [Limaien and ElMaraghy, 1999], [Fisher, 2004], [Thompson et al, 1999]. The need for reverse engineering typically arises when:

- No drawings or design models exist for a product that must be replaced (worn, broken, damaged) and the original manufacturer no longer exists or produces that product [Langbein, 2003], [Thompson et al, 1999].

- Drawings/models have been created, but the components have been modified during iterative prototyping/design, testing and use; hence, the existing documentation is no longer relevant.
- Comparing a fabricated part to its CAD description or to a standard item for inspection and/or quality assurance purposes [Yuan et al, 2001].
- Documenting and/or measuring cultural objects (sculpture or other artwork) or artefacts in archaeology, palaeontology and other scientific fields [Tsakiri et al, 2003].
- Generating data to create dental or surgical prosthetics, or fitting clothing or footwear to individuals [Au and Yuen, 1999], Kolmanic and Guid, 2003].

The reverse engineering (reverse surface modelling) tools focus on efficient and robust automatic generation of free form shapes from point cloud data [Attene and Spagnuolo, 2000], [Azernikov and Fischer, 2003], [Bernardini et al, 1999], [Krause et al, 2003], [Kruth and Kerstens, 1998], [Limaiem et al, 1996], [Motavelli, 1998], [Zhang et al, 2002], [Zhongwei and Shouwei, 2003]. Researchers are concerned about mesh construction, [Chappuis et al, 2004], [Li et al, 2003], [Fischer, 2002], [Botsch and Kobbelt, 2001], [Karbacher et al, 2001, 1999], [Dey et al, 2001], [Liu and Ma, 2001], [Sun et al, 2001], [Attene and Spagnuolo, 2000], [Bradley et al, 1999], [Turk and Levoy, 1994], surface continuity [Chappuis et al, 2004], [Knopf and Sangole, 2004], [Krause et al, 2003], [Huang and Meng, 2001], sharp edge detection [Vanco and Brunnett, 2004] and reducing measurement and registration noise [Vadde et al, 2004], [Page et al, 2003], [Kverh and Leonardis, 2002], [ElMaraghy and Rolls, 2001], [Luck et al, 2000], [Yau, et al, 2000], [Chalermwat, 1999], [Gagnon et al, 1998], [Eggert et al, 1994]. There are several state of the art commercial reverse engineering software packages, such as Paraform®, which are very powerful. However, the reconstructed surfaces and edges have no functional meaning, may have self -intersections, and may not be continuous. These issues make it difficult to edit the base geometry for subsequent design modifications and manufacturing tool path creation.

Features such as stepped holes, gear teeth, keyways, sprockets, splines, V-grooves for belts and so forth have precise mathematical definitions or standard specifications for their geometry. Tapped holes, slots, grooves and keyways have specific relationships and tolerances depending on the functional requirements and mating components. The existing reverse engineering tools

cannot effectively deal with this type of geometry, as the reverse engineering modelling tools capture a precise best-fit polynomial representation of the data, but do not generate a functional engineering representation. The data will contain noise due to measurement errors, manufacturing variations, and wear and damage on the part. This noise is not Gaussian (i.e. it does not have a zero mean value and a normally distributed variation). The resulting best-fit geometry will not reflect the designer's intent. Not only must the individual features within the component be reconstructed accurately, there are structural relationships. There are aggregates of features; therefore, there should be a methodology to recognize this. With engineered components, the feature shapes are neither arbitrary, nor is their pattern of arrangement. There are identifiable characteristics at the feature level and the system level. Several researchers recognize that 'designed in' geometric relationships exist, and that exploiting these geometric constraints (e.g. primitive shapes and symmetry) improves the reconstruction process for the design features [Benko and Varady, 2004], [Benko et al, 2002], [Benko et al 2001], [Gao et al, 2004], [Langbein et al, 2004], [Langbein, 2003], [Langbein et al, 2001], [Fisher, 2004], [Tangelder et al, 2003], [Thompson et al, 1999], [Werghi et al, 2002], [Werghi et al, 1999]. General shape knowledge can allow recovery even when data is very noisy, sparse or incomplete [Werghi et al, 2002], [Fisher, 2004]. The geometry should be compared based on similarity measures for both the individual elements and their arrangement. Most of the existing research focus has been on reconstructing the general form or individual features using data from scanning systems. At the system level, neither a pattern matching methodology has been performed, nor have the functional requirements been taken into consideration when recovering the feature's form. To reconstruct the product architecture, information and data must be collected from several sources. This cannot be automated, but multi-level, intelligent, interactive tools can be developed to assist in transforming the collected data into relevant design knowledge that can be then edited for downstream applications.

1.1 REVERSE ENGINEERING BACKGROUND

To capture the aspects of the reverse engineering process, an Integration DEFinition 0 model (IDEF0) model was created. IDEF0 modelling techniques are used, as they are an effective, structured, graphical tool that was specifically developed to model decisions, actions, and activities of a given system, either at an overview or at a detailed level [NIST - Anonymous, 1993]. The general IDEF0 activity block is shown in Figure 1-2.

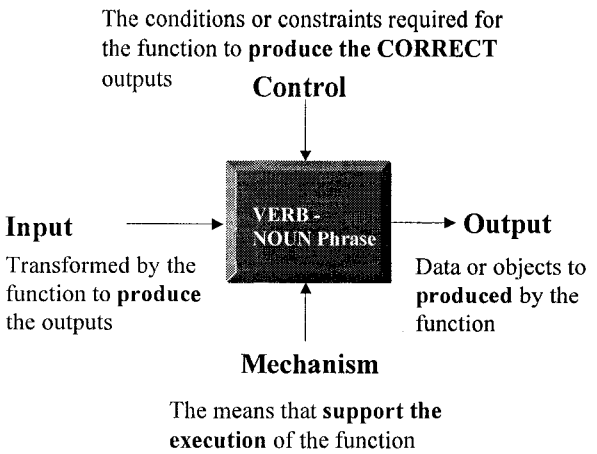

Figure 1-2: General IDEF0 Activity Block

A sample of the reverse engineering IDEF0 model is presented here. When reverse engineering, a deductive process is combined with data gathering techniques to migrate from a physical 'WHAT' to the hypothetical 'WHY' and a conjectured final model. The existing product, related documentation, and the functions the product performs are inputs into the reverse engineering system. The device functional requirements, the link between the form and function, the product model and the documentation are the desired outputs. The mechanisms to generate the desired output from the input are the technical resources, the design and analysis tools, the information systems and the human resources. The controlling aspects of the reverse engineering process consist of the available product documentation, available information with regard to the mating components and the knowledge of the operating environment. This is illustrated in Figure 1-3. The fabrication techniques are essentially out of the reverse engineering design loop, although the fabrication techniques influence the final model.

An iterative, incremental approach is required when performing reverse engineering. Just as the forward engineering methodology cannot be fully automated, neither can reverse engineering. However, like forward engineering, a design framework and various tools can be used to assist with the process. The reverse engineering problem is broken into a series of smaller tasks, each of which requires a toolbox, the designer's knowledge and experience, in combination with data for proper interpretation. In-depth analysis, deductive techniques, physical and virtual tests are some of the techniques that are required to transform the

information gathered by studying the product into knowledge that can be cascaded to the fabrication, inspection and testing processes.

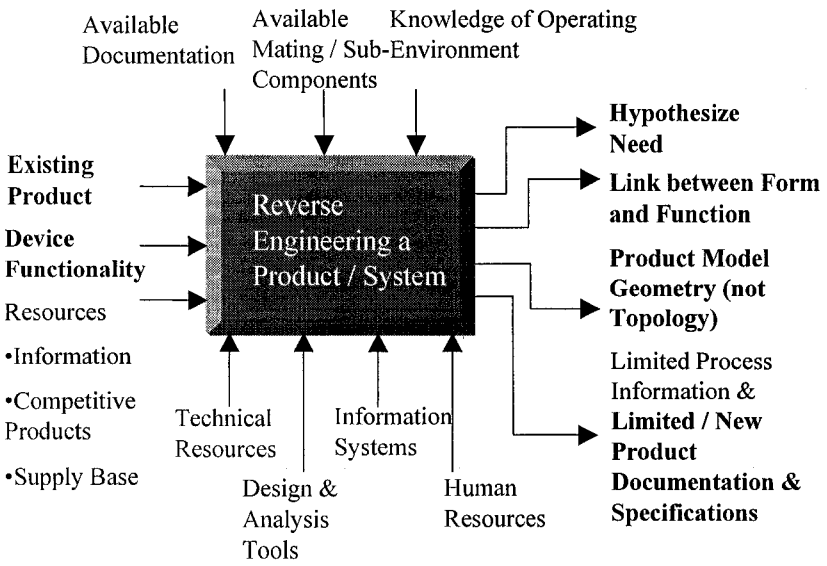

Figure 1-3: Reverse Engineering

This goes beyond capturing the general shapes of the product. The factors that need to be considered are the:

- Functional, form and fabrication features,
- Interface, and assembly features, and the
- Material and tolerance characteristics.

A functional feature assists with meeting the product related FRs, e.g., utilizing an 'I' shape to minimize deflection or bending. Form features consist of the geometry and topology used to meet the FRs. Interface features exist where independent and unrelated systems meet. For example, automobile manufacturers may use the same engine in many vehicles. The independent transmission, coolant, air conditioning, fuel and electrical systems must interface with the engine. Fabrication features facilitate the component manufacturing. If an alternative manufacturing process were used, these features would not be required. Assembly features allow related features to be joined. An example for an aluminum connecting rod is presented in Figure 1-4 and Table 1-1.

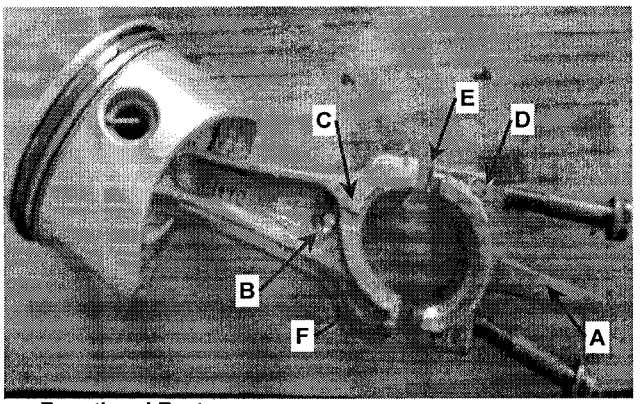

Functional Features
Feature A: Oil Splasher (lubricates engine case interior)
Feature B: Lubrication Hole (1 per side)
Feature C: Oil Grooves (3 per side)
Assembly Features:
Feature E: Horizontal Split
Feature F: Mounting holes (2)

Figure 1-4: Connecting Rod and Piston

Table 1-1: Feature Type Examples for a Single Cylinder Engine Connecting Rod

Feature Type	Description	Comment
Functional Features (Fig. 1-4)	Functional requirement: Lubrication Feature A: Oil Splasher Feature B: Oil Lub. Hole Feature C: Oil Grooves	There is no oil pump on this engine. There is a hydrodynamic bearing between the crankshaft and connecting rod.
Form Features	Except for the oil splasher, the connecting rod is symmetric along the parting line (top and bottom) and left to right.	The form is altered due to the casting process. There is draft varying between 3 - 6.5°.
Interface Features	Not applicable	
Fabrication Features	A permanent mould casting process is used to generate the initial shape; hence, ejector pins, a parting line and gating to feed the material into the die are required. If the part were machined, these features would not be required.	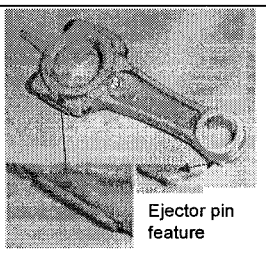
Assembly Features (Fig. 1-4)	Two M7 x 1.0 bolts are used to assemble the cap onto the connecting rod body.	There is a torque specification to ensure the parts are retained during usage.
Material Attributes	Aluminum, 93 HB	The part should be porosity free.
Tolerance Attributes	Connecting rod big end bore 30.010 mm	Ovality: 0.004 mm

The data collected (available information) with respect to these factors must be translated into knowledge that is required for fabrication and usage purposes. Information is gathered at the

detail level when reverse engineering. However, when manufacturing the designed product, the collected information must be transformed into knowledge at both the detail level (tolerances, draft angles, surface treatments, etc.) and the embodiment level (sealing surface, mounting point, hardness, etc.). Transformation into the appropriate design and manufacturing specifications such that there are no functionality problems, premature failures or exorbitant manufacturing costs is a significant challenge. A comparison of forward and reverse engineering is presented in Table 1-2, and the full IDEF0 model is developed in Appendix A.

Table 1-2: A Comparison between Forward and Reverse Engineering

Description	Forward Engineering	Reverse Engineering
Functional Features	Designed elements are defined explicitly to satisfy the need. The designs are optimized based on the problem's constraints [Pahl and Beitz, 1988], [Suh, 2001], [Dixon and Poli, 1995], [ElMaraghy and ElMaraghy, 1994].	Features are implicitly defined or deduced.
Form features	Geometry, Topology and Structure are explicitly defined and optimized. Process considerations influence the shape.	Geometry and Structure are deduced. Distortion due to wear, corrosion, and other causes introduce noise into the model. *A geometric healing process must be applied to address these issues.*
Interface features (places at which independent and unrelated systems meet)	An interface may consist of a modular or customized structure. A modular component has standardized features and dimensions (i.e., modular fixture components used for a variety of parts). A customized structure utilizes an unique design specific to its purpose (i.e. custom work holding devices).	Implicitly defined and depends on the availability of super structure, sub components and commercial product information.
Nominal values	The designer explicitly defines nominal values for ease of understanding and cost minimization throughout the design, manufacture, and usage phases.	The values can be distorted due to the quality of the part(s) being analysed. *A dimensional healing process must be applied to address these issues.*
Tolerances	The designer explicitly defines tolerances to balance manufacturing feasibility with overall product quality.	Dimensional and geometric tolerances are implicitly defined due to assumed functionality and process capabilities.
Manufacturing process	The manufacturing processes are explicitly (and/or implicitly) defined. They are an important aspect in design and detailing the final product (concurrent engineering and DFX), and determining the product testing, verification and process capability requirements [Benko et al, 2002], [Tichkiewitch and Veron, 1998], [Van Vliet et al, 1999], [Dixon and Poli, 1995], [Wiendahl, and Scholtissek, 1994].	Some original processes may be inferred by characteristic tool marks, and analysis of physical properties; however, this information may be changed if the remanufacturing volumes and other constraints are different.
Process capability	The process capability requirements are explicitly (and/or implicitly) defined. Process capability ≡ conformance to specification (or product quality and reliability aspects)	Process capability and other quality related information cannot be deduced.
Overall	Shape, dimensions, tolerances and specifications defined by design.	Information is transformed into the most probable and relevant design.

The state of the art for reverse engineering of physical components is represented using a modification of the Zachman Framework [Zachman, 2002] in Table 1-3. The Zachman framework was originally created for developing and/or documenting enterprise wide information systems architecture. The framework matrix consists of columns that provide various focii of the overall architecture and rows, which provide the various perspectives within the architecture. The detail layer has been added for this depiction.

Table 1-3: Zachman Framework Representation for Reverse Engineering Present State of the Art

	What	How	Where	Who	When	Why
	Data	**Function**	**Inter connections (Network)**	**People**	**Event Relation-ships (Time)**	**Motivation**
Contextual			Product architecture			Design Recovery
Conceptual		Linking the FRs, Form, Material and Manufacturing Processes		Multi-discipline resources required to navigate between the conceptual to detail phases - depends on the product / component complexity	Iterative cycle between the conceptual to detail phases	Ensure product form and materials addresses the FRs, design and manufacturing constraints
Logical	*Logical Data Model - Functional Requirements (FRs)*	*Description how the FRs are met*	*Product, component behaviour reconstruction & energy flows*			The product / product elements to address the FRs
Physical	*Physical Model or Physical Data Model - CAD model*	*Surface modelling techniques*				Produce replicas that have the desired form, physical, mechanical and interface characteristics
Detail	Point cloud data, other measurement data from instruments, manuals, etc.	*Contact and Non-contact data collection devices*				Generate process plan to manufacture replicas in an optimal manner (new constraints)

In the logical, physical, and detail domains for the data gathering and manipulation (italicized text), much work has been done in academia and industry. However, the physical models consist of 'best fit' surfaces to the point cloud data, and the interconnectivity between these

domains has not been addressed. The present reverse engineering techniques focus on 'form recovery', not 'design recovery'. When engaging in design recovery, the engineer is assessing the information to determine a function at the detail level. Simultaneously, the engineer has a general concept of the overall purposes and how they might be accomplished. As recognized in the area of reverse engineering legacy software systems, the functions and the interactions of the system and each element are defined in a synchronized manner [Tilley, 1998], [Rugaber, 1994]. This concept of assessing the functional requirements at the system and elemental level in a coordinated manner can be applied to mechanical components. In the mechanical application, the system consists of the product architecture, the elements are the components and the features, and the interactions consist of the feature and component relationships. Researchers, such as Otto and Wood [2001,1996], have presented methodologies that focus on the recovery of the functional aspects, but not on the form features. Unconstrained form recovery using surface modelling techniques is not appropriate for engineered components; consequently, several researchers are endeavouring to exploit geometric constraints when recovering the form of an object [Langbein, 2004, 2003], [Benko et al, 2002], [Mills et al, 2001], [Thompson, 1999]. For effective design recovery, all of these aspects must be combined. The form must be considered with respect to the function. In addition, the inter-relationships between the features and the component in its environment must be assessed. To this end, a full set methodologies and tools that assist with the design recovery process need to be developed for mechanical components. Data gathering for the form and the functions must be performed at the system level and at the detail level, and then combined. Exploiting realistic constraints by assessing the component at different levels of granularity will improve the reconstruction process for the individual features, pattern of features and the final component architecture. Mating components provide insight into the functional requirements and their implementation method. Common engineering features (e.g. tapped holes, keyway pockets), and components types, where the application influences the base parameters and specifications, provide specific design knowledge in the physical and logical domains. The gathered information and data must be transformed into design knowledge: this cannot be done automatically as the examination, construction and modification of relevant geometry, dimensions and tolerances is an iterative process. The existing surface modelling techniques (presented in the physical-data rubric) must be complemented with other modelling techniques that extract relevant function related geometry. This geometry can be subsequently modified in

a straightforward manner to accommodate changes. The part design and the manufacturing processes are highly coupled. Understanding the interconnections between the domains is necessary for effective design recovery, design modifications and manufacturing process planning. The proposed Zachman framework for the reverse engineering of engineered components is presented in Table 1-4.

Table 1-4: Proposed Zachman Framework for Reverse Engineering

	What	How	Where	Who	When	Why
	Data	**Function**	**Inter connections (Network)**	**People**	**Event Relation-ships (Time)**	**Motivation**
Contextual			Product architecture			Design Recovery
Conceptual		Linking the FRs, Form, Material and Manufacturing Processes	Product Functional Requirements and Interface link	Multi-discipline between the conceptual to detail phases - depends on the product or component complexity	Iterative cycle between the conceptual to detail phases	Ensure product form and materials addresses the FRs, design and manufacturing constraints
Logical	Logical Data Model - Functional Requirements (FRs) use Product Design Functional vocabulary (NIST) [Hirtz et al, 2002]	Description how the FRs are met	Product/ Element Functional Requirements link			The product / product elements to address the FRs
Physical	Physical Data Model - CAD model	Functional modelling techniques, consider Design and Mfg techniques	Product Form and Material - Process link			Produce replicas that have the desired form, physical, mechanical and interface characteristics
Detail	Point cloud data, other measurement data from instruments, manuals, etc.	Contact and non-contact data collection devices Process con-siderations	Tolerances, Feature Associations			Generate process plan to manufacture replicas in an optimal manner (new constraints)

1.2 PROBLEM STATEMENT

Mechanical components are designed to satisfy a specific need for a given set of constraints: the form, functions, material and the manufacturing processes are all interrelated. The component interfaces with other components. The features, nominal values of the dimensions, and the tolerances are selected for functionality, assemblability, ease of understanding, and cost minimization throughout the design, manufacture, and usage phases.

No comprehensive reverse engineering methodology exists that assesses an engineered component at various levels of granularity, linking the form and functional aspects in a systematic manner. The functional requirements must be taken into consideration when recovering the design parameters for a feature's form and its structural relationships. The model should be extensible, i.e. it should integrate smoothly into other design and manufacturing tools. It should be easy to analyse the reconstructed design and incorporate subsequent design modifications. An innovative, holistic approach needs to be taken in order to comprehensively capture the designer's intent and model the product/component/feature when performing reverse engineering tasks.

The goals of this research are to develop a framework, a set of methodologies, and reverse engineering design tools to assist an engineer to:

(i) Construct an ideal geometric model that captures the intended geometric regularities,

(ii) Identify, extract and ignore (if necessary) process related irregularities and geometry,

(iii) Capture the relevant engineering specifications by linking multiple perspectives in a structured, organized manner, and

(iv) Provide a foundation to enable the designer to assess and make modifications to the original design in a straightforward manner.

The design recovery process cannot be fully automated because of the various sources of noise, and the necessity of merging information from several design disciplines. The proposed approach integrates the bottom-up reverse engineering and top-down forward engineering processes in an opportunistic manner to create a robust model. A systematic approach is

required in order to generate a framework to capture the key elements that reflect the design intent and meet the functional requirements.

The existing reverse engineering software tools focus on reverse surface modelling. The final model consists of a set of precise surfaces and curves that will not represent the desired ideal model. Any distortion, wear or other flaws are captured in the model, as shown in Figure 1-7. For organic shapes, accuracy, precision, functional, and structural relationships do not have the same importance as with engineered shapes. Although engineered shapes have free form components, they typically have features with common primitive shapes and theoretical sharp edges. The reverse engineering software tools: (i) have problems with sharp edge definitions, (ii) capture noise within the model (due to distortion, wear, manufacturing variations, measurement and registration errors), (iii) create a CAD model that does not reflect the intended 'designed-in' relationships, and (iv) generate CAD geometry that is difficult to modify.

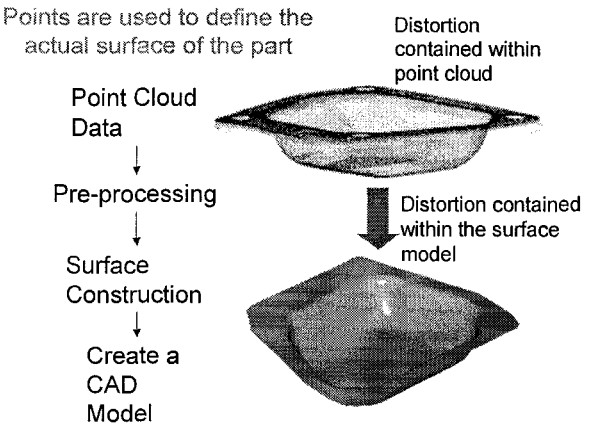

Figure 1-5: Traditional Point Cloud to CAD Model Transformation Steps (created using Paraform®) [Metris, 2006]

For functional shapes, the generic reverse surface modelling tools must be complemented by application specific modelling techniques. Tools that assist with the geometry reconstruction process need to be developed that complement the design recovery framework. These tools focus on transforming point cloud data into functional wire frame geometry.

1.3 RESEARCH APPROACH

To compare and contrast a reverse engineered part with the original and to highlight the design recovery issues, first a literature review was performed which covered the forward and reverse engineering design processes. An IDEF0 model was then created to capture the factors that contribute to the differences between forward and reverse engineering. The forward and reverse IDEF0 models are presented in Appendix A. A brief review of the contemporary reverse engineering techniques, which focus on general form recovery, is presented in Chapter 2.

Using the IDEF0 models as a platform and the sample components shown in Figure 1-6 and Table 1-5 as test pieces, a reverse engineering framework that integrates reverse and forward engineering techniques was developed. The framework consists of structured guidelines to obtain the relevant design information at different perspectives. This includes providing specific information of the context of the component's application, its operating environment, the component and feature functions, information on feature patterns and relationships, and instructions for geometry reconstruction. The design recovery framework is presented in Chapter 3, using a cylinder valve cover and a power steering pump pulley to illustrate the methodology.

Tools have been developed to transform the specified point cloud data into relevant geometry. It is recognized that 2D geometry, consisting of lines and arcs, forms the foundation of engineering design; hence, geometry reconstruction tools have been developed that focus on emulating this design practice. The point cloud data is transformed into wire frame geometry consisting of lines and arcs using the point cloud data as a template. Adjustments to the reconstructed geometry are made by leveraging standard geometric constraints in order to capture aspects of the design intent. The information contained in the design recovery framework is used to guide the reconstruction process and refine the results. The final surface or solid model can be subsequently constructed from the critical wire frame geometry using standard CAD tools. The algorithms were developed and tested using Excel® spreadsheet tools, Matlab® and Mastercam®, a common commercial computer aided manufacturing (CAM) package. The geometry construction, manipulation and pattern recognition algorithms are described in Chapter 4.

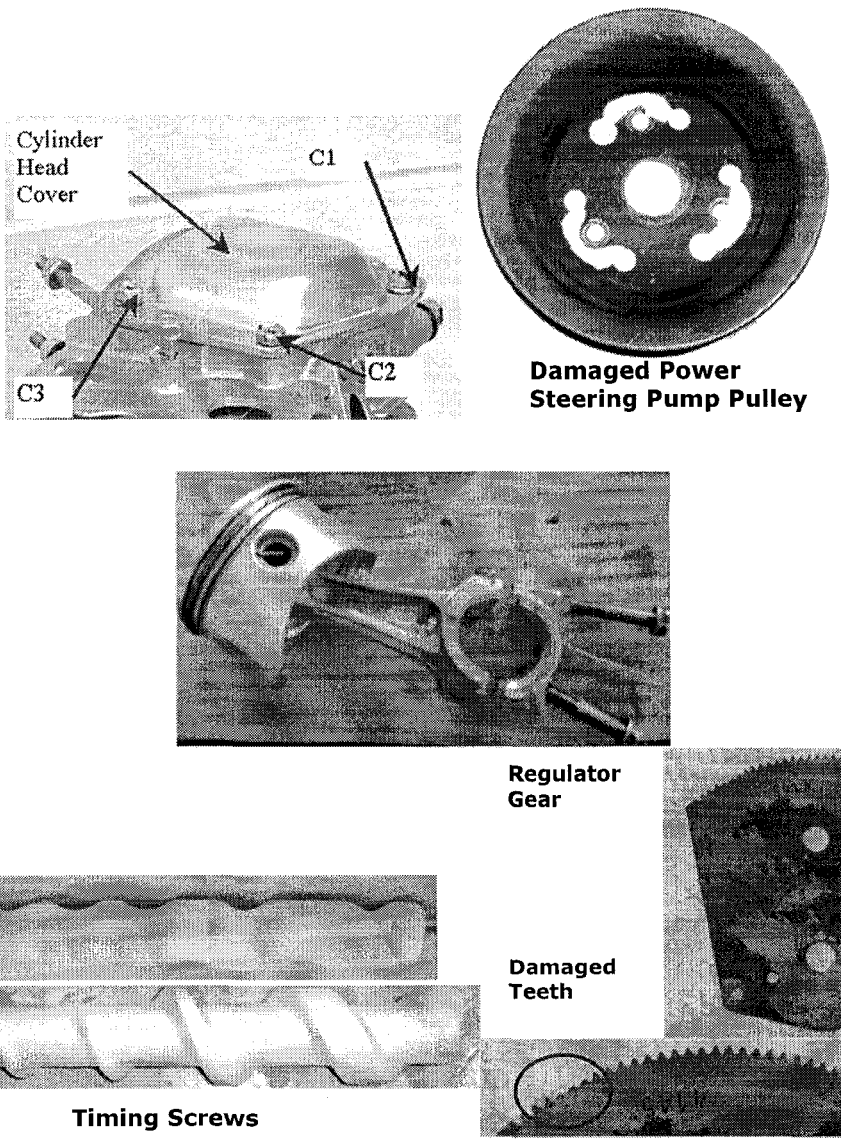

Figure 1-6: Valve Cover, Power Steering Pump Pulley, Connecting Rod, Timing Screws, and Regulator Gear

Table 1-5: Test Components Summary

Component	Manufacturing Process	Comments
Cylinder Valve Cover	Stamped	3D thin walled part, bent and distorted gasket sealing face
Power Steering Pump Pulley	Rolled, Drawn, Punched	Rotary part with damage on the flange face
Connecting Rod	Die Cast and Machined	3D axially symmetric part with draft and ejector pin bosses, ground off runners, gates and trimmed flash
Timing Screws	Machined	3D part with variable pitch screw used to control motion
Regulator Gear	Punched	2D profile part with damaged gear teeth

In Chapter 5, it is shown how the framework can be directly associated with formal engineering design tools in order to assess the design and provide a foundation for design improvements. The design recovery framework is linked to the Axiomatic Design methodology [Suh, 2001] and the product complexity assessment metrics developed by ElMaraghy and Urbanic [2004, 2003]. The connecting rod and timing screws are used as case studies to illustrate this.

The summary and conclusions, and future work are presented in Chapters 6 and 7 respectively.

Chapter 2

RELATED REVERSE ENGINEERING RESEARCH

2 REVERSE GEOMETRIC MODELLING

This chapter focuses on point cloud data collection techniques and surface reconstruction, which in essence is not reverse engineering, but reverse geometric modelling. Significant research has been performed on scanning systems that quickly collect point cloud data corresponding to the surface of the part. When creating a CAD model from these techniques, there are four major steps: data acquisition, pre-processing, surface construction and creating the final CAD model (Figure 2-1).

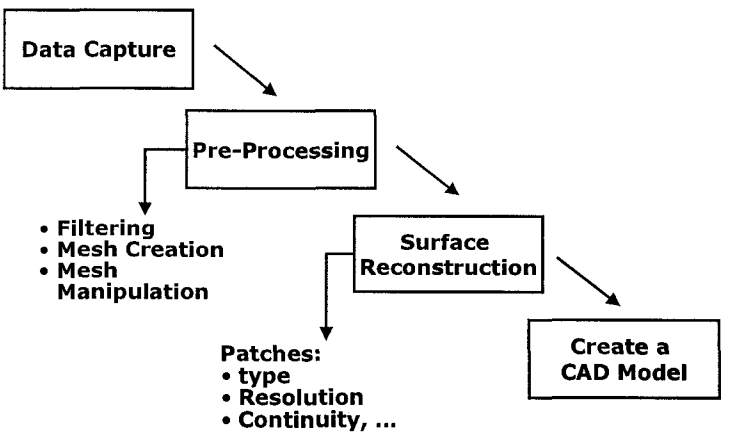

Figure 2-1: Reverse Geometric Modelling

Scanned data must be filtered to reduce noise and the decrease the number of data points to improve processing times. Sophisticated algorithms are utilized to generate a surface model from the filtered data directly from the points [Fischer and Park, 1998], [Limaiem and ElMaraghy, H., 1999], [Krause, 2003], [Phillipe et al, 1998] or an intermediary mesh is constructed and the surface is constructed from the mesh [Attene and Spagnuolo, 2000], [Azernikov and Fischer, 2003], [Azernikov and Fischer, 2004], [Barhak and Fischer, 2001], [Barhak and Fischer, 2002], [Benko et al, 2002], [Benko et al, 2001], [Bernardini et al, 1999],

[Fischer and Park, 1998], [Gao et al, 2004], [Huang et al, 2003], [Karbacher, and Hausler, 1998], [Page, 2003], [Steiner and Fischer, 2001], [Volodine et al, 2003], [Zhang et al, 2002]. A brief description of data collection techniques, filtering, meshing, surface reconstruction and measurement related sources of error follow.

2.1 SCANNING SYSTEMS

The geometry acquisition is a digitization process whereby a scanning system is used to produce a set of unsorted 3D data points, called a point cloud. There are several data acquisition scanners, which can be categorized as tactile or remote (Figure 2-2). The scanners are mounted on a coordinate measuring machine (CMM), a robot or on a special purpose machine. A CMM is a 5-axis robot, consisting of three translational axes for X, Y and Z motions, and two rotary motions: around the y-axis (A) and around the z-axis (B) on the wrist upon which the measuring devices (physical contact probes, scanners) are mounted.

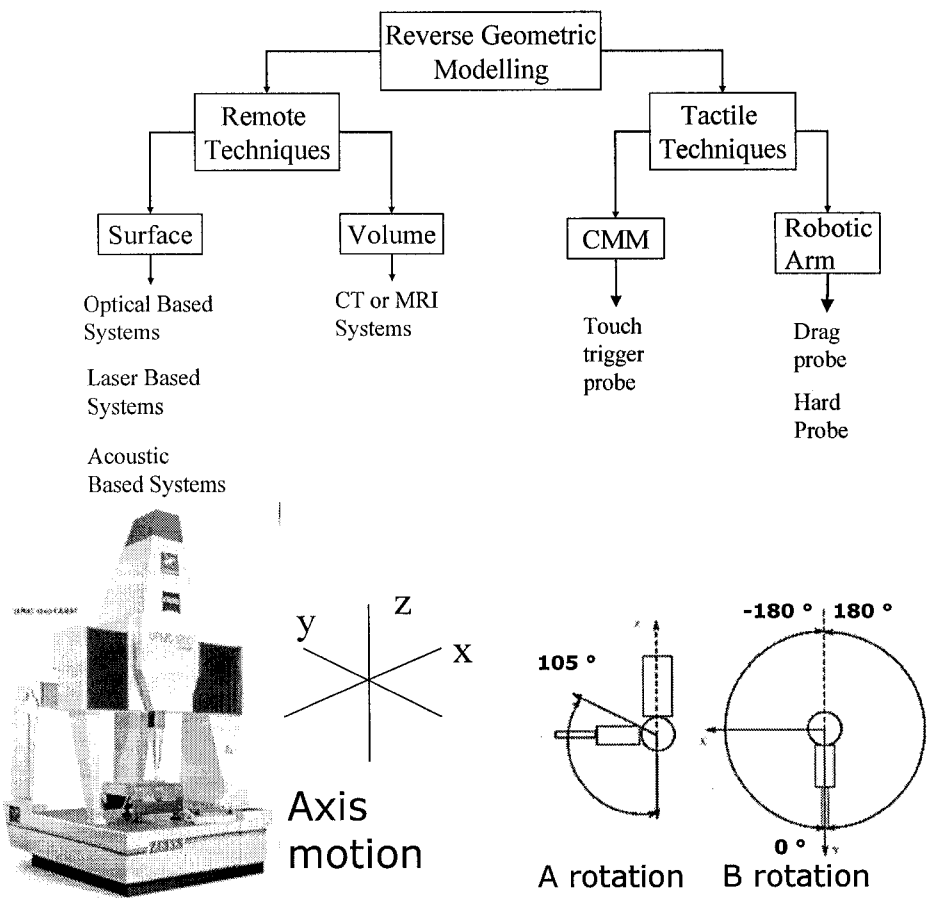

Figure 2-2: Zeiss CMM and Probe A and B Travel Limits

There are three main types of tactile sensors:

(i) touch trigger probes mounted on a CMM, which temporarily contact with the measured surface at a specified point,

(ii) hard probes mounted on a robot or CNC machine, which also temporarily contact with the measured surface at a specified point; and

(iii) analogue probes, which are dragged along the surface of the artefact along a specified line.

The geometry and material of the component to be measured influences the stylus geometry and material. The probe must have the reach and shape to be able to access the features that are to be measured without compromising the process (i.e. shank interfering with an obstacle, accessing deep features, or determining tapped hole positions).

The stylus ball material influences the long-term accuracy of scanning results. The ball material can wear, or pick up material (adhesion wear) from the components being measured, which may be an issue with analogue probe scanning. Both wear types result in permanently changing the shape of the stylus ball, which in turn compromises the accuracy of the data. Ruby styli are good for general purpose applications, but silicon nitride is the best choice for aluminum, whereas zirconia is ideal for cast iron [Renishaw, 2004]

With remote non-contact sensing devices, light, sound or magnetic devices are used to capture information about the surface or volume of the artefact. Typically with remote sensors, large amounts of point data are collected quickly. There are several methods which are briefly discussed here: stereovision using existing illumination (passive triangulation), active triangulation (light is projected onto the artefact), ranging, structured light (Moiré fringe), image analysis, computer tomography (CT scan), echography (sonar), and magnetic resonance imaging (MRI).

Triangulation techniques allow the depth to be inferred (Figure 2-3). Given H, L and A, the height of the object D is determined by:

$$D = H - R = H - L\cot A \tag{2.1}$$

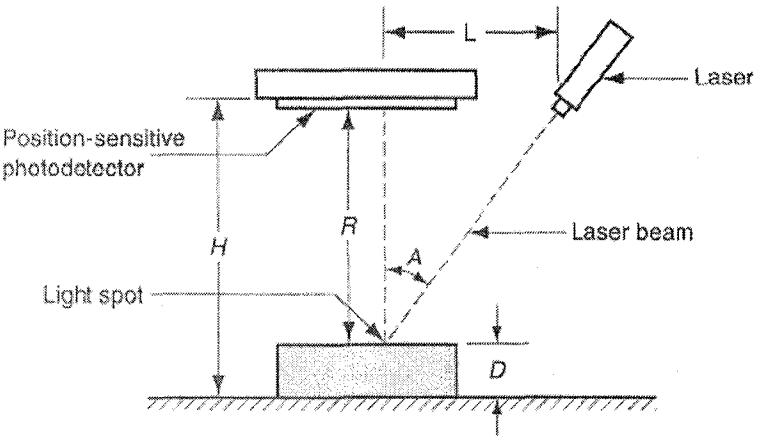

Figure 2-3: Laser Triangulation for Measuring Dimension D [Feng, 2002]

With stereovision techniques, a camera with two lenses or multiple cameras are used to obtain information necessary to infer depth by corresponding the features in both stereo images. Passive triangulation may lead to ambiguous results. The correspondence problem is ill-posed, and therefore, leads to either sparse distance measurements or erroneous results based on mismatches. Additionally, the stereovision techniques are susceptible to spectral highlights, harsh shadows, and surface inter-reflections [Page et al, 2003].

With active triangulation, a light source such as a laser (for a "sheet of light" the beam is expanded by a special lens) and a charge couple device (CCD) camera are used to collect the point cloud data. The laser beam is projected onto a surface, which is observed by the camera at a different angle (Figure 2-4). By analysing the distortions created by the target's topology using simple trigonometric rules, the 3D position of the points on the surface can be determined.

Triangulation methods can acquire data at very fast rates; however, there are shortfalls. The accuracy falls off as the angle increases [Feng, 2002]. There may be problems at fine edges, sharp corners and grooves [Wohlers, 2001]. This methodology is not appropriate for long-range application. The longer the range, the larger the scanner system needs to be.

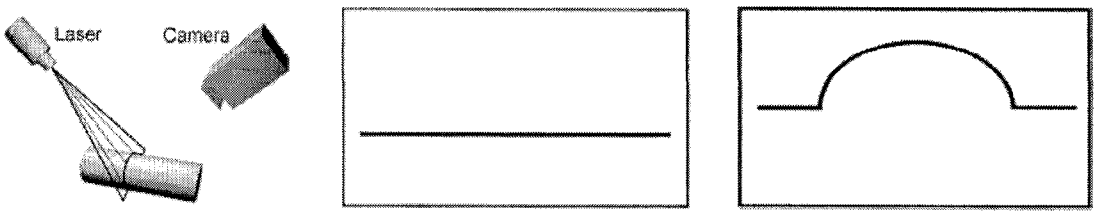

(a) Overview of the setup. (b) Laser line as "seen" by the laser. (c) Laser line as seen by the camera.

Figure 2-4: Images Seen by the Laser and Camera for Active Triangulation [Teutsch, 2003]

Structured light techniques involve projecting patterns of light (grid, stripes, ellipses) onto the surface of the artefact. An interference pattern such as a Moiré fringe is projected onto the surface producing distorted contour lines (Figure 2-5), which are captured by a CCD camera and subsequently analysed. With a Moiré fringe, a grating is projected onto an object and an image is formed with respect to a reference grating. Knowledge of the reference grating, master grating, the position of the camera and projector in space is required so that the depth can be calculated by triangulation [Clarke et al, 1993]. The distance between the lines is proportional to the height of the points of interest on the surface.

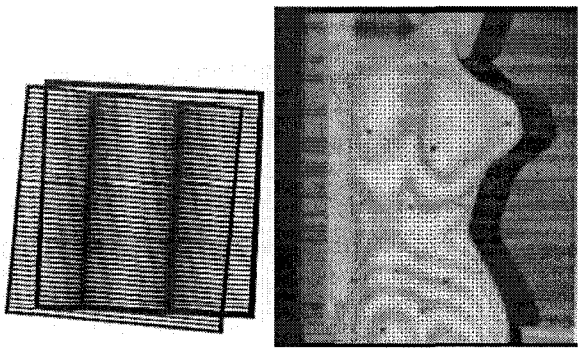

Figure 2-5: Moiré Fringe [Ypsilos, 2004] and Image Distorting the Fringe [Bujakiewicz et al, 2004]

Ranging or "time of flight" systems, illustrated in Figure 2-6, measure the distance of an object by calculating the time it takes for a wave (e.g. optical or ultrasonic) to travel to an object and return [Ypsilos, 2006], [Lichti and Harvey, 2002]. Large objects (i.e. landscapes) can be digitized using this technique, as well as objects with fine detail. Acoustic methods or echography calculate distance (knowing the speed of sound) using sound waves that reflect

from the surface of a part. This method is similar to ranging. Acoustic interference is a problem with this technique.

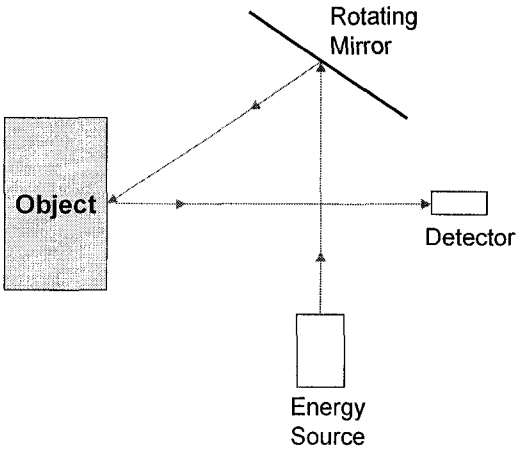

Figure 2-6: Time of Flight System [Ypsilos, 2004]

A Computer Tomography (CT) scan produces a gray scale cross sectional image of features within the body. The features are made visible by how much they attenuate (absorb or deflect) x-rays that have been passed through them. Brain tissue grey scale characteristics are illustrated in Figure 2-7. To create 3D image, data is collected from various cross sections by scanners positioned at multiple intervals and merged. CT scans are not limited to medical uses. A CT scan cross sectional slice of a cylinder head is illustrated in Figure 2-8. Industrial systems are available that are used to compare "as built" parts to "as designed" models [Hytec, no date].

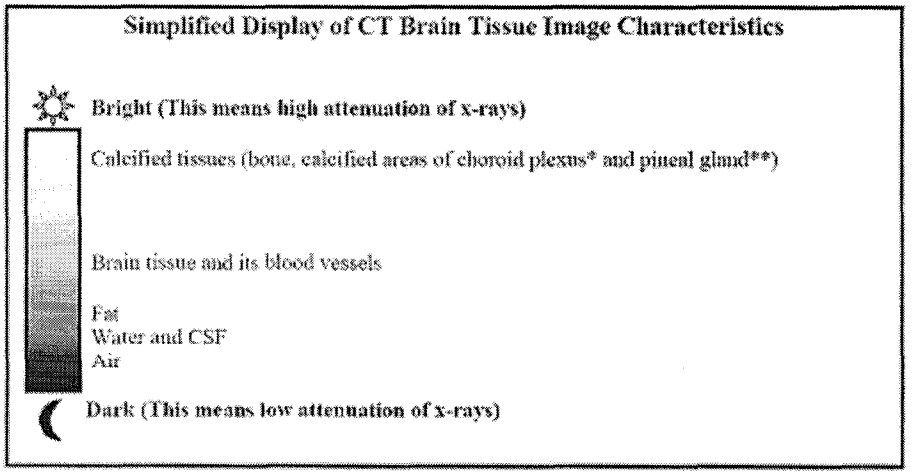

Figure 2-7: Grey Scale for CT Scanning System
[StrokeStop, 2000]

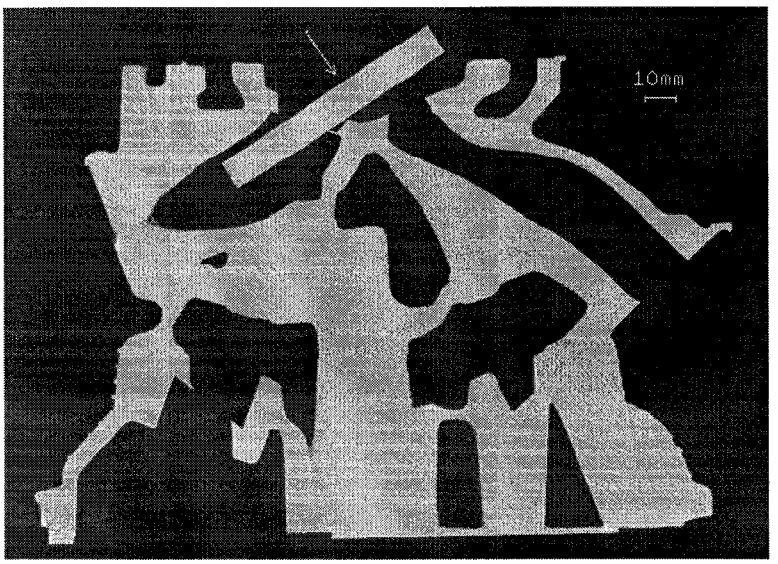

Figure 2-8: Single Slice Tomogram of a Cylinder Head
[Flisch et al, 1999]

Similar to CT scans, Magnetic Resonance Imaging (MRI) generates a cross sectional image that differentiates between tissues that contain water (fat, discs in the spine) and do not contain water (bone, cartilage) [Hornak, 2006], [Ballinger, 2004]. Magnetic resonance is used to obtain the tissue information, not x-rays as with the CT scanning. Multiple scans are required to produce a full 3D image.

2.1.1 Summary

Tactile systems are prevalent in the manufacturing arena, mainly for inspection, but laser-scanning techniques are making inroads. All measuring systems must interact with the object being analysed. Many issues for generating relevant, accurate data quickly for reverse engineering mechanical components, performing body scans for medical purposes, collecting information on architecture or archaeological objects and remote satellite scanning are common. Each system has its advantages and disadvantages. Table 2.1 summarizes the advantages and disadvantages of classic mechanic touch probe systems and laser scanning systems.

Table 2-1: Comparison of Touch Probe and Laser Scan Systems

Mechanical CMM Measurement		Laser Scanner CMM Measurement	
Advantages	**Disadvantages**	**Advantages**	**Disadvantages**
Very accurate over a large volume	Limited accuracy when measuring soft objects	Non-contact	Measurement errors due to equipment accuracy or resolution
Not affected by colour, transparency or surface reflections	Time consuming	Dense, "accurate" coordinate data	Problems with reflections, scatter with sharp edges and transparent materials
Quickly collect data for simple geometry (plane, circle, cylinder, etc.	Sparse amount of data points; therefore difficult to collect data on complex surfaces	Fast	Data must be filtered or resampled to reduce the point cloud density
Collect data for slots, holes, faces and quickly determine GD&T relationships	Skill intensive (path planning, number of points, data interpretation)	Portable	It is timing consuming and difficult to construct surfaces (10:90 ratio of scan time to surface creation)
Data density is not fixed		Ease of use	Data density is fixed
Little noise		Measure data for an object in its native environment	Computer intensive processing
Very repeatable			

2.2 FILTERING AND POINT THINNING

The goal of reverse engineering is to convert the discrete data points acquired through the sampling device into a continuous surface or set of curves and surfaces. There are regions of overlap when merging multiple scans of an artefact (variable point cloud density), as well as noise due to reflection, bright lights, laser light energy, sharp edges or foreign objects. Data filtering is performed to reduce the quantity of data points without reducing information with respect to the object. Different smoothing algorithms can be incorporated. Each algorithm looks at each point within the point cloud and its neighbours to intelligently reduce the data set. Common filtering strategies are:

(i) Noise filtering: Points that are furthest from their neighbours may be considered noise and eliminated.

(ii) Grid filtering: This filtering method reduces the data points such that they are regularly spaced in a cubic grid.

(iii) Curvature filtering: This filtering method analyses the curvature or the rate of change of the slope between points. The amount of data points in areas perceived to be flat is reduced, while more points in regions of curvature are retained.

Some noise filtering may need to be done interactively, since no algorithm can foresee all circumstances [Boehler et al, 2002].

2.3 REGISTRATION

Multiple views of an object are necessary to ensure that there is a digital coordinate representation for all the surface features (Figure 2 – 9). To capture this information, either the camera or the part must move; hence, the resulting point cloud coordinate data is relative to the new view position. Registration is the process whereby these multiple views are aligned into a single global frame as each scan has its own local coordinate system. [Page et al, 2003], [ElMaraghy and Rolls, 2001], [Li et al, 2000], [Chalermwat, 1999], [Besl and MacKay, 1992], [Chen and Medoni, 1992]. If y is defined as a point in the world coordinate system, and x is the point in the camera frame coordinate system, y is related to x by:

$$y = Rx + \vec{T} \tag{2.2}$$

where **R** is the rotation matrix, and

T is the translation vector.

Existing registration techniques can be mainly categorized into surface matching and feature matching [Zonghua et al, 2000]. The iterative closest point (ICP) algorithm, used to register two sets of points representing free form surfaces, was introduced by Besl and McKay in 1992. Other researchers, such as Chen and Medioni [1992] and Zhang [1994], have extended the basic ICP algorithm to improve rates of convergence and computational time. The accuracy of registration obtained using the ICP algorithm depends on the surface shape. If insufficient shape information is available then inaccurate or incorrect registration may occur [Page et al 2003], [Zonghua et al, 2000], [Hilton, 1997].

Predefined features may be used to establish a link between the multiple views. When utilizing feature-matching techniques these features must be common between the point cloud data sets. Correspondence is established between the features within the views: the point cloud data

to be aligned is manipulated (transformed and rotated) to register its features to the corresponding features on the reference (fixed) point cloud. Ideally, the registration features are non-symmetrical in geometry, orientation and placement; however, this typically is not the case. Additional markers may be placed on the artefact to be scanned in order to augment the feature matching registration process.

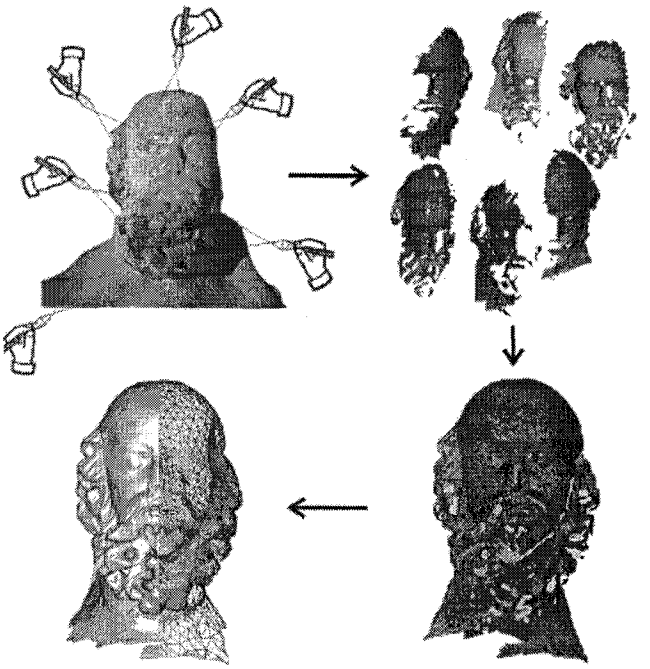

Figure 2-9: Multiple Scans, Point Clouds Data,
Registration and Surface Generation for a Sculpture
[Karbacher et al, 2001]

2.4 POLYGONAL MESH

Polygonal meshing (triangulation) is a standard method of defining a curvilinear object as a set of piecewise linear triangles or planar facets. This method is based on interpolation, not approximation techniques, and is suitable as a first estimate for subsequent surface or solid generation. Essentially, topology is inferred from the vicinity of the points in 3D space. Interpolation techniques based on Voronoi diagrams and Delaunay tessellations are common as they are robust, but they are computationally expensive [Bernardini et al, 1999], [Volodine, 2003], [Dey et al, 2001]. Few CAD/CAM packages can import and manipulate a mesh file. The polygonal mesh contains no topological information, and the file size is large.

True 3D meshing is required for closed objects. The polygonal mesh may require editing if there are holes in the mesh, invalid geometry (self intersecting surfaces, non-manifold structures, triangles with an angle less than 30°), or a ragged edge is created due to improper selection of vertices and line segments. The Standard Triangulation Language (STL) format is one way of representing a polygonal mesh. Tools are available that allow interactive mesh modifications by manipulating the facet normals (i.e. smoothing), subdividing or decimating the planar facets, and creating and manipulating sub-meshes [Chappuis et al, 2004], [Li et al, 2003], [Fischer, 2002], [Botsch and Kobbelt, 2001], [Karbacher et al, 2001, 1999], [Dey et al, 2001], [Liu and Ma, 2001], [Sun et al, 2001], [Attene and Spagnuolo, 2000], [Turk and Levoy, 1994].

2.5 SURFACE RECONSTRUCTION

For CAD/CAM applications, connectivity and continuity are important parameters. For aesthetic parts such as body panels on a car, at least second order continuity must exist between the various surface elements. Many commercial software packages such as Imageware Surfacer® (SDRC), Maya® (Alias), Geomagic Raindrop®, Nvision®, Paraform® etc. allow Bézier, Bspline or Non-Uniform Rational Bspline (NURBS) surfaces to be created from the polygonal mesh with interaction from the user. Curves can be generated to use for skinning and lofting operations. Surfaces patches can be created from the boundary curves or by using the polygonal mesh as a template. Subsequently the surfaces can be modified and blended. The Least Squares Method is commonly used to generate the curve or surface geometry from the mesh components. The degree of the curve, resolution for u and v, the method of creating the control hull lead to approximation and numerical errors in the reconstruction process. Regular features such as planes, cylinders, parallel or perpendicular alignments, feature similarities and symmetry may not be captured properly, although they were part of the original design intent. The final results are dependent on the skill level of the user as well the quality of the point cloud data.

2.6 SOURCES OF ERROR

There are several errors associated with the reverse engineering process. They are as follows:

- Scanning system and sensors based errors, which occur during the data acquisition phase;

- Approximation and numerical errors, which occur when refining the point cloud, creating a polymesh and reconstructing a surface;
- Artefact based errors: the actual product may have worn features, exhibit distortion, corrosion, etc. as well as variations due to the actual manufacturing process.

During the data acquisition phase, the error is influenced by the accuracy of the positioning system and sensors, the calibration of the system, occlusions and associated registration errors, the surface reflectivity (optical and laser systems), the material of the component to be measured, missed measurements, "mis-measurements" and accessibility errors. These errors lead to scattered data, uneven distribution of points, outlying points, gaps, and holes, which in turn leads to misarranged meshes.

2.6.1 Calibration

Any sensing system must be calibrated to a known reference to accurately determine the system parameters such as the home position and the measurement reference planes (consists of the orientation of the sensing device such as a camera or a tactile probe with respect to a known home position). Proper calibration reduces accumulative system errors.

2.6.2 Accuracy

Within both the hardware and the software components of the system, there is a limit to their accuracy. The accuracy of the data collection device must be combined with the positioning device. The state of the art CMMs with a touch trigger probe have a resolution of 0.000008 inches (0.00002032 mm) over a wide measurement volume [Sandia National Laboratories, 2004]. To obtain this accuracy the CMM must be vibration isolated in a temperature and humidity controlled environment. With optical systems, the accuracy is related to the resolution of the system. Within the reverse engineering vendor literature, accuracy of a laser scanning system is typically quoted as being between ± 0.0005 to ± 0.002 inches (± 0.0127 to ±0.0508 mm). The measurement accuracy will be compromised if a coating is applied to a transparent or reflective surface.

2.6.3 Shadows and Occlusions

Based on the size, complexity and geometry of the part, it may take several scans to generate a suitable point cloud. One reason for this is optical occlusions and/or shadows. If the laser or

light cannot reach a portion of the object being scanned (the geometry is in an area of shadow) then no data can be collected. Conversely, the surface may be seen by the laser beam, but not the camera. Abrupt changes in geometry can lead to partial occlusions, where the laser beam perceives one surface and the camera another. Discontinuities can also cause to questionable data points to be generated. These phenomena are illustrated in Figure 2-10 and 2-11 respectively. To address these issues, more than one scan is required to capture the geometry. For a large part, more than one scan may be required for a given plane, and to capture all surfaces the part may need to be shifted or rotated in its fixture.

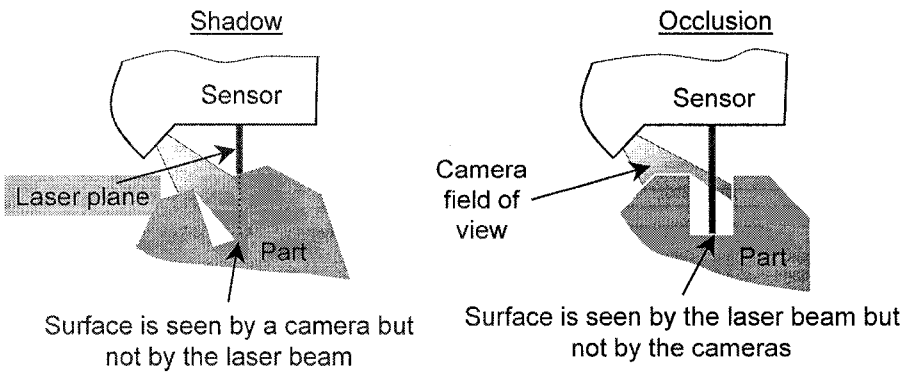

Figure 2-10: Shadow and Occlusion

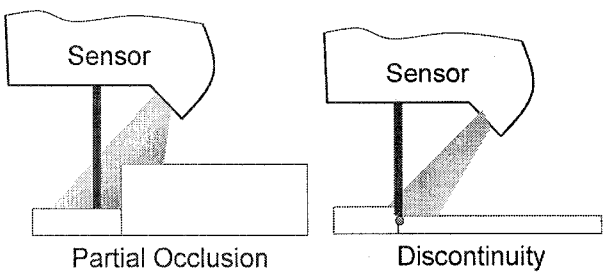

Figure 2-11: Partial Occlusion and Discontinuities

2.6.4 Surface Reflectivity, and other Material Properties

When using optical or laser scanners, the scan quality will vary depending on the type of material or the colours of the object to be scanned. Objects that are transparent, translucent, or have surfaces that are fuzzy, glossy, or highly reflective, made of fabric or of dark colours such as black, blue or green may require the use a matte-finish overcoat or another temporary surfacing agent [Roland, no date]. The underlying hypothesis of active optical geometric measurements is that the imaged surface is opaque and diffusely reflective [Tsakiri, 2003]. For

tactile systems, "soft" artefacts such as car seats (fabric supported by foam) may deflect creating distorted point cloud data. For the CT and MRI scans, the tissue type significantly affects the image of the captured data. For any system, the type of material and the material properties must be considered in order to determine the best data acquisition strategy.

2.6.5 Accessibility

It is difficult to capture information on deep features, recessed features and features in areas of shadow. As well, physical logistics must be taken into consideration. The object to be scanned should be set up to allow access to as many surfaces as possible; however, there may be obstruction due to the fixture configuration.

2.6.6 Missed Measurements and Mis-Measurements

Due to reflected light, occlusions or obstacles, insufficient data may be collected to define the object at a particular view plane. As well, the point density may be insufficient in areas of high curvature if a constant velocity is used during the scanning process, as illustrated in Figure 2-12.

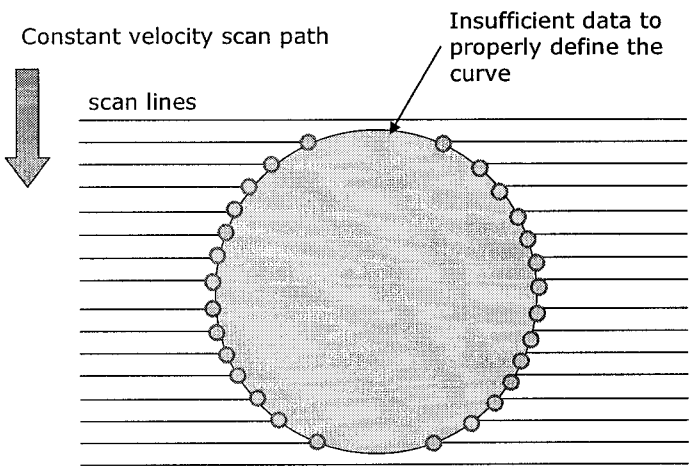

Figure 2-12: Variable Point Cloud Data Set due to Measurement Velocity

The surface roughness may be a problem: craggy surfaces may cause multiple reflections and shadows, which in turn will cause indefinite point correlations. Sharp edges (i.e. punched part) will also cause multiple reflections, creating false measurement data.

2.6.7 *Modelling Errors*

When filtering the spatial coordinates of the surface, the number of points must be minimized without losing information, as reconstructing the unorganized points is an "under-constrained problem". Without the appropriate number of points, several valid solutions may be possible, as illustrated in Figure 2-13 [Bernardini et al, 1999].

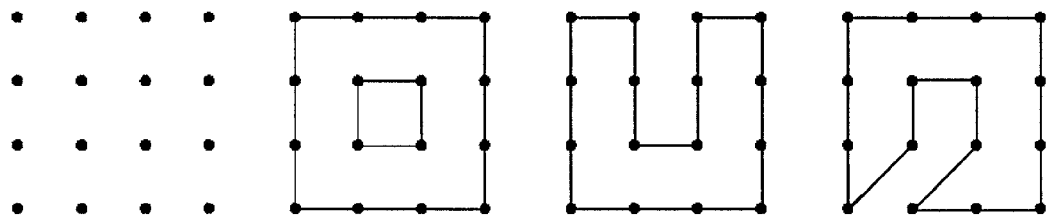

Figure 2-13: Ambiguous 2D Reconstruction from Points [Bernardini et al, 1999]

The surface quality is intertwined with the quality of the polygonal mesh. Data acquisition errors, approximation and numerical errors from creating the polygonal mesh cascade into cumulative errors in the final surface. Skinny or intersecting tetrahedrons can potentially cause problems with the surface fitting algorithms. Bernardini et al [1999] describe a re-triangulation algorithm to search and repair undesirable geometry (such as triangles that have an angle less than 30°); however, interaction with the user may be required with commercial products [Paraform® trainer, 2004].

As well, there is difficulty reconstructing sharp edges and areas of high curvature (singularities occur at sharp points and edges). Some algorithms can only construct surfaces from a point set of uniform density, or can only construct objects without holes [Attene and Spagnuolo, 2000]. The Least Squares Method may produce a surface having extraneous parts [Bernardini et al, 1999].

There is another consideration to be considered. The surfaces are fit together independently; hence, any relationship between the surfaces and other geometric entities, such as orthogonality, will not exist. Prioritizing geometric regularities (planes, natural quadratics, translational and rotational sweeps), and detecting similarities and symmetry within a model is called beautification. Beautification aims to improve the model so that it exhibits exact geometric regularities representing the original, ideal design intent [Langbein, 2002].

2.7 SUMMARY

When using reverse engineering techniques to reconstruct an object, many 3D data points are collected along the object's surface. Surfaces are constructed from the point cloud data using best-fit polynomial methods. Models of free form objects can be readily constructed in this manner. Although these reverse engineering techniques recover the form of an object, the model does not contain information suitable for subsequent design and manufacturing operations for an engineered component. Because of errors (due to scanning and manufacturing techniques, wear, etc.), the point cloud data does not correspond to an ideal replica; therefore, design modifications may be necessary. In order to create a more suitable model for engineered components, a different approach is required. Feature geometry should consist of lines and arcs. Surfaces, where needed, should be created from critical wire frame geometry. The user should be able to easily modify the geometry based on new design or manufacturing constraints. Within the design recovery framework, described in the next chapter, the engineer defines specific geometry construction criteria in a structured manner for a component/feature. Geometry construction tools need to be developed which utilize the design criteria and the collected point cloud data to create functional geometry. The digitized data is used as a template, but the data undergoes a series of transformations in order to create the final model.

Chapter 3

THE DEVELOPMENT AND APPLICATION OF THE DESIGN RECOVERY FRAMEWORK

3 THE SYSTEMATIC DESIGN RECOVERY FRAMEWORK

3.1 BACKGROUND

A product consists of a system of components, and meets an overall set of functional requirements. Each component has its set of functional requirements, and consists of functional features, process related features, and assembly features. Each component interfaces with another component. It is made from materials with certain mechanical and physical properties; it has a specific shape, features and feature patterns. The component must be manufactured in an efficient and cost effective manner; hence, the product design will be adapted to facilitate the manufacturing and assembly operations. There are geometric, dimensional and tolerance attributes for each feature, system of features and the overall shape, which are influenced by the functional requirements and the manufacturing processes. The general structure for a product is shown in Figure 3-1.

When analysing the component for design recovery, it needs to be assessed at the system level to understand its overall functional requirements, its method of implementation and the components with which the component of interest interfaces. The functional requirements of the individual features and their physical attributes need to be identified. This includes detailed information with respect to the form, the feature relationships and associations. A collaborative, integrated approach is essential in order to collect and link general design information and the detailed form characteristics to create an appropriate engineering model. Information must be integrated from different design domains and must be transformed into knowledge that can be effectivley used with computer aided engineering design, analysis and manufacturing tools. Gathering this information in a modular, systematic, comprehensive manner allows the designers the means to make informed decisions as to whether the current

component design is adequate, or how may it be modified to add value and/or address the present set of design and manufacturing constraints.

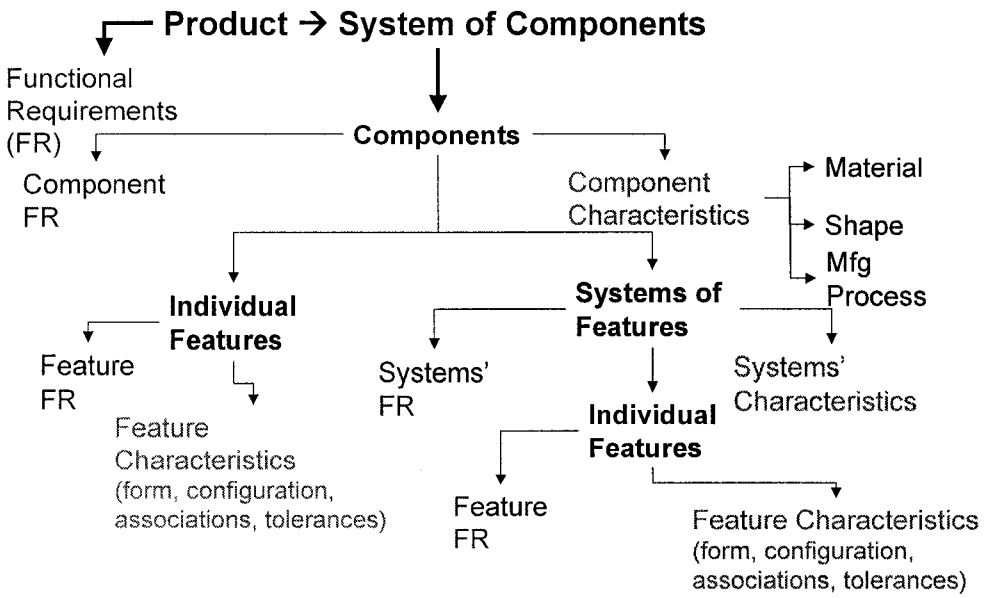

Figure 3-1: Product Taxonomy

In the area of reverse engineering of legacy software, this synergistic systems level – detail level procedure for analysing a program (code) and its interactions (data flow) is recognized as a technique for facilitating program comprehension [Tilley, 1998], [Rugaber, 1995]. Code reverse engineering focuses on understanding about how information is processed, while data reverse engineering tackles the question of what information is stored and how this information can be used in a different context [Hausi et al, 2000]. The multi-perspective approach for reverse engineering legacy software can be transformed to represent the appropriate activities and tasks that are necessary for design recovery of a physical object. A framework developed for legacy software, which encompasses different design domains and recognizes that there are various aspects to the data gathering and analysis activities, has been adapted to reflect the design recovery characteristics for engineered components (Table 3-1). Within this framework, it is recognized that there are differing levels of granularity in the data gathering and analysis activities, but the framework does not provide a suitable guide to allow the designer to move from one design domain to another in a comprehensive manner. Consequently, existing enterprise architectures are assessed to determine whether one can be effectively adapted to support reverse engineering of mechanical components.

Table 3-1: Overview of the Reverse Engineering Process, adapted from [Tilley, 1998]

Reverse Engineering Tasks	Component Analysis	Implementation	Implementation of individual features
		Structural	Structural relationships between features
		Functional domain	Functional relationships between structures (geometry and constraints)
		Physical domain	Physical domain: environment, substructures, super-structures, materials, production volumes, manufacturing processes
	Planning Recognition	Physical domain	
	Concept Assignment (FR) and application	Functional domain	
		Physical domain	
	Redocumentation	Detail level	
		Embodiment level	
	Architecture Recovery	System Level	
Formal Reverse Engineering Activities	Data Gathering	System Examination	Superstructure
			Substructure
		Product Documentation	Geometry, Topology
			Mechanical properties
			Physical properties
	Information Exploration and Transformation	Navigation	Pattern selection
			Editing patterns/attributes
		Analysis	Type
			Level
			Verification
		Presentation	Multiple perspectives
			Visualization tools and techniques
			User Interface
	Knowledge Management	Organization	Extract selected details and information, capture common characteristics and classify features and patterns
		Discovery	Structural relationships between features and their properties and the relationships among them within the system (iterative)
		Evolution	Dynamic development of structured framework (iterative)
Quality Attributes	Applicability	Application domain (end use)	
		Implementation domain (manufacturing and assembly)	
	Extensibility	Integration mechanisms to CAE and CAM and other design and manufacturing tools	
		End-user usability for modifications and redesign	

Enterprise Architecture defines how information and technology will support business operations within an organization. This involves applying a framework to detail the models, which comprehensively describes the actual or desired business activities throughout an organization. The framework serves as road map to provide a reference that is well documented and easily understood, so that stakeholders within an organization can assess the existing processes and the impact of changes on each of the enterprise architecture components. At varying levels of detail, the entities, roles and relationships are explicitly described. Internal core competencies and procedures are documented for an organization as well as external interactions with customers and suppliers. The framework also provides a rigorous taxonomy and ontology that clearly identifies what processes are performed, and how these processes are executed. Upon documenting an organization's structure and business processes, the specific elements pertaining to the information technology are illustrated, such as interfaces between applications, and network connectivity diagrams.

A direct analogy can be made between a business system and a physical product/subassembly/component. A business's organizational structure is comparable to a product structure. A department, application or other element within the organization is comparable to a subassembly or component. Likewise, technical elements such as infrastructure hardware, design specifications, and development languages which support the business structure, are analogous to form, features, materials and interface specifications, which allow the component to achieve the design objectives. Tasks within an organization support a business process. Features within a component or components within a product are designed to meet specific functional requirements. This similarity can be leveraged to develop a formal framework for design recovery using Systems Analysis techniques. Using these techniques, questions pertaining to 'what, how, where and why' with respect to the components and their features can be answered in an explicit, well thought-out manner.

The framework must provide a multi-level roadmap to allow the functional, structural and data information related to mechanical components to be accumulated at different levels of abstraction or 'resolution'. Detailed data, such as the diameter, depth, positional coordinates and the related tolerances for a hole corresponds to a high resolution condition. Conversely, a low resolution condition corresponds to a high level of abstraction (Figure 3-2).

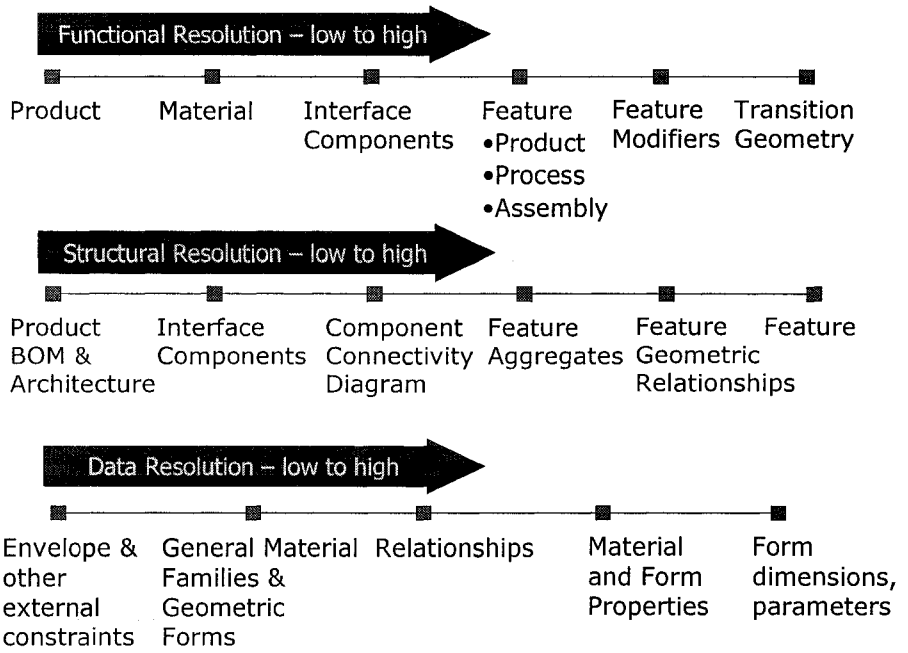

Figure 3-2: Resolution Levels for the Design Recovery Process

At a low resolution, a comprehensive overview of the component within the 'product system' is required, whereas at the detail level (high resolution), specific detailed data values with respect to the individual features must be obtained. The embodiment information is associated with a medium level of resolution. The information in the physical and logical design domains should be captured at the varying resolution levels and linked.

3.2 APPLYING THE ZACHMAN FRAMEWORK FOR REVERSE ENGINEERING

There are several recognized Enterprise Architecture frameworks, such as the U.S. Department of Defense Architecture Framework (DoDAF), the U.S. Federal Enterprise Architecture (FEA), the Extended Enterprise Architecture Framework (E2AF) and the Zachman Framework (introduced in Chapter 1). The DoDAF is aimed at military systems, but it is also suitable for large systems with complex integration and operational issues in non-military domains. The DoDAF focuses on four basic areas or view sets of a system:

- The overarching All View (AV), which defines the scope and context of the architecture;

- The Operational View (OV), which provides the descriptions of the tasks and activities, operational elements, and information exchanges required to accomplish DoD missions;

- The Systems View (SV), products provide graphical and textual descriptions of systems and system interconnections that provide or support DoD functions, and the

- The Technical Standards View (TV), define technical standards, implementation conventions, business rules and criteria that govern the architecture. [United States Department of Defense, 2006]

The FEA is designed to ease sharing of information and resources across federal agencies, reduce costs, and improve citizen services. This framework consists of a set of reference models designed to facilitate cross-agency analysis and the identification of duplicative investments, gaps, and opportunities for collaboration within and across federal agencies. The FEA reference models are:

- The Performance Reference Model,
- The Business Reference Model,
- The Service Component Reference Model,
- The Data Reference Model, and
- The Technical Reference Model [Federal Enterprise Architecture, 2006].

The FEA also contains a common taxonomy and ontology to describe the information technology resources within the federal agencies.

The Institute for Enterprise Architecture Developments has developed the Extended Enterprise Architecture Framework (E2AF). This framework consists of four viewpoints, which focus on privacy, security, governance and other. These viewpoints are analysed in conjunction with a framework matrix that consists of a vertical axis, which concentrates on the business information and information technology areas, and a horizontal axis, which combines the Zachman classifications and perspectives [IFEAD, 2006].

Although these frameworks are very powerful for examining aspects of a business and its interactions, the Zachman Framework provides a solid, non-specific structure that can be readily transformed to support the design recovery process, as many perspectives must be considered to effectively reverse engineer a product or component. The key perspectives and classifications that are applicable for the design recovery process at the component level and the feature level are shown in Figure 3-3.

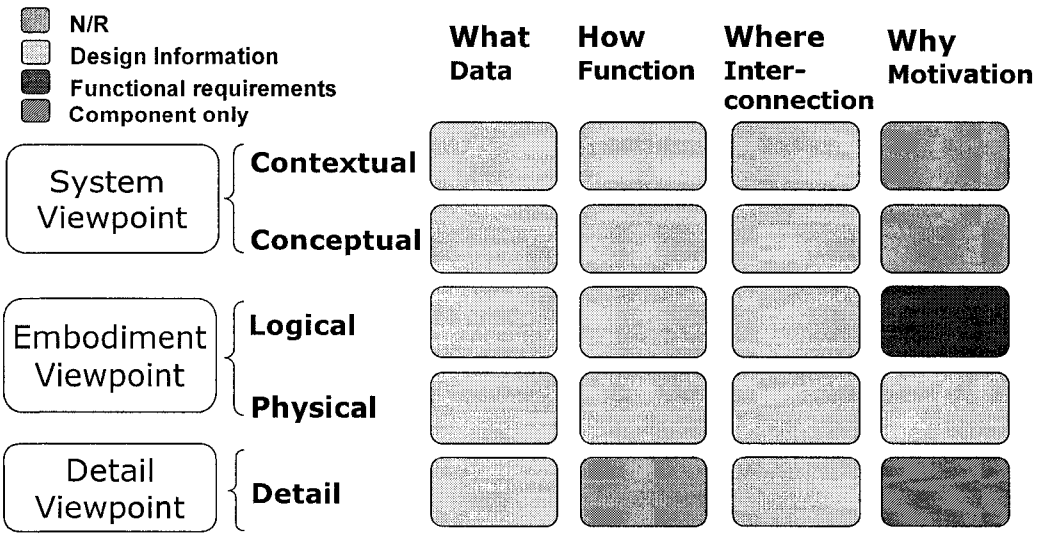

Figure 3-3: Design Recovery Framework (Component and Feature Levels), adapted from Zachman [2002]

3.3 COMPONENT LEVEL ANALYSIS

The design recovery framework is used to capture concise information for the component and each feature at the different resolution levels. The component functional requirements, structure, features, material and interface components are highly coupled. A methodology for driving collaboration across the different design domains is needed in order to improve the design reconstruction process. The material and functional requirements influence the base form. In turn, the base form is modified by the interfacing components and the manufacturing processes. The tolerances must be selected to satisfy the functional requirements and to establish cost effective manufacturing and assembly processes. The coupling of the component attributes amplifies the design recovery issues illustrated in Figure 3-4.

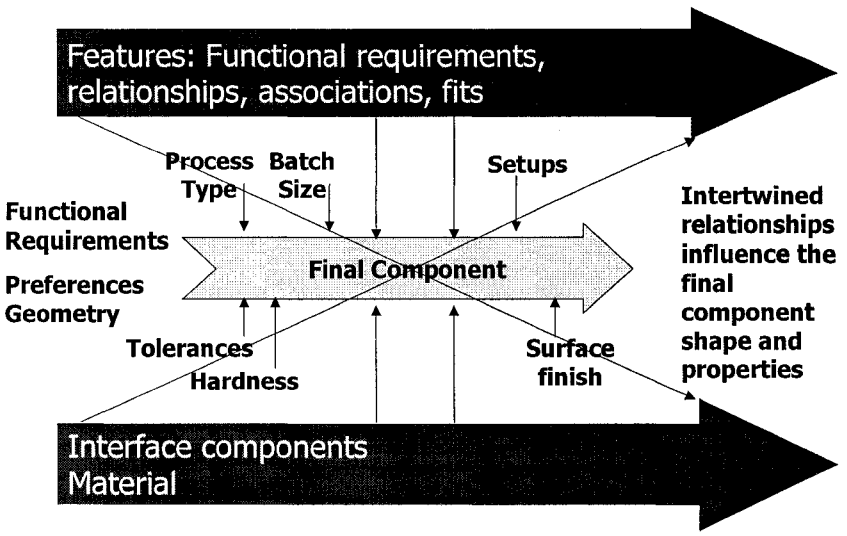

Figure 3-4: The Coupling of the Component Attributes

At the low resolution or the system level perspective, the context of the component of interest within the product architecture is defined, as well as the generic concepts used to address the specific circumstances. The contextual and conceptual 'what, how, where and why' questions are answered by considering the component in its entirety within the product architecture.

At the medium resolution or the embodiment level, the logical and physical perspectives are analysed. At the logical layer, the functional are enumerated for the 'Logical: What' rubric using the National Institute of Standards and Technology (NIST) design vocabulary. NIST research partners developed a comprehensive, standardized terminology to reflect the intended reasons for a component's architecture [Hirtz et al, 2002]. Identifying the component's functions in this manner provides a rational basis for evaluating the design. The information contained in the ' Logical: How' rubric provides a brief description as to how the functions are met in the design. The hypothesized functional requirements are presented in the 'Logical: Why' rubric.

When assessing the component as a whole at the physical level, one is interested in collecting overarching information: the material and material treatments, the part envelope, the basic shapes, the base manufacturing processes, and the interface components that influence the component design. At the physical level, assessing the 'Physical: What' aspects take precedence. Limited information is required for the 'Physical: How' aspects as this is process related. The material family, physical and mechanical (and other) characteristics are considered

for the 'Physical: Why' rubric. Many attributes could be taken into account when assessing the component material and its properties. The various material related characteristics need to be determined in order to rationalize as to why this material is required. The original material may not be appropriate based the new design/manufacturing constraints. Understanding the motivation for the material selection provides the designer a basis for selecting a practical alternative material. A summary of the general material families and some typical reasons for justifying a material selection is presented in Table 3-2.

Table 3-2: General 'Physical Level' Material Characteristics

Material	
Physical: What	
Ferrous	Cast iron
	Steel
	Stainless steel
Non-Ferrous	Aluminum
	Copper
	Magnesium
	Zinc
	Titanium
Superalloys	Superalloys
Polymers	Thermoplastic
	Thermoset plastic
Ceramics	Porcelain
Composite Materials	Fiberglass
	Carbon fiber
	Kevlar
Other	Glass
	Wood
	Other

Material
Physical: Why
Cost
Strength
Weight
Appearance
Wear Resistance
Corrosion resistance
Thermal expansion characteristics
Manufacturability
Fatigue resistance
Ductility
Stiffness
Springiness
Good high temperature properties
Electrical conductivity
Electrical resistance
Thermal conductivity
Insulation
Other (waterproof, ...)

The detailed information related to the material and processes that modify the material properties is summarized in Table 3-3.

Table 3-3: General 'Detail Level' Material Characteristics

Material	
Detail: What	
Type	Material composition / specifications
Heat Treatment	Surface hardening
	Through hardening
	Annealing
Surface Finishing Treatments	Coating (galvanizing)
	Texture modification (peening)
	Deburring

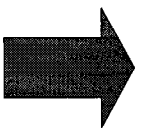

Material
Detail: Why
Cost
Strength
Appearance
Wear Resistance
Corrosion resistance
Fatigue resistance
Safety

The component is either static or dynamic, and it interfaces with static or dynamic parts. The envelope is defined by the components that contact or surround the component of interest, and influence the component and feature structures. The operating conditions have an effect on the material type and treatments and the component structure. Concerns about the temperature extremes, the corrosiveness level, dirt level, exposure to vibration, forces and stresses (static or cyclical) need to be itemized. These traits are ranked, where 0, 0.5 and 1 indicates no or minimal concern, moderate concern, and a high concern, respectively.

The initial stock condition, finished shape type, volume and mass are considered with assessing the general shape characteristics (Table 3-4). There are two basic shape types: (i) natural free form shapes, and (ii) engineered shapes. Objects that have a free form shape may be standalone entities, such as statue or a solid toy model, and are not considered here. In contrast, all engineered components and features have a basic characteristic shape with associated inherent design constraints. There are five part families established for engineered components:

- Prismatic parts (i.e. a cylinder head),
- Rotational parts (i.e. pulleys and shafts),
- Axially symmetric parts (i.e. a connecting rod),
- 3D-2D parts, (i.e., stamped parts consisting of a thin sheet with a free form shape such as body panels for an automobile), and

- 3D-3D parts, (i.e., weldments, castings, and casting patterns, which have free form shapes in combination with prismatic or rotary shapes).

Table 3-4: Form Related 'Physical: What' Cell Attributes

Form		
Physical: What		
Envelope	Shape (prismatic, cylinderical, other...)	
	Components	
	Packaging characteristics	
	Clearance (tight, loose, in vicinity)	
Operating Conditions	Temperature (Heat or Cold) / Humdity	
	Vibration / Fatigue	
	Corrosiveness / Dirt Levels	
	Forces / Stresses	
General Type	Static / Dynamic	
	Interface with Static / Dynamic	
General Fundamental Shape	Initial stock condition	
	Finished shape type (prismatic, rotary...)	
	Weight / Mass	
	Volume	
General Process Type	**Casting**	Investment Casting
		Permanent Casting
		Sand Casting
		Shell Casting
		Die Casting
	Total Deformation	Cold Extrusion
		Hot Extrusion
		Cold Forging
	Local Deformation	Stamping / Stretching
		Deep Drawing
	Polymer Molding	Injection Molding
		Compression Molding
		Transfer Molding
		Thermoplastic Extrusion
	Machining	Machining
	Other	Other

For prismatic parts, the part faces consist of planar surfaces. This is the basic characteristic shape for this family. Other features are added (bosses, ribs) or subtracted (holes, pockets) from a planar face. Typically, the features appended on the base shape are extrusions from a primary reference surface. Three dimensional parts are built from entities that have a two dimensional cross section and a depth. There are other cases however where there are two reference surfaces for an attached feature, such as a support structure like a gusset. This case is defined as a 3D-3D case, as there are multiple reference planes for a feature.

Rotational parts consist of a profile swept around a central axis. Any cross section perpendicular to the axis of rotation will be circular. There are several sub-families for rotary parts. They are parts that have: (i) a rotary profile, (ii) a rotary profile plus appended features (slots, holes) (iii) a profile that is swept to produce helical geometry, (iv) flanges and other disk like components, which combine prismatic and rotary aspects, and (v) offset diameters (crankshaft). A special case exists when there is a cylinder with appended features, such as a roll die. The cylinder can be flattened (unwrapped), and geometry reconstructed on the flattened face. Reconstructing this type of rotary geometry is similar to reconstructing geometry on a planar prismatic part. Specific data transformation and analysis techniques for several rotary component types have been developed by Urbanic et al [2006].

When an irregular shape is mirrored about an axis, the part is axially symmetric. Rotary parts and several prismatic parts are axially symmetric, but have other associated constraints. Stamped panels have a 3D free form shape. The panels may have contoured shapes created by the stretching or drawing processes. Unique feature geometry can be created by the stamping processes (i.e. lancing, bending). Typically with stamping geometry, there is a sheet thickness associated with critical geometry, such as a cross section; hence the designation 3D-2D. Modelling this geometry is challenging, as there are free form shapes (body panels) blended with engineered shapes (mounting tabs). This is also true for complex 3D shapes created by the casting and welding processes. The designation for these types of components is 3D – 3D. This geometry can be very intricate, includes 3D fillets and blending, and the component may consist of multiple materials (cast in liner for a cylinder block). Free form shapes are a consequence of DFX practices (Appendix B) as well as for aesthetic appeal. Specific geometry reconstruction instructions such as the slice plane depth for the point cloud geometry or surface construction information (i.e. fillet data) for 3D-2D and 3D-3D components may be included in the component analysis or in the feature analysis, as appropriate.

Including information with respect to the component type, the work envelope and operation conditions, the general shape characteristics, the mating components, and the functional requirements puts the component of interest in context with the total system, and establishes a platform that can be leveraged for subsequent product/process modifications. The attributes associated with the shape aspects for the 'Physical: What' rubric are summarized in Table 3-4.

General process information is itemized at the 'Physical' layer. Explicit process characteristics are obtained at the detail level. Each feature, and system of features within the component, is given a label that is used for identification in subsequent analyses.

At the detail level, specific data regarding the envelope (i.e. dimensions, clearance conditions) and the component shape is collected. The component is positioned in Cartesian space and the datum features to be used for feature relationships and dimensioning are identified. Specific numerical values and observations relating to the form and the manufacturing processes (presented in Table 3-5) are also performed when assessing the component at the detail level. Much relevant information is contained in existing design repositories. By assessing the component in this manner, pertinent information can be retrieved when querying existing design databases.

Table 3-5: Detail: What Cell for the Component Analysis

Form		
Detail: What		
Envelope	Dimensions	
	Details for special definition	
	Detailed clearance conditions	
General Fundamental Shape	Dimensions for bar stock, tubing	
	Finished shape type (prismatic, rotary…)	Component level critical cross sections
	Datum points / features	Primary, secondary, tertiary datum definitions
General Product-Process Characteristics	Porosity / inclusions	Process dependent
	Non-uniform hardness, strength	
	Surface discontinuity	
	Lower limit surface finish (mm)	
	Section thickness (min/max) (mm)	
	Surface detail	
	Internal geometry	
	Undercuts – internal / external	
	Large radii	
	Draft angle	
	Parting plane(s)	
	Minimal no. of distinct features	
	Closely spaced features	
	Narrow cut outs/ projections	
	Bend axes / Bends greater than 90 deg.	
	Long, thin sections	
	Semi-hollow features	

The general process characteristics vary per process. Process cross-reference summary tables are presented in Appendix B.

A summary of the component level analysis is illustrated in Figure 3-5.

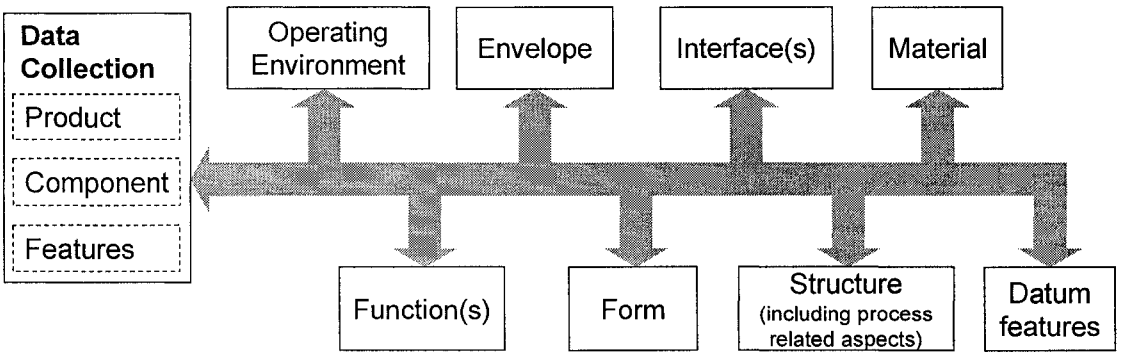

Figure 3-5: Component Level Analysis Summary

The component taxonomy is illustrated in Figure 3-6.

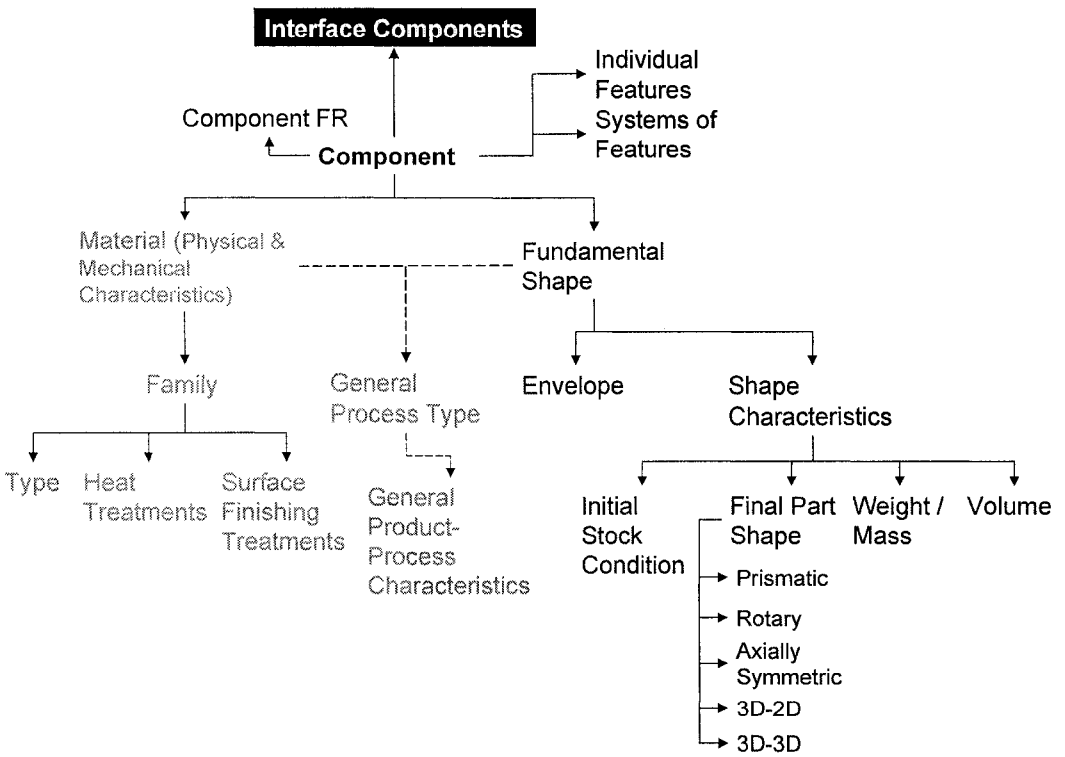

Figure 3-6: General Component Attribute Taxonomy

3.4 FEATURE LEVEL ANALYSIS

Each feature must be systematically analysed at the different resolution levels. The features must be placed in context, and the general conceptual applications need to be defined. As with the component analysis, the feature related system level analysis information is abstract. The context for the feature defines the circumstances that make this feature applicable. An explicit analysis is performed for the embodiment and detail viewpoints. Each feature is an entity within the component. It has a name, a function, a set of attributes and relationships that are assessed at the elemental level. Any feature within a component has a product, process or assembly related function. Analogous with the component functional requirement descriptions, the NIST design vocabulary is used to specify the feature related functions. In general, the feature functional requirements will be a sub-set of the component level functional requirements. Consequently, there may be some overlap between the component and feature analyses for the 'Logical: What, How and Why' elements.

When assessing the feature at the physical level, the general descriptors are used to depict the form, pattern of arrangement, the chosen manufacturing process and the components to which the feature is physically connected ('Physical: Where'). The basic feature form may have been modified based on the chosen manufacturing process (i.e. draft, large radii), or external constraints (envelope). Each feature is coupled or associated with another feature (internal link) or component (external link). The feature form, process modifications, pattern associations and relationships are elaborated on when performing the analysis at the detail level. A summary of the feature types and modifiers is presented in Table 3-6.

Table 3-6: Feature Summary

Type	Description	Modifiers
Product-based	A form that assists with meeting the product related FRs, i.e. 'I' shape to minimize deflection / bending.	Process related modifications to the product form that optimized the manufacturing process, i.e. draft, large radii, etc.
Process-based	A feature that assists with meeting process related FRs, i.e. adding ejector pin geometry to assist with the die casting process or adding features that allow for transport throughout the manufacturing process.	
Assembly-based	Assembly features that allow the product to be assembled, i.e. tapped holes for fasteners.	Assembly related modifications to the product form that assists with the assembly process, i.e. introducing symmetry or fool proofing geometry.

Four categories are used classify feature shapes in engineered components. They are:

- Geometric primitives, such as cylinders and cubes;
- Engineering primitives, such as stepped holes, keyways, slots, splines and gear teeth, and so forth;
- User defined profiles / shapes (i.e. specialty grooves), and
- Critical cross sections for free form shapes (traditionally used in design of free form shapes).

Geometric primitives are simple 3D shapes that are used in solid modelling CAD systems. Standard geometric primitives are the block, cylinder, cone, sphere, wedge and torus; these shapes can be specifically defined by a minimal set of parameters. A variation of these geometric primitives is used in feature based modelling systems to serve as a foundation for computer aided process planning [Changchien and Lin, 1996], [Dong et al, 1991], [Krause et al, 1991], [Kumara et al, 1994], [Logar and Peklenik, 1991], [Mantyla et al, 1994], [Peklenic and Grum, 1982], [Owodunni et al, 2002], [Tonshoff et al, 1996], [Venuvinod and Yuen, 1994], [Wang et al, 2002], [Zimmerman et al, 2002]. Feature based modelling systems support composite simple shapes such as a chamfered hole, which consists of a cylinder plus a cone. The 'engineering primitives' introduced here are an extension of the feature based composite shapes. Engineering primitives have:

(i) specific form - function relationships,

(ii) standardized (i.e. ANSI or ISO Standard) key parameters, and

(iii) defined tolerances and relationships (i.e. ANSI or ISO Standard) based on the form and / or application.

Engineering primitives encompass geometric primitives that have defined form-function relationships (i.e. ISO standard shaft / hole size and fit relationships), common feature based

primitives (fastener hole geometry, thread type, and class of fit), and other forms such as grooves, keys, splines and gear teeth, all of which are defined by parameters, and have explicit form, function and fit relationships. Not all parameters may be predefined (i.e. the depth of a tapped hole). The engineering primitives considered here focus on fasteners and components used in power transmission. A user defined profile is comprised of a set of user defined parameters and relationships that defines the feature geometry (i.e. a dovetail slot or specialty o-ring grooves). Each feature must be classified appropriately, and provided with the necessary parameters and data in order to be able to properly reconstruct it (Figure 3-7).

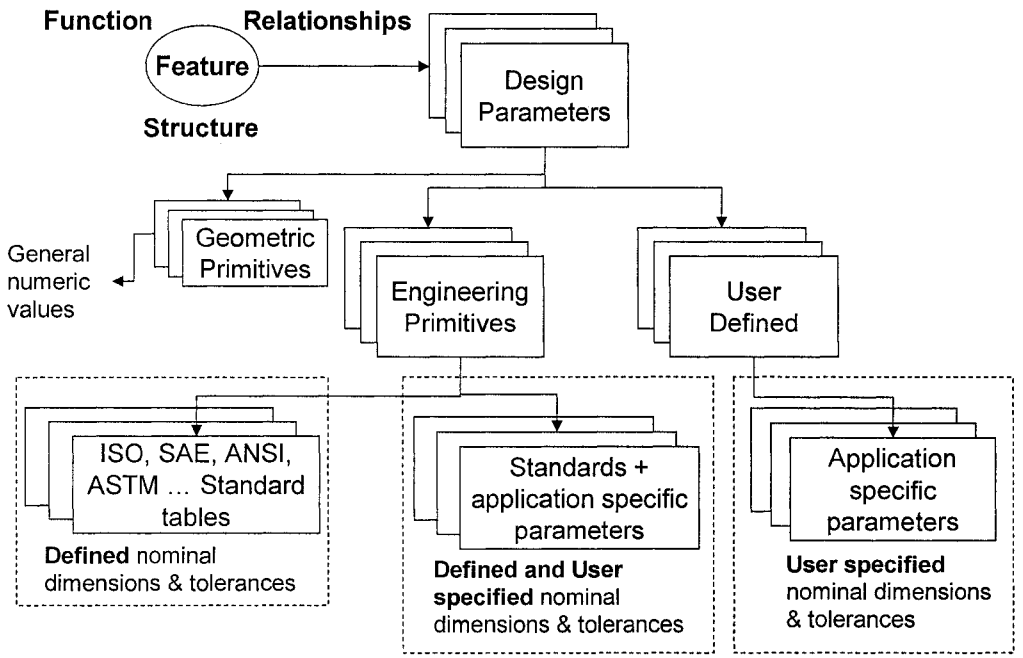

Figure 3-7: Design Parameters for Different Feature Types

Critical cross sections consist of a user defined planar slice through the part point cloud data. The slice plane information is provided to isolate the data to be used to construct the wire frame boundary curve geometry. From these boundary curves, surfaces and solids can be constructed. The algorithms used to fit geometry to noisy point cloud data is presented in Chapter 4.

The form category, general information, and the reason 'why' (the motivation) this feature is necessary are specified at the physical level. The corresponding parameters and numerical values are specified at the detail level. Feature form alterations are based on physical

constraints, design for 'X' (DFX) considerations, and the material selection. The form alterations are specified in the 'Detail: What' rubric.

The features may be aggregated in a pattern; consequently, they have associations. There may be ideal physical relationships with respect to the form (i.e. flatness, cylindricity) and to other features on the component (i.e. parallelism, perpendicularity, and concentricity). This information is explicitly defined at the detail level in the 'Detail: Where' rubric. The geometric dimensioning and tolerancing (GD and T) method specifies these relationships in unambiguous terms; therefore, it is used to represent the ideal feature relationships (Table 3-7). To ensure the assemblability to the mating parts, they should also be assessed in order to have confidence with both the nominal dimensions and any assigned feature tolerances. For the design recovery process, there may be other location and fit relationships that may need to be considered. This information must be gathered from the design and manufacturing domains for effective model reconstruction. This information is used to create an ideal CAD model as well as provide supporting documentation.

Table 3-7: Geometric Dimensioning and Tolerance Relationships

GD and T Callout	Feature	Primary Datum	Secondary Datum	Tertiary Datum	Tolerance Value	Comment
Cylindricity						
Circularity						
Flatness						
Straightness						
Parallelism						
Perpendicularity						
Angularity						
Concentricity						
Symmetry						
True Position						
Line Profile						
Surface Profile						
Circular run out						
Total run out						

Common ancillary location and fit attributes are presented in Table 3-8.

Table 3-8: Ancillary Location and Fit Relationships

	Datum	Feature	Comment
Location Callout			
Aligned			
Along			
Axial			
Radial			
Centred			
Collinear			
Coplanar			
Mirror			
Offset			
Fit Callout			
Clearance			
Interference			
Running Fit			

The general feature taxonomy is shown in Figure 3-8.

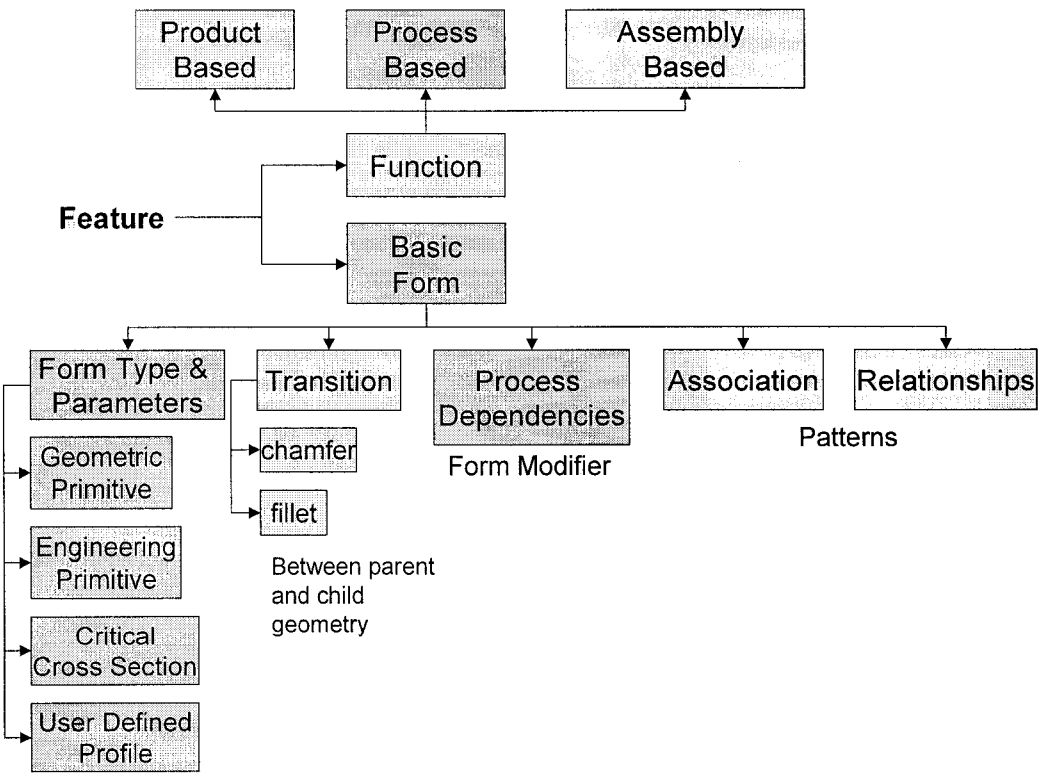

Figure 3-8: General Feature Attribute Taxonomy

3.5 CONNECTIVITY DIAGRAM AND THE DESIGN STRUCTURE MATRIX

A connectivity diagram is used to illustrate physical feature links within a component, and the interface components. A connectivity diagram is a technique used in network design and is employed to illustrate the logical and physical connections (essential data flows) within a system. Here it is used to show how the features are interconnected within the component of interest. The rules developed for constructing an artefact connectivity diagram are as follows:

- Each feature must be identified, and provided with a concise, descriptive label.
- Feature patterns and pattern types must be identified and labelled. The pattern types are linear, circular, polar grid, linear grid, and peripheral.
- The mating components for each feature must be identified. If the mating component is an external component, it must be included and labelled appropriately.
- Critical external components, which influence the design of the component being analysed, must be also included in the connectivity diagram.
- Each feature type has a distinct font and connector style, as shown in Table 3-9. The appropriate connector style is drawn between the features.
- Transition geometry is included in the model at the discretion of the engineer.

Table 3-9: Feature Summary for Connectivity Diagrams

Feature Type	Font	Connector Style
External component, special	Italicized, Blue	Solid
External component, standard commercial item	Italicized, Black	Phantom
Product	Normal, Black	Solid
Process	Bold	Dashed
Assembly	Normal, Red	Solid

The connectivity diagram for a single cylinder engine cylinder valve cover case study is illustrated in Figures 3-9 and 3-10. The valve cover encompasses the valve train, sits on a cork gasket, and is mounted to the cylinder head via four zinc plated M6 bolts. Although the bolts and gasket are the external components with direct contact with the valve cover, the cylinder

head must also be taken into consideration. The cylinder head tapped holes theoretically have the same positional coordinate relationships as the valve cover bolt mounting holes. The fillets between the valve enclosure and sealing surface, and between the sealing surface and lip are included in this model shown in Figure 3-10.

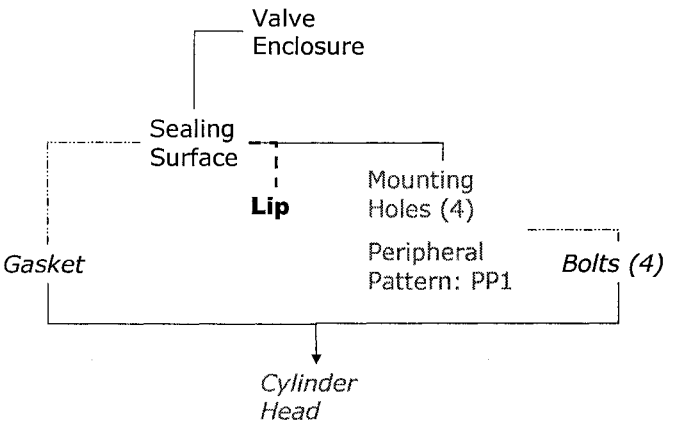

Figure 3-9: Connectivity Diagram for a Single Cylinder Engine Valve Cover

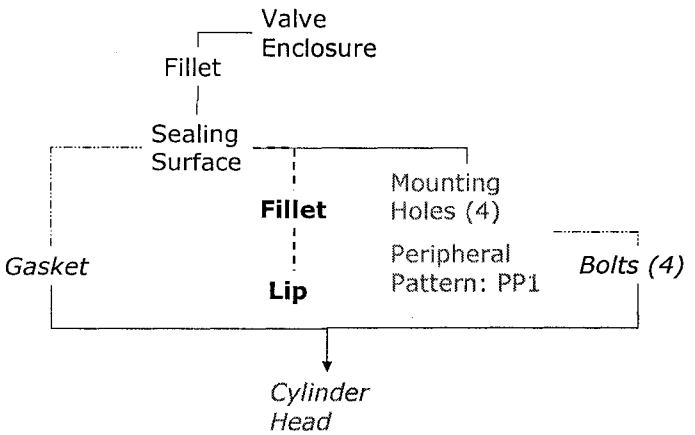

Figure 3-10: Connectivity Diagram for a Single Cylinder Engine Valve Cover Including Transition Geometry

The design structure matrix is employed to evaluate the actual design structure coupling based on the designer's understanding of the functional requirements and the features contained in the component being assessed. The design structure matrix (DSM) is a project development tool used to illustrate task coupling for individual activities in a matrix format. There are three different matrix structures to reflect activity types. Activities that occur independently are

represented as a parallel structure. Activities that occur in a sequence, or have dependencies, are presented as a serial structure. Highly coupled activities, where the parameters are interdependent, as represented as a crossover structure. These relationships and the associated design matrices are illustrated in Figure 3-11.

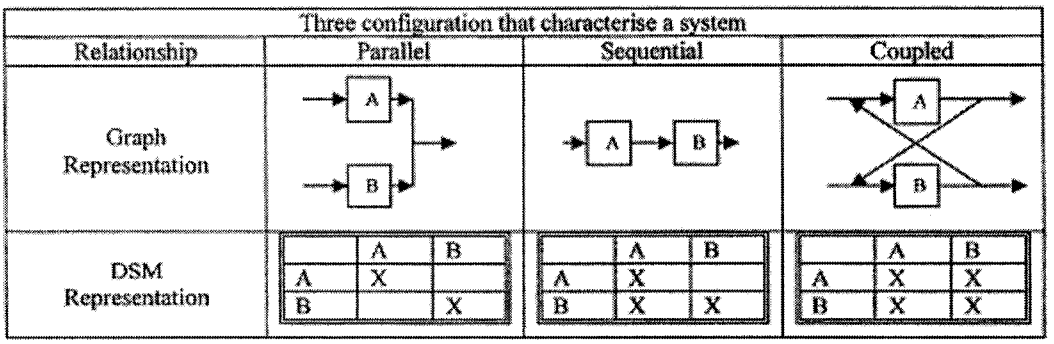

Figure 3-11: DSM Configurations [Guenov and Barker, 2004]

This design structure matrix representation is used to illustrate the physical interconnections of the features within a component. Independent features correlate to parallel activities, dependent features (i.e. a boss containing a feature that interfaces with another component) correlate to serial activities, and coupled features correlate to interacting activities. Coupled and dependent features are sensitive to geometric, material and surface related variations. Understanding this coupling is important when assigning tolerances, and introducing any variations to the original product design.

3.6 HEALING PROCESSES

Engineering design methodologies in combination with assessing the collected data can be used to determine the design parameters and infer the final product documentation such as nominal dimensions, tolerances and specifications. This is speculative in nature, and highly dependent on the quality of the available data and existing relevant knowledge. In order to produce a model that contains the ideal geometry, appropriate nominal dimensions and tolerances, a three-tiered healing process assessing these aspects of the model should be conducted. The geometric healing process is employed to determine the ideal nominal geometry from the available measurement data by exploiting realistic constraints that represent the design intent. For example for prismatic parts, the surfaces are flat, and holes are round

and typically perpendicular to the surface. Multiple diameters within a hole are concentric. In many components, there is symmetry – and features are mirrored. This should be captured in an "idealized form". Geometric variations may be introduced from several sources. It is good manufacturing practice to break all sharp edges, apply chamfers to assist in assembly operations, and to maximize radii to reduce stress concentrations or to facilitate ease of manufacturing. Typically, there are high levels of variation with these features because of the loose tolerances associated with them. The surfaces should be reconstructed, intersected and the features reapplied, using appropriate, consistent, nominal values.

The part geometry is strongly influenced by the manufacturing process. Several parts may have critical cross-sections or contours defined; however, the surface blending between these curves is left to the designer. Consequently, creating wire frame profiles from the point cloud data, which represent the design intent and can be easily modified, is more appropriate than surface patches for engineered parts. Variable draft angles as shown in Figure 3-12 are common in moulding processes. However, if the same processes are not to be used when remanufacturing the part, the essential embodiment level information must be extracted. In essence, the draft angles in this example would be considered noise. Computational tools assist in the geometry healing process, but because the component may be complex, or there may be insufficient or noisy information, a synergistic man-machine approach is necessary.

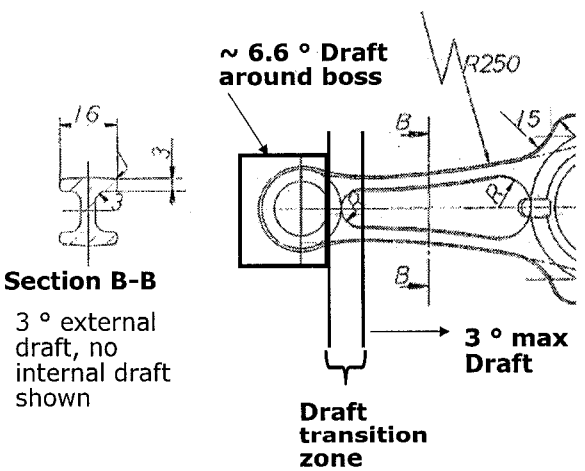

Figure 3-12: Draft for a Die Cast Connecting Rod

In tandem with the geometry healing process, a dimensional healer should be applied. Dimensional healing consists of determining the ideal nominal dimensions by analysing the component, its mating pieces and the functional requirements at the component and feature level. It is important to look for patterns and interrelationships between features. Assessing common features and attributes of the product, along with the standard industrial components (bearings, gaskets, fasteners, and so forth) associated with it and the product's environment (i.e., mating pieces) provides a baseline to establish nominal dimensions. Multiple tools such as least squares method and statistics need to be utilized to gain insight as to the nominal dimensions. However, these tools cannot be applied to the base part alone. They should also be applied to the mating pieces to reduce distortion resulting from the manufacturing process, usage and measurement related noise. The resulting nominal dimensions need to be considered in light of their functional requirements and balanced with common sense. For example, a clearance hole that has a computed diameter of 15.98 mm should be set to 16 mm.

A tolerance is the range of allowable variation to order to maintain a specified dimension when manufacturing a component. Tolerances are critical to both the product and process design. Tighter tolerances optimize product performance, allow assembly of parts in the desired way, and ensure component interchangeability, whereas looser tolerances maximize production yields and lower production costs. ISO 286 implements 20 grades of accuracy to satisfy the requirements of different functional requirements:

- IT01, IT0, IT1, IT2, IT3, IT4, IT5, IT6 - Production of gauges and specialized instruments
- IT 5, IT6, IT7, IT8, IT9, IT10, IT11, IT12 - Precision and general industry
- IT11, IT14, IT15, IT16-Semi finished products
- IT16, IT17, IT18 - Structural engineering

The ISO 286 tolerance grade for the standard manufacturing processes is summarized in Table 3-10. Tolerance healing consists of determining functional tolerances by analysing the component, its mating pieces, the feature's functional requirements and considering realistic geometric and manufacturing constraints. Again, an integrated approach that considers the subcomponents, super structure and the coupled features highlighted in the design structure matrix, is required to establish tolerances of the component of interest with confidence. The

allocation of tolerances is challenging. This is an important step in both the forward engineering and reverse engineering design processes. Minimum cost is a main criterion for specifying dimensional tolerances; hence, knowledge of the employed manufacturing process is required. The mismatch probability methodology proposed by Nassef and ElMaraghy [1997] complements the healing strategies by presenting solutions applicable to the tolerance healing. The geometric tolerance allocation problem is converted from a trial and error based process into a mathematically formulated problem to search for the best solution [Nassef and ElMaraghy, 1997]. Since both the manufacturing processes and the assembly surfaces and features are considered, this tool could be extended to encompass reverse engineering applications.

Table 3-10: Tolerance Grades for Manufacturing Processes

IT Grade	2	3	4	5	6	7	8	9	10	11	12	13	14	15	16
Lapping															
Honing															
Super finishing															
Cylindrical grinding															
Diamond turning															
Plan grinding															
Broaching															
Reaming															
Boring, Turning															
Sawing															
Milling															
Planing, Shaping															
Extruding															
Cold Rolling, Drawing															
Drilling															
Die Casting															
Forging															
Sand Casting															
Hot rolling, Flame cutting															

3.7 TESTING AND VALIDATION

Testing and verification is a critical phase in forward engineering, and is no less so for reverse engineered parts. The verification process presented in this research flows from the logical

domain, then to the virtual and physical domains, and may involve multiple steps in each. In the logical domain, potential design variations and flaws, which could lead to a loss of functionality or failure, are diagnosed. In the virtual domain, simulations using different design alternatives are used to determine the response characteristics; whereas in the physical domain, a component is manufactured to be used for physical testing and validation purposes. A cumulative approach is presented here: a failure analysis is initially performed. Based on the results of this analysis, virtual testing simulations may be recommended. The next level of the testing and verification process is to construct a physical prototype after completing a set of simulations. A physical prototype may not be required for all cases. They are expensive and time consuming to produce; hence, this avenue is recommended only if the component has several high precision features.

There are several methods to determine potential failure modes such as the Failure Modes and Effects Analysis (FMEA) and the Fault Tree analysis. The FMEA is one of the formal techniques used in the product development process to analyse potential product failure, either due to the product design (design FMEA), or due to the chosen manufacturing processes (process FMEA). The purpose of an FMEA is to detect and address weaknesses in the product design. The general FMEA structure is illustrated in Table 3-11.

Table 3-11: Standard FMEA Table

Item	Potential Failure Mode	Potential Failure Effect	S	Class	Potential Failure Causes	O	Current Process Control Prevention	Current Process Control Detection	D	RPN	Re-commended Action	Actions taken
			7			8			9	504		

S - severity
O – occurrence
D – detect
RPN - risk priority number = S*O*D

The generic failure effect is failure to perform the function and the generic cause is variation in the design variables. The explicit failure modes need to be determined. The generic failure modes are (Table 3-12):

(i) Absence of a feature (process dependent);

(ii) Improper design parameter selection (design dependent);

(iii) Geometry variations leading to improper size or physical geometric characteristics (design and process dependent);

(iv) Improper surface characteristics, which includes smoothness, heat and surface treatments (design and process dependent); and

(v) Improper material selection, material composition or structure (design and process dependent).

Table 3-12: Generic Failure Modes, Effects and Causes

Failure Mode	Failure Effect	Failure Cause
Missing	Feature cannot perform function Undesirable behaviour occurs with coupled features	Improper design, tolerance or properties selection (material) Poor process control
Improper design parameter selection		
Improper size		
Improper form		
Improper position		
Improper orientation		
Improper run out		
Improper profile		
Improper surface characteristics		
Improper material selection		
Improper material composition		
Improper material structure		

The Function-failure methodology by Arunajadai et al [2002] enhances the FMEA procedure by implementing an extended standard vocabulary for the description of functions and the failure modes of components. A formal procedure is applied to identify primary and secondary identifiers to aid in selecting the appropriate failure mode and composite function-failure matrix is used to assist with the analysis. This approach complements the function-form analysis utilized in the design recovery framework; however, this work focuses primarily on failure due to wear or deformation and there is no concise means to visualize the results. In general the FMEA process is labour intensive, there are problems with consistency, or the information is too vague to be able to effectively assess the potential failure modes, effects, and causes [Teng et al, 2004], [Arunajadai et al, 2002]. For design recovery, these issues can be overcome by performing a modified version of the FMEA that focuses on the failure modes

in a systematic manner and graphing the results. These results can provide insight into potential subsequent testing in the virtual and physical domains. The modified FMEA focuses specifically on the failure modes. At the design level, there are three main failure modes: improper design parameter selection, improper allowable tolerance variations and improper material selection. When reverse engineering, the key failure mode focuses on the geometric variations. The design parameters and the material properties should be reconstructed with confidence when analysing the component at the different levels of resolution; however, the procedure described here can be extended to encompass design and material failure modes. The relevant data should be contained in the design recovery framework, as tolerances are assigned based on understanding the component functions and the potential manufacturing processes. The tolerance variations may be coupled; therefore, a potential failure may be due to an accumulative effect. Variations with one attribute (i.e. hole size) can amplify or attenuate other variations (i.e. position). This is illustrated in Figure 3-13.

	Size +	Size -	Roundness	Taper	Position	⊥	∠	Depth +	Depth -	Concentric
Size +			+	+	+	+	+			+
Size -			-	-	-	-	-			-
Roundness	Δ	Δ								
Taper	Δ	Δ								
Position	Δ	∇				∇	∇			Δ
⊥	Δ	∇			∇			∇		Δ
∠	Δ	∇			∇			∇		Δ
Depth +						∇	∇			
Depth -										
Concentric	Δ	∇			∇	∇	∇			

+	direct, measureable influence, allows for greater variation
-	direct, measureable influence, allows for less variation
Δ	indirect influence, other variable has positive influence
∇	indirect influence, other variable has negative influence

Figure 3-13: Coupling of Geometric Variations

The geometric sources of variation, which consist of the GD and T callouts, the size, depth and surface characteristics, are considered simultaneously for each feature (Table 3-13) in order to address this issue. Each relevant factor is assigned a weighting factor value, as described in Table 3-14. These factor values are summed. The higher the number the more precise the feature is. As well, the total number of factors is considered. The higher the number of factors, the more difficult it is to manufacture that feature.

Table 3-13: Failure Modes Analysis Table

	Fit		Size		Depth		Form (1 of 4)				Orientation			Location			Profile		Surface				
Feature Name	Description	Standard Table	Size +	Size -	Depth +	Depth -	Roundness	Cylindricity	Straightness	Fatness	Perpendicularity	Parallelism	Angularity	Position	Concentricity	Symmetry	Linear	Surface	Thread form	Finish	Characteristics	No. of Factors	SUM

Table 3-14: Standardized Failure Mode Weights

Factor Value	Description
Blank	Do not need to consider
1	Very weak (low precision, general tolerance)
3	Weak (loose tolerance)
5	Moderate (moderate tolerance)
7	Strong (tight tolerance)
9	Very strong (high precision)

The modified FMEA is performed on the component from the data contained in the design recovery framework using the following steps:

- List the feature names and their descriptions and link the features to a design table if standard design parameters are used.
- For each relevant factor, assign a weight.
    - Sum and enumerate the number of factors.
    - Plot the results in the Failure Mode chart.

- Determine the subsequent testing and validation procedures based on the levels and zones in which the features within the component fall (Figure 3-14).

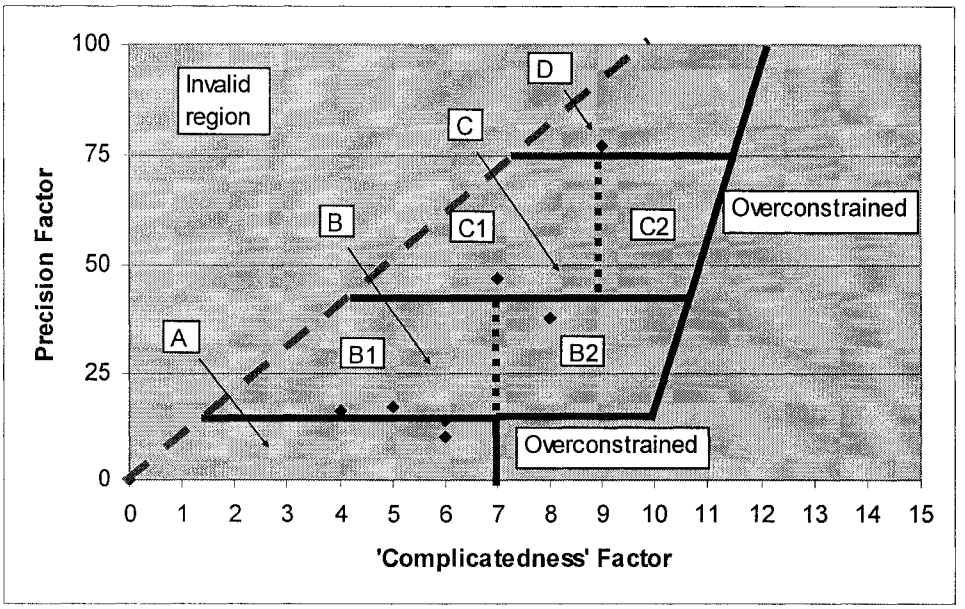

Figure 3-14: Charting the FMEA Results

In the over constrained regions, the designer should look at the number of attributes used to determine the precision factor. There are too many attributes for the precision of the feature. In the labelled regions, the other testing and verification tasks are recommended depending on the number of features within the each region (Table 3-15).

Table 3-15: Chart Regions

Region	Testing and Verification
A	Review form-function relationships to ensure loose tolerances and minimal information is appropriate
B	Review tolerances and perform a detailed tolerance stack up
B1	Higher level of precision required – review potential finishing processes as well as near net shape processes
B2	Lower level of precision required – review processes that can generate a near net shape, review factors to ensure that the number of attributes is appropriate
C	Perform virtual simulation: such as finite element modelling, kinematic analysis, mould flow analysis (structural defects), and so forth.
C1	Higher level of precision required – review potential finishing processes, and process related simulations, benchmark competitive processes; consider a physical prototype
C2	Relatively lower level of precision required – review potential finishing processes, and process related simulations, benchmark competitive processes
D	Construct a physical prototype or prototype sets for physical testing: the manufacturing processes depend on the number and type of features within this zone

A tolerance stack up is performed to ensure that the assembly operations can be performed with confidence. Virtual tools such as finite element modelling (FEM) and kinematics analysis tools can provide perspective into the part's response to different test conditions. If the part is to be cast, mould flow analysis can predict defects that influence the structural integrity of the component. Multiple scenarios can be readily scripted using these simulation tools. Information with respect to the material characteristics, boundary conditions, load characteristics, joint and spatial relationships, and constraints should be contained within the design framework matrices. Competitive benchmarking of process alternatives should be considered for high precision features, and process related simulations might be required to supplement the product simulations.

A physical prototype may be required for physical testing. The nature of an applicable physical prototype depends on the functions, materials and tolerances. Understanding the context of the application assists with decision to fabricate a physical prototype. Rapid prototyping technologies can be used to easily create a physical model with undercuts, overhangs, free form shapes, as well as elementary shapes for physical verification. However, there are limited materials that can be utilized, and RP processes have limited accuracy. For a review of the state of the art options in the area of rapid prototyping, see Levy et al [2003]. If a rapid prototyping is not appropriate, traditional technologies must be used. Again, this is dictated by the level of precision required, and the context of the application.

3.7.1 Summary

Multiple levels of analysis may be required in the verification and testing stage of the design recovery process. A procedure that flows from the logical to the virtual and physical domains is presented here. The design recovery framework contains the design concepts, variables and structural relationships at different levels of granularity that can be used as the basis for an FMEA. However, the traditional approach for an FMEA is time consuming, does not consider multiple sources of variation in an intuitive manner, and does not directly provide any insight as to the next stages of the testing and verification process without the designer performing extensive analysis. A streamlined methodology has been developed that quickly and graphically highlights the characteristics of the features. Subsequent testing and verification

strategies are proposed after all the features are analysed, based on the location of the precision and complicatedness factors on the graph.

3.8 CASE STUDY 1: CYLINDER VALVE COVER

The cylinder valve cover, shown in Figure 3-15 (a), is the first case study used to illustrate the design recovery framework. The cylinder valve cover is a 3D thin walled part. It must provide clearance for the valves (Figure 3-15 (b)) and be contained within the envelope constraints (gas tank, brackets and other shrouding as shown in Figure 3-15 (c)). The external and internal cylinder head profiles should be followed. The cylinder head valve cover base is a sealing surface. The intermediary cork gasket that is placed in between the cylinder head valve cover and the head is not illustrated. There is a lip on the valve cover to avoid sharp edges near the gasket, and the fillet radius could be used as a pry point. The cover must be smooth, wrinkle and crack free, as well as corrosion and crack resistant. During disassembly, it was evident that the cylinder valve cover has undergone distortion through usage.

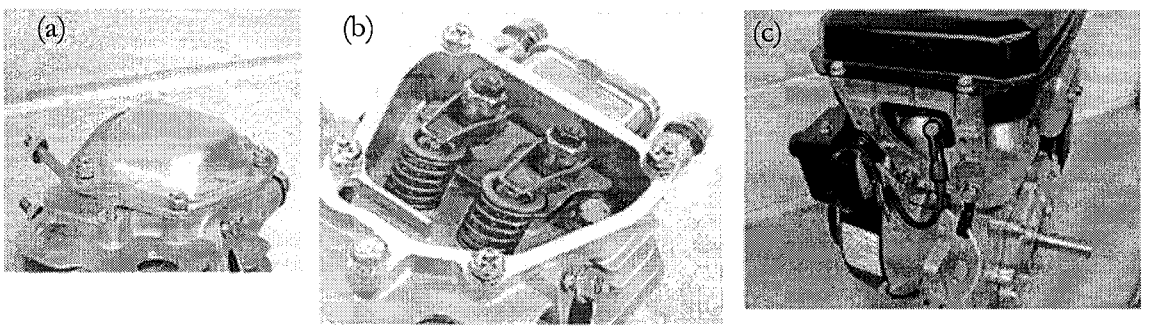

Figure 3-15: (a) The Valve Cover, (b) the Rocker Arm Assembly, (c) the Engine Assembly

Manual measurements were taken using precision micrometers and the top and under sides of the cylinder head valve cover were scanned using a Metris® LC50 laser scanner mounted on DEA CMM. The laser scanner is mounted on a Renishaw® PH10M indexing probe head, which effectively provides a 5 axis optical digitising device. The data was filtered using the Metris® scan curvature filter software. The data analysis was performed on the underside, as there was less surface damage on the part. From a sample of five parts, data was collected with respect to several features, and a statistical analysis was performed to determine the sample means, standard deviations and sampling error. Selected data is employed to illustrate the necessity of considering the super structure and the functional requirements.

Contextually, the cylinder valve cover protects the valve train mechanism from the external environment, and the external environment from the lubrication oil. Hence, the general design concept of enclosing the space using a metal barrier. The engine may need to be rebuilt; therefore, one must be able to assemble and disassemble the components with ease using common commercial fasteners. The functions the cover performs, using the NIST terminology, are:

- Contain – separate
- Couple – join, and
- Support – locate.

The cylinder valve cover contains the valve train, and separates it from the rest of the engine assembly. Four threaded fasteners connect the valve cover to the cylinder head through clearance holes punched in the cover. The valve cover clearance hole positions correspond to the cylinder head tapped hole positions. They also locate the cover around the cylinder head's periphery profile. The internal edge of the sealing surface overlaps the valve train cavity slightly. The low resolution analysis for the component is summarized in Table 3-16 (a).

Table 3-16 (a): Low Resolution Analysis for the Cylinder Valve Cover using the Design Recovery Framework

Component: Cylinder Valve Cover				
	What	**How**	**Where**	**Why**
	Data	Function	Interconnections	Motivation
Contextual	Leak proof barrier	Sealed enclosure encasing the valve train	Air cooled, overhead valve, single cylinder engine	
Conceptual	- Enclosure feature - No oil leakage desired - Easy assembly and disassembly	Metal barrier mounted on the cylinder head	Over the valve train mechanism; On the cylinder head; Within the envelope constraints	
Logical	Contain - separate	Enclosure envelops the valve train, sealing face is mounted on a gasket	See connectivity diagram Figure 3-9 or 3-10	Protects the valve train mechanism and prevents oil leakage onto other engine components
	Couple - join	4 threaded fasteners connect the valve cover to the cylinder head through clearance holes		
	Support - position	Valve cover clearance hole positions = cylinder head tapped hole positions & locate enclosure around the valve train profile periphery		

The material is galvanized steel. This low cost material presents no unusual manufacturing challenges. The galvanizing inhibits corrosion. The cover shape consists of a free form surface blended with a flat sealing and cover surfaces, combined with four stamped, circular holes. The selected datum features are the lip edge -A-, the perpendicular line drawn from the midpoint of the bolt hole centres -B- & -C-, and the sealing surface for datum -D-. This is illustrated in the summary Table 3-16 (b). As the enclosure geometry is composed utilizing a free form surface, the surface's bounding wire frame geometry needs to be constructed from the point cloud data at user defined reference intervals. The designer defines critical cross section positions to be used for the edge curves and intermediate construction geometry. In this example, six different heights are delineated for the reference wire frame creation. For the outer boundary, the point cloud data is used as a profile template. The medium and high resolution analysis for the cylinder valve cover is summarized in Table 3-15 (b).

Table 3-16 (b): Medium and High Resolution Analysis for the Cylinder Valve Cover using the Design Recovery Framework

Component: Cylinder Valve Cover					
	What		How	Where	Why
	Data		Function	Interconnections (Network)	Motivation
Physical	Material	Steel			Cost Manu-facturability
	Envelope	Gas tank, gas tank mounting brackets, cylinder head, valve train		*Cork Gasket* *Mounting Bolts* Cylinder Head	
	Form initial	Thin sheet			
	Form final	3D-2D - free form thin sheet	Stamped		
	Type	Static part			
	Interface with:	Static components			
Detail	Material	Coating: galvanizing			Corrosion resistance
	Stock	1mm sheet			
	Shape	Trimmed planes - flat		z = 0, z = 21 mm	
		Holes - circular		Match cylinder head hole centres	
		Free form surface - use critical cross sections - use the point cloud data as a profile template		6 layers in the top view defined by z = 0, z = 6, z = 12, z = 15, z = 18, z = 21	
	Datum	Lip Edge -A-; Bolt hole centres -B- & -C-; Sealing surface, -D-; Perpendicular line through the midpoint of -B- and -C-, and the part edges		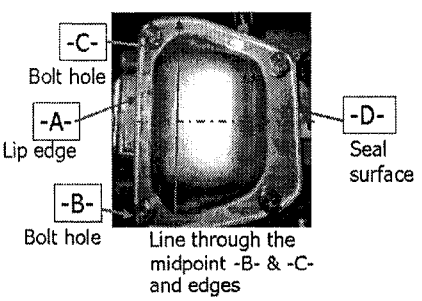	

The design structure matrix is constructed for the cylinder valve cover (Table 3-17). The valve enclosure is influenced by the seating surface and mounting hole positions. The lip height is influenced by the sealing surface; consequently, these features have a dependent relationship.

The seating surface flatness is influenced by the mounting holes (burr, deflection in the region around the hole) and in turn, the mounting hole positions are influenced by the flatness of the sealing surface; hence, these features have a coupled relationship.

Table 3-17: Design Structure Matrix for the Cylinder Valve Cover

	Valve enclosure	Sealing surface	Mounting holes
Valve enclosure		X	X
Sealing surface			X
Mounting holes		X	
Lip		X	

The feature analysis is now presented for the valve enclosure, sealing surface, mounting holes and the lip. The local feature information, connections, relationships and associations are presented in the following tables. Components in italicized text are external components.

Much of information for the valve enclosure and sealing surface feature is a direct subset of the component analysis (Tables 3-18 and 3-19 respectively). However, additional information is included for the geometry construction. The geometry reconstruction instructions are highlighted with bold text in the Physical and Detail 'What' rubrics.

The mounting hole positions must be determined with respect to each other and the reference datum points. Upon measuring the mounting bolthole centre positions for five cylinder valve covers and the accompanying cylinder heads, the results are compared. The valve covers are distorted through usage. The measured flatness is approximately 0.50 mm on average, which in turn influences the centre positions of the holes. The positional differences varied between 0.06 mm to 0.19 mm between the valve cover and the cylinder head (Table 3-20). This example illustrates the importance of extracting and utilizing information from the surrounding environment appropriately. Without gathering data from the cylinder head, incorrect conclusions can be drawn resulting in an imprecise CAD model. The individual feature labels and measurements for the cylinder valve cover are shown in Figure 3-16. The italicized numerals represent the measured values; the plain numerals represent the nominal values. The final positional results are summarized in Figure 3-16 and Table 3-20, and the mounting hole feature summary is presented in Table 3-21.

Table 3-18: Valve Enclosure Summary

Component: Valve Cover – Feature: Valve Enclosure (Product Feature)			
	What	**How**	**Where**
	Data	Function	Interconnections (Network)
Contextual	Leak proof barrier	Cover	Air cooled, overhead valve single cylinder engine
Conceptual	Boundary/enclosure feature	Metal barrier	Enclose the valve train mechanism with cover within the envelop constraints
Logical	Contain - separate	Enclosure envelops the valve train, using the profile of the cylinder head boundary as its periphery	Internal feature to internal feature
Physical	**Free form thin sheet: 1 mm**	Stamped	Sealing Surface
Detail	**Critical cross sections - 6 layers in the top view defined by z = 0, z = 6, z = 12, z = 15, z = 18, z = 21**		Relationships: Profile Top plane – parallel to -D- Associations: None

Table 3-19: Sealing Surface Summary

Component: Valve Cover – Feature: Sealing Surface (Product Feature)			
	What	**How**	**Where**
	Data	Function	Interconnections (Network)
Contextual	Leak proof barrier	Cover	Air cooled, overhead valve single cylinder engine
Conceptual	Boundary/enclosure feature	Metal barrier	Enclose the valve train mechanism with cover within the envelop constraints
Logical	Connect - join Support - position	Face of the joint that connects the valve cover to the cylinder head using 4 threaded fasteners	Internal feature to internal feature Internal feature to external feature
Physical	**Free form thin sheet - flat trimmed plane**	Stamped	Valve Enclosure Lip Mounting Holes *Cork Gasket*
Detail	**User defined: use the point cloud data as a profile template in the top view** **Blend fillet to enclosure: 2.0 mm**		Relationships: Flat Associations: None

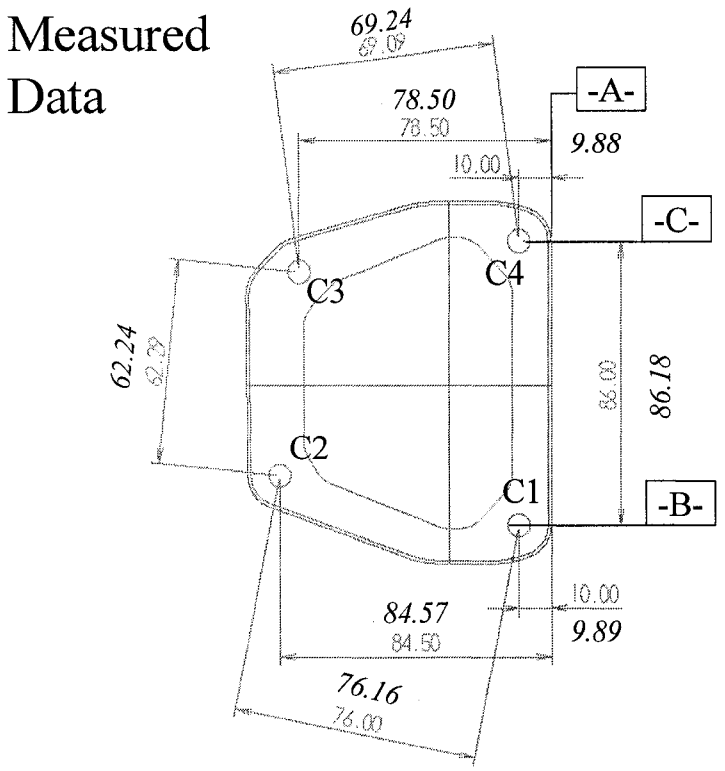

Figure 3-16: Datum Features and Data Values

Table 3-20: Positional Analysis for the Fastener Features

Feature	Valve Cover Sample Mean (mm)	Cylinder Head Sample Mean (mm)	Difference (mm)
X: C1 – C2	74.68	74.55	0.13
X: C3 – C4	68.62	68.56	0.06
Y: C1 - C4	86.18	86.06	0.12
Y: C2 - C3	62.14	61.95	0.19

The lip is a process related feature; as such, the perspectives for this feature are different when compared to the other product related features. If the cylinder valve cover were cast, this feature would not exist. Typically cast or moulded valve covers are much thicker and have no sharp edges. Adding the lip is a safety feature. It protects the cork gasket from a sharp edge and provides a pry point. Due to the distortion, the lip height with respect to the sealing surface varies significantly for the five piece sample (between 4.46 +/- 0.30). The localized lip measurements varied between 4.13 +/- 0.15 mm. The minimum value was 4.00 mm; consequently, the lip height is determined to be this value. The lip is perpendicular to the

periphery, and can be modelled as a ruled surface. The lip feature summary is presented in Table 3-22.

Table 3-21: Mounting Hole Summary

Component: Valve Cover – Feature: Mounting Holes (Assembly Feature)			
	What	**How**	**Where**
	Data	Function	Interconnections (Network)
Contextual	Leak proof barrier	Cover	Air cooled, overhead valve single cylinder engine
Conceptual	Assembly feature	Clearance holes	Mounting point for the valve cover onto the cylinder head
Logical	Couple - join	Connection for joining several components using threaded fasteners	Internal feature to external feature
Physical	**Cylinder**	Punched	Sealing Surface *Bolts* *Cylinder Head*
Detail	**Diameter: 6.98 mm average → use 7.00 mm** **Depth – through hole** **Position – see Figure 3-11 and Table 3-14**		Relationships: True Position -B- & -C- aligned to -A- Associations: Bolt hole periphery pattern: PP1

Table 3-22: Lip Summary

Component: Valve Cover – Feature: Lip (Process Feature)			
	What	**How**	**Where**
	Data	Function	Interconnections (Network)
Contextual	Leak proof barrier	Safety feature	Air cooled, overhead valve single cylinder engine
Conceptual	Safety feature - Protect the valve train mechanism's **seal**	Eliminates sharp edges and provides a pry point	Enclose the valve train mechanism with cover within the envelop constraints → sealing surface
Logical	Channel - guide	Protects the gasket from engaging a sharp edge, and could guide a tool used as a pry	Internal feature to internal feature
Physical	Free form thin sheet - swept/ruled feature following flat trimmed plane periphery	Stamped	Sealing Surface
Detail	Ruled surface using the profile periphery as the reference edge Height: 4.00 mm Average Internal fillet: 1.0 mm		Relationships: Perpendicular to -D- Associations: None

An ideal CAD model is reconstructed from the essential design recovery information contained in the framework, and point cloud data generated from the non-contact scanner. The wire frame geometry constructed from the inner and outer point cloud data at position z=0 is illustrated in Figure 3-17, and the final CAD model is shown in Figure 3-18. The planar surfaces are trimmed to the boundaries defined by the point cloud data. The valve enclosure is a lofted surface constructed from the wire frame geometry created at the various z depths specified in the framework. Constant fillet blending is applied between the gasket sealing surface (2 mm radius) and between the sealing surface and the lip (1 mm radius). Standard engineering design tools are utilized to create the final surface model from the wire frame data.

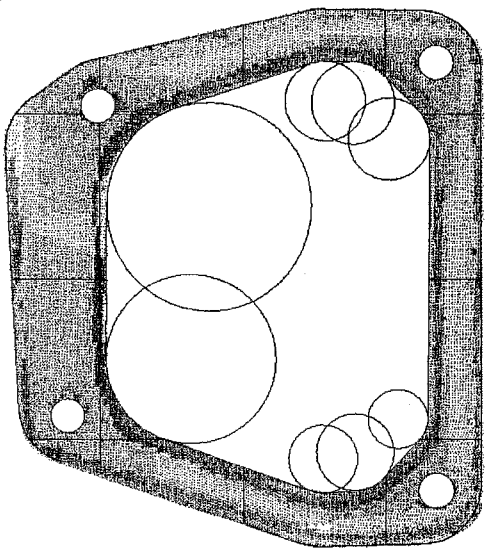

Figure 3-17: Gasket Sealing Surface Creation

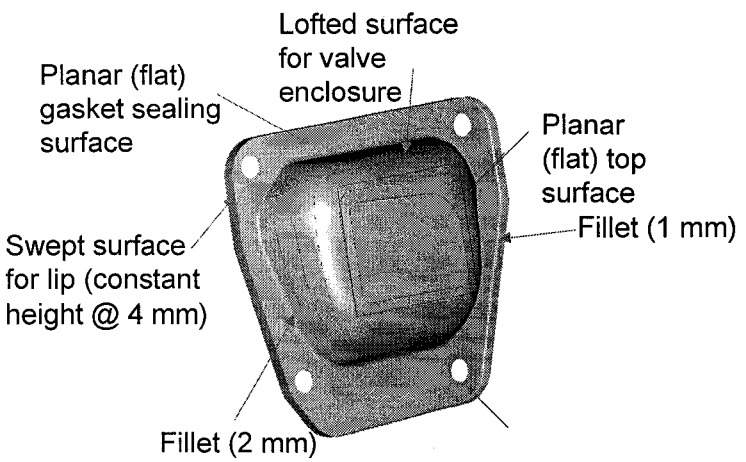

Figure 3-18: Final CAD Model

The feature relationships highlighted in the analysis are presented in Tables 3-23 and 3-24. Tolerance values have been assigned based on assessing the nominal tolerances associated with the stamping process, and considering the observed variations of the mating components.

Table 3-23: GD and T Feature Relationships

	Feature	Primary Datum	Secondary Datum	Tertiary Datum	Tolerance Value	Comment
Cylindricity						
Circularity						
Flatness	Seal Face				0.10	-D-
Straightness						
Parallelism	Valve Enclosure				0.20	-E- (in-process dimensional check)
Perpendicularity	Lip	-D-				
Angularity						
Concentricity						
Symmetry						
True Position	Mounting Holes	-D-	-B-	-C-	0.25	
Line Profile		-D-	-B-	-C-	0.50	Critical cross sections
Surface Profile						
Circular run out						
Total run out						

Table 3-24: Auxiliary Feature Relationships

	Datum	Feature	Comment
Aligned	-A-	Mounting holes C1 & C4	
Along			
Axial			
Radial			
Centred			
Collinear			
Coplanar			
Mirror			
Offset			
Clearance		Mounting holes C1 - C4	1 mm

A partial FMEA table is presented in Table 3-25(a). The main failure modes are interference related, which in turn is caused by geometric variations. Proper tolerance selection is necessary. If special process controls are required, this should be included as a note on the model, such as a "no burr on edges" notation. The FMEA information contained in Table 3-25(a) is of limited use. The modified failure mode analysis is presented in Table 3-25 (b) and charted in Figure 3-19. The feature description and standard table information columns are not shown for clarity. Ancillary functions have been added to the table as an alignment attribute is utilized. Based on the results, the next step is to perform a formal tolerance stack up of the selected tolerances to ensure assemblability.

Table 3-25 (a): Valve Cover FMEA (partial)

Feature Name	Failure Mode	Failure Effect	Failure Cause
Valve enclosure	Out of shape Out of position	Interference with rocker arm assembly	Geometric variation Process problem
Sealing surface	Out of flat	Leak Distort hole positions - cannot assemble	Geometric variation Process problem
Mounting holes	Out of size Out of position	Cannot assemble	Geometric variation Process problem
Galvanized coating	Missing, partial coating	Corrosion	Process problem

Table 3-25 (b): Failure Analysis for the Valve Cover

	Feature (Geometry)								Feature and Pattern Inter-relationships																				Feature				
	Size		Depth		Form (1 of 4)				Orient-ation (max 2)			Location (max 2)			Run-out (1)		Profile (1)		Ancillary (max 2)										Surface				
Feature Name	Size +	Size -	Depth +	Depth -	Roundness	Cylindricity	Straightness	Flatness	Perpendicularity	Parallelism	Angularity	Position	Concentricity	Symmetry	Circular	Total	Linear	Surface	Aligned	Along	Axial	Radial	Centred	Collinear	Coplanar	Mirror	Offset	Thread form	Finish	Characteristics	No. of Factors	SUM
Valve cover mounting holes	3	3	1									5							5												5	17
Valve cover enclosure	1	1	1	1													5												5		6	14.0
Valve cover sealing surface	3	3						5																					5		4	16.0
Valve cover lip	1	1	1	1					3																				3		6	10.0

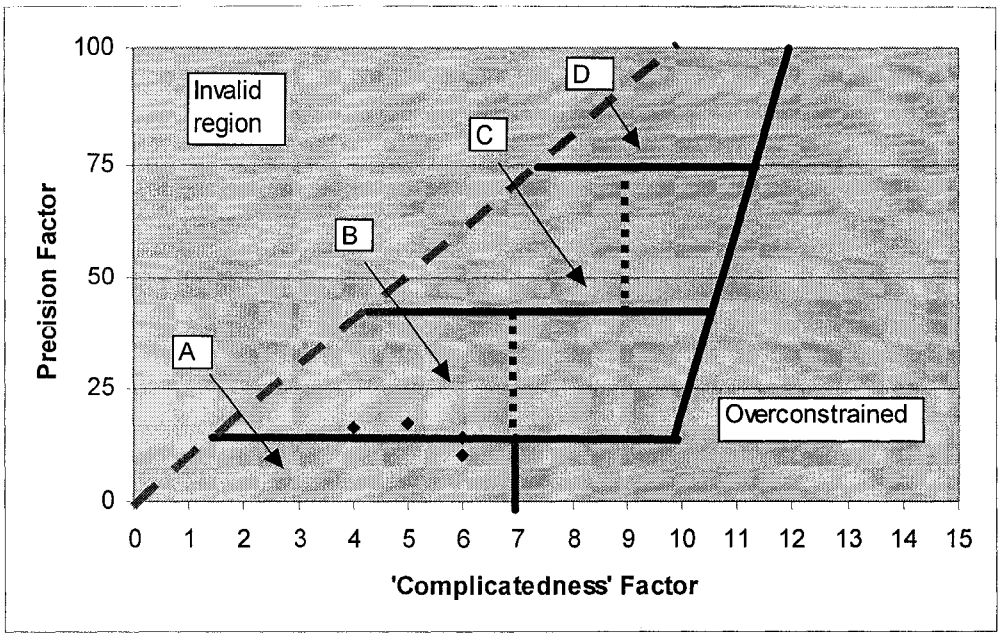

Figure 3-19: The Failure Mode Chart for the Valve Cover

3.9 CASE STUDY 2: POWER STEERING PUMP PULLEY

Cases may exist where the existing part needs to be redesigned in tandem with its interface components based on a new set of operating conditions. The modular structure of the design recovery framework can be extended to capture data from several components, so that key information can be extracted and utilized in the design and manufacture of the replacement component. This case study highlights this situation. The power steering pump pulley for a mid-70's high performance vehicle, shown in Figure 3-20, is significantly damaged, and cannot be purchased from the original manufacturer. This pulley is joined to a dual groove pulley via two locating holes (D1 and D2). The dual groove pulley drives the air conditioning compressor and the water pump. This pulley system is fastened to the dampener using three 3/8-24 inch bolts through holes B1-B3, and is radially located on the crankshaft. (Note: all units are in inches.)

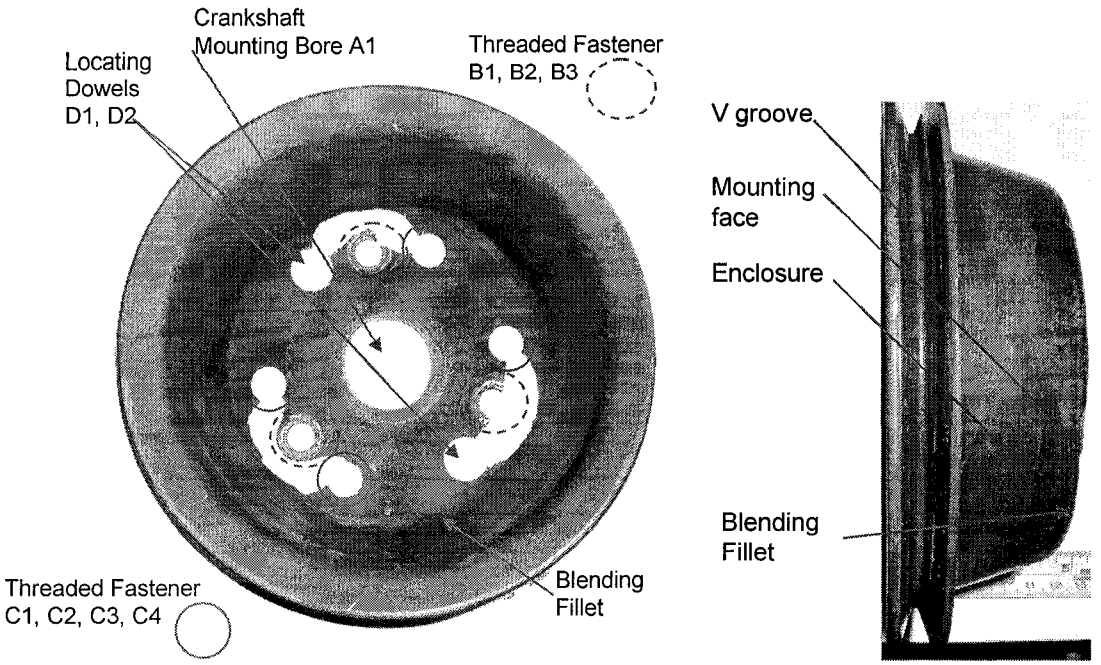

Figure 3-20: Power Steering Pump Pulley

Flexible belt-pulley systems are used to transmit power and motion between widely spaced shafts, or when the driver and driven shafts must rotate at different speeds. This power transmission method is simple, easy to install and maintain and can be used in a variety of applications. The crankshaft is the driver for this system, and the power steering pump is the driven component using a standard V groove and belt configuration. The functions performed by the power steering pump pulley are: channel – transfer, couple – join and support – position. A summary of the low resolution information for the power steering pump is presented in Table 3-26.

Table 3-26: Power Steering Pump Pulley Low Resolution Analysis Summary

Component: Pump Pulley				
	What	**How**	**Where**	**Why**
	Data	Function	Interconnections	Motivation
Contextual	Power & rotary motion transmission	Flexible belt drive - pulley system	Crankshaft to power steering pump	
Conceptual	Link crankshaft output to peripheral engine devices	Standard V groove sheave Power steering pump pulley bolted onto dual sheave pulley System bolted onto dampener & located on the crankshaft output shaft		
Logical	Channel - transfer	Standard belt-groove system used to transfer rotary motion and power from one device to another	See connectivity diagram (Appendix C)	Simple, efficient, cost effective and low maintenance method of transmitting power and motion between widely spaced shafts
	Couple - join	2 threaded fasteners types connect the pulley / system to the dampener		
	Support - position	Dowel holes locate pump pulley onto water pump / A-C pulley Pulley system located onto crankshaft-dampener		

The pulley is made from steel (with an average wall thickness of 0.095 inches) and is painted black. Its envelope is influenced by the water pump / air-conditioning pulley design and the dampener. The pulley has a rotary profile and a flange face. The features consist of three hole patterns, the V groove, the mounting face, the enclosure, and the blending fillet as labelled in Figure 3-20. The V belt has a trapezoidal shape. Upon measuring the maximum width and height, it is determined that the V belt conforms to the standard SAE 440 size. There are standard dimensions that should be used for this belt type [Machinery's Handbook, 2003]. The selected datum features are the crankshaft mounting hole, -A-, the threaded fastener hole -B-, and the mounting face -C-. This high resolution information is summarized in Table 3-27.

Table 3-27: Power Steering Pump Pulley High Resolution Analysis Summary

Component: Pump Pulley					
	What		How	Where	Why
	Data		Function	Interconnections	Motivation
Physical	Material	Steel			Cost Manufacturability
	Envelope	Dampener, Crankshaft mounting bolt & Water pump / A-C pulley			
	Form initial	Cylindrical sheet stock			
	Form final	Rotary design with mounting face 0.095 inch wall thickness	Rolled, drawn & stamped		
	Type	Dynamic component			
	Interface with:	Static: bolts Dynamic: Dampener			
	Feature labels	Crankshaft mounting bore A1 Threaded fasteners B1-B3 Threaded fasteners C1-C4 Locating holes D1, D2 V Groove, V1 Mounting Face, Enclosure, and blending Fillet		Crankshaft mounting bolt - dampener Water pump / A-C pulley *SAE standard V belt - size 440* *3/8 - 24 inch bolts &* *0.675 inch* diameter washers	
Detail	Shape	Sheave groove		**SAE standard pulley dimensions for 440 V belt**	Transmit power and motion
		3 hole patterns: B_C1, C_C2, D_C2		See detailed feature information	Locate and assemble pulley
		Rotary profile		Unroll methodology Urbanic et al [2006] & extract from front view	Contain pulley in envelope and support V groove
	Datum	Shaft mounting hole centre -A- Bolt hole centre -B- Planar face -C- - as labelled		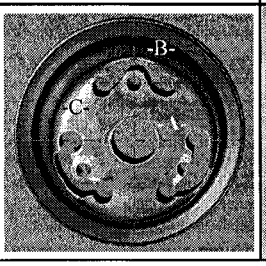	

This analysis is extended for each of the identified features. The feature functions, attributes, and pattern information is summarized in Appendix C for this part. This includes notes on the damage, which appears to have propagated from the blending fillet between the mounting face

and the enclosure. This feature must be included in the analysis, as this failure mode should be dealt with for the redesigned component. Nominal dimensions are generated by measuring the pulley, its interfacing components and by using the standard design parameters for an SAE 440 size belt. A larger corner radius (0.15 inches as opposed to 0.063 [1/16] inches) between the mounting face and enclosure is used to reduce stress concentrations at this edge. There is still clearance for the washers (0.675 in diameter) and a socket wrench using this fillet radius. The CAD model for the power steering pump pulley is illustrated in Figure 3-21.

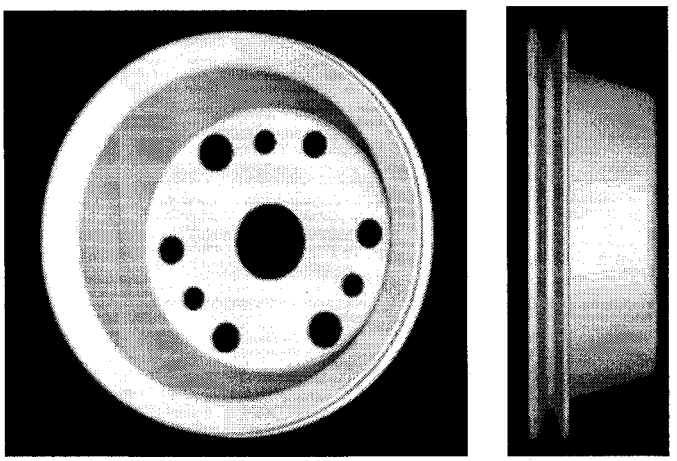

Figure 3-21: CAD Model of Reconstructed Pulley

However, further design is required to optimize the pulley system for this application – there is no air conditioning in this vehicle, and there is no apparent use for the bolt holes C1 – C4. It is speculated that these pulleys were used on multiple engine families. Based on this, it was determined to redesign and manufacture a pulley system appropriate for this vehicle using an alternate material and manufacturing processes. The modular nature of the design recovery framework allows the inclusion of ancillary components with minimal adjustment. The low resolution information should remain the essentially the same, as the context should be consistent within the product architecture; however, some modification to the functional requirements may occur. The high resolution information is collected for all related components (water pump/air conditioning pulley and dampener), and the relevant system information, which forms the basis for the final design, is extracted for the new component. In this example the -C- datum is adjusted to be the system mounting face, but datum features -A- and -B- remain consistent. Information with respect to the water pump pulley groove V2 and the mounting hole A1 must be added. The cross section of the water pump V belt is identical

to the power steering pump; hence, both grooves must conform to a standard SAE 440 type. Information with respect to the C1-C4 bolt holes and the locating features D1 and D2 on the respective pulleys is eliminated as these features serve no function. The enclosure is of no concern, but an appropriate body to support the grooves must be developed, along with an applicable material. The new part is machined (mill, drill, and turn) as opposed to utilizing deformation processes. The bolded items in Table 3-28 reflect the component level changes.

Table 3-28: Pulley System High Resolution Analysis Summary

<table>
<tr><th colspan="5">Component: Pump Pulley System</th></tr>
<tr><th></th><th colspan="2">What</th><th>How</th><th>Where</th><th>Why</th></tr>
<tr><td></td><td colspan="2">Data</td><td>Function</td><td>Interconnections</td><td>Motivation</td></tr>
<tr><td rowspan="8">Physical</td><td>Material</td><td>Steel or Alternative</td><td rowspan="4"></td><td rowspan="2"></td><td>Cost
Manufacturability</td></tr>
<tr><td>Envelope</td><td>Crankshaft mounting bolt & Dampener</td><td rowspan="6"></td></tr>
<tr><td>Form initial</td><td>Cylindrical bar stock</td></tr>
<tr><td>Form final</td><td>Rotary design with mounting face</td><td>Machined (mill, drill, and turn)</td><td rowspan="2"></td></tr>
<tr><td>Type</td><td>Dynamic component</td><td></td></tr>
<tr><td>Interface with:</td><td>Static: Bolts
Dynamic: Dampener</td><td></td><td></td></tr>
<tr><td>Feature labels</td><td>Crankshaft mounting bore A1
Threaded fasteners B1-B3
V Groove V1 & V2
Body</td><td></td><td>Crankshaft mounting bolt - dampener
SAE standard V belt - size 440
3/8 - 24 inch bolts & 0.675 inch dia. washers</td></tr>
<tr><td rowspan="4">Detail</td><td rowspan="3">Shape</td><td>Sheave groove (2)</td><td rowspan="4"></td><td>SAE standard pulley: 440 V belt</td><td>Transmit power and motion</td></tr>
<tr><td>1 hole pattern: B_C1</td><td>See detailed information</td><td>Assemble pulley</td></tr>
<tr><td>Rotary profile</td><td>Develop</td><td>Support V grooves</td></tr>
<tr><td>Datum</td><td>Shaft mounting hole centre -A-
Bolt hole centre -B-
Planar face -C-
- as labelled</td><td colspan="2"> 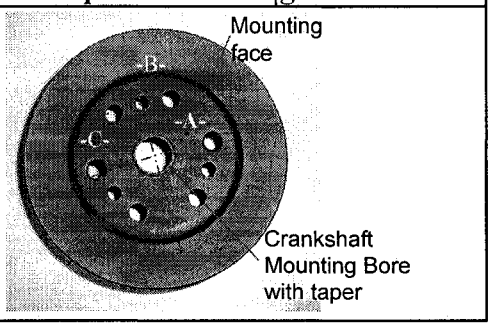
</td></tr>
</table>

Aluminum is chosen as the material due to its weight, machinability and corrosion resistance. All wall thicknesses are increased by at least a factor of 3.0, due to the strength and fatigue characteristics of alumimum as compared to steel. The mounting face blending fillet and the face thickness is increased by a factor of 4.0 to prevent cracking and damage in the area around the fasteners, and the features used to drive the air-conditioning compressor are eliminated. The fillet size is constrained by the diameter of the washers (0.675 inches). Chamfers have been added to the fastening clearance holes. A short (1/4 inch) internal cylindrical feature is added at the lip for locating purposes. The final CAD design and machined part is illustrated in Figure 3-22. The critical tolerances for the features are presented in Tables 3-29 and 3-30.

Table 3-29: Pulley GD and T Data

	Feature	Primary Datum	Secondary Datum	Tertiary Datum	Tolerance Value	Comment
Flatness	Mounting faces				0.010	Flat, smooth surface
Angularity	Mounting holes	-A-	-B-	-C-	0.015	
Angularity	Grooves	-A-	-B-	-C-	0.010	Per side of groove
Line Profile	General body	-A-	-B-	-C-	0.030	Profile
Total run out	Grooves	-A-	-B-	-C-	0.020	Use 0.3750 ball per SAE guidelines

Table 3-30: Pulley Ancillary Geometric Data

	Datum	Feature	Comment
Location			
Radial	-A-	Mounting holes B1-B3	120° apart
Centred	-A-	Locating hole	
Fit			
Clearance		Mounting holes	1/32 inch
Clearance		Crankshaft	1/8 inch
Clearance		Dampener	1/32 inch

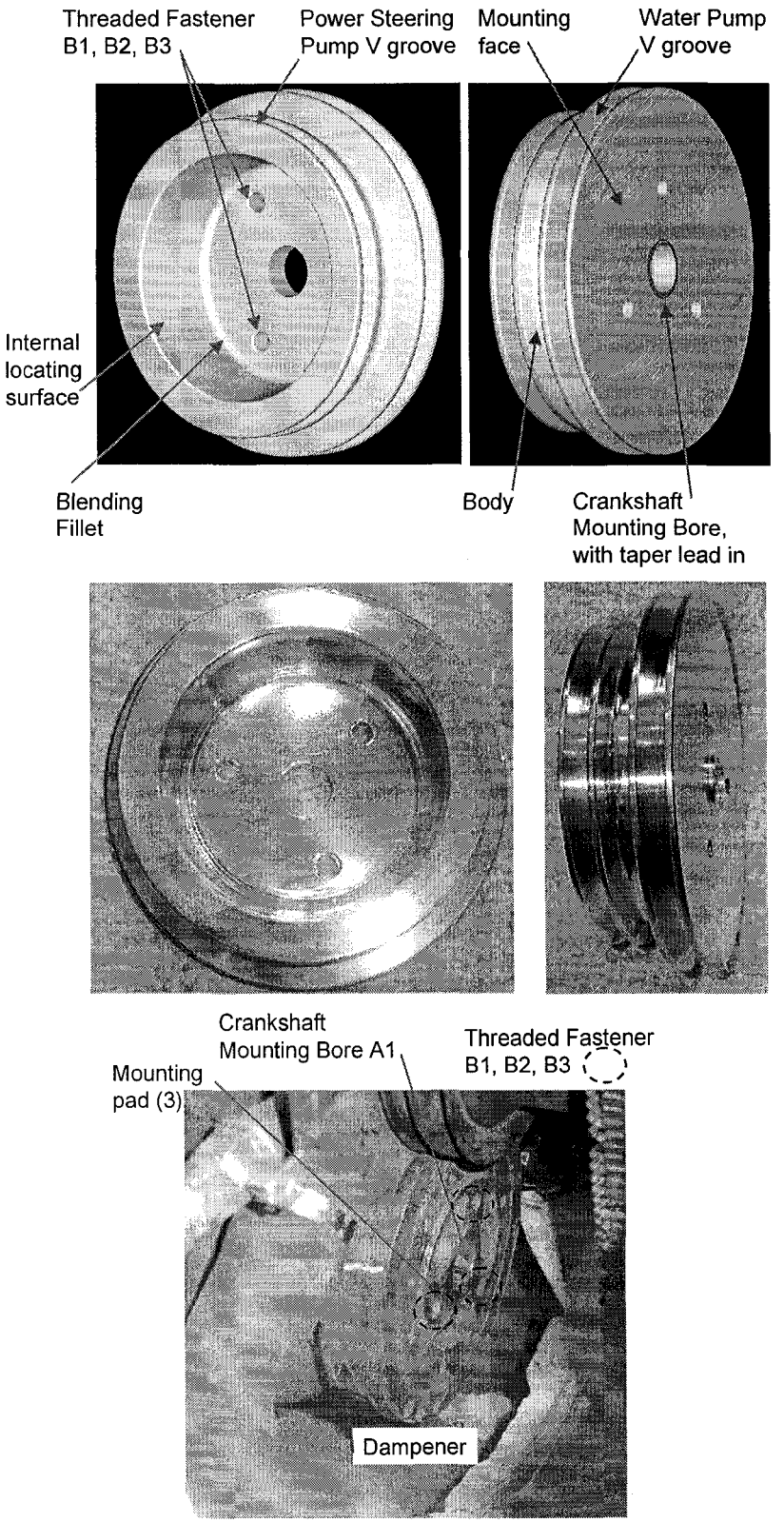

Figure 3-22: New Pulley to Drive the Water Pump and Power Steering Pump – CAD model and machined part, and Interfacing Dampener

3.10 SUMMARY

For effective design recovery of an engineered component, the form, functions and the features must be reconstructed to fit within the product architecture. A collaborative effort is required to effectively recover a design because of the coupled nature of the component structure, features, material, work envelope, operating conditions and interface components. Information from several perspectives and sources must be merged in order to extract the relevant data. Consequently, a framework was developed to drive collaboration across the different design domains in order to improve the design reconstruction process. A modular, structured, multi-perspective approach is essential as knowledge from many disciplines may be required to encompass all of the relevant aspects. For effective design recovery, there must be data sharing along the design recovery chain. The Zachman Framework has been selected as a basis for a design recovery framework, as the perspectives and classifications within the Zachman framework can be utilized with minimal adaptation. The design recovery framework structure is a sub-set of the basic Zachman framework, but the conventions that were developed in this research focus on the reverse engineering process. By analysing the component and features at difference resolutions, and documenting the results at the various perspectives, the designer(s) creating the final model has a comprehensive representation of the component and its features. This approach for recovery of the functional aspects of a design complement the product benchmarking methodology developed by Otto and Wood [1996]. An ideal CAD model should be generated from the point cloud data (and other supplementary data) using the information presented in the design recovery framework as the design reference. The critical form recovery specifications are captured in the framework; therefore, independent of the designer, the characteristics of the component and its features should be captured in a consistent manner when constructing the final CAD model. There may be minor variations with the transition geometry or other non-critical entities, but the core design aspects should be constant. Understanding the design based on the various perspectives allows the designer(s) to modify the structure, materials, or manufacturing processes without compromising the basic integrity of the component. A modified FMEA procedure is introduced to diagnose the recovered design, and to provide insight into suitable supplementary testing and verification procedures.

A cylinder valve cover and a pulley set are used to illustrate the design recovery framework. Although these are relatively simple parts, extensive analysis is required in order to develop an engineering model in which one has confidence, as damage and distortion altered the characteristics of several features. By analysing the functional requirements and identifying the ideal geometric conditions, the influence of the observed noise is reduced. Understanding the environment, the components within the system, along with the nominal tolerances of which the manufacturing processes are capable [Schey, 1987], [Dixon and Poli, 1995], [Auto/Steel Partnership – Anonymous, 2000] is essential to generate relevant dimensions and tolerances and to infer the original needs. The component reference information (datum features and critical cross sections) should be integrated into any subsequent manufacturing and inspection processes. The design recovery framework provides a road map in order to accomplish this.

When reverse engineering a component, conditions may exist where the design needs to be modified before the component can be remanufactured. The pulley set illustrates this scenario, as it is redesigned for the present operating conditions and available manufacturing processes. The overall system is improved for the pulley set: the critical groove and mounting features are retained, but the failure mode has been addressed and ancillary features are eliminated. The design recovery framework allows for information to be cross-referenced between components in a structured manner. The relevant information can then be extracted and utilized in the updated design.

A formal ontology and a spreadsheet application (Excel®) have been developed using the design recovery framework described in this research as the foundation. This is contained in Appendix C. To complement the design recovery framework, a set of algorithms has been developed to construct the critical section wire frame geometry directly from the point cloud data. This is described in the next chapter.

Chapter 4

CURVE DETECTION AND CAPTURING GEOMETRY RELATED DESIGN INTENT

4 SHAPE AND GEOMETRY RECONSTRUCTION

4.1 INTRODUCTION

Form recovery is a critical element of the design recovery process. With the contemporary form recovery reverse engineering techniques, the point cloud data is transformed directly into 'mathematically exact' surface geometry. Improvements to the physical modelling approach are necessary as the resulting geometry may not reflect the original design intent, or may not be ideal for subsequent product modifications or remanufacture. The methodology presented here mimics the forward design process. Typically, there are three geometric levels within a design: (i) the 2D curve primitives, (ii) the 3D features constructed from the curve primitives, and (iii) the aggregates of features, which are placed in a pattern or have geometric relationships amongst them. When the original component was designed, the designer created basic wire frame geometry using line and arc segments on a reference plane. The majority of engineering features can be related to a minimal amount of 2D geometry in a specific spatial orientation. A surface or solid model can then be constructed from the wire frame boundary curves.

The necessary design recovery information regarding the point cloud data is contained in the framework. This information is used to select the points (in a particular orientation) that should be converted into the line and arc curve primitives. Once the points are converted into curve primitives, adjustments are made to capture the design intent. Other researchers create B-spline contour segments from layer measurement data (CT scans) to serve as the basis of their reverse engineered surface model [Liwei and Minghui, 2004], [Liu and Ma, 2001], but a fitted spline curve contains no relevant information other than G^0 and G^1 continuity where:

- G^0 continuity corresponds to end point continuity, and

- G^1 continuity corresponds to tangent continuity.

Curve fitting may be performed on partial arcs and small line segments. This can be done using several techniques. However, presence of noise from several sources will influence both the analysis techniques and the final results. Point to point analysis generates misleading results; consequently, a multi-step process is required to go from the point cloud data to the final curve entities. The points are sorted, and placed in an array in an orderly manner using a nearest point algorithm. Noisy points are adjusted by projecting them onto a line or arc, using the 'in-line' points as a reference. The points are then spaced equidistantly along a curve created by point-to-point line segments or 'polylines'. The final point data modification step is applied on clusters of points. The perimeter to chord ratio is calculated for a fixed number of points. Based on this ratio value, the number of points on the polyline curve segment is adjusted. This completes the pre-processing phase.

From this modified point set, the inflection points between curve entities are detected, and the curve entities generated. The curves may not have continuity. An intelligent bounds checker is applied to systematically adjust the curve primitives such that they have G^0 and/or G^1 continuity. The bounds checker is not limited to ensuring continuity; it also checks for design intent with respect to form. A set of rules is applied to extract the relevant geometric structure. The curve primitives may represent a common shape and the planar slice may capture a set of features. Common feature shapes and patterns are detected from the closed curve geometry.

Although the point cloud data is transformed into basic curve primitives and common features and patterns are identified, the resulting CAD geometry may not reflect the original design intent for all situations. However, using the methodology presented in the next sections, the reverse engineered geometry is constructed in a form that allows the designer to easily adjust the relevant particulars.

The right hand coordinate system is used for all the algorithms. For the world coordinates, the following convention is used:

- Plan or top view consists of the x and y axes
- Elevation view consists of the x and z axes

- Side view consists of the y and z axes.

Standard x and y axis notation is used to describe any two dimensional geometry. The appropriate substitutions must be made for each view.

4.2 POINT SELECTION AND PRE-PROCESSING THE DATA POINTS

For a given planar slice, there is an associated layer thickness tolerance, *l_tol*, as there is no guarantee that there will be a sufficient number of points directly on the slice plane. The points lying within the tolerance band are projected onto the slice plane for the subsequent analysis. From this set of unordered points, the edge boundary points must be determined. The boundary evaluator algorithm detects the edges of the boundaries for each layer using modified ray tracing techniques. There are three cases to consider: (i) layers which consist of the dense point cloud, with or without feature related spaces; (ii) layers which have a scattering of points along an edge, and (iii) layers with both a surface and an edge (Figure 4-1).

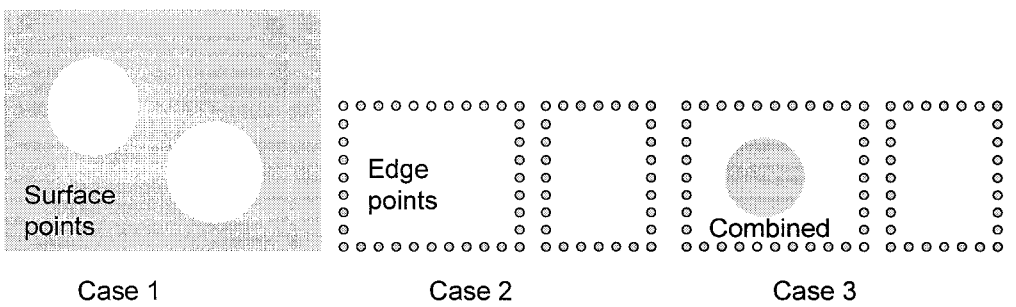

Figure 4-1: Point Distribution Types on the Layers

To initiate the sorting process, the points are sorted in y, and then x. Scanning from left to right, a boundary edge will occur when there is a positive change in y coordinate values for a large negative change in x coordinate values, as shown in Figure 4-2. There is a gap in the points representing a feature when there is no (or a minimal) change in the y coordinate for a large change in the x coordinate.

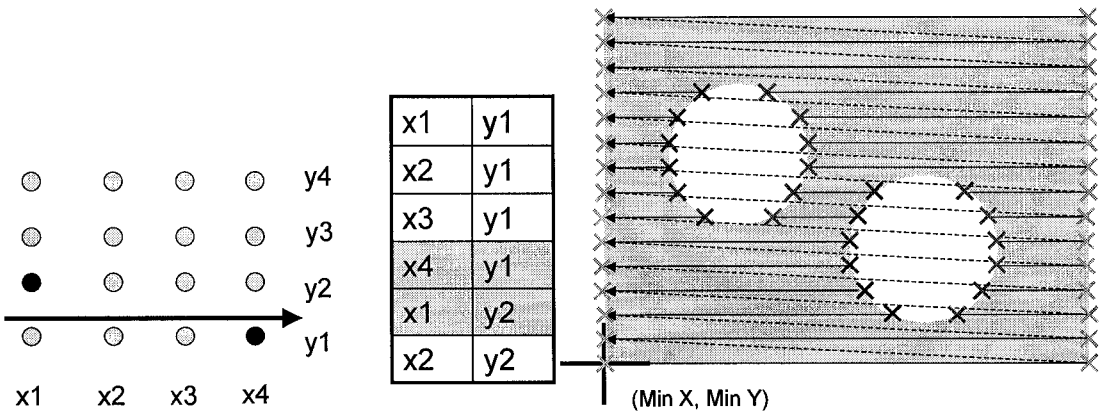

Figure 4-2: Boundary Edge Detection with Sorted Points

The scan line is incremented in the y direction until the maximum y value is reached. In the example shown in Figure 4-2, there are only two points on the top and bottom edges, and the hole geometry is only partially captured. In order to collect points to ensure a complete representation of any feature, the scanning and boundary identification process is repeated at specific x intervals to complement the data collected at y intervals. Several practical considerations must be addressed: (i) the points are not on an even grid; (ii) the scan line positions will not have matching x or y coordinate values; and (iii) if the boundary edge is on a sharp corner, the data points are scattered. Additionally, if the data is pre-filtered and there is a surface combined with features, the points are unevenly spaced on the surface. This makes it difficult to determine which points lay on feature boundaries. Based on this, features smaller than maximum filtered point distance may not be detected properly. A filtered point cloud sample is shown in Figure 4-3.

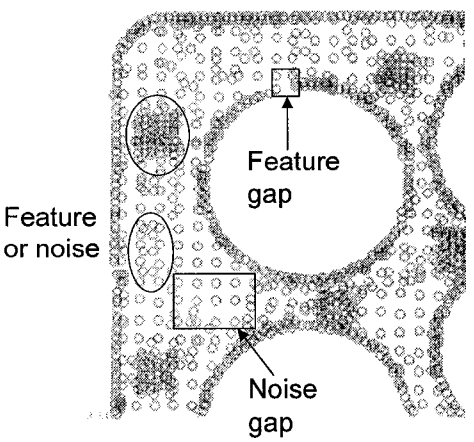

Figure 4-3: Identifying Features from Noise Challenges

Boundary Point Algorithm

(For a selected set of points at z height ± tolerance)

- Get array of points – fix z
- Create array of integer values for x and y coordinates
- If metric, round coordinate values to nearest integer
- Else inch, multiply by 100 and round coordinate values to nearest integer
- Sort by y integer values, then by x integer values
- Scan for transition large negative x transition for positive y transition
    - If only one set of points per scan line is desired, ignore duplicates
- Set valid boundary point flag on appropriate points
- Scan for transition positive x transition (greater than a defined constant) for no y transition
    - If only one set of points per scan line is desired, ignore duplicates
- Set valid boundary point flag on appropriate points
- Sort by x integer values, then by y integer values & repeat process
- Extract all points with a valid boundary point flag
- Delete all duplicate points

A 'nearest point' algorithm is used to sort the points and identify the curve. Starting from the minimum x coordinate the closest point is found. This point is put into a new array and marked such that it is not included in subsequent checks. This nearest point is now set as the reference point, and the process is repeated until all points in the original array are marked selected. If the distance between two points is greater than the 1.5 * the scan line increment value, then the point belongs on a new curve. If the new curve has less than four points, the points are assumed to be noise and discarded. To test for whether the curve is an internal or external curve, the bounding rectangle coordinates, defined by the (*min* x, y), (*min* y, x), (*max* x, y), and (*max* y, x) points are compared. If the bounding rectangle coordinates for a curve are contained within an external curve, it is an internal curve. If the curve is contained within an internal curve, it is a sub-external curve and so forth.

Once the boundary points are identified, the boundary curves that these points lie upon must be labelled appropriately. The curves' labels consist of the boundary type and a unique number. As illustrated in Figure 4-4, there are four boundary types: external (E), internal (I), sub-external (ES), and sub-internal (IS). No distinction is made beyond one nesting level.

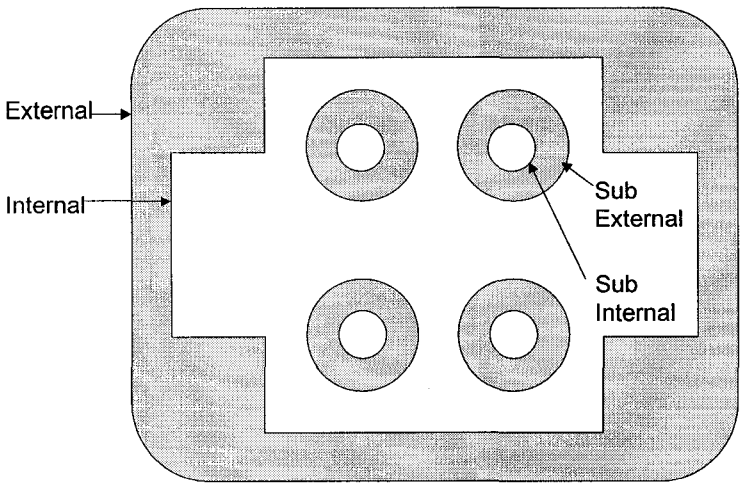

Figure 4-4: Boundary Labels

Nearest Point Algorithm

- Get array of points
- Find the nearest point by calculating the distance between points
- Put into new array
  - Give selected point with a curve id
  - Mark selected point so it is not rechecked
- Increment to next point, test and iterate
- If the distance between points is greater than 1.5 times the increment distance, set new curve id
- If there are less than four points for a curve, remove points from the array
- Find the bounding rectangle defined by (*min x, y*), (*min y, x*), (*max x, y*), (*max y, x*) for each curve
- For curves 1 to I
  - If bounding rectangle coordinates for curve *i* are inside *i-1,* AND curve *i-1* is an external curve, then curve *i* is an internal curve
  - If bounding rectangle coordinates for curve *i* are inside *i-1,* AND curve *i-1* is an internal curve, then curve *i* is a sub-external curve
  - If bounding rectangle coordinates for curve *i* are inside *i-1,* AND curve *i-1* is a sub-external curve, then curve *i* is a sub-internal curve
  - Else curve *i* is an external curve

4.3 POINT MODIFICATIONS

To reduce the influence of noise, a variation of interpolation techniques is used to shift noisy points onto the boundary. The angles $v_0v_1v_2$ and $v_1v_0v_2$ are calculated between three points, *v0*, *v1* and *v2* using the cross product ($v_{01} \times v_{12}$, $v_{10} \times v_{12}$). If the absolute value of the v_0 v_1 v_2 angle is less than the critical angle (175.5°), a flag is set. The point may contain noise, or the points could represent an arc curve. The angles between *v0*, *v1* and *v3* are calculated. If the $v_1v_0v_3$ angle is less than the previous angle, the point is assumed to contain noise, and is

projected onto a line created from *v0* and *v3* or an arc created from *v0*, *v1* and *v3*. The linear example is illustrated in Figure 4-5.

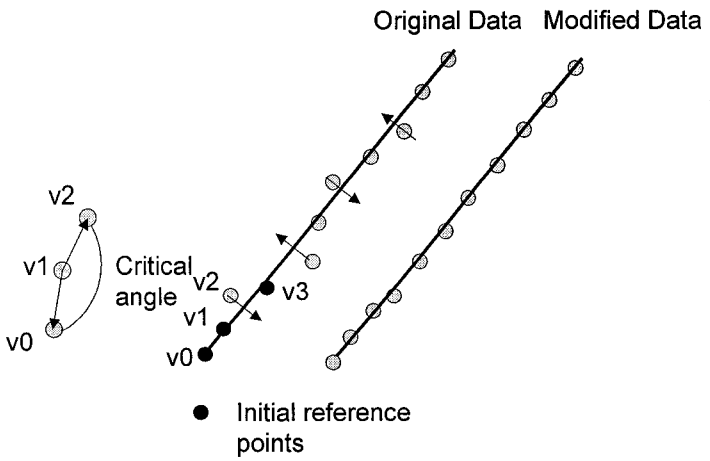

Figure 4-5: Adjsuting Noisy Points

A test for linear and arc geometry must be conducted by assessing the angle generated from *v0*, *v1* and *v3*. If the calculated absolute angle is approximately 180° (tolerance +0, -0.50°), the geometry is assumed to lie on a line. If the linear projection method is used for all the data, the points representing an arc are linearised if the points are widely spread; therefore, if the angle is less than 175.5°, a circumcircle is created from points *v0*, *v1* and *v3*, and *v2* is adjusted if necessary. All boundary points are tested and adjusted as appropriate.

Project Point Algorithm

- Get array of points
- For i +2 to array size
- Calculate angle *j* from points *v0, v1, v2*
- If angle 180°-*j* is less than critical value (175.5°), set transition flag
- Increment to next point and calculate *v0, v1, v3*
- If angle *j* is less than angle *j-1* AND set transition flag = TRUE
  - Project point onto appropriate entity (line or arc)
  - Set transition flag = FALSE
- Else Set transition flag = FALSE (may be a curved entity)
- Increment to the next point

A 'parse polyline' algorithm is used to space the points at predefined intervals. The perimeter is calculated for a set of points, and a travel distance (distance between adjacent points) is generated based on the number of desired points within the limits. New points are placed

within the line segments at the appropriate travel distances. The total travel distance remains constant. This is illustrated in Figure 4-6.

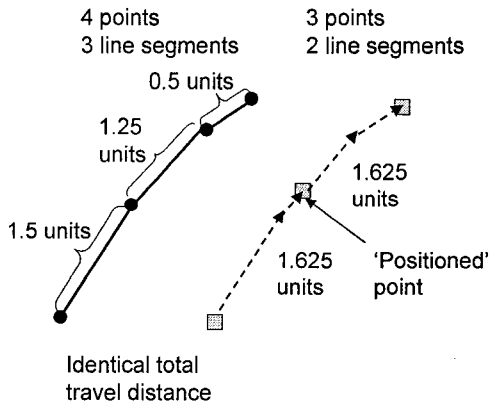

Figure 4-6: Parse Polyline Example

Parse Polyline Algorithm

- Get array of original points and the desired number of points
- Calculate perimeter from the point set
- Calculate travel distance (perimeter/ desired number of points)
- Find the distance between points *i* and *i-1*
- If the distance is less than the travel distance,
  - Accumulate the point to point distance
  - Increment *i* (to the next point pair) until the accumulated distance is greater than the travel distance
- When the accumulated distance is greater than the travel distance, determine the coordinate value for the new points position on the appropriate line segment
- Reset the accumulated distance and continue distance checking from the new point position
- Increment until an array of new points has been generated

After the data is sorted and the noisy points adjusted, the boundary points are spaced at uneven intervals, and there is no relationship between the spacing and the geometry. Initially, the 'parse polyline' algorithm is used to space the boundary points at an even interval. Then the parse polyline algorithm is executed for clusters of points. The angle *CAB* is generated from the perimeter, *s*, to chord, *c*, relationship for the point cluster (equations 4.1- 4.5, Figure 4-7). If the angle is small, it is assumed that the points lie on a line, and minimal amount of information is required to generate the geometry (i.e. two points define a line); whereas, if the angle is large, a curvilinear feature exists. More data is required to reconstruct the geometry.

The distribution of points based on the angle CAB is for a cluster of 30 points is provided in Table 4-1. A sample part is illustrated in Figure 4-8.

$$Perimeter\ s = \sum_{i=2}^{I} \sqrt{(x_i - x_{i-1})^2 + (y_i - y_{i-1})^2} \tag{4.1}$$

$$c = \sqrt{(x_I - x_1)^2 + (y_I - y_1)^2} \tag{4.2}$$

where x is the x coordinate value

y i is the y coordinate value

I is the total number of points

$$s \approx \sqrt{c^2 + \frac{16}{3}h^2} \text{ [Weisstein, 2003]} \tag{4.3}$$

$$\therefore h \approx \sqrt{(s^2 - c^2)\frac{3}{16}} \tag{4.4}$$

where h is the height of the arced portion illustrated in Figure 4-7.

$$angle\ BAC = \arctan(\frac{h}{c * 2}) \tag{4.5}$$

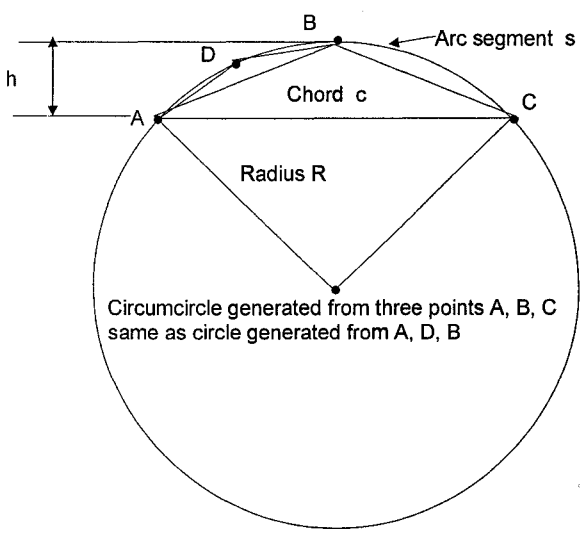

Figure 4-7: Circle Relationships

Table 4-1: Point to Angle Relationships

No. of Points	Angle *CAB*
4	< ½°
11	½° — 3°
16	3° – 10°
18	10° – 15°
21	15° – 22.5°
26	22.5° – 40°
29	>40°

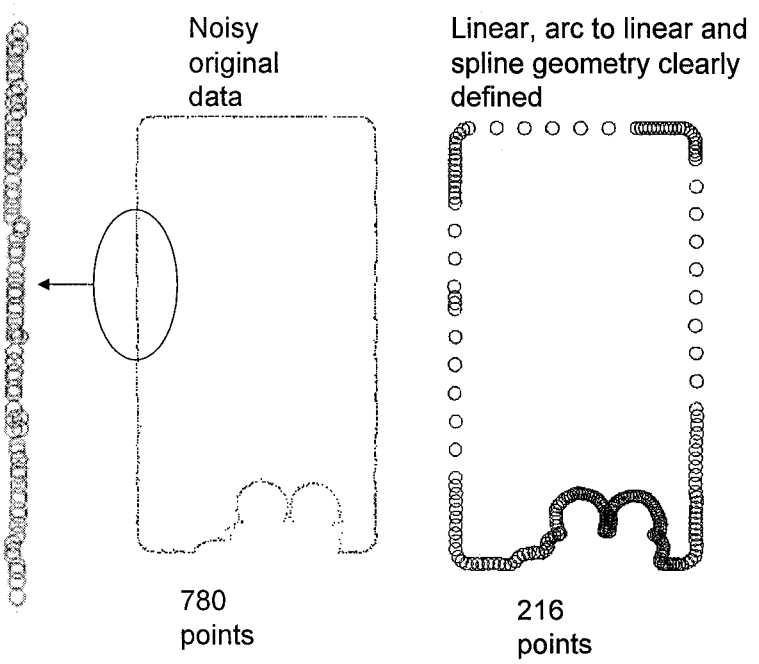

Figure 4-8: Dynamic 'Filtering' Algorithm Used to Generate Points

From this modified set of points, the inflection points are determined by analysing the angle relationships between points, and the curve primitives created. Feature transition geometry, which consists of short lines or small arcs, such as a corner or tangent arc blending (Figure 4-9) must also be detected and accommodated. There are five cases to be considered:

1) Line to line transitions

2) Line to arc transitions

3) Arc to line transitions

4) Arc to arc transitions – same direction (Case 1 in Figure 4-9)

5) Arc to arc transitions – opposite direction (Case 2 in Figure 4-9).

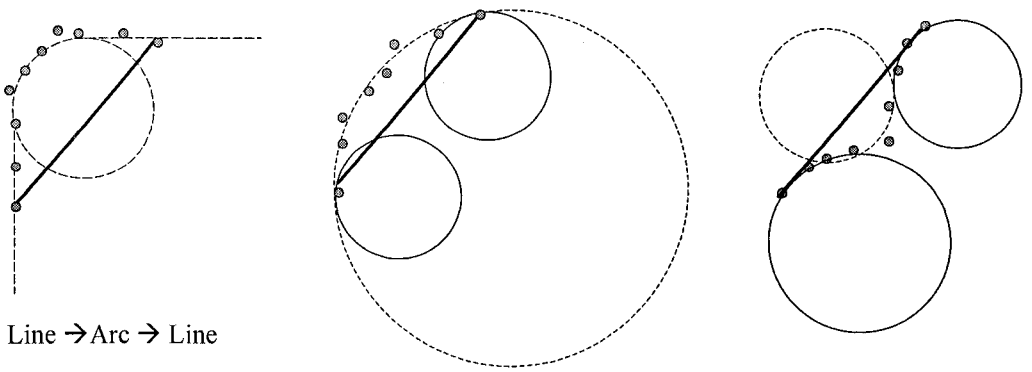

Figure 4-9: Feature Transition Geometry Examples

Point to point geometric analysis is performed on the modified point set to determine the inflection points. To detect line to line and line to arc transitions, the relative angle between points is compared. If the relative angle starts to increase, then an inflection point exists. To detect arc to line and arc to arc transitions, a combination of geometric and statistical methods is utilized. To detect whether point *i* belongs to the arc of interest, an arc is created from points 1 to *i-1*. Point *i* is projected onto the constructed arc. If the projected distance is within the tolerance band, then that point belongs to the arc, else an inflection point exists. Point sets that are neither linear nor circular are stored as splines. An example is illustrated in Figure 4-10, where arcs have been fitted to a French curve.

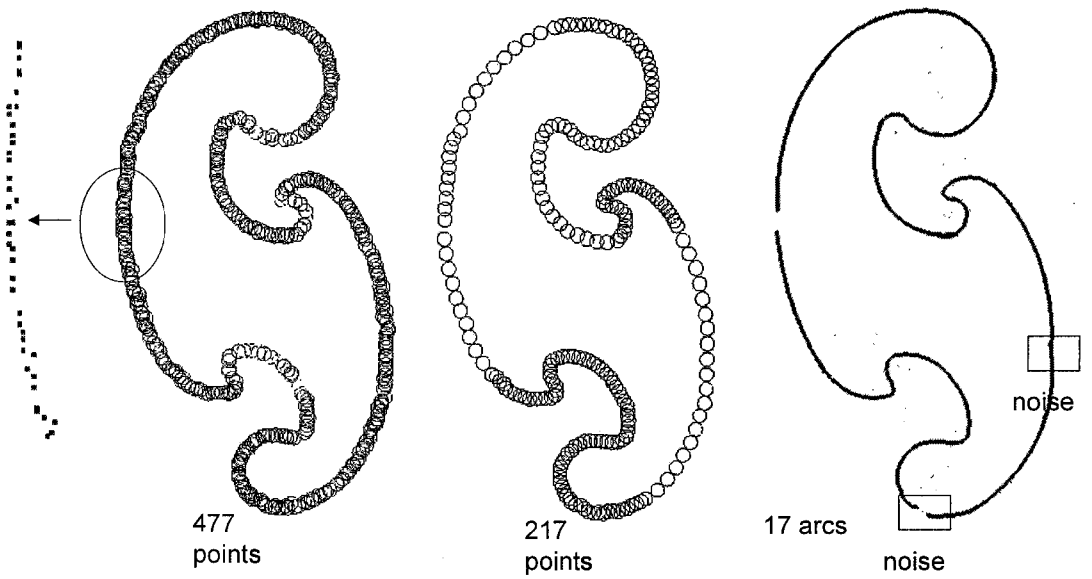

Figure 4-10: Original Points, Modified Points and Constructed Arcs for a French Curve Template

Iterative techniques are computationally expensive, and result in "mathematically" accurate curves, but an exact solution may not be a correct solution. Therefore, non-iterative techniques are investigated and the appropriate ones are utilized to create the applicable curve primitives. This is presented in Appendix G. The basic primitives under consideration are the line, circle, circular arc, and ellipse.

4.4 CAPTURING THE CURVE DESIGN INTENT

The curve segments of the boundary curve may not have the desired geometric structure, or have G^0 and G^1 continuity, as shown in Figure 4-11. The boundary curve segments must be evaluated to extract the relevant geometric structure. A series of rules are implemented to create a final curve that contains relevant geometry and has G^0 and G^1 continuity. The rules base for line segments, line to arc blending, arc to arc blending and non-standard line to arc blending are described in the following sections.

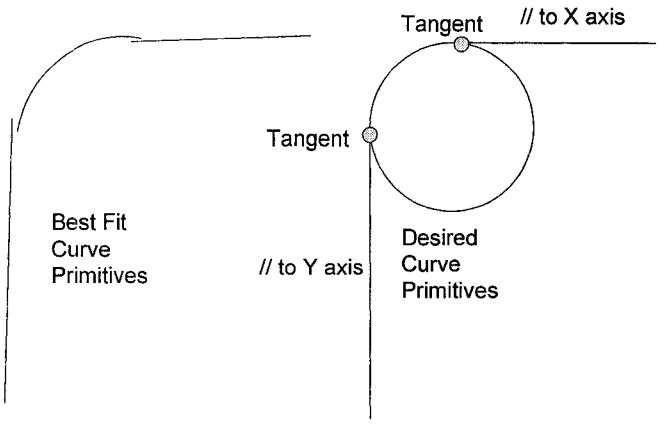

Figure 4-11: Generated Curve Primitives and Desired Curve Primitives

4.4.1 Design Intent for Linear Segments and Standard Line to Arc Blending

The longest line is set as the primary datum line. From this datum line, a series of tests for standard structural relationships are conducted using the cross product. The datum line is tested with respect to the *x*-axis, and the other lines are tested with respect to the datum line. The tests on the other line segments are summarized in Table 4-2.

Table 4-2: Linear Design Intent Tests

Line Check	Angle Value	Comment
Parallel lines	0	Assume condition if lines are within ± 2 °
Perpendicular lines	$n^*\pi/2$	Assume condition if lines are within ± 2 °
45 ° angle – each quadrant	$n^*\pi/4$	Assume condition if lines are within ± 2 °
22.5 / 67.5 ° angle – each quadrant	$n^*\pi/8$	Assume condition if lines are within ± 2 °
30/60 ° angle – each quadrant	$n^*\pi/3$	Assume condition if lines are within ± 2 °

where n is an integer value from 0 – 3 (for each quadrant)

If an angle adjustment is required on the secondary line, that line is rotated around its midpoint to the desired angle, the endpoints recalculated and stored in the database. Once all of the linear segments for the closed boundary curve are assessed and adjusted as necessary, continuity rules are applied. Four conditions are tested for: trimmed, normal fillet, inverse fillet and clearance fillet. The geometry, conditions and resulting continuity are presented in Table

4-3. Only the radius value is used for the fillet (Figure 4–12). The endpoints and arc centre shift to ensure tangency conditions (where required) between the linear and arc segments.

Table 4-3: Line –Arc –Line Relationships

Description	Figure	G^0 continuity	G^1 continuity	Comment
Trimmed lines		yes	no	No fillet
Normal fillet	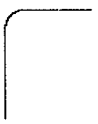	yes	yes	Arc sweep angle is less than 180 °
Inverse fillet		yes	yes	Arc sweep angle is greater than 180 °
Clearance fillet	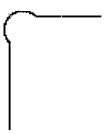	yes	no	Arc sweep angle is greater than 180 °. No relationship between the arc centre coordinate and the line end point coordinates

Trim and Fillet Line Algorithm

- Offset the lines by the value of the arc radius
- Test for an intersection point before the original endpoints
- Trim lines to the valid intersection point
  - End here for trim only condition
- Set the fillet arc centre to the intersection point
- Intersect the lines to the arc radius to establish the new end points for the lines and fillet

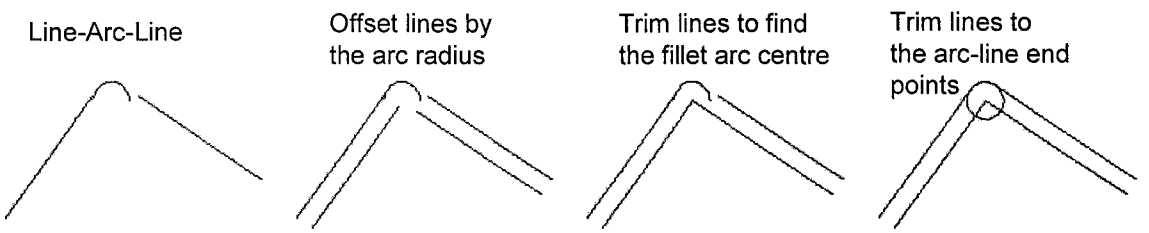

Figure 4-12: Normal Fillet Example

4.4.2 Design Intent for Circles/Ellipses

Embedded circular and elliptical curves are assumed to be concentric if their centres are within 0.5 mm. The outer circle is assumed to be the primary datum, and the embedded curve centre coordinate is adjusted to match. This is shown in Figure 4-13.

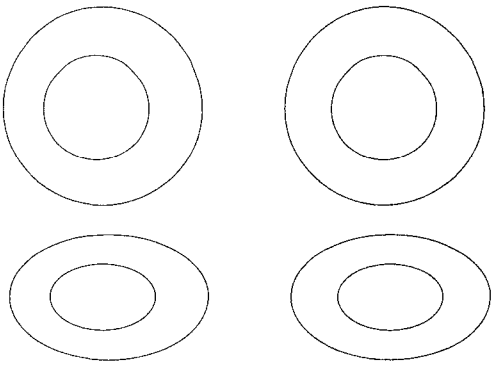

Figure 4-13: Test for Concentricity and Corrected Geometry

4.4.3 Design Intent for Arc – Arc Combinations

There are two arc-to-arc blending conditions as illustrated in Figure 4-14. The arc with the largest sweep angle is selected as the primary arc. The radius size is used as the secondary check. From the primary arc, n, and the arc n+2, a tangent fillet is generated using the radius of arc n+1 (Figure 4-15). The endpoints and the radius centre point are adjusted to suit. The primary datum is shifted to the arc n+2, and the process is repeated until the initial arc is reached. The fillet algorithm is illustrated in Figure 4-16.

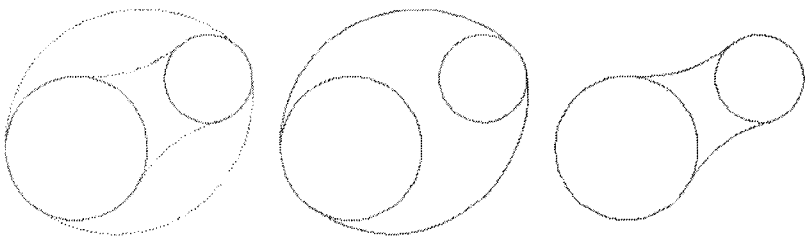

Figure 4-14: Arc to Arc Combinations

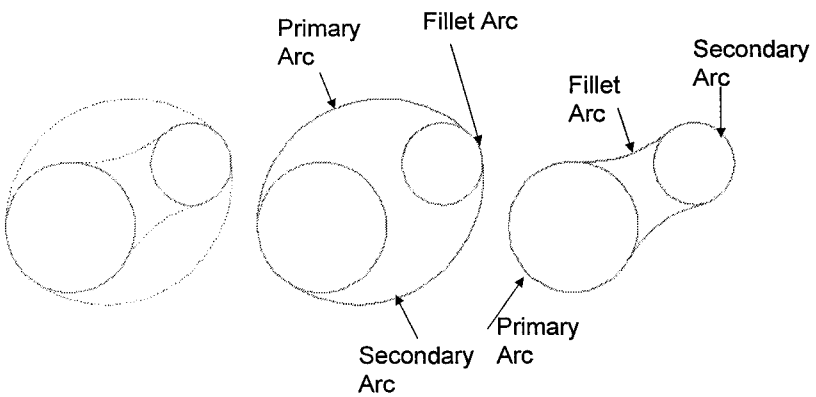

Figure 4-15: Arc Fillets to Ensure Tangency

Fillet Arc Algorithm

- Create circle C1 from centre R1 with diameter R fillet – R1
- Create circle C2 from centre R2 with diameter R fillet – R2
- Find the two intersection points of C1 and C2
- Select the intersection point closest to the R fillet centre
- Set this point as the R fillet arc centre
- Intersect the R1 to the arc R fillet to establish the new end points for the R1 and R fillet
- Intersect the R2 to the arc R fillet to establish the new end points for the R2 and R fillet

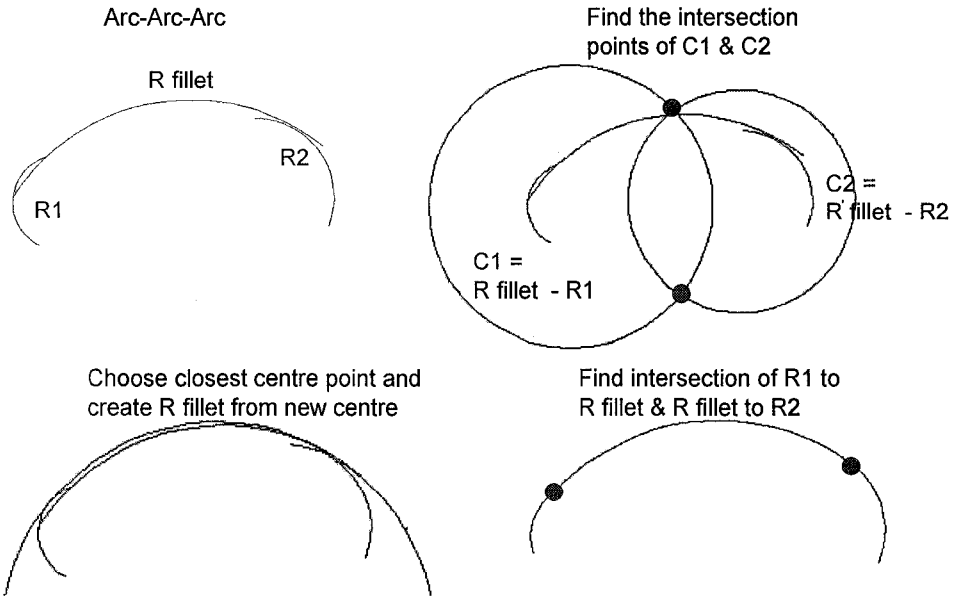

Figure 4-16: Arc-Arc-Arc Fillet Example

4.4.4 Design Intent for General Line-Arc Combinations

The general line to arc case is illustrated in Figure 4-17. There are *m* line segments, and *n* arc segments. The longest line segment is set as the primary datum, the linear tests are performed and the linear geometry modified as necessary. If there is a standard line-arc-line relationship, the intermediate arc radius is established as the fillet radius. The remaining curve segments are modified using an 'entity-arc-entity' approach: any arc between two entities is assumed to be a fillet.

Line - Arc - Arc Algorithm

- Offset the line by the value of the arc radius R fillet
- Create circle R2 from centre R1 with diameter R fillet + R1
- Find the nearest intersection point of C1
- Set this point as the R fillet arc centre
- Intersect the line to the R fillet to establish the new end points for the line and R fillet
- Intersect the R1 to the R fillet to establish the new end points for the R1 and R fillet

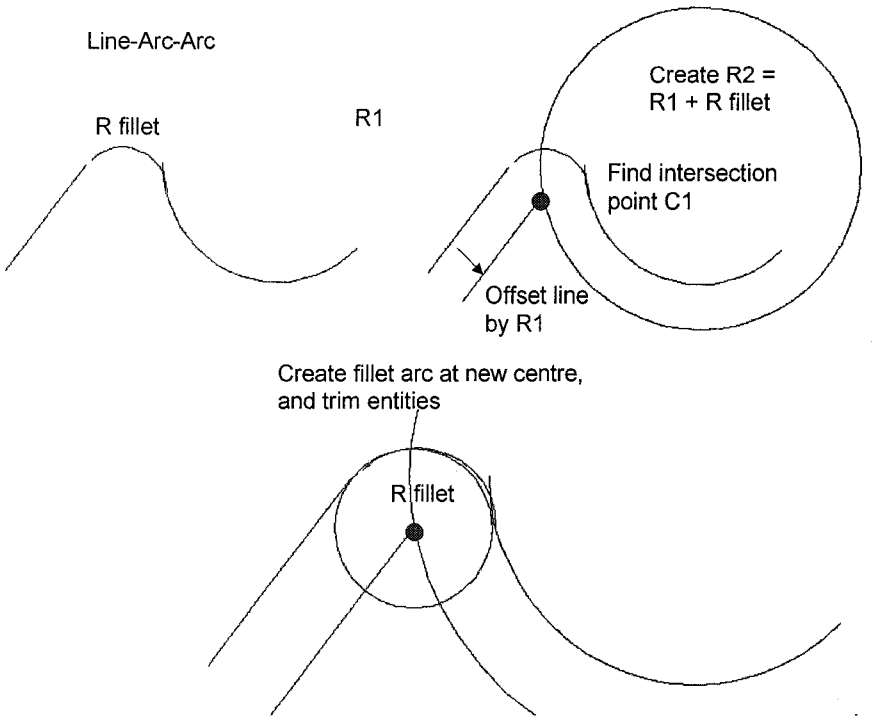

Figure 4-17: Random Line - Arc Combinations

4.4.5 Test for Symmetry

A test for a symmetrical curve is performed on any curve with a non-standard shape. The centroid of the curve is used as a base point. For a curve with symmetric geometry, it is assumed that there are multiple choices (within a tolerance zone) for the nearest endpoint coordinate from an entity to the centroid. The steps to determine symmetrical entities follow:

- Find centroid C of the closed curve
- Find the nearest point A, and flag that point
- Find the next nearest point B, and test whether it lies within the acceptable tolerance zone, and set a flag (Create a circle with radius CB at centre point C, and determine intersection points. The valid point B occurs when angle $CAB \equiv CBA$).
- Find the midpoint M of the line between A and B
- Create a line through CM that intersects the boundary curve in two places – this is the axis of symmetry (Figure 4-16).

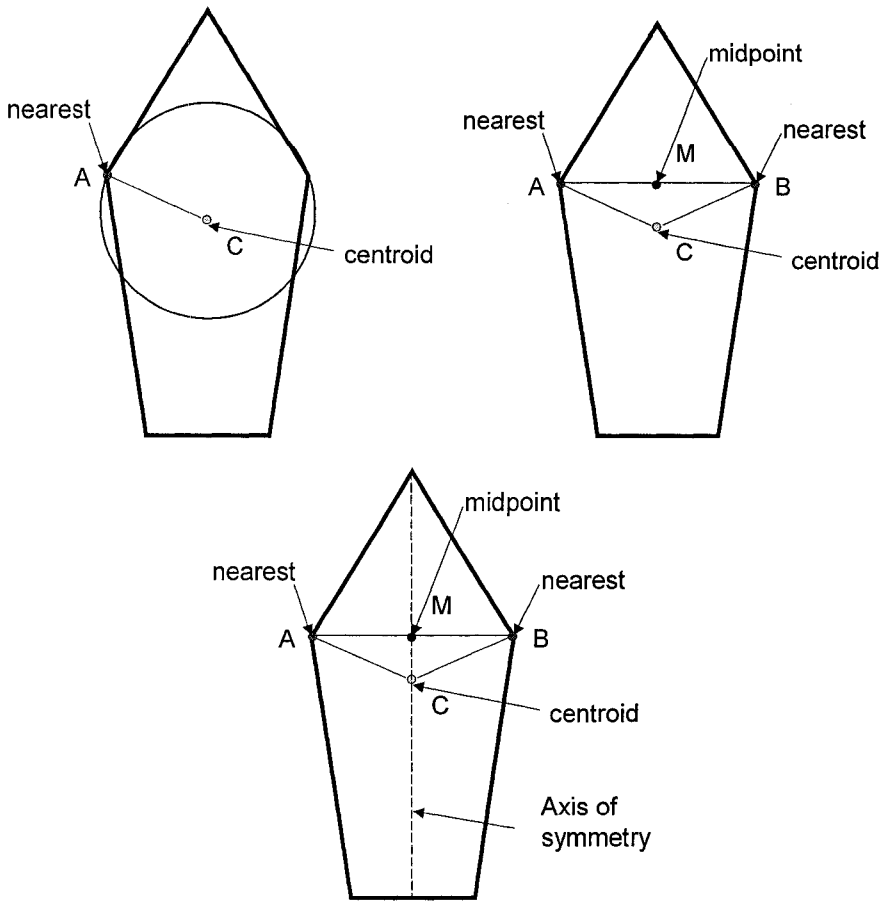

Figure 4-18: Setup for Symmetry Assessment

The parameters of each entity are mirrored through the axis of symmetry, and a comparison is conducted to determine if there is an 'equivalent' entity. If there is, both entities are flagged as symmetric, and the parameters of the 'equivalent' entity are updated to have identical properties as the mirrored entity. Entities to the 'left' of the axis of symmetry are set as the reference entities. Upon completion of the symmetry test, it is verified that the boundary curve is closed. If it is not, the checks listed above are conducted again.

4.4.6 Capturing Curve Design Intent Summary

In order to ensure that the curves are closed, have the appropriate geometric structure, and to enforce G^0 and G^1 continuity, a series of tests are performed and the curve primitives are altered to suit. It is assumed that a tangency condition exists between arc entities. Tests are performed for to check for common fillet radii (within a tolerance), but the radii are not changed to a common value unless the boundary curves represent a common shape (section

4.6), nor is additional geometry generated to enforce continuity. The number of curve primitives remains constant throughout the evaluation and modification process. Between initial the curve primitive generation, and the subsequent curve evaluation and modification, the structural design intent that covers straightness, circularity, parallelism, perpendicularity, specific standard angles, symmetry, and concentricity conditions are addressed. This in fact encompasses most of the standard geometric tolerance and dimensioning conditions (Figure 4-19) that are applicable for 2D geometry.

Form	 Flatness	 Straightness	 Circularity	 Cylindricity
Orientation	 Parallelism	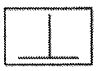 Perpendicularity	 Angularity	
Location	 Position	 Concentricity	 Symmetry	
Profile	 Section Profile	 Surface Profile		
Runout	 Circular Runout	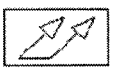 Total Runout		

Figure 4-19: Geometric Tolerancing and Dimensioning Symbols

4.5 GEOMETRY CONSTRUCTION VALIDATION

To evaluate the geometry construction, the results are compared with the original part for several test cases. A set of points on six circles, a French curve, the cylinder valve cover (introduced in Chapter 3) and a regulator gear (case study 3) are used for the validation process.

Six circles were created, and points interspersed at 1.0 mm intervals. The diameters and positions are calculated for these holes. The Algebraic Fit (AF) algorithm is used to calculate the circle parameters (using the procedure described in Appendix G) using the algorithms described in the earlier sections. The larger the circle, it is observed that there are less

variations in the calculated diameter. This is expected: if the data points are sampled along a small circular arc, the AF tends to return small circles [Chernov and Lesort, 2005]. The maximum diameter deviation is 0.040 mm (illustrated in Figure 4-20), and the maximum position variation is less than 0.025 mm.

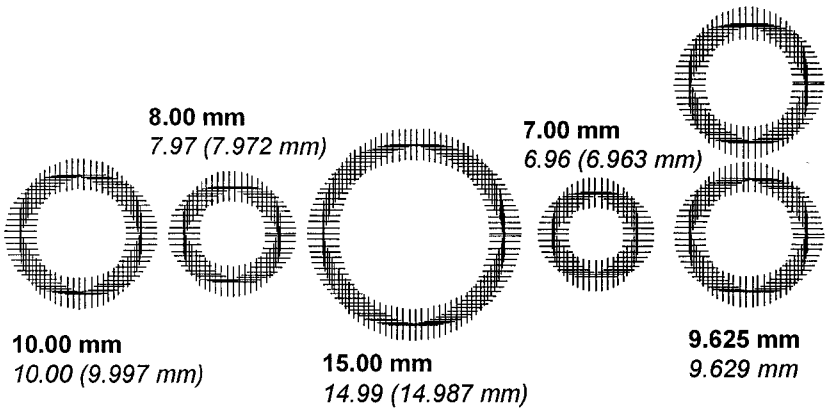

Figure 4-20: Circle Test

The French curve was tool frequently used prior to the sophisticated CAD systems prevalent today as a template to create free form geometry, projection geometry or ellipses. The curve geometry blends from one radius curve to another smoothly. Consequently, results that are comparable but not exact are expected. To assess the French curve geometry, a picture of the part was taken using a Toshiba camera, model PDR-M71, at 2048 x 1536 resolution. A machinist's scale is used to calibrate the pixel raster image into vector dimensions. For this example, the calibration ratio is 5.7 pixels per mm. Points are selected along the French curve and the resulting geometry calculated and compared to the results generated by the curve creation algorithm. Care must be taken to select the points on the edges, as there is some shadow and blurring at the boundaries. The measurement results are similar, as shown in Figure 4-21. The measured and calculated length and width are within 1% of each other; the selected radii are within 5%.

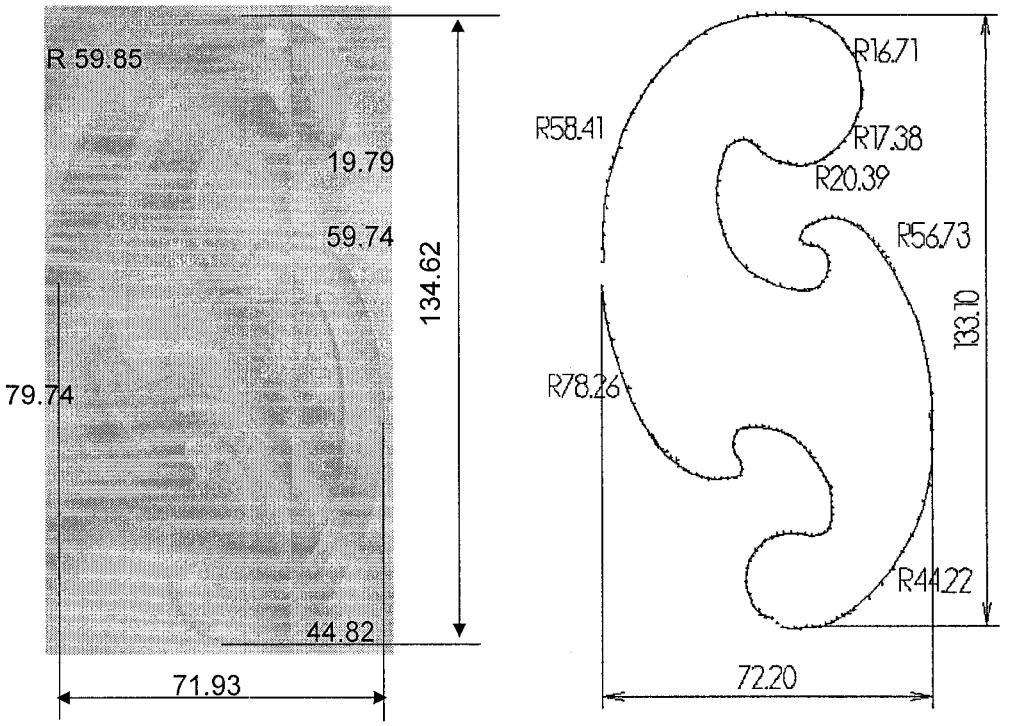

Figure 4-21: French Curve Analysis Results (not to scale)

The cylinder valve cover CAD model (case study 1) is compared to the wire frame geometry created from the 2D part model. The comparison of the outside and inside perimeters for the CAD model and reconstructed model is illustrated in Figure 4-22. For the inside perimeter, there are some minor differences in the corner geometry. The maximum difference is 0.74 mm. There is a more significant dissimilarity for the upper left hand corner geometry (2.88 mm), but as shown in the point cloud data, this variation represents actual physical discrepancies in the point cloud data. These discrepancies are not significant in this application, as they occur on non-critical boundary edges. However, there are applications where blindly reconstructing damaged or worn features will lead to developing a model of a non-functional part. This scenario is highlighted in the next case study.

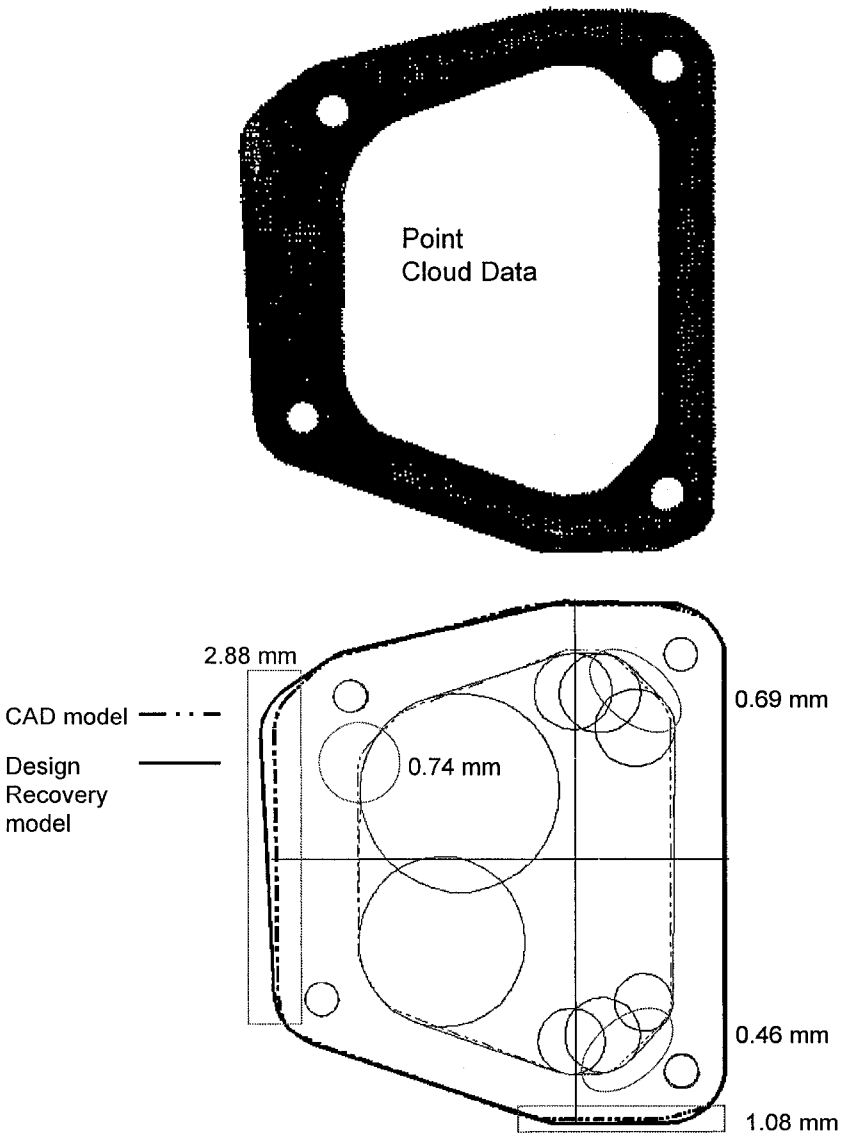

Figure 4-22: Cylinder Valve Cover: Bottom

A comparison of the constructed surfaces to the original point cloud data is presented in Figure 4-23. Distortion is present on the sealing surface. The average flatness is 0.46 mm for a five part sample of these components. The maximum distortion occurs in the mounting hole regions. This distortion is due to the torque load applied when assembling the cylinder head cover onto the engine. For this part, the maximum distance from the fitted planar sealing surface to the point cloud data is 0.42 mm. The maximum variations from the point cloud data to the enclosure surface are observed to be at the corners. Upon projecting the corner points onto this surface (normal projection), the maximum observed variation is 0.66 mm.

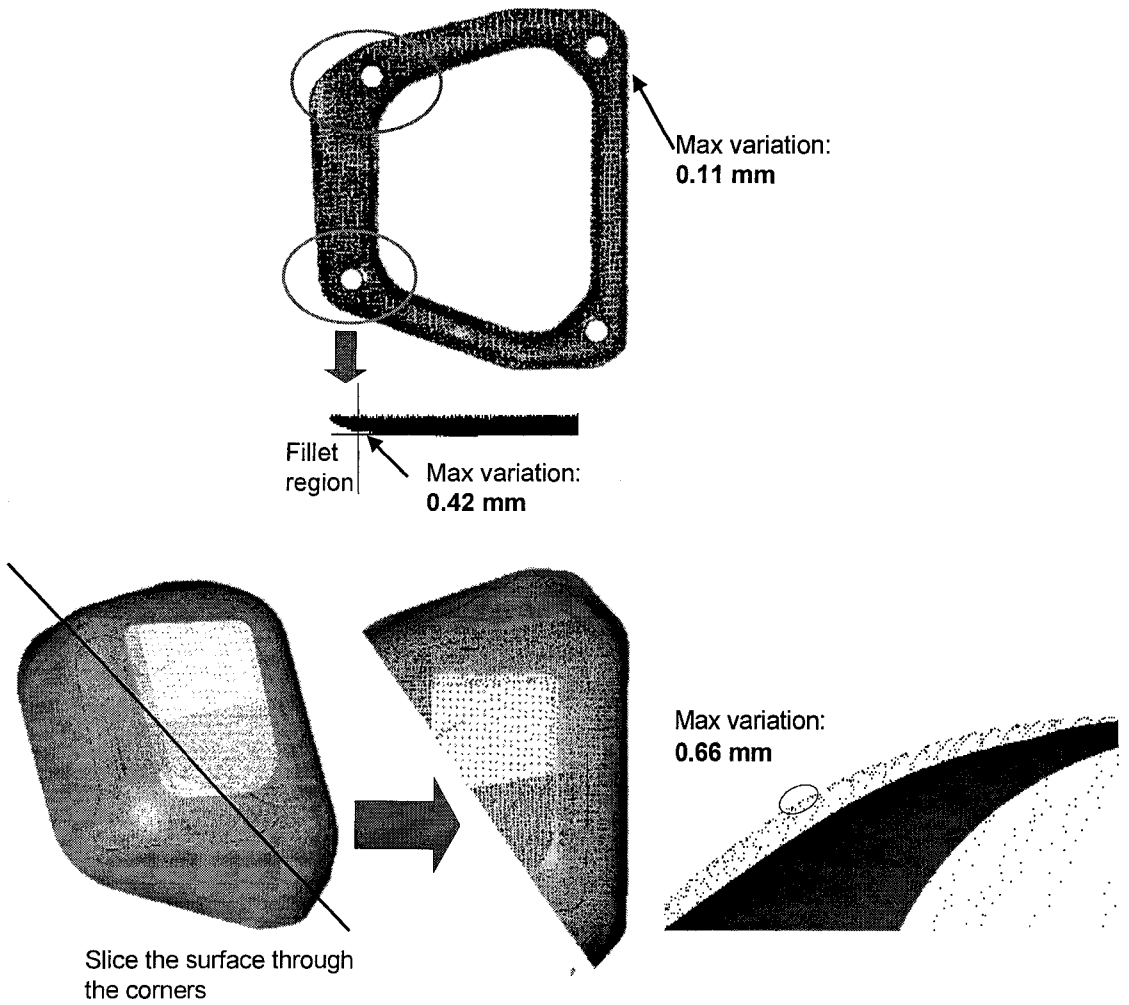

Figure 4-23: Variations from the Surface

4.5.1 Case Study 3: Regulator Gear

The final component evaluated is the regulator gear used in a power window system. The driver's side power window, for a mid-70's performance vehicle, would not raise the glass all the way up. Upon disassembly it was found that the actuating gear (regulator) was badly damaged. Not only were teeth missing for the end of the stroke, but also along the arc of travel many teeth were severely deformed (Figure 4-24). *Note, for this example all dimensions are in inches.*

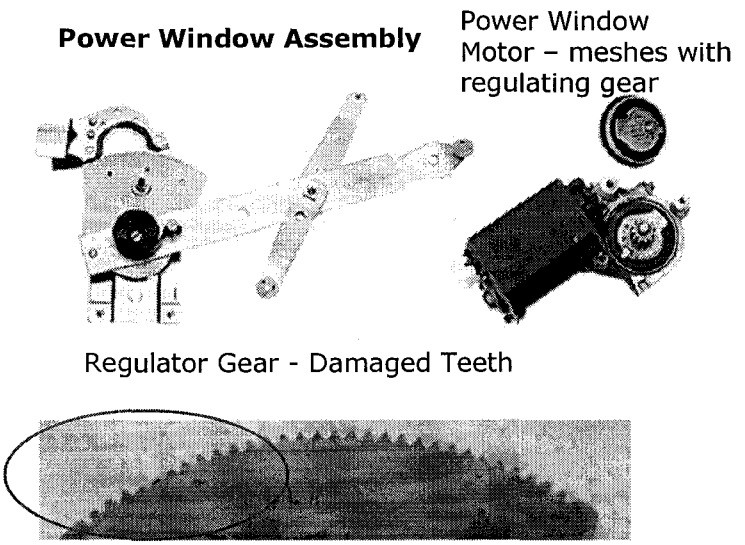

Figure 4-24: Regulator Gear System and Damaged Part

Manual measurements were taken using precision micrometers and the front and back sides of the gear were scanned using a Metris® LC50 laser scanner mounted on DEA CMM. The data was subsequently filtered using the Metris® scan curvature filter software. The scanned part and the feature labels are shown in Figure 4-25.

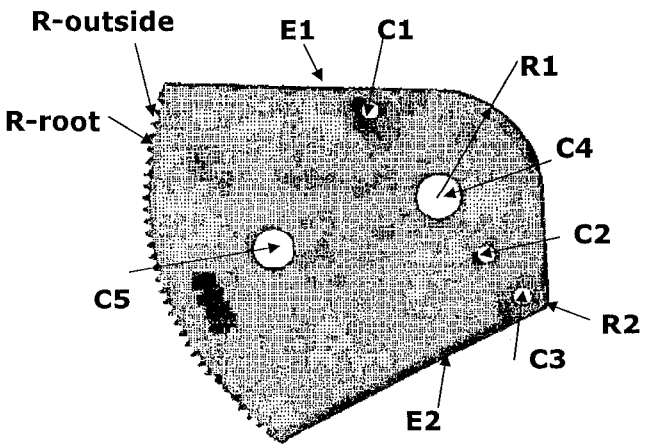

Figure 4-25: Power Window Regulator Gear

The dense regions in the point cloud data highlight the areas where rust remained on the surface and where grinding had occurred due to the rivet removal.

Upon collecting the data it was observed that there are several sources of noise: (i) there was rust on the part; (ii) the surface was modified when removing the mounting rivets and by the subsequent cleaning process; (iii) manufacturing irregularities were evident with the tapered holes, offsets with the hole positions and an offset edge, (iv) the gear teeth were heavily worn and deformed; and (v) measurement error was evident when comparing the scanned data results with physical measurement results. The Metris® and AF least squares algorithms were used to generate the diameter data for holes C1-C5 (Table 4-4). The diameters generated from the scanned data were consistently larger than those measured using micrometers. Changing the points to be included for a given hole can cause variations of 0.001 to 0.003 inches in the computed diameter because of the observed ovality. Another source of the error is due to the fact that the holes are tapered, which is typical for a punched component.

Table 4-4: Diameter Data for Holes C1 – C5

	Micrometer		Scanned Data Result (Metris®)	Difference between Min. Gage and Scanned Data	Scanned Data Result (Urbanic)	Difference between Min. Gage and Scanned Data
	Max. Hole Diameter	Min. Hole Diameter	Hole Diameter		Hole Diameter	
Label	(in)	(in)	(in)	(in)	(in)	(in)
C1	0.264	0.262	0.290	0.028	0.291	0.027
C2	0.261	0.259	0.295	0.036	0.291	0.032
C3	0.263	0.260	0.299	0.039	0.297	0.034
C4	0.691	0.688	0.719	0.032	0.718	0.031
C5	0.629	0.625	0.657	0.032	0.655	0.029

Using the scanned data, it was determined that the gear teeth are symmetrical around centre line between C4 and C5. There are differences between the scanned and measured data for the gear teeth.

- OD(scanned) = 2*R-outside ≈ 9.478 inches
- OD(gage) = 2*R-outside ≈ 4.798 *2 = 9.596 inches
- ID(scanned)) = 2*R-root ≈ 9.290 inches
- ID(gage)) = 2*R-root ≈ 4.679*2 = 9.358 inches

This is to be expected, as the measured points were taken from the undamaged teeth, whereas the scanned data is a least squares method approximation utilizing several points. The gear

teeth are engineering primitives; consequently, the key gear tooth parameters need to be determined from the noisy data and damaged teeth. Information from the scanned data (angle between teeth, pressure angle) along with the measured root diameter and outside diameter are necessary to generate the parameters used to construct the gear tooth involute curves, and position the teeth appropriately. This is described in Urbanic et al [2005].

The hole and radii positions and relationships must be determined. As the gear teeth are symmetric around holes C4 and C5, datum –A– was chosen to be this centreline. Datum –B– was chosen to be the centreline of the mounting holes, as shown in Figure 4-26. This will establish the hole relationships to each other, but the holes must also be positioned relative to the edges, hence a reference edge is established for datum -C-.

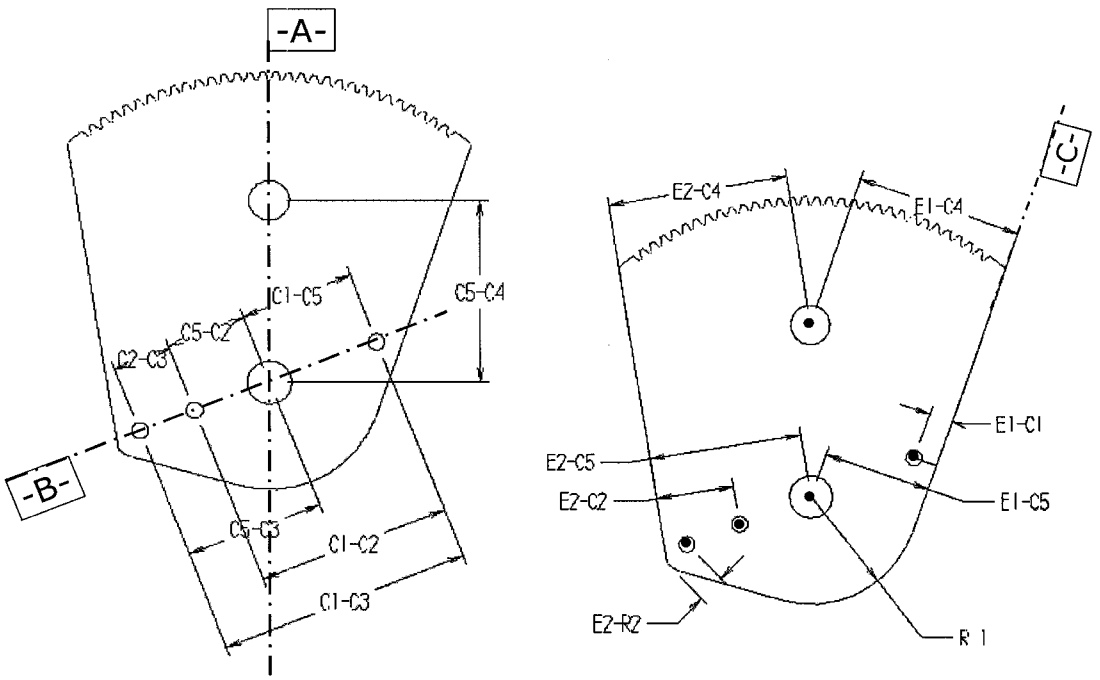

Figure 4-26: Positional Measurements

The concentricity of the radial features (R1, R2, R-outside and R-root) cannot be established with a high level of confidence directly from the scanned data due to the gear teeth damage. It was found that the centre position of holes C1, C2, and C3 are within 0.0025 inches to each other, while hole C5 is approximately 0.006 inches away from a line drawn between C1 and C3. It is assumed that this hole should be aligned based on the nature of the assembly. It is standard practice for punching to cluster similar geometry in one station, as the tooling for

different features has different wear rates [Dixon and Poli, 1995]. Therefore, it is assumed that this offset is because these holes were punched in different stations, and this is an allowable variation.

For the final model, the gear tooth geometry and R1 were set to be concentric with C5. R2 was determined to be concentric with C3. Edge E2 was offset in the part. This offset has no functional purpose; hence, the edge was redesigned to be tangent to R2 and gear tooth pattern (Figure 4-27).

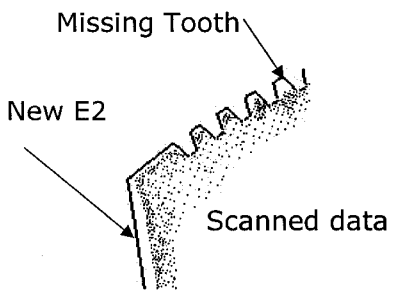

Figure 4-27: Geometric Healing (Modifying) Edge E2

Standard values (for the imperial system) were used as nominal dimensions for the holes and the centre distances (i.e. 0.688 inches = 11/16 inches), and the geometry redrawn (Figure 4-28). The primary datum is the surface of the part, the secondary datum is hole C5, and the tertiary datum is hole C1. A summary of the differences in the part geometry (generated from the scanned data) and the final geometry is presented in Table 4-5 for selected features.

Table 4-5: Geometry Difference Analysis

Feature Label	Geometry Differences	Comment
C1 – C3	Diameter: 0.031 in (0.79 mm) Position: 0.0025 in (.064 mm)	Diameters adjusted for 1/4 in rivets Positioned in a straight line
C4	Diameter: 0.030 in (0.76 mm)	Safety feature - standard imperial size (5/8 in)
C5	Diameter: 0.030 in (0.76 mm) Position: 0.006 in (0.15 mm)	Diameters adjusted for mating pin Positioned in a straight line with C1 - C3
E2	Position: 0.125 in (3.13 mm)	Redesigned to be tangent to R2 and gear tooth pattern
Gear teeth	N/A	Must reconstruct using standard design parameters for an involute stub gear tooth

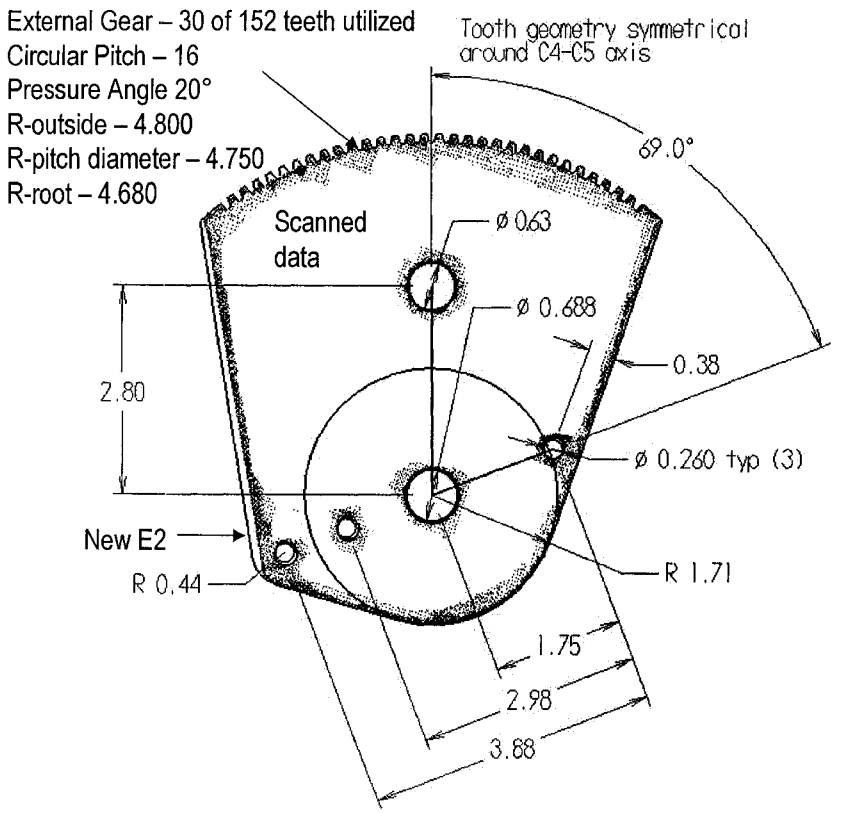

Figure 4-28: Final Part Geometry

4.5.2 Discussion

The algorithms presented here create curves that are similar to the original part, but not the same. The point cloud data is transformed into a set of line and arc entities that are adjusted in order to generate geometry that reflects the original design intent using the GD and T principles as a foundation. As shown by the cylinder valve cover, and amplified by the regulator gear case, the differences between the CAD model and reconstructed model exist because the part itself contains variations. Analysing the scanned data points exclusively cannot lead to an adequate model. For example, the scanned hole diameter nominal values are on average 0.031 inches (0.79 mm) larger (due to taper in the hole and measurement / modelling errors) than the diameters measured with precision micrometers. The error associated with the diameter calculation is approximately 0.015 inches (0.38 mm). The scanned data could not be used to generate the gear tooth involute curves. The gear tooth geometry was reconstructed from first principles in conjunction with the collected data. As no functional purpose for the offset in Edge E2 could be established, it was reconstructed with no offset.

To summarize, the geometry creation tools generate sets of line and arc geometry by using the point cloud data as a template. However, additional analysis and modifications may be required in order to generate a useful model. This information and the relevant design parameters should be contained in the design recovery framework. Elements of the final CAD can be generated automatically, but an iterative, incremental approach is required when reconstructing the CAD model. Just as the forward engineering process cannot be fully automated, neither can reverse engineering. However, like forward engineering, a design framework and various tools can be used to assist with the process.

Once the closed curves are generated based on the presented methodology, a series of tests are implemented to assess whether there are common shapes amongst the set of curves, and whether the curves are placed within a standard pattern. This is presented next.

4.6 FEATURE AND PATTERN DETECTION

Various 2D shapes and patterns can be determined when assessing the closed curve. Many features tend to have standard characteristics, and can be identified using geometric relationships. This is outlined in detail in the next subsections, and summarized in Table 4-6. The general algorithm used to detect a standard shape follows:

- Count line segments and arc segments
    - Test entities to determine that an line-arc repeatable pattern exists
- Test for shape relationships based on the:
    - Number of line and arc segments,
    - Line lengths and arc radii
        - Determine the angle between the line segments
        - Check for common fillet diameter between line segments
    - Line angle relationships, and
    - End point of the last entity is the same as the first entity start point
- Determine the shape, and its parametric variables (including shape orientation)
- Assign a shape code and a unique identification number in the format: *code.number*

Table 4-6: Summary of the Common Shape Characteristics

Standard Shapes		Lines	Arcs	Angle	Other Relationships	Parametric Variables	Shape Code ID
Circle	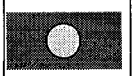	0	1	-		Radius, Centroid	C.1 …C.j
Triangle		3	0 or 3	-	Equation 4.6a, 4.7, 4.8, and 4.9	Side1, Side2, Side3, Fillet	TI, TR, TE, T
Square	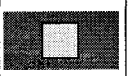	4	0 or 4	90°	Equation 4.10	Width, Length, Centroid, Fillet, θ	S.1…S.j
Rectangle	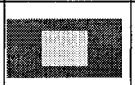	4	0 or 4	90°	Equation 4.11	Width, Length, Centroid, Fillet, θ	R.1…R.j
Pentagon		5	0 or 5	108°	Equation 4.14, 4.15, 4.16	Inscribed Circle, Number of Sides, Length, Fillet, θ	P.1…P.j
Hexagon		6	0 or 6	120°	Equation 4.14, 4.15, 4.17	Inscribed Circle, Number of Sides, Length, Fillet, θ	H.1…H.j
N-gon		*n*	0 or *n*	180-360/*n*°	Equation 4.14	Inscribed Circle, Number of Sides, Length, Fillet, θ	N.1…N.j
Obround	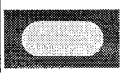	2	2	180°	Equation 4.19	Width, Length, Centroid, θ	O.1…O.j
Single D	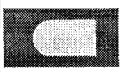	3	1	90° & 180°	Equation 4.20	Width, Length, Centroid, θ	D.1…D.j
Irregular		*n*	*m*	-	Equation 4.21	Curve Primitives	I.1 … I.j

Where m and n are integer values and θ is the rotation angle. Note: the rotation angle parameter θ is not used when comparing common shapes in the pattern analysis module.

4.6.1 Triangle

For a triangle, the number of line segments equals three or there are three line segments interlaced with three equal arcs. Tests are conducted for an equilateral, isosceles, right angle, and an irregular triangle. The tests are based on the cross product of the lines:

Equilateral triangle: $angle\ 1 \cap angle\ 2 \cap angle\ 3 = 60°$ (4.6a)

$$\left(Line\_segment_1 = Line\_segment_2 = Line\_segment_3\right) \cap \left(Arc\_segment_1 = Arc\_segment_2 = Arc\_segment_3\right) \cap \left(\vec{u} \times \vec{v} = \frac{2\pi}{3}\right) \quad (4.6b)$$

Isosceles triangle: $(angle\ 1 = angle\ 2) \cup (angle\ 1 = angle\ 3) \cup (angle\ 2 = angle\ 3)$ (4.7)

Right angle: $angle\ 1 \cup angle\ 2 \cup angle\ 3 = 90°$ (4.8)

Irregular triangle: $(angle\ 1 \neq angle\ 2 \neq angle\ 3) \cap (angle\ 1 \cup angle\ 2 \cup angle\ 3 \neq 90°)$ (4.9)

The parametric representation for a triangle consists of the three lines trimmed to a common fillet radius. If there is no fillet radius, this value is set to zero, and the line segments will have common endpoints.

4.6.2 Square, and Rectangle

For the square and the rectangle, the number of line segments equals four. To determine if the geometry represents a square or rectangle, the cross product of two lines sharing the same vertex point is $\pi/2$. The start point of the first line is equivalent to the end point of the last line, or these points are separated by the diameter of the fillet radius.

$$\left(\overrightarrow{u_4} \times \overrightarrow{v_1} = \left|\frac{\pi}{2}\right|\right) \cap For\ i = 2\ to\ 4, \left(\overrightarrow{u_{i-1}} \times \overrightarrow{v_i} = \frac{\pi}{2}\right) \tag{4.10}$$

For a rectangle, the two sets of line segment lengths are not equal (4.11a), whereas for a square the length equals the width (4.11b).

$$(Line\_segment_1 = Line\_segment_2) \neq (Line\_segment_3 = Line\_segment_4) \tag{4.11a}$$

$$(Line\_segment_1 = Line\_segment_2 = Line\_segment_3 = Line\_segment_4) \tag{4.11b}$$

If there are four lines interlaced with arc segments, the tests for a square and rectangle are as follows:

Square -

$$\left(\overrightarrow{u_4} \times \overrightarrow{v_1} = \frac{\pi}{2}\right) \cap For\ i = 2\ to\ 4, \left(\overrightarrow{u_{i-1}} \times \overrightarrow{v_i} = \frac{\pi}{2}\right) \cap$$
$$(Line\_segment_1 = Line\_segment_2 = Line\_segment_3 = Line\_segment_4) \cap \tag{4.12}$$
$$(Arc\_segment_1 = Arc\_segment_2 = Arc\_segment_3 = Arc\_segment_4)$$

Rectangle –

$$\left(\overrightarrow{u_4} \times \overrightarrow{v_1} = \frac{\pi}{2}\right) \cap For\ i = 2\ to\ 4, \left(\overrightarrow{u_{i-1}} \times \overrightarrow{v_i} = \frac{\pi}{2}\right) \cap$$
$$(Line\_segment_1 = Line\_segment_2) \neq (Line\_segment_3 = Line\_segment_4) \cap \quad (4.13)$$
$$(Arc\_segment_1 = Arc\_segment_2 = Arc\_segment_3 = Arc\_segment_4)$$

A sample algorithm is presented below for the square and rectangle shapes.

Detect Square / Rectangle Algorithm

- Check for 4 line or 4 line and arc (total 8) curve primitives
  - Check that arcs are interspersed between the lines
  - Check to ensure that the curves are closed
- Compare angles and line segment lengths (should be within 10%) for adjacent lines
- Compare arc radii (should be within 10%)
- Set as square or rectangle
- Calculate the bounding rectangle, establish rotation angle
- For shape type, store parameters: width, length, and fillet radius, and rotation angle

The orientation is determined by comparing the area of the bounding rectangle to the shape. If the area of the bounding rectangle does not equal the area of the closed curve identified as a square or a rectangle, the feature has been rotated in space. The rotation angle is determined by calculating the cross product of the vector **u** with the horizontal axis (Figure 4-29).

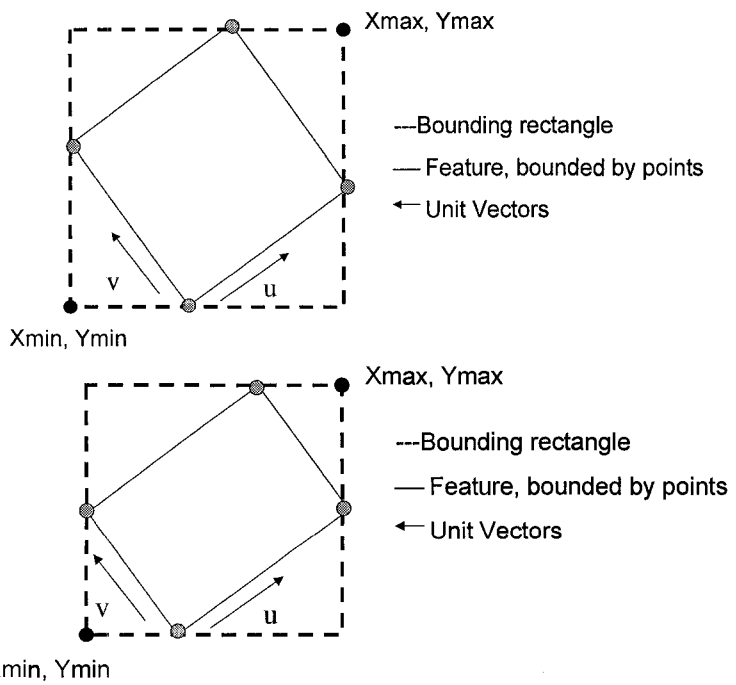

Figure 4-29: Square and Rectangle Feature in Random Orientation in Space

4.6.3 N-gon

For a curve with n lines, or n lines and arcs (where $n \neq 3$ or 4), the inscribed circle must be determined. If the line distance between the centroid and the end points of a given line segment equal R for all lines, and the angle satisfies the relationship below, the curve is an n-gon (Figure 4-30):

$$\left(R_1 = R_2 ... = R_n\right) \cap \left(\vec{u} \times \vec{v} = \pi - \frac{2\pi}{n}\right) \tag{4.14}$$

$$\left(R_1 = R_2 ... = R_n\right) \cap \left(arc_1 = arc_2 ... = arc_n\right) \cap \left(\vec{u} \times \vec{v} = \pi - \frac{2\pi}{n}\right) \tag{4.15}$$

For a pentagon, $n = 5$ and $\mathbf{u} \times \mathbf{v} = 108\ °$ (4.16)

For a hexagon, $n = 6$ and $\mathbf{u} \times \mathbf{v} = 120°$ (4.17)

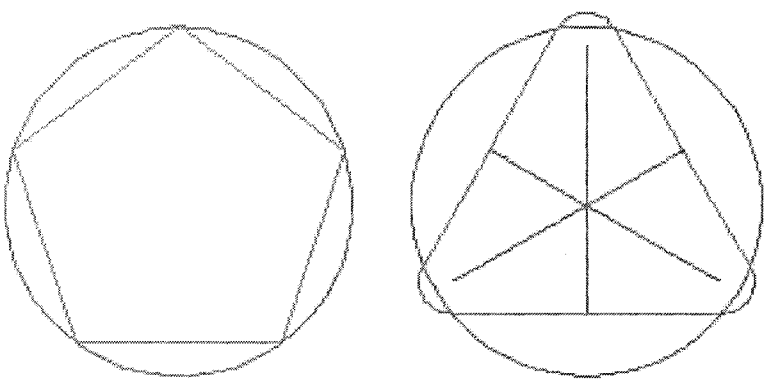

Figure 4-30: Inscribe Circle for an N-gon without and with Fillets

The rotation angle is determined finding the minimum value of the cross product of each vector **u** with the horizontal axis:

$$\theta_{rotation} = \min\left[\overrightarrow{u_n} \times \vec{x}_{axis}\right] \tag{4.18}$$

4.6.4 *Obround and Single D*

The obround and single D shapes are representative of common keyway geometry. For the obround shape, shown in Figure 4-31, the number of line segments and arcs equals two each. The arc sweep angle is π, the cross product of two line entities is 0, and the bounding rectangle area can be explicitly defined from the basic geometry (equation 4.19). The boundary rectangle area must be determined relative to the rotation vector.

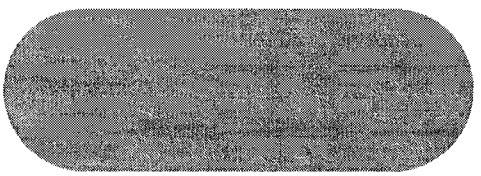

Obround: 2 arcs 2 parallel lines

Bounding rectangle of the line segments + radii = bounding rectangle of the shape

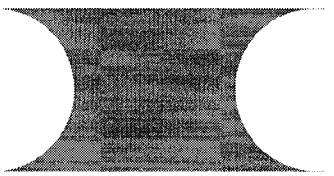

Same geometry as obround

Bounding rectangle of the line segments = bounding rectangle of the shape

Figure 4-31: Obround Shape

$$\begin{aligned}&\left(\vec{u} \times \vec{v} = |\pi|\right) \cap \left(Line\_segment_1 = Line\_segment_2\right) \cap \\ &\left(Arc\_segment_1 = Arc\_segment_2\right) \cap \\ &\left(Bounding\ Area_R = radius * (line\_segment + 2 * radius)\right)\end{aligned} \tag{4.19}$$

For the single D shape, there are three line segments and one arc, and the arc sweep angle is π. The cross product of two lines sharing the same vertex point is $\pi/2$, and as with the obround shape, there is a specific relationship for the bounding rectangle area. This is shown in Figure 4-32 and equation 4-20.

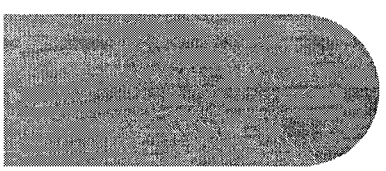

Single D: 3 lines & 1 arc

Bounding rectangle of the line segments + radius = bounding rectangle of the shape

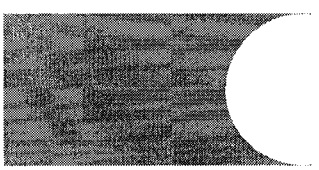

Same geometry as single D

Bounding rectangle of the line segments = bounding rectangle of the shape

Figure 4-32: Single D Shape

$$\left(\vec{u} \times \vec{v} = \left|\frac{\pi}{2}\right|\right) \cap \left(Line\_segment_1 = Line\_segment_3\right) \cap$$
$$\left(Arc\_segment\_radius_1 = Line\_segment_2\right) \cap \qquad (4.20)$$
$$\left(Bounding\ Area_R = radius * (line\_segment + radius)\right)$$

4.6.5 Irregular Shape

A common set of features, which have a non-standard shape (Figure 4-33), can be identified using the area, perimeter, bounding rectangle, and centroid to point of minimum distance on the curve h_{min} to identify closed curves with common shapes, as expressed below:

$$\left(Area_1 = Area_2\right) \cap \left(Perimeter_1 = Perimeter_2\right) \cap \left(h_{\min 1} = h_{\min 2}\right) = TRUE \qquad (4.24)$$
$$\therefore common$$

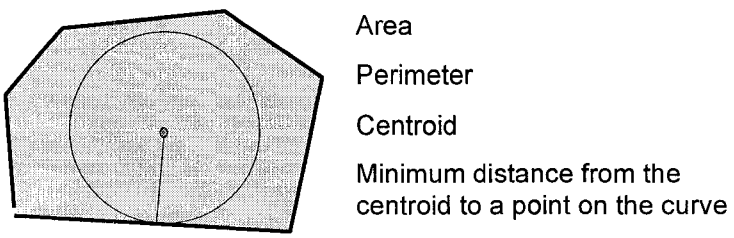

Figure 4-33: Irregular Shape Critical Features

4.7 SYSTEM OF FEATURES

There are many standard patterns commonly used for prismatic parts and on the planar faces of disk-like rotary components, and machined faces on 3D-3D castings and weldments. A matrix of prevailing patterns for common feature types is presented in Figure 4-34. To determine whether the curves that have a common shape are intended to be within a pattern, analysis is performed on the centroids of each set of common shapes. The first test performed ascertains whether the centroids are placed in a 1-D linear or circular pattern. If this test fails, a test is performed for multiple line and arc patterns. Subsequent tests check for the presence of linear or polar grid patterns. If a pattern type is detected, each curve within the pattern is labelled with a pattern identification code.

4.7.1 *Linear Pattern*

The centroid coordinates are used as input data for the equation of a line. If the line fit is good (the coefficient of correlation ≥ 0.90), the x increment, y increment, and the rotation angle θ from the horizontal axis are determined (Figure 4-35).

	Planar Face ***System*** of Features							
Feature Familly -->	Hole	Round Boss	Pocket	Projections	Slot (one or two radial ends)	Groove (both ends open/u'cut)	Pockets for Ribs (ends closed)	Ribs (subset of projections)
Straight Pattern	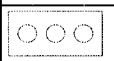		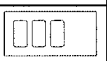	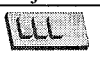	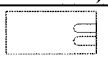			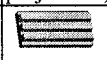
Angular Pattern	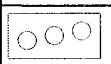							
Square Pattern	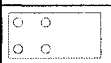							
Rectangular Pattern	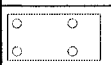							
Corner Pattern								
Arc Pattern	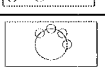							
Circle Pattern		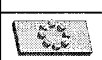				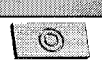	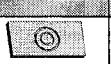	
Grid Pattern			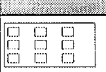	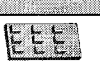		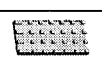	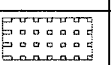	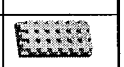
Staggered Pattern	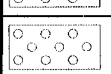		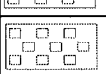	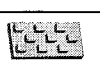				
Angular Grid Pattern								
Polar Grid Pattern Radial								
Polar Grid Pattern Axial								
Mirror X Axis								
Mirror Y Axis								
Mirror Vector Axis								
Rectangular Non Symmetric Pattern								
Circular Non Symmetric Pattern								
Polar Non Symmetric Pattern								
Peripheral Pattern								
Random Pattern	user defined	user defined	user defined	user defined			user defined	user defined

Figure 4-34: Common Planar Patterns

If this test fails to find a line, vector tests are performed on centroid point pairs. Each centroid point is compared to another once. If the vectors are equal (length within 1.0 mm and the angle within 5.0 degrees) and collinear (within 0.5 mm), the centroids lie on a line. These centroid points are collected, appropriately flagged, and the line parameters calculated. This algorithm is looped until all unique line patterns are found.

Detect Line Pattern Algorithm

- Collect all 'like' shapes
- Analyse all centroids to determine if they lie on a line
  - If yes, determine parameters
- For i = 2 to number of like shapes
  - Calculate vectors (magnitude and distance) between centroid i & i-1
- Collect all shapes with parallel and collinear vectors
  - Flag all collected shapes
- Determine line parameters [if there are uneven intervals detected for Δx or Δy, these values are set to 10^{37} and the original positional data is stored unadjusted]
- Loop until all lines are found

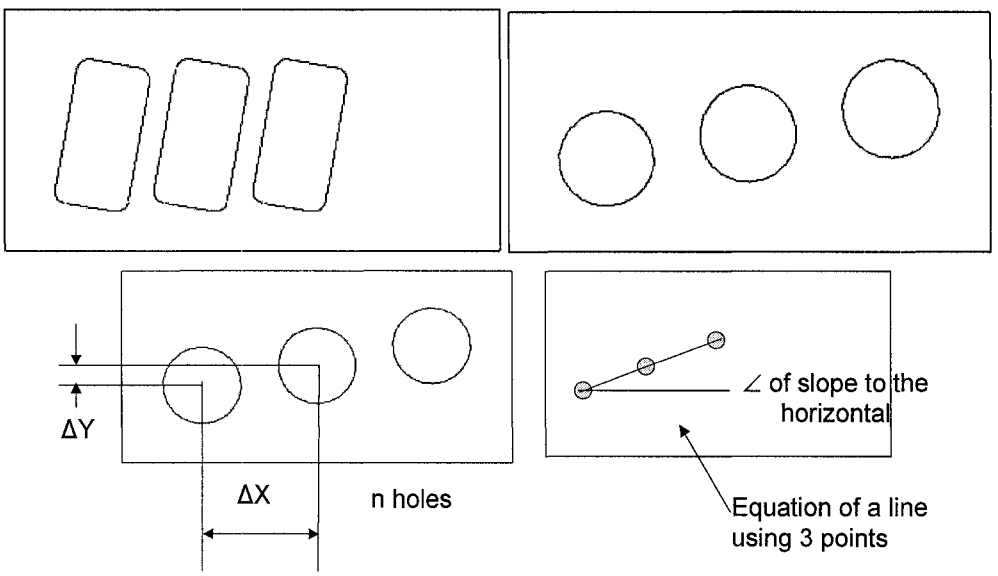

Figure 4-35: Linear Arrangement of Features

4.7.2 Circular Pattern

If the line fit is poor (the correlation coefficient < 0.9), the next test checks for a circular pattern. If the circle fit is good (standard deviation of the points with respect to the calculated circle is less than 0.25 mm), the radius R, pattern circle centre coordinate, angular increment ϕ, and rotation angle θ from the horizontal axis are determined for both a complete circle pattern

and an arc pattern (Figure 4-36). No distinction is made between radial and axial circular grids, as shown in Figure 4-37.

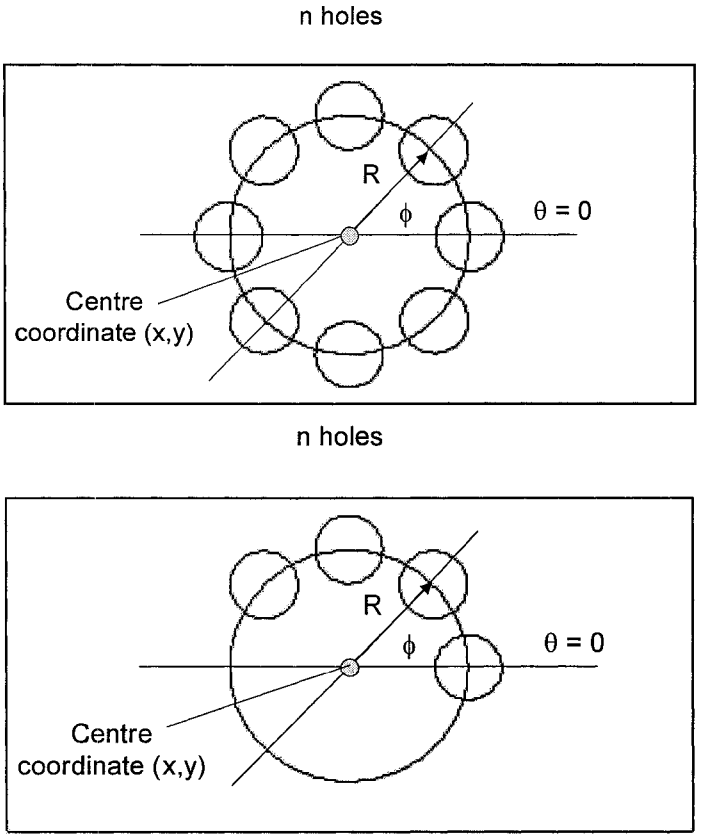

Figure 4-36: Circular Pattern of Features

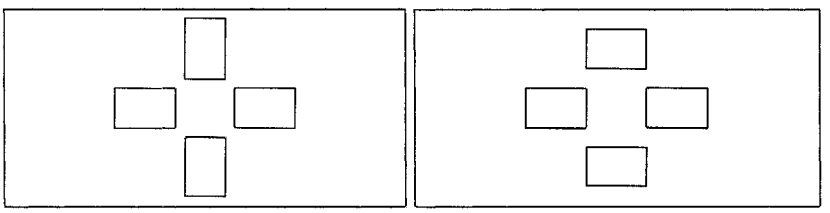

Figure 4-37: Radial and Axial Circular Grids

4.7.3 Grid

There are three cases for the grid pattern that can be determined from the same analysis: the full grid, which consists of parallel lines of centroids, (Figure 4-38), peripheral rectangle (Figure 4-39), and the corner pattern (Figure 4-40). The first line (primary line) is detected using the algorithm in section 4.7.1. The vector, **u,** distance between points, *delta X*, and the number of

centroids (counter *i*) are parameters associated with this line. The start coordinate consists of the primary line start point. From this centroid point, the next nearest centroid point is determined and an initial baseline vector generated. Using the initial baseline as a reference, all 'like' shape centroids are compared. If the vector magnitude and direction is consistent, and the normal distance of the centroid to the extended baseline is within an acceptable tolerance (0.5 mm), the centroid points lie on the same line. A counter enumerates the centroids along the vector. This check is performed until it fails. This generates vector **v,** the distance between points, *delta Y*, and counter *j*. Tests for the three cases are conducted as follows:

Test whether each centroid on the grid lies on a scalar multiple of *delta X* and *delta Y* ((*1 to j)*delta X and (1 to i)*delta Y).* All centroids that meet this condition are extracted.

If the number of centroid points = *i * j*, then the features are contained in a regular grid.

If the number of centroid points = *2*(i + j)-4* then the features are contained in a rectangular grid pattern.

If the number of centroid points = *i + j-1*, then the features are contained in a corner pattern.

u × **v** = angle of the grid

u × **x axis** = angle of orientation of the grid

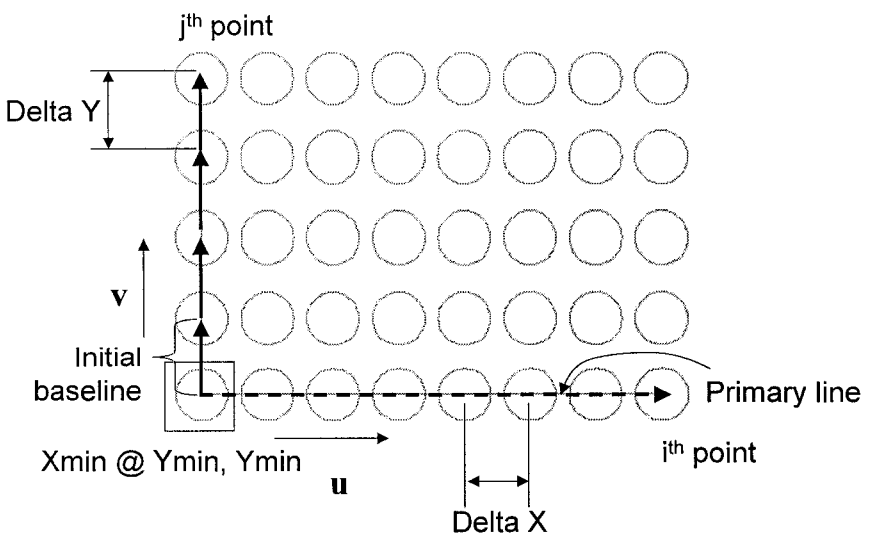

Figure 4-38: Case 1 - Standard Grid

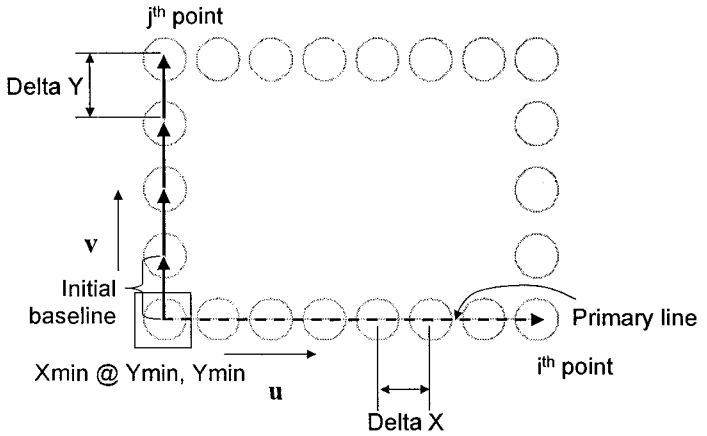

Figure 4-39: Case 2 – Rectangular Pattern

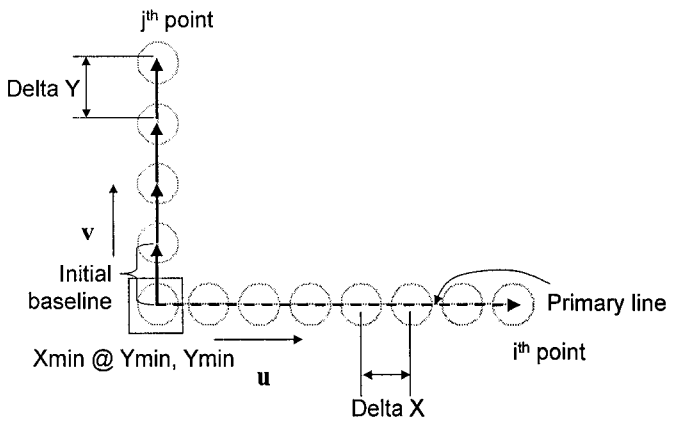

Figure 4-40: Case 3 - Corner Pattern

Detect Grid, Rectangle, Corner Pattern Algorithm

- Collect all 'like' shapes
- Analyse all the centroids to determine if they lie on a line
  - If yes, find the 'first line' and determine parameters (*u, delta X, i*)
  - Set as primary line
- Set the primary line start centroid as the start point
  - Find the nearest point (not on primary line), and create a vector
- Collect all shapes with parallel vectors
  - Determine *v, delta Y*, and *j*
  - Flag all collected shapes
- Compare all centroid to determine whether they lie on a grid pattern
  - For (i = 1 to I)
    - For (j = 1 to J)
      - If grid centroid = *i*delta Y* AND *j*delta X* -> good point
- Loop until all acceptable centroids are found
- Perform grid, rectangle, and corner tests, and if TRUE, set appropriate flags
- If grid like, set appropriate flag

4.7.4 *Grid Like*

If none of the above cases is true, yet the two vectors and counts are generated, the features may be placed in a 'grid like' pattern. An example is shown in Figure 4-41. This is actually a combination of two patterns: a rectangular pattern and a two-line grid pattern. When a grid like condition occurs, a flag is set. Tests must be conducted for all of the centroid coordinates in order to isolate the individual patterns. The algorithm isolating a rectangle pattern is illustrated in Figure 4-41.

Detect Embedded Rectangle Pattern Algorithm

- Generate primary and baselines (Detect Grid Pattern)
- Create an offset set of geometry for the primary line set of centroids
  - Offset equals baseline distance, start point = baseline end point centroid
- Create an offset set of geometry for the baseline set of centroids
  - Offset primary line distance baseline, start point = primary end point centroid
- Compare all remaining centroids to determine whether they lie on the offset lines
- Loop until all acceptable centroids are found
- If TRUE, set appropriate flag for rectangle pattern, and reanalyse remaining points

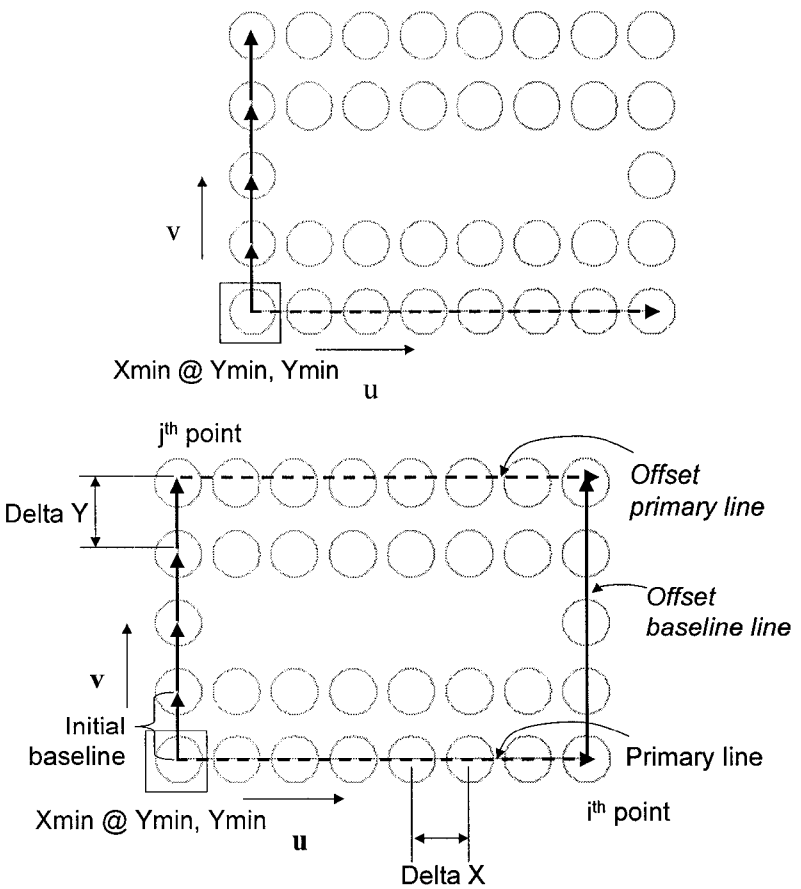

Figure 4-41: Partial Grid and Method of Detecting an Embedded Rectangle Pattern

If there is a staggered pattern, as illustrated in Figure 4-42, there exists two embedded grid patterns. The secondary grid has an offset from the primary grid, and may have a different number of holes per line (case 2). If a staggered grid case is detected, each hole needs to be evaluated separately to determine to which grid it belongs. This staggered grid case is detected by counting the number of centroids that fall within the circle defined by the radius value of the vector **v** (next nearest point distance and magnitude after the primary line has been detected). If there are more than two centroids within the radius circle, there is a staggered grid pattern. The primary line detection remains constant. The baseline next point is established by calculating the minimum distance from the start centroid point for all the centroid points lying on the circle. Once these parameters are determined, the detect grid pattern algorithm can be used. If the offset for the staggered grid is such that vector **v** is determined from the centroid on the next grid line parallel to the primary line, the detect grid algorithm will filter out any shapes do not meet the centroid grid position test (i.e. each centroid on the grid must lie on a scalar multiple of *delta X* and *delta Y* (*(1 to j)*delta X and (1 to i)*delta Y).*

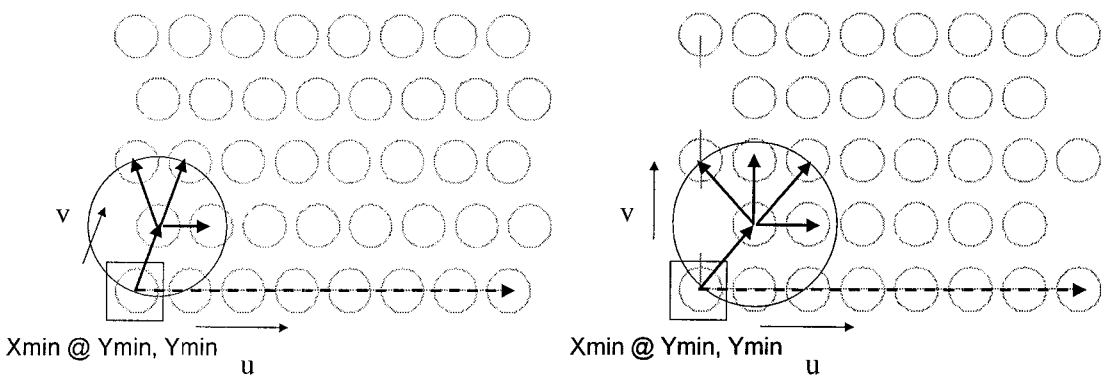

Figure 4-42: Staggered Grid Case 1 and Case 2

4.7.5 Polar

The features may be placed in a polar pattern (Figure 4-43), where circle patterns are nested with a common centre point. The relevant parameters must be established for each bolt circle (Table 4-7) and the common centre point flagged. The individual circle patterns may be detected by selecting sets of three centroids, and testing whether the other features have centroids that lie on the calculated bolt circle defined by the three reference centroid points. This is inefficient, as all centroid combinations must be tested; however, non-symmetric polar patterns (illustrated in Figure 4-34) can be detected with approach. For this work, it is

assumed that the features are equidistantly spaced (common angle increment), and that the vectors for the "nearest point" centroids (from a reference centroid) are not collinear. The feature that has the centroid with the minimum x value is set as the start point. For sets of three 'pre-selected' centroids with appropriate attributes, a bolt circle radius and centre point is calculated. Then all other pre-selected feature centroids are tested.

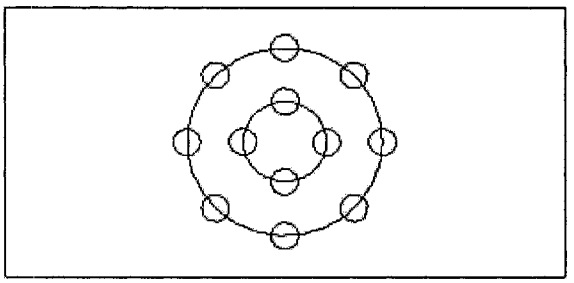

Figure 4-43: Polar Grid Pattern

Once all valid centroid points are established for a bolt circle, the parameters are generated and the relevant features are flagged. The start point is then reset and the process repeated. All the pre-selected centroid point sets must be tested. The bolt circle must have a minimum of three points. A polar pattern exists when multiple bolt circles have the same centre point.

Detect Polar Pattern Algorithm

- Collect all 'like' shapes
- Find the centroid coordinate that has the minimum x value (start point)
- Find the nearest centroid point and flag
    - Calculate the distance and angle to the horizontal
    - Reset the reference to this nearest point
- Find the nearest unflagged centroid point, calculate distance and angle to the horizontal
- Compare angle and distance
- If distance is equal, and angle is not, Flag as pre-select, and iterate until all points are tested
    - Flag all collected shapes
- Collect all shapes with common attributes
- Calculate the Radius and Centre point for a bolt circle for the first three pre-selected centroids
    - For (i = 4 to I) {I is number of features with appropriate attributes}
        - Test for all acceptable centroids on bolt circle→ Flag valid feature as TRUE
    - Loop until all acceptable centroids are found
- Reset to new start point and retest
- Find all bolt circles → compare bolt circle centre points to determine if polar pattern exists, and flag as TRUE and calculate common centre point (average value)

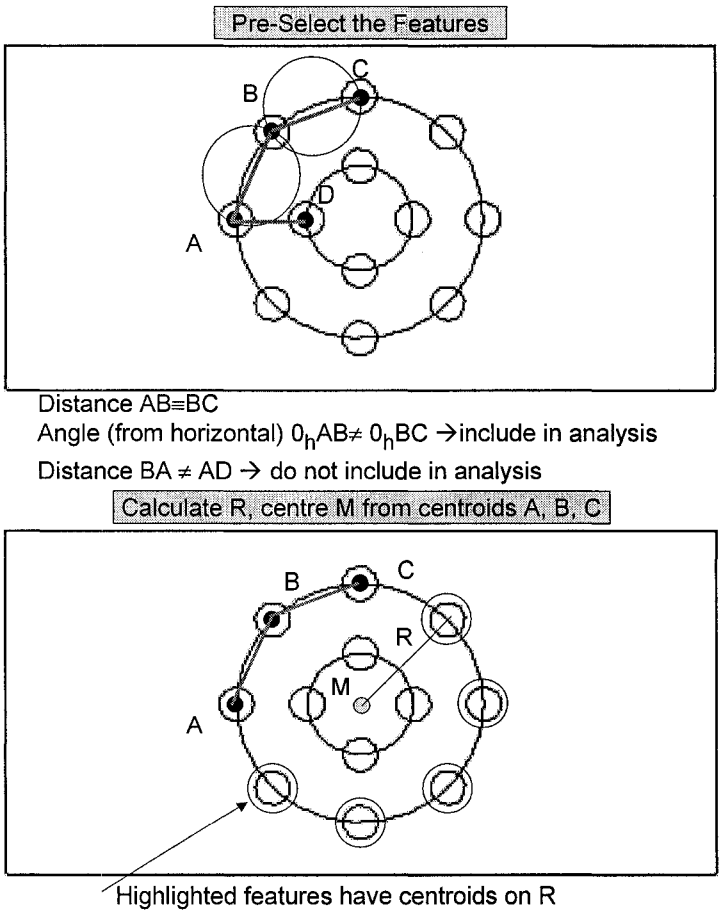

Figure 4-44: Polar Grid Pattern

The patterns, their parameters, and the pattern identification codes are presented in Table 4-7.

Table 4-7: Patterns and their Associated ID Codes

Pattern	Pictorial	Parameters	Pattern ID Code
Linear	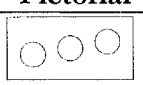	*N, Δx, Δy, θ, start pt* (x_s, y_s)	PATTERN_LINE
Circular	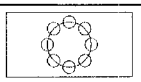	*N, R, Δϕ, θ, start pt* (x_s, y_s)*, centre* (x_c, y_c)	PATTERN_CIRCLE
Grid – standard	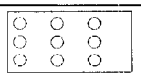	*N, Δx, Δy, i, j, θ, start pt* (x_s, y_s)	PATTERN_GRID_S
Grid – rectangle	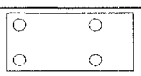	*N, Δx, Δy, i, j, θ, start pt* (x_s, y_s)	PATTERN_GRID_R
Corner Pattern		*N, Δx, Δy, i, j, θ, start pt* (x_s, y_s)	PATTERN_CORNER
Polar	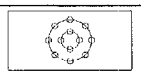	*N, R, Δϕ, θ, start pt* (x, y)*, centre* (x_c, y_c) *centre* (x_c, y_c) *is common for all circle patterns*	PATTERN_POLAR

Patterns that consist of disparate shapes are not automatically detected. In addition, polar arc patterns and several other standard patterns that are commonly used, such as a mirroring pattern, non-symmetric placement of features and a peripheral pattern, are not addressed in this work.

4.8 SUMMARY

Once the curve primitives are detected, common shapes and patterns can be identified by analysing the curve entities and the curve centroids. The 2D curve generation and feature detection algorithms can be summarized as follows:

- Project selected points onto the slice plane, and then sort the points to determine the boundary curve points.
- Apply the 'nearest point' algorithm to isolate the unique curves and remove small clusters of noisy data points.
- Apply the 'project point on entity' algorithm to shift individual noisy points.
- Apply the 'parse polyline' algorithm to place points at fixed travel distance intervals, then to place points at intervals depending on the curvature.
- Determine the inflection points and create the entity parameters.
- Adjust the entity parameters to generate the desired geometry relationships and G^0/G^1 continuity.
- Detect common shapes by assessing the curve entities, and then generate the shape parameters.
- Detect common patterns for 'like shapes', and then generate the pattern parameters.

This approach, moving from the detailed point cloud data to identifying systems of patterns, is illustrated in Figure 4-45.

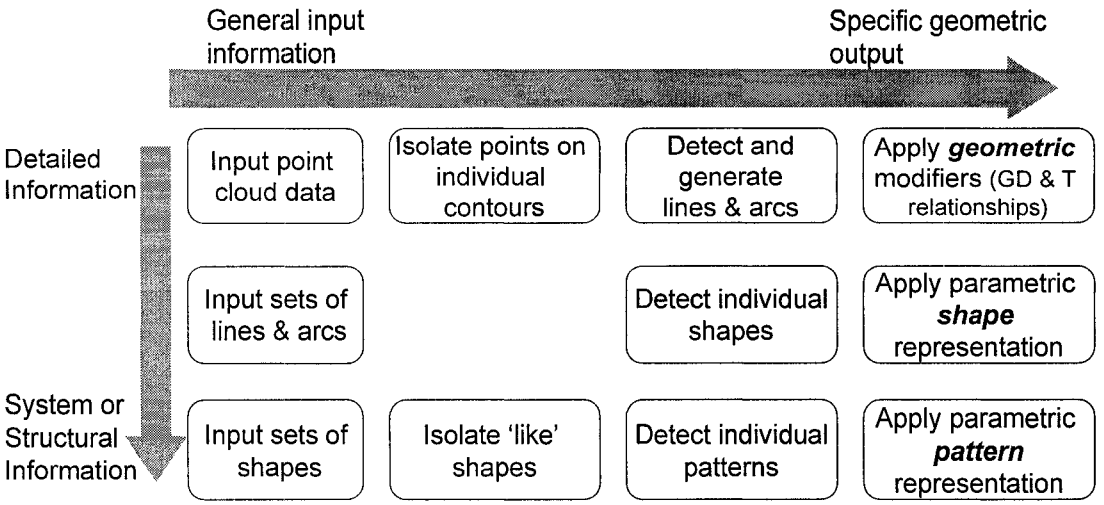

Figure 4-45: Algorithm Summary

The point cloud data manipulation algorithms outlined here have been designed to create geometry that mimics the standard forward engineering design process. This wire frame geometry can be readily modified, and for features not represented by the point cloud data (internal hole geometry), additional geometry can be easily included. The design recovery framework contains the guidelines for the point selection, geometry creation for all features, critical dimensional and tolerance information. This information is used to refine the final CAD model.

Chapter 5

THE DESIGN RECOVERY FRAMEWORK IS LEVERAGED TO ASSESS AND IMPROVE UPON THE ORIGINAL DESIGN

5 DESIGN IMPROVEMENT METHODOLOGIES

The original design may not be effective or other new design and manufacturing constraints may exist; consequently, the recovered 'original' design will need to be modified. In this chapter the design recovery framework is linked to other formal design tools in order to assess the original design and to highlight areas of improvement. It is proposed to use the Axiomatic Design (AD) methods developed by Suh [2001], which consist of a formalized methodology to map the design requirements to physical design parameters, in conjunction with the design recovery framework. To evaluate the original design using the Axiomatic Design techniques, the information contained within the design recovery framework must be rearranged into a specific matrix format in an appropriate manner and the results assessed to highlight potential areas of improvement. The design recovery framework can also be leveraged to quantify the original design and subsequent design alterations using a variant of the product complexity analysis methodology developed by ElMaraghy and Urbanic [2003]. A structured feature and component code has been developed to facilitate assessing the product complexity and the testing and validation processes.

5.1 INTRODUCTION TO AXIOMATIC DESIGN

Axiomatic Design is a systematic, rational design method created to improve design activities in the various design domains. The design domains are defined as: the customer needs, the product functional requirements, the design parameters that satisfy the functional requirements, and the process variables. The Axiomatic Design approach consists of a decomposition process that traverses through the four design domains in a logical, organized manner. The product design consists of mapping from the functional domain to the physical domain, and the process design consists of mapping from the physical domain to the process domain. The designer starts with the most general functional requirements, which are then

decomposed into lower-level functional requirements until the design can be implemented. Simultaneously, the designer conceives a physical embodiment or a design containing a set of design parameters. These parameters are key variables in the physical domain that characterize the design in order to satisfy the specified functional requirements. The choice of the design parameters is governed by the two design axioms: the independence axiom and the information axiom.

- Axiom 1: Independence Axiom- Maintain the independence of all functional requirements.
- Axiom 2: Information Axiom- Minimize the information content of the design.

Axiom 1 states that one should maintain the independence of the functional requirements (FRs). This means that in a system with two or more FRs, the design solution should be such that one can control the FRs independent of each other. In other words, each design parameter (DP) should only affect only one FR. Such a system is called an uncoupled system. If some DPs influence multiple FRs, but there is a specific order through which one can adjust the DPs without a need for iteration, the design is called decoupled. In a coupled system, iteration is required to satisfy all FRs. The three design systems (uncoupled, decoupled, and coupled) are illustrated in Figure 5-1. Axiom 2, or the information axiom, states that one should minimize the information content of the design (i.e.—the design with the highest probability of success is the best design). The design matrix [A] relates the FRs and the DPs, as shown in equation 5.1:

$$\begin{Bmatrix} FR_1 \\ \vdots \\ FR_n \end{Bmatrix} = [A] \begin{Bmatrix} DP_1 \\ \vdots \\ DP_n \end{Bmatrix} \tag{5.1}$$

	DP 1	DP 2	DP 3
FR 1	X	0	0
FR 2	0	X	0
FR 3	0	0	X

Uncoupled

	DP 1	DP 2	DP 3
FR 1	X	0	0
FR 2	X	X	0
FR 3	X	X	X

Decoupled

	DP 1	DP 2	DP 3
FR 1	X	X	X
FR 2	X	X	X
FR 3	X	X	X

Coupled

Figure 5-1: Design Coupling

The mapping between the design recovery framework and the axiomatic design matrix is illustrated in Figure 5-2. The functions and hypothesized functional requirements are stated in the 'Logical' layer. Aspects of the physical design are identified in the physical and detail layers. This data (features, dimensions, and tolerances) corresponds to the design parameters used to satisfy the functional requirements.

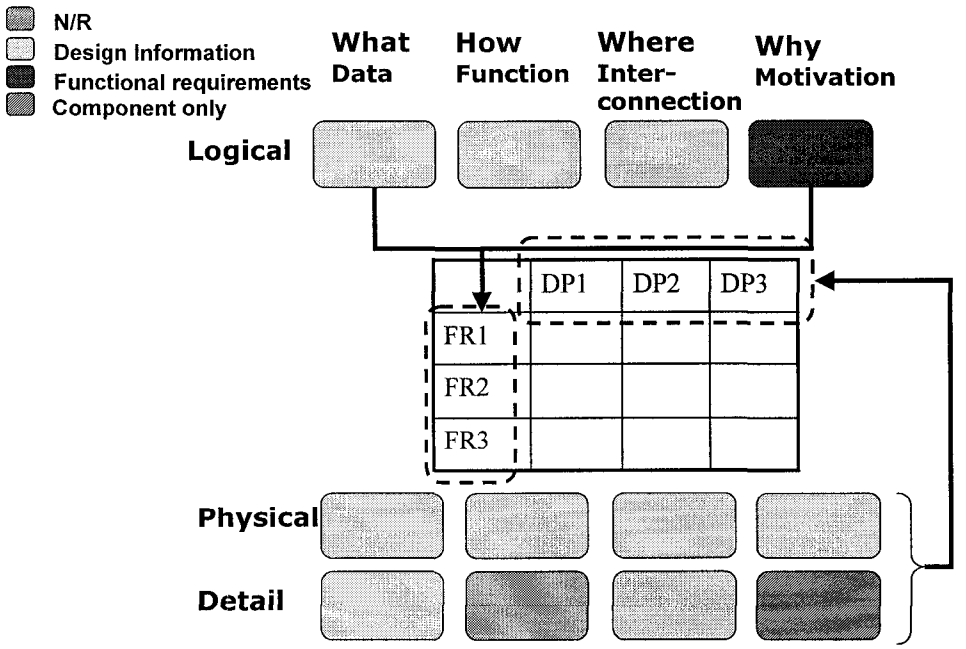

Figure 5-2: Transforming the Design Recovery Framework Information into the AD Matrix Format

5.2 INTRODUCTION TO THE MANUFACTURING COMPLEXITY MODEL

Evaluation of a product's complexity is not as simple as determining the physical characteristics of an object, as each person has a unique perception of complexity. There are highly coupled relationships between the product design, the materials, the manufacturing processes, and support systems. These elements are integrated with activities within all levels of an organization and capturing a relevant perception of complexity can be problematic. A proper understanding of the nature of complexity is required in order to be able to determine its characteristics, and provide an effective relative measure, as the areas of complexity need to be identified before they can be effectively managed [Corbett et al, 2002], [Bainbridge, 2002]. Complexity may be, in part, associated with understanding and managing a large volume or quantity of information, as well as a large variety of information. The general manufacturing

complexity model introduced by Urbanic and ElMaraghy [2003] and ElMaraghy and Urbanic [2003] is a heuristic model that focuses on these elements. The model is composed of three basic components – the absolute quantity of information, the diversity of information and the information content or the "relative" measure of effort to achieve the required results (Figure 5-3).

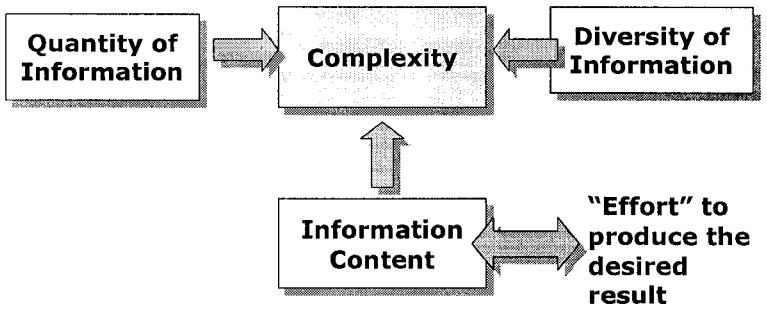

Figure 5-3: Elements of Complexity

Although the quantity of information is a factor of complexity, the absolute quantity of information may contain much redundancy. Therefore a compression factor, the information entropy measure H, is used to represent the quantity of information element:

$$H = \log_2(N+1) \tag{5.2}$$

where N is the total quantity of information.

The measure of uniqueness or the diversity ratio D_R is defined as a ratio of distinct information to total information, as given by:

$$D_R = \frac{n}{N} \tag{5.3}$$

where n is the quantity of unique information and N is the total quantity of information.

Information content is defined here as a "relative" measure of effort to achieve the required result, not a measure of the probability of success as per the Axiomatic Design Theory [Suh, 2001]. The higher the effort (i.e. the more required stages or tools), the more complex the

feature or task is. Each work environment has a different perception of complexity, but is typically consistent. The complexity index needs to effectively capture this. To this end, the relative complexity coefficient, c_j is introduced and a matrix methodology is used to determine the relative complexity coefficient. This coefficient has a value between 0 – 1, complementing the diversity ratio D_R.

The product complexity analysis is performed independently from any process plan, and focuses on the product features and specifications. The product complexity indices visibly reflect the influences of the feature quantity, variety and the characteristics of the product features. The product complexity index $CI_{product}$ is a combination of the diversity ratio and the relative complexity, and is scaled by its information entropy. This is expressed as:

$$CI_{product} = (D_R + c_j) * H \tag{5.4}$$

There are three types of complexity to be considered in a manufacturing environment: product complexity, process complexity and operational complexity, and each one flows into the other as shown in Figure 5-4. Only the product complexity can be assessed within the bounds of the design recovery framework.

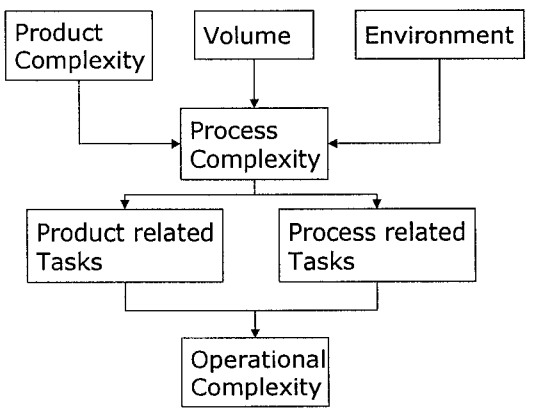

Figure 5-4: Manufacturing Complexity Cascade

Aspects associated with complexity such as the material, tolerances, and shape are specified and assessed in a simple concise manner to calculate the relative complexity coefficient, c_j. The method of determining the relative complexity coefficient, c_j is described in Appendix D, along with some examples.

In order to streamline the complexity analysis for a recovered design, and provide a basis for other tasks such as process planning, a code is introduced to classify the component and its features. Coding methods are employed in classifying parts into part families. Product codes are used with the group technology manufacturing philosophy and computer aided process planning. The product code consists of a set of alphanumeric values each of which represents design attributes. There are three types of code styles:

(1) Monocode or hierarchical code,

(2) Polycode or attribute code, or

(3) Hybrid or mixed code.

The monocode system was originally developed for biological classification in the 18th century. Each symbol depends on all of the information provided in the previous digits; hence, resulting in a hierarchical structure. The polycode symbols are independent of each other. Each digit in a specific location of the code describes a unique property of the component. Therefore, each code character represents a distinct piece of information, regardless of values in other code positions. The hybrid or mixed coding method combines characteristics of the monocode and polycode systems. The Opitz classification system, widely used in industry for process planning, is an example of a hybrid code. The form is represented in the first five digits, supplementary information that represents the size, material type, raw material shape, and accuracy is contained in the next four digits. An optional four digit secondary code is utilized to identify the production operation type and sequence [Groover, 2001].

5.3 COMPONENT AND FEATURE CODES

In order to link the design recovery framework to the product complexity index, a complexity code that represents the essential information with representative fields needs to be developed. A feature code, used to generate the feature and component complexity indices, contains information with respect to the feature quantity and variety, its form and structure, and a selection of attributes that influence the complexity (Figure 5-5). The attributes being considered are: the component material, the feature shape, the pattern placement for a set of features, the tolerances related to the feature, the surface finish and the spatial relationships

with respect to the feature – all information contained within the design recovery framework. A factor level is associated with each attribute highlighted with an asterisk (*) in Figure 5-5. The factor level corresponds to the level of "effort" to produce the feature based on the attribute being considered. A multi-tier ranking system is used where low, medium, and high effort levels correspond to factor levels 0, 0.5 and 1 respectively.

Feature Code									
Feature Related				**Complexity Analysis Attributes**					
Total Number of Features, N	Number of Distinct Features, n	Basic Geometry	Type	Material	Shape	Pattern	Tolerance	Surface Finish	Spatial Relations
N	n	*1-7*	*1-12*	*	*	*	*	*	*

Figure 5-5: Feature Codes

The total and distinct number of the general feature types, N and n, the basic construction geometry and the general feature type is contained in the feature related fields. A large variety of elements is used in design; however, standard design methods are used to create any given feature. The basic geometry can be modeled as an extrusion, a surface or solid of revolution, a swept or lofted surface or solid, a 'net' or combination of surfaces, a fillet or a blended chamfer/bevel edge. The generic set of feature types, as defined in the design recovery framework database, is presented in Table 5-1.

Certain materials are easier to manipulate than others are. This is based on both the material characteristics (i.e. formability, castability, and machinability) and the experience base within the manufacturing environment. The shape or geometry of the feature influences the value of the shape attribute. The more faces and edges within a feature (i.e. multiple step bore) or the more curve primitives defining an edge (i.e. an irregular shaped pocket), the higher the effort to produce the feature. The pattern type (i.e. linear or circular grid, mirror pattern, peripheral pattern), the positional relationships between features and the number of unique features within the pattern dictate the values for the pattern attribute. The effort decreases with the amount of allowable variations for the feature's dimensions and interrelationships. The tighter

the tolerances, the more material removal steps are required. This is also true for the surface finish requirements. The geometry of the feature may not be challenging, but the feature's position or orientation may provide a manufacturing challenge, i.e. if the features are positioned at an oblique angle, are recessed or an under cut, or contain an internal intersection (e.g. oil holes within engine components). This effort is reflected in the spatial relationships attribute. In addition, effort levels associated with fixturing are included in this attribute.

Table 5-1: Feature Complexity Code

	Digit No. and Value
1	*N* – total number of feature types
2	*n* – number of distinct feature types
3	**Feature Basic Construction Geometry:** 1 - Extrusion 2 - Revolved 3 - Swept 4 - Loft 5 - Surface net 6 - Fillet 7 -Blended chamfer/bevel edge
4	**Basic Feature Types** 1 - Clearance features 2 - Complex features 3 - Enclosing or container features (cover, o-ring groove, ...) 4 - External protrusion (boss, cooling fin, tab, ...) 5 - Fastening features (threads, rivets, ...) 6 - Free form feature (aesthetic features, contours, 3D fillets, ...) 7 - Locating features (dowels, tongue and groove ..) 8 - Planar faces (mounting faces) 9 - Precision feature (shaft / hole) 10 - Precision / complex feature (multiple step bore, gear teeth) 11 - Seating features 12 - Support features
5	**Material** 0 - Low effort 0.5 - Medium effort 1 - High effort
6	**Shape** 0 - Low effort 0.5 - Medium effort 1 - High effort
7	**Pattern** 0 - Low effort 0.5 - Medium effort 1 - High effort
8	**Tolerances** 0 - Low effort 0.5 - Medium effort 1 - High effort
9	**Surface Finish** 0 - Low effort 0.5 - Medium effort 1 - High effort
10	**Spatial Relationship** 0 - Low effort 0.5 - Medium effort 1 - High effort

Rules have been developed to be able to apply these codes in generating the complexity indices, and are listed below.

- Each feature is associated with a feature type. Feature types are clustered to generate a complexity index for the various feature types within the component.

- When assessing the feature complexity, only the information entropy measure H and the relative complexity coefficient, $c_{j,\,feature,}$ are used. If there is only one feature for a given feature type, D_R will equal one, significantly distorting the feature complexity value.

- The maximum values for the attributes for a set of feature types are used for the complexity analysis.

- The total number of features N for a feature type is multiplied by a factor related to that type prior to calculating the information quality variable H. This is done as the explicit number of dimensions and geometric modifiers are not being assessed. Typically, there are three dimensions to locate a feature in space. Maximum and minimum values or GD and T dimensions are used to describe the allowable variation for the form and to establish feature interrelationships. There are five basic GD and T categories (form, orientation, location, profile and run out). As a rule, the profile and run out categories are not used simultaneously for a feature, nor are profile and size; therefore, four categories are considered feasible for a 'simple' feature, generating a base information quantity factor of '7'. This factor is used for feature types 1, 4, 8 and 12. Other feature types (i.e. threaded fasteners, complex features such as a gear form or a free form feature) contain more information than these '7' basic factors in order to convey the essential manufacturing information. Locating features and precision external features (feature types 7, 9) typically have simple geometry with precision tolerances; therefore, the factor is set to '8'. Fastener features typically include chamfer and thread information; free form features may have sets of specific curvature information; multiple step bores and seating features (i.e. bearing) have additional geometry and specification; hence, the factor for these features (3, 5, 6, 11) is '10'. For complex features (gear teeth, non-standard thread forms and so forth), is factor is set to '12' (feature types 2 and 10). The feature type and default factors are presented in Table 5-2.

- If there are noticeable differences for features that are categorized within the same feature type (i.e. pipe thread and deep hole fastening features), a separate analysis can be performed if desired. However, features with similar characteristics (i.e. same hole size, but slightly different depths) should be clustered.

- The average 'relative effort' values for each attribute should be calculated and compared. Attributes that have higher values should be thoroughly reviewed, as the manufacturing challenges increase with higher values.

Using these rules, a feature and a component complexity index can be quickly extracted from the description codes.

Table 5-2: Default Factors used to Calculate H for the Different Feature Types

Feature Number	Feature Types	Factor
1, 4, 8, 12	1 - Clearance features 4 - External protrusion (boss, cooling fin, tab) 8 - Planar faces 12 - Support features	7
7, 9	7 - Locating features (dowels, tongue and groove) 9 - Precision feature (shaft / bore)	8
3, 5, 6, 11	3 - Container feature 5 - Fastening features (threads, rivets, ...) 6 - Free form feature (aesthetic features, contours, ...) 11 - Seating features	10
2, 10	2 - Complex features 10 - Precision / complex feature (multiple step bore, gear teeth)	12

A code that captures the essential component information has also been developed. This code could be used as a basis to generate values for the material and shape feature aspects automatically, and serve as a foundation for comparison amongst other components. The form, material, function and external conditions are captured in this code. The form fields focus on the shape and the number of each general feature types. There are eight initial shape types. The X values for the parameters and final shape fields depend on the values for the previous entries. The total amount of each feature type N and the unique amount of feature type n is listed in the appropriate fields. This is shown in Table 5-3.

Table 5-3: Component Code for the Form

Component Code															
Form															
Shape				No. of Each Basic Feature Type											
Initial Shape	Parameters	Final Shape	Part Datum Points	1	2	3	4	5	6	7	8	9	10	11	12
1-8	*X*	*X*	1-*n*	*N.n*	*N.n*	*N.n*	*N.n*	*N.n*	*N.n*	*N.n*	*N.n*	*N.n*	*N.n*	*N.n*	*N.n*

The material code contains information in relation to the material family, type, and treatments. As with the shape codes, the *X* value depends on the value in the previous field and the fields marked with an asterisk (*) have a value of 0, 0.5 and 1 to represent the various levels of intensity. In lieu of developing function codes, the function codes created by Jordan et al [2005] are utilized for *FF1, FF2*, and *FF3*. The detailed component code breakdowns are presented in Appendix E. The general component code record format for the material, function and external conditions are shown in Table 5-4.

Table 5-4: Component Code for the Material, Function and External Conditions

Component Code															
Material				Function			External Conditions								
				A	B	C	Envelope		Operating Conditions						
Material Family	Material Type	Treatment Family	Treatment Type	Function 1	Function 2	Function 3	Shape	Parameters	Heat / Cold	Vibration	Corrosive Environment	Pressure / Vacuum	Humidity	Dirt Levels	Force / Stress Levels
1-9	*X*	0-3	*X*	*FF1*	*FF2*	*FF3*	1-4	*	*	*	*	*	*	*	*

To summarize, a structured feature and component code has been developed to facilitate associating information in the design recovery to a product complexity index, in order to generate complexity measures for both the features and the component.

To illustrate how the Axiomatic Design methods can be implemented, the design recovery framework is applied to two new case studies: (i) a connecting rod, and (ii) a timing screw. The design matrix relating the FRs and DPs for the connecting rod is constructed and assessed, and design changes are recommended to reduce the observed coupling. Complexity indices are

generated for the original design and an alternative decoupled design for the connecting rod. A complete design and inspection process is developed for the timing screws employed in container motion control applications (i.e. filling, capping and labelling) using the design recovery framework with the Axiomatic Design methodology. The steps are presented in detail in Appendix F. The aspects pertaining to the design recovery framework and the Axiomatic Design method are contained in this chapter.

5.4 CASE STUDY 4: CONNECTING ROD

5.4.1 Connecting Rod Description

The connecting rod connects the crankshaft to the piston in an internal combustion engine. For this example, the engine is a single cylinder, overhead valve, air-cooled engine. The linear reciprocating motion of the piston is transformed into the rotary motion of the crankshaft using a slider-crank mechanism, where the connecting rod undergoes both linear and oscillating motions. Structurally, a connecting rod has a small end that connects to the piston through the wrist pin, a rod or strut, and a big end that connects to the crankshaft (Figure 5-6). The combustion and reciprocating inertia loads from the piston produce both tensile and compressive stresses in the connecting rod. The combustion load is compressive; the inertial loads contribute to both tensile to compressive loads. The connecting rod must be durable enough to withstand these forces and must be low in weight. The inertial forces increase by the square of the crankshaft rotational velocity, and the connecting rod mass contributes to these forces. The length of the rod influences the side thrust forces, the inertial forces and the torque curve for the engine. The connecting rod cross section is typically H-shaped as this offers the greatest opposition to bending for a given weight, and provides adequate resistance to twisting and buckling [Heisler, 1999]. The rod must blend smoothly into the big and small end hole bosses to prevent stress concentrations. The big end of the connecting rod is connected to the crankshaft journal. The cap is split from the rod horizontally to facilitate assembly and disassembly.

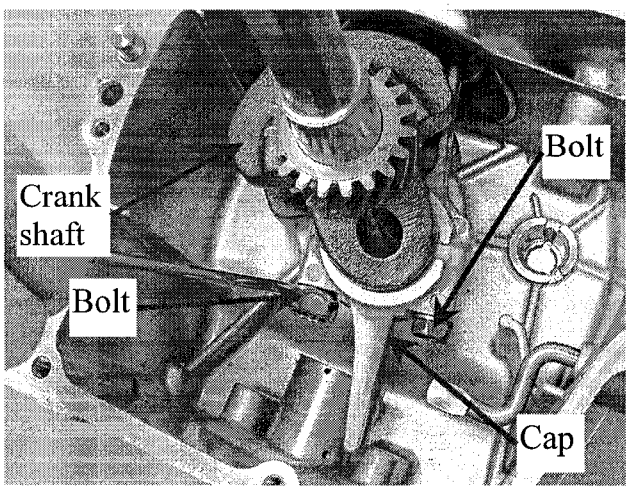

Figure 5-6: Functioning Connecting Rod

The piston pin operates at a temperature of about 140-180°C, due to the oil temperatures and the friction between the pin and the pin locating system [Heisler, 1999]. There is no oil lubrication system within this engine; hence, an 'oil splasher' has been incorporated on the connecting rod cap. This 'oil splasher' is used to whip up the oil to create an oil mist in lieu of using an oil pump and drilling oil passages in the cylinder block and cylinder head. In this engine, oil is circulated to the cylinder head in the form of an oil mist created by the splasher. The oil condenses from the mist to return to the sump via gravity. Hydrodynamic lubrication occurs between the crank journal and the connecting rod. Symmetrically opposite lubrication holes are positioned along the central axis and drilled at an oblique angle to provide oil for the hydrostatic bearing between the crank and the connecting rod. These holes allow oil to be fed under the force of the moving piston to keep the journal oiled. Since the oiling system is not through pressure via an oil pump, there are grooves on the connecting rod to aid in the oiling process. This helps the oil enter/exit the journal surface so that the contact portion can remain oiled at all times.

The connecting rod bores should be cylindrical when assembled. Threaded fasteners are used to bolt the rod and cap sections together. To retain the cap during usage, the fasteners are torqued to 16 N.m. Alignment between the cap and the rod is achieved using knurled bolts in order to locate the rod cap to the rod more precisely. This information, summarized in the design recovery format, is contained in Appendix F.

The product and assembly related features that need to be assessed are the piston linkage features (small end bore, boss and chamfers), the crankshaft linkage features (big end bore, boss and cap, bolt hole mounting faces and tapped holes), the neck or rod with the recessed 'weight savers', and the lubrication related features (the oil lubrication holes, big boss chamfers, oil grooves and the oil splasher). These features are illustrated in Figure 5-7.

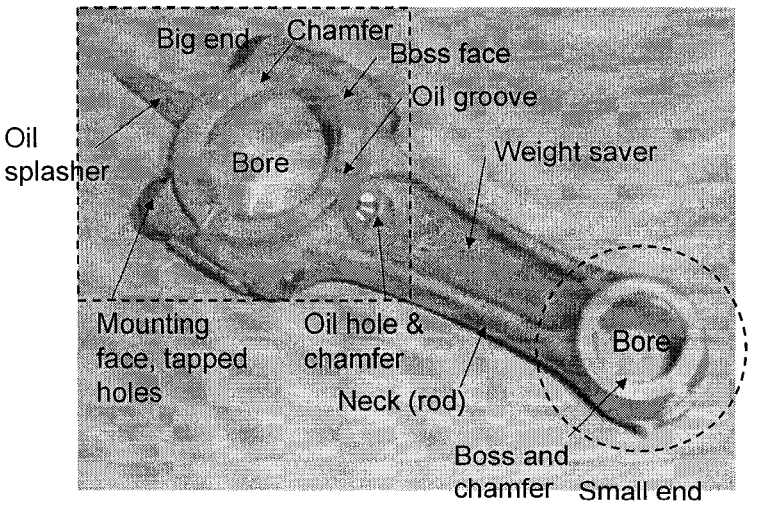

Figure 5-7: Connecting Rod Features

For this part, there are features and shape characteristics specifically related to a permanent mould casting process, e.g. die casting. There are parting lines, draft, and multiple ejector pin related features to assist in the ejection of the part from the die. A connectivity diagram illustrates the product, process and assembly features, and the physical connections within the component and the interfacing components. The connectivity diagram for the connecting rod is illustrated in Figure 5-8. The fillet blending between features is not included.

The DSM representation for the connecting rod is presented in Table 5-5 to illustrate the structurally independent and coupled features. Some subtle design couplings are highlighted that are not immediately obvious when assessing the overall design. The big end and small end bosses influence the neck length. Not only are the oil splasher design parameters influenced by the big end boss and the internal engine case, the neck, another structural element, could influence the oil splasher length. The small and big end boss sizes influence the weight saver pocket profile. The reason for a coupling may not be obvious unless the functions are clearly identified and the functional requirements understood. Having a round bore and smooth

surface finish for the bores connecting to the piston pin and crankshaft relates to having a smooth, continuous motion. The oil holes may influence the surface finish at their junction on the big end bore. There may be a burr at the intersection of these features. Proper selection of the cutting tools and process parameters may eliminate the burr with the appropriate process sequence. If the burr is not eliminated, it would effect the robustness of the dynamic component interface. Because there is sensitivity between the oil holes and the big end bore this coupling must be identified, although it can be resolved at the process level.

Table 5-5: The Connecting Rod DSM Representation for Product and Assembly Related Features

Feature	X	Small end boss	Small end bore	Small end chamfer	Neck	Big end boss	Weight saver	Oil Holes	Big end bore	Split	Clearance	Big end chamfer	Oil Grooves	Mounting faces	Mounting holes	Oil splasher
Feature	X	A	B	C	D	E	F	G	H	I	J	K	L	M	N	O
Small end boss	A	X	X		X											
Small end bore	B		X													
Small end chamfer	C		X	X												
Neck	D	X			X	X										
Big end boss	E				X	X				X	X	X	X	X	X	X
Weight saver	F	X			X	X	X		X							
Oil Holes	G						X	X								
Big end bore	H							X	X	X	X	X			X	
Split	I									X						
Clearance	J										X	X				
Big end chamfer	K					X						X				
Oil Grooves	L												X			
Mounting faces	M					X								X		
Mounting holes	N					X				X				X	X	
Oil splasher	O				X	X										X

Point cloud data and manual measurements were collected for the connecting rod. The connecting rod was scanned as an assembly. To collect data with respect to the bore positions, bolt holes, and the obliquely angled oil holes, the connecting rod was disassembled. The precision bores were measured with a micrometer, and the surface finishes measured with a profilometer. For each feature, the design must be analysed. Examples are presented for the bores and the weight saver features in Appendix F.

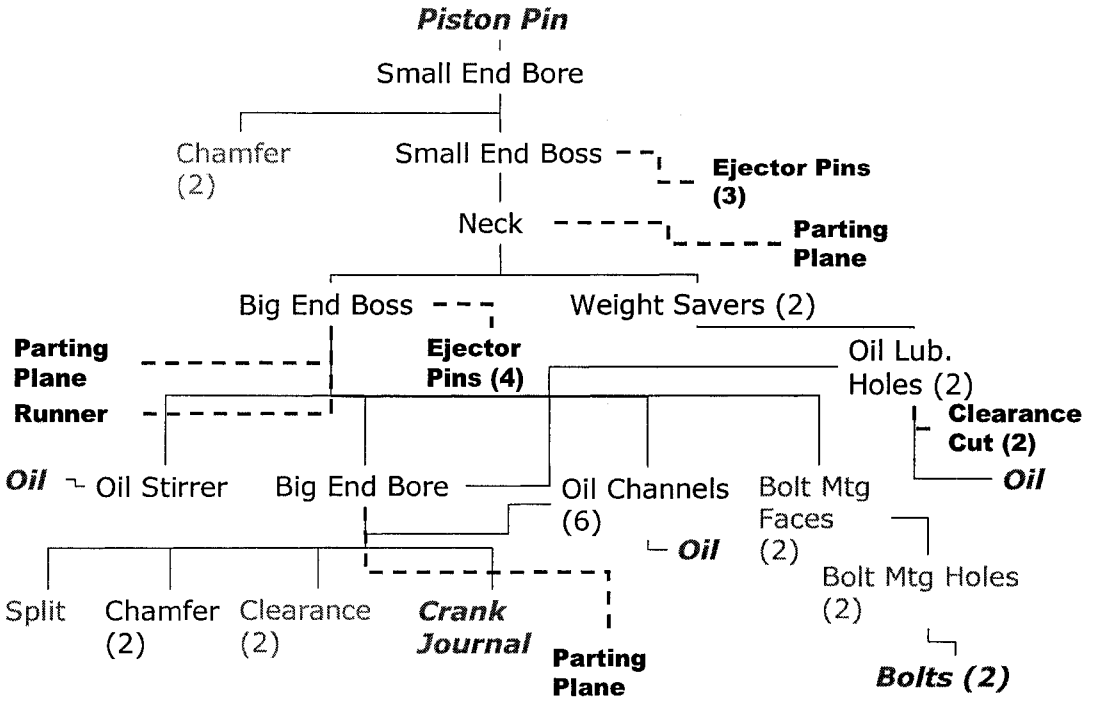

Figure 5-8: Connecting Rod Connectivity Diagram

The feature type, functions, functional requirements and the design parameters for each feature are summarized in Table 5-6. The highlighted features in this table incorporate multiple functions. Consequently, there is some coupling between the functional requirements and the design parameters. The design recovery information must now be restructured using the Axiomatic Design methodology.

Table 5-6: The Features, Feature Type, Functions, FRs and DPs

Feature	Type	Function	Functional Requirements	Design Parameters
Small end bore	Product	Couple - link	Interface to the piston pin	Cylinder - precision clearance to the piston pin Polished surface
Small end boss	Product	Couple - link	Interface to the piston pin	Cylinder + split draft Symmetric
Small end chamfer	Ass'y	Channel - import	Guide feature to assist with the assembly to the piston pin	Cone concentric to small end bore
Neck	Product	Couple - link Support – position Support- secure	Strut to position the piston to the crank Sustain tensile and compressive forces	Trapezoid shape + split draft, fillets blending into the small and big end bosses Symmetric
Weight savers	Product	Reduce inertia	Minimize the inertial load	Generate H cross section on neck (front view section) Symmetric design and location
Oil lubrication holes	Product	Channel - transport	Transport oil for the hydrostatic bearing between the crankshaft and the big end bore	Cone + cylinder, 25° angle Symmetric No burr
Big end boss	Product	Couple - link	Interface to the crankshaft Supports assembly features and the oil stirrer	Symmetric
Big end bore	Product	Couple - link	Interface to the crankshaft	Cylinder - precision clearance to the crankshaft Polished surface
Oil stirrer	Product	Channel - transport	Splash the internal engine components with oil	Thin protrusion that blends into the big end boss
Chamfer	Product	Channel - transport	Transport oil	Cone concentric to bore Symmetric
Oil grooves	Product	Channel - transport	Transport oil	Slots placed at 90° intervals Symmetric in design and location
Orientation boss	Ass'y	Support - position (orient)	Assembly feature – used for proper cap positioning	Raised linear feature
Split	Ass'y	Assemble rod to crankshaft	Assembly feature – to ensure that the connecting rod can be connected to the crankshaft	Horizontal split at the big end bore centreline Polished surface, No burr Flat surfaces
Mounting faces	Ass'y	Connect - couple – join	Join the rod and cap segments Retain the cap during usage	Flat surfaces
Bolt holes	Ass'y	Connect - couple – join Support- position Support- secure	Join the rod and cap segments Locate the cap onto the rod Retain the cap during usage	Tapped holes with concentric, precision counter bores Perpendicular to mounting surfaces
Ejector Pins	Process	Part removal	Contact points for part removal mechanisms in the die	Cylinder + draft
Parting Line - neck	Process	Part removal	Remove part from the die easily	Centreline of part
Parting Line - oil stirrer	Process	Part removal	Remove part from the die easily	Centreline of the stirrer (offset from the centre of the part)
Parting Line - big bore	Process	Part removal	Remove part from the die easily	Offset from the centre of the part

5.4.2 *Axiomatic Design Approach*

As presented in the design recovery framework, the main functional requirement of the connecting rod component is to transmit the piston linear reciprocating motion into the crankshaft rotary motion. This is achieved through utilization of a slider crank mechanism. There are several constraints: the motion must be transformed smoothly, the component must be able to withstand the stresses, and should introduce minimal inertial forces and side thrust. The component should withstand 10^9 cycles, and operate through the normal temperature range experienced by the operating environment. The component level design characteristics are summarized in Figure 5-9.

***FR0**: Linkage to convert translational piston motion to the crankshaft rotary motion*
***DP0**: Slider-crank "hinge joint" system*
C1: Smooth, continuous motion
C2: Withstand compressive and tensile stresses
C3: Minimal inertial reciprocating forces
C4: Minimize the side thrust
C5: High fatigue strength → 10^9 cycles
C6: Function between -40°C and 200°C (oil temperatures)
C7: Low-cost

Figure 5-9: Component Level Design

This basic functional requirement must be decomposed into the lower level functional requirements, and mapped to the physical domain via zigzagging (Figure 5-10). The Layer 1 FRs are:

FR1: Connect piston to crankshaft
FR2: Sustain loads: compressive / tensile stresses, side thrust/piston slap
FR3: Small inertial forces or minimize mass
FR4: Smooth continuous motion or minimize friction

These FRs must be linked to the DPs via the design matrix. The design parameters that satisfy the FRs consist of the interface features, the structure and material, and the lubrication features (Table 5-7).

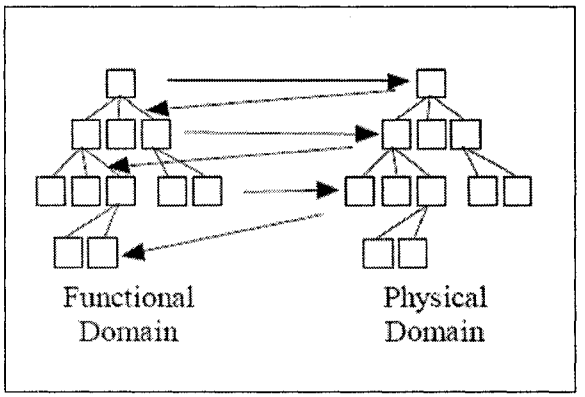

Figure 5-10: Decomposing the Design Problem and Zigzagging between Domains

Table 5-7: Layer 1 FRs and DPs

	DP1: Linkage interface features	DP2: Linkage structure	DP3: Linkage material	DP4: Features to transport lubrication oil
FR1: Connect piston to crankshaft	X	0	0	0
FR2: Sustain loads: compressive / tensile stresses, buckling, side thrust/piston slap	0	X	X	X
FR3: Small inertial forces or minimize mass	X	X	X	0
FR4: Smooth continuous motion or minimize friction	X	0	0	X

These four FRs must be further decomposed. The FR decomposition for this example is illustrated in Figure 5-11. The detailed physical domain composition and mapping is not shown for clarity.

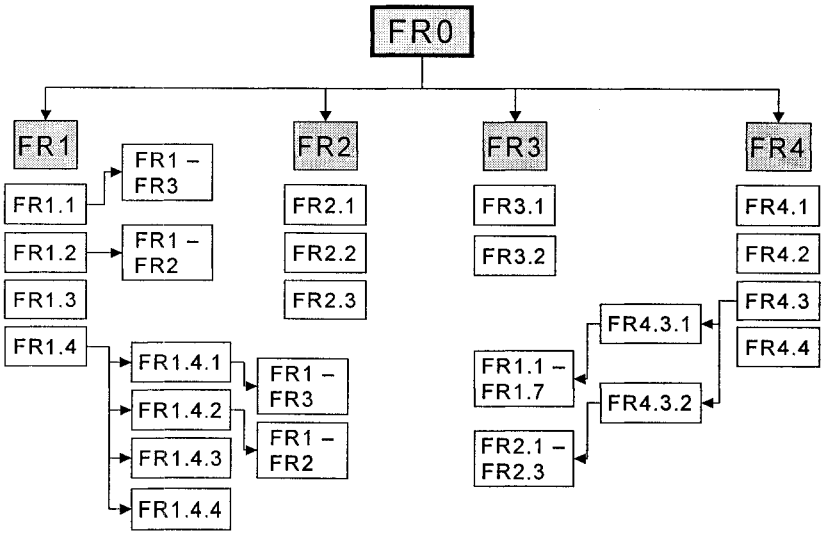

Figure 5-11: Connecting Rod FR Decomposition

FR1, which consists of the direct interface connection, can be broken down into specific features that link and position the external components. The length of the connecting rod influences the torque and power curves. An assembly feature must be considered for the big end bore, as the crank cheeks do not allow for a slip on assembly method. The next layer of FRs for FR1 are:

FR1.1: Interface with the piston (via the piston pin)
FR1.2: Interface with the crankshaft (via the journal)
FR1.3: Locate piston-crankshaft with respect to each other to achieve desired output characteristics
FR1.4: Assemble onto crankshaft

The FRs, DPs and the corresponding design coupling, is illustrated in Table 5-8. There is limited coupling for this set of FRs. The interface between the crankshaft and the big bore are both influenced by the bore geometry and the bore split. The other DPs are uncoupled.

Table 5-8: FRs and DP for FR1, Layer 2

	DP1.1: Small end bore	DP1.2: Big end bore	DP1.3: Connecting rod neck to position features	DP1.4: Big end bore/ boss split - assembly feature
FR1.1: Interface with the piston (via the piston pin)	X	0	0	0
FR1.2: Interface with the crankshaft (via the journal)	0	X	0	X
FR1.3: Locate piston to crankshaft	0	0	X	0
FR1.4: Assemble onto crankshaft	0	0	0	X

For FR2, the decomposition focuses on identifying and addressing the specific force related failure modes. The connecting rod should not buckle, flex or twist, and the side thrusts should be minimized. The hydrodynamic lubrication should be readily established and maintained in order to prevent flexing and twist. The presence of ribs or bosses placed in critical locations can reduce or prevent flexing and twist. Bosses on the rod and cap sections are located on the split joint interface to reduce flex at this junction. The neck length influences both the buckling and the side thrust. The FR2 decomposition is:

FR2.1: Prevent buckling
FR2.2: Prevent flexing / twist
FR2.3: Reduce side thrust/piston slap

The DPs and the coupling are presented in Table 5-9.

Table 5-9: FRs and DP for FR2, Layer 2 (-ve sign used to indicate a contradiction)

	DP2.1: Dynamic interface	DP2.2: Reinforcement boss/ribs at split	DP2.3: Neck Length
FR2.1: Prevent buckling	0	0	-X
FR2.2: Prevent flexing / twist	X	X	0
FR2.3: Reduce side thrust/piston slap	0	0	X

To reduce the inertia of the component, the material density and volume (controlled by the shape) must be minimized. Therefore the decomposition for FR3 is (Table 5-10):

FR3.1: Minimize Density
FR3.2: Minimize Volume

Table 5-10: FRs and DP for FR3, Layer 2

	DP3.1: Beam shape for neck	DP3.2: Material
FR3.1: Minimize Density	0	X
FR3.2: Minimize Volume	X	X

FR2 and FR3 are tightly coupled, as indicated in Table 5-7. The buckling (FR2.1), and flex behaviours (FR2.2) are governed by the component shape (DP3.1) and material properties (DP3.2). The FR2.3 (reduce side thrust) is also linked to the shape design parameter (DP3.1).

To provide smooth and continuous motion, a hydrodynamic bearing between the moving components is utilized. The surfaces must be smooth, have the appropriate clearances, and oil

transported to the areas of motion. These are the decomposed FRs for FR4. The design parameters that address these FRs focus on specific design features and tolerances, and are listed in Table 5-11.

FR4.1: Smooth surface
FR4.2: Clearance between interfacing components
FR4.3: Provide lubricant

Table 5-11: FRs and DP for FR4, Layer 2

	DP1: Define surface finish	DP2: Tolerance stack up between components	DP3: Features to transport lubrication oil
FR4.1: Smooth surface	X	0	0
FR4.2: Clearance between interfacing components	0	X	X
FR4.3: Provide lubricant	0	0	X

FR1.4, assemble onto the crankshaft, is further decomposed into four unique FRs. This is a coupled design, as the locating details, fastening and retaining features are combined with the bolt and bolt hole fastening system (Table 5-12).

FR1.4.1: Position cap onto rod
FR1.4.2: Join cap onto rod
FR1.4.3: Retain cap during usage
FR1.4.4: Orient the cap during assembly

Table 5-12: FRs and DP for FR1, Layer 3

	DP1.4.1: Locating detail	DP1.4.2: Threaded fastener	DP1.4.3: Torque loads on threaded fastener	DP1.4.4: Orientation Detail
FR1.4.1: Position cap onto rod	X	X	0	0
FR1.4.2: Join cap onto rod	X	X	X	0
FR1.4.3: Retain cap during usage	0	X	X	0
FR1.4.4: Orient cap during assembly	0	0	0	X

FR1.1, FR1.2, FR1.4.1, FR1.4.2 are decomposed to another layer to link the identified form characteristics to more refined FRs. A detailed analysis is not presented, as each FR is satisfied by a unique DP. The complete decomposition for the original FR1is presented in Table 5-13. Tables 5-8 and 5-12 are subsets of Table 5-13.

Table 5-13: The Final Decomposition for FR1

	DPs	Small End Bore shape	Small End Boss shape	Small End Chamfer shape	Big End Bore shape	Big End Boss shape	Neck length & bosses	Big Bore Split position	Concentricity	Perpendicularity to mounting faces	Feature surface finish	Threads / Threaded fastener	Torque level on threaded fastener	Raised Orientation Detail
FRs		**1.1**	**1.1.1**	**1.1.2**	**1.2**	**1.2.1**	**1.3**	**1.4.1.1**	**1.4.1.2**	**1.4.1.3**	**1.4.2.1**	**1.4.2.2**	**1.4.3**	**1.4.4**
Interface to piston	**1.1**	X												
Support interface to piston	**1.1.1**		X											
Assy guide for piston pin	**1.1.2**			X										
Interface to crankshaft	**1.2**				X			X					X	
Support interface to crankshaft	**1.2.1**					X								
Position piston to the crankshaft	**1.3**						X							
Assemble connecting rod onto crank	**1.4.1.1**							X						
Position cap onto the rod - align mounting hole bore to fastener	**1.4.1.2**								X			X		
Position cap onto the rod - align bolts to mounting features	**1.4.1.3**									X				
Bearing surface on the split joint	**1.4.2.1**										X			
Join cap onto rod	**1.4.2.1**								X			X	X	
Retain cap during usage	**1.4.3**											X	X	
Orient the cap properly during assembly	**1.4.4**													X

Functional requirement FR4.1 could be broken down into two sub FRs: the desired initial surface finish of the big end bore (FR4.1.1), and the long term surface characteristics (FR4.1.2). Fine particulate matter will be generated during usage due to metal on metal contact; hence, contaminating the oil. This should not influence the engine performance. FR4.1.1 is met by specifying a maximum acceptable surface finish. The DP that addresses FR4.1.2 is met by selecting a crankshaft—connecting rod interface material that will embed fine particles, and not gall. Other engines, which have do not have an aluminum connecting rod, incorporate aluminum (or other non-ferrous material) shell liners to address FR4.1.2. As this connecting rod is fabricated from aluminum, this is not an issue here.

Functional requirement FR4.3 is broken down into two more layers to correlate the FRs and DPs for the various features associated with the lubrication system. There are internal and external lubrication features. The oil holes introduce oil for the hydrostatic bearing between the connecting rod and the crankshaft at the centre of the big end bore. The oil hole chamfer aids in collecting and channelling the oil that pools in the weight saver pocket. The oil hole geometry size must be balanced between the oil flow requirements and weakening the neck. The rib chamfer provides an external flow path. Where there are clearance grooves in the big end bore at the junction of the cap and rod, there are surface grooves on the face of the big end boss, as well as surface grooves aligned with the oil holes. These grooves also assist with the channelling of the lubricating oil. The oil splasher stirs oil to lubricate the internal components within the engine. It is offset to prevent interference with other components, and has a large fillet radius in the direction of motion to provide extra strength. These functional requirements and design parameters are summarized in Table 5-14.

Table 5-14: Decomposition of FR4.3 (FR and DP Prefix '4.3.' eliminated for clarity)

	DPs	Oil hole size	Oil hole position/ orientation	Oil hole chamfer angle	Oil hole chamfer depth	External chamfer on big end boss	Groove position on big end boss chamfer	Grooves width on big end boss chamfer	Oil stirrer length	Oil stirrer depth offset	Oil stirrer blend fillet
FRs		**1.1**	**1.2**	**1.3**	**1.4**	**1.5**	**1.6**	**1.7**	**2.1**	**2.2**	**2.3**
Provide internal flow path	1.1	X									
Locate internal flow path at center of the hydrostatic bearing	1.2		X								
Channel oil from atmosphere (cavity)	1.3			X	X						
Minimize material removal in neck	1.4			X	X						
Provide general external flow path	1.5					X					
Provide specific external flow path zone at areas of high flow / clearance	1.6						X	X			
Limit flow at the specific external flow path zones	1.7						X	X			
Contact the oil sump	2.1								X		
Do not interfere with other components	2.2									X	
Strong in direction of rotary motion	2.3										X

The data contained in the design recovery framework is correlated to the Axiomatic Design FRs, and DPs to compare the results for the two methods. The features, their FRs, the Axiomatic Design FR decomposition identifier, the DP descriptions and their identifiers are mapped in Table 5-15. The highlighted features have multiple FRs and DPs that were not clearly defined during the initial design recovery process. Using the Axiomatic Design methodology rigorously clarified the coupling for several features.

Table 5-15: Mapping the Design Recovery Feature to the Axiomatic Design Decomposition

Feature	FR	AD FR	DP Description	AD DP
Small end bore	Interface to piston	1.1	Bore shape	1.1
	Clearance	4.2	Bore size	4.2.1
	Smooth surface	4.1	Bore surface finish	4.1.1
Small end boss	Interface to piston	1.1	Boss shape	1.1
Small end chamfer	Ass'y guide	1.1.1	Chamfer shape	1.1.1
Neck	Position piston to the crankshaft	1.3	Neck length	1.3
	Prevent buckling	2.1	Neck general shape, including the length	2.1
	Prevent flex	2.2	Boss shape on neck	2.2.1
	Reduce side thrust	2.3	Neck length	2.3
Cap	Prevent flex	2.2	Boss shape on cap	2.2.2
Weight savers	Reduce inertial mass	3.2	Weight saver shape	3.2
Oil lubrication holes	Transport oil	4.3.1.1 – 4.3.1.4	Oil hole parameters	4.3.1.1 – 4.3.1.4
Big end boss	Interface to crankshaft	1.2	Shape	1.2
Big end bore	Interface to crankshaft	1.2	Bore shape	1.2
	Clearance	4.2	Bore size	4.2.2
	Smooth surface	4.1	Bore surface finish	4.1.2
Oil stirrer	Transport oil	4.3.2.1 – 4.3.2.3	Stirrer parameters	4.3.2.1 – 4.3.2.3
Chamfer	Transport oil	4.3	Chamfer parameters	4.3.1.5
Oil grooves	Transport oil	4.3.1.6 – 4.3.1.7	Groove parameters	4.3.1.6 – 4.3.1.7
Orientation boss	Ass'y feature to match mark rod and cap	1.4.4	Feature shape that is common on both the cap and rod	1.4.4
Split	Ass'y feature	1.4.1	Feature tolerances: flatness, surface finish, and orientation	1.4.1.1
Mounting faces	Position cap onto the rod	1.4.1	Feature tolerances, flatness, perpendicularity	1.4.2
Bolt holes	Position cap onto the rod	1.4.1	Feature tolerances: Perpendicularity to mounting faces, Concentricity to tapped portion	1.4.1.2
	Join cap onto rod	1.4.2	Threaded fastener	1.4.2
	Retain cap during usage	1.4.3	Torque level on threaded fastener	1.4.3

5.4.3 Incorporating Potential Design Improvements for the Connecting Rod

From the design recovery framework, the neck and mounting bolt holes are quickly highlighted as features that perform multiple functions. Using the Axiomatic Design

methodology, this coupling is clarified. Other couplings are highlighted, such as the coupling between the big end bore and the assembly features. Some features, such as the oil lubrication holes, perform many sub-functions that were not specifically identified during the design recovery process. Another level of detailed analysis is needed to be performed to link the observed DPs to FRs. This is done when constructing the Axiomatic Design matrix in a rigorous manner.

To develop a design capable of sustaining the forces while reducing the inertia, iterative analysis is typically performed for the neck and weight reduction geometry, as the shape, material and manufacturing processes are highly coupled. (The achievable wall thickness and the fillet geometry are limited by the chosen manufacturing process). The common neck / weight saver shape consists of an H beam or an I beam. Several designs have been developed to maximize the strength to weight ratio [Heisler, 1999], [Mrdjenovich and Yeager, 1992]. However, multiple material connecting rods would combine the strength of one material with the light mass of another. Yoon and Kim [1994] have incorporated a stainless steel mesh in an aluminium connecting rod to decouple the weight and strength FRs.

There are common design alternatives to decouple the location, joining and retention of the cap to the connecting rod. A sample of these methods are: locating the cap using dowel pins, incorporating oblique cut with a locating detail, or incorporating a tongue and groove detail. These options introduce extraneous components and extra process steps. However, these features locate the cap and rod elements independently from the joining features. Locking devices such as a nut could be added to ensure the cap is retained during usage; however, an extra face needs to be machined (a spot-face into the shoulders of the rod) to locate the nut or bolt head. Care must be taken to ensure that the spot face operation does not generate a failure point within the connecting rods. The fastening system can be placed at an oblique angle, or an alternative fastening system, which incorporates a tension band to enclose the rod and cap, may be implemented. This alternative has by proposed by Beckmann and Oberg [1988]. These alternatives introduce an extra process steps; however, the location, joining and retaining FRs are decoupled with these design strategies.

The neck length parameter is coupled to several FRs. The neck length can be effectively increased without adding mass by altering the connection with the piston. The piston

connection is design as an arced track slot. A rider pin, which connects to the connecting rod small end, is guided by the piston track. Therefore, both ends of the connecting rod oscillate [Towler, 2003]. This design concept for the connecting rod effective length was generated by considering the system as a whole.

The analysis with respect to the lubrication aspects of the design could be extended to the microscopic level. By studying the coupling between the lubrication oil viscosity and journal bearing design parameters, Hirania and Suh [2005] have determined that improved hydrodynamic lubrication can be established by incorporating microgrooves, which retain oil, or by generating a surface that reduces particle agglomeration.

The appropriate solution depends on the context of the application, as there are various levels of effort that must be applied at the process level in order to produce the DPs that satisfy the FRs. Other design quantification tools, such as the product complexity assessment tools developed by ElMaraghy and Urbanic [2003, 2004] are necessary to determine a suitable resolution.

5.4.4 Complexity Analysis for the Connecting Rod

The complexity analysis for the original connecting rod is shown in Table 5-16. Each feature is enumerated and associated with a feature type. The feature codes and relative complexity values $c_{feature}$ are developed in Table 5-16 (a) and the feature and component complexity calculations are demonstrated in Table 5-16 (b).

The connecting rod is cast to the near net shape. Finish machining is required for the precision and fastening features. There are six feature sets being considered. For the component complexity analysis: $N = 12$ and $n = 7$. The sum of $N^{*}factor = 102$, hence $H = 6.687$. The diversity ratio $D_R = 0.583$ and the relative complexity coefficient = 0.20. This provides a product complexity index $C_{Iproduct} = 5.25$.

If alternative manufacturing processes are being considered, such as machining the complete part, all features must be included and assessed.

Table 5-16 (a): Individual Feature Codes and Complexity Aspects for the Connecting Rod

Feature Label	Feature Type	N	n	Basic	Type	Material	Shape	Pattern	Tolerance	Surface Finish	Spatial Relations	Sum of Fields 5 - 10	Average of Fields 5 - 10
Small end bore	Precision features	1	1	1	10	0	0	0	0.5	0.5	0	1	0.167
Oil lubrication holes	Container feature	2	1	2	3	0	0.5	0.5	0	0	0.5	1.5	0.250
Big end bore	Precision feature	1	1	1	10	0	0.5	0	0.5	0.5	0	1.5	0.250
Split	Planar surfaces	4	2	1	8	0	0.5	0	0.5	0.5	0	1.5	0.250
Mounting faces	Planar surfaces	2	1	1	8	0	0	0	0.5	0	0	0.5	0.083
Bolt holes	Fastening features	2	1	2	5	0	0.5	0	0.5	0	0	1	0.167

Table 5-16 (b): Feature and Component Complexity Analysis for the Connecting Rod

Feature Label	Feature Type	N*factor	H, feature	DR, part	c, feature	CI feature	Weighted c, feature
Small end bore	Precision features	10	3.459	(Sum of n) / (N)	0.167	0.577	0.014
Oil lubrication holes	Container feature	20	4.392		0.250	1.098	0.042
Big end bore	Precision feature	10	3.459		0.250	0.865	0.021
Split	Planar surfaces	28	4.858		0.250	1.214	0.083
Mounting faces	Planar surfaces	14	3.907		0.083	0.326	0.014
Bolt holes	Fastening features	20	4.392		0.167	0.732	0.028
	Sum	**102**	**6.687**	**0.5833**			**0.201**
	Complexity Index: product		**5.247**				

The average relative effort for the attributes is plotted in Figure 5-12. The effort associated with producing the product to the required tolerances and surface finish is moderate (0.42 and 0.25 respectively). No other attributes are a concern.

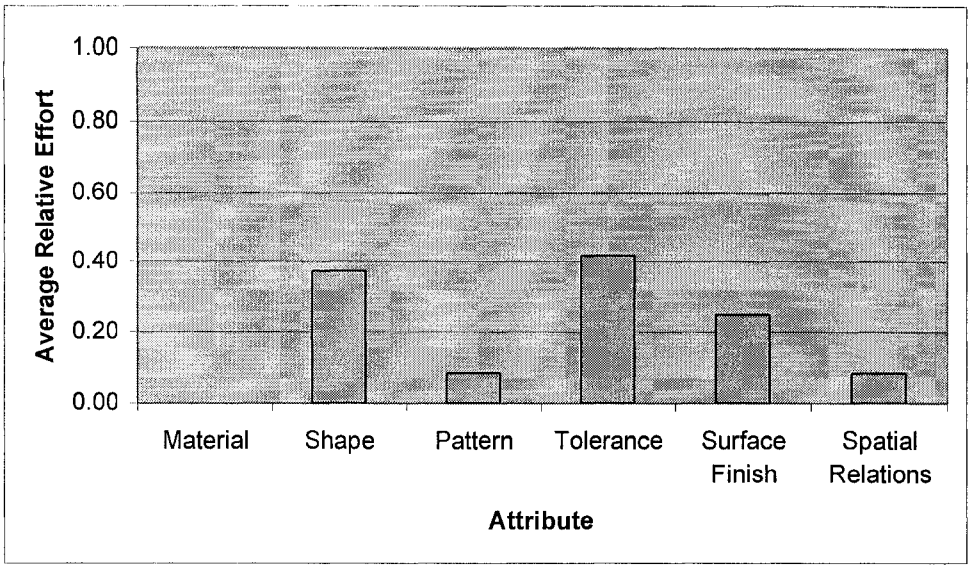

Figure 5-12: A Comparison of the Relative Effort for each Attribute for the Base Connecting Rod

If dowel holes and locking nuts are included, additional machining is required. Incorporating these features, a modified small end piston interface slot (arced slot) as suggested by Towler [1993], and multiple materials as presented by patent Yoon and Kim [1994] higher individual feature complexity indices (bolded text) and a much higher product complexity index results. For the product complexity analysis, the sum of $N^{*}factor$ = 132, hence H = 7.055. The diversity ratio D_R = 0.563. The relative complexity coefficient = 0.38, which provides a product complexity index $CI_{product}$ = 6.65 (Table 5-17 (b)).

As shown in highlighted cells in Table 5-17 (a), the non-standard precision hole and the material aspects are assigned much higher values. Specialized tools are necessary to produce the special small end interface slot. Different tool geometries and cutting parameters are required for aluminum and stainless steel metal removal. The relative effort for each attribute for the modified connecting rod design is illustrated in Figure 5-13. The material attribute stands out as being problematic. This material combination is not common in industry, and specialty tools and process operations would have to be developed in order to generate the desired geometry and surface finish consistently and in a cost effective manner. There are some moderate issues with the shape as well as the tolerances and surface finish. The results from the attribute analysis highlight the general product characteristics and potential areas of concern.

Table 5-17 (a): Individual Feature Codes and Complexity Aspects for the Modified Connecting Rod

Feature Label	Feature Type	N	n	Basic	Type	Material	Shape	Pattern	Tolerance	Surface Finish	Spatial Relations	Sum of Fields 5 - 10	Average of Fields 5 - 10
Small end specialty hole	Precision features	1	1	1	10	1	1	0	0.5	1	0	3.5	0.583
Oil lubrication holes	Container feature	2	1	2	3	1	0.5	0.5	0	0	0.5	2.5	0.417
Big end bore	Precision feature	1	1	1	10	1	0.5	0	0.5	1	0	3	0.500
Split	Planar surfaces	4	2	1	8	1	0.5	0	0.5	1	0	3	0.500
Mounting faces	Planar surfaces	4	2	1	8	1	0	0	0.5	0	0	1.5	0.250
Bolt holes	Fastening features	2	1	2	5	1	0	0	0.5	0	0	1.5	0.250
Dowel holes	Locating features	2	1	1	7	1	0.5	0	0.5	0	0	2	0.333

Table 5-17 (b): Feature and Component Complexity Analysis for the Modified Connecting Rod

Feature Label	Feature Type	N*factor	H, feature	DR, part	c, feature	CI feature	Weighted c, feature
Small end specialty hole	Precision features	10	3.459	(Sum of n) / (N)	**0.583**	2.018	0.036
Oil lubrication holes	Container feature	20	4.392		**0.417**	1.830	0.052
Big end bore	Precision feature	10	3.459		**0.500**	1.730	0.031
Split	Planar surfaces	28	4.858		**0.500**	2.429	0.125
Mounting faces	Planar surfaces	28	4.858		0.250	1.214	0.063
Bolt holes	Fastening features	20	4.392		0.250	1.098	0.031
Dowel holes	Locating features	16	4.087		0.333	1.362	0.042
	Sum	**132**	**7.055**	**0.5625**			**0.380**
	Complexity Index: product		**6.651**				

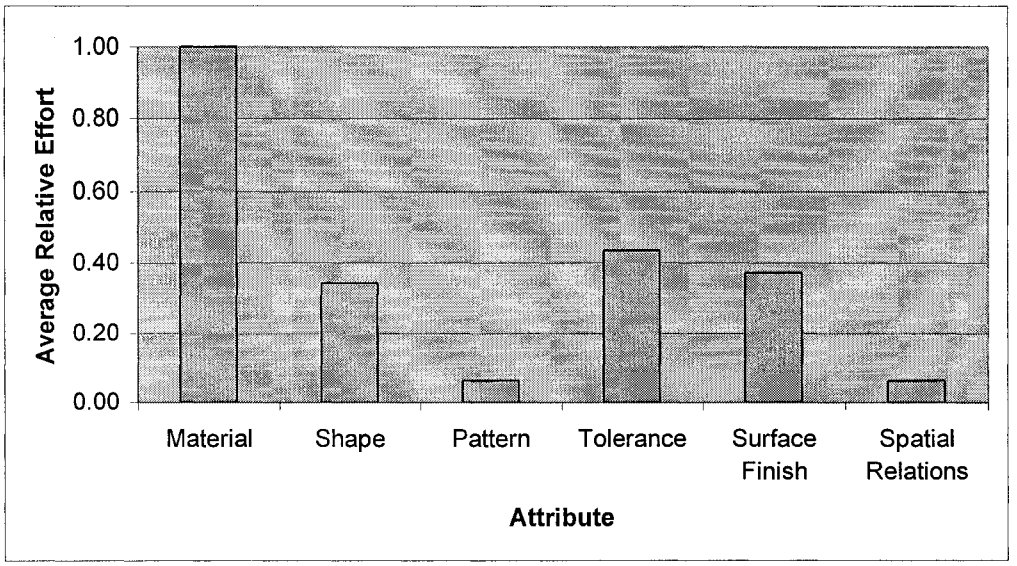

Figure 5-13: A Comparison of the Relative Effort for each Attribute for the Modified Connecting Rod Design

5.5 CASE STUDY 5: TIMING SCREWS

5.5.1 Introduction

Cams and variable pitch screws are used to change motion. A cam is a rotating lobe or eccentric device that is used with a cam follower. The cam's input rotary motion is transformed into the reciprocating motion of the follower. There is a specific displacement response based on the angular position of the cam, and a typical application is a rise-dwell-return sequence for a plate or disk cam. Variable pitch screws are used in metering and bulk material handling applications. Timing screws are subsets of variable pitched screws, and are used in high volume material handling applications. They interface with filling, capping, labelling and pressure testing machines. The variable pitch causes containers being moved to accelerate or decelerate to a different velocity or dwell in position. Understanding the FRs is essential in order to reverse engineer the critical geometry for a variable pitch timing screw. A timing screw example is illustrated in Figure 5-14.

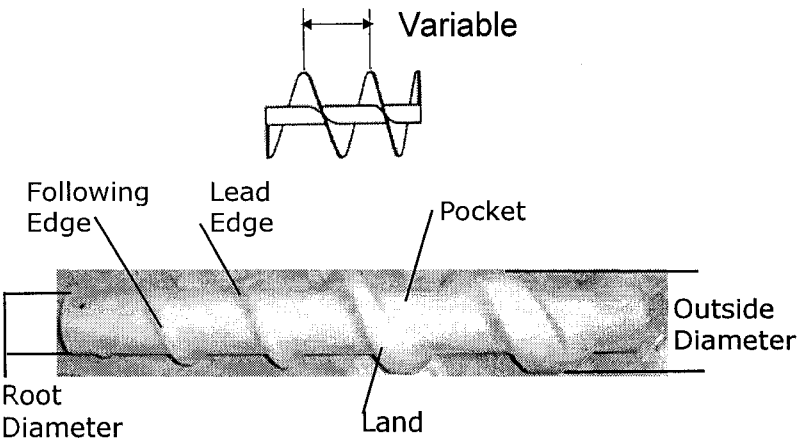

Figure 5-14: Variable Pitch Screw Terminology

Variable pitch screws can be considered a variation of a cylindrical or spatial cam, and the cam follower is represented by the container being conveyed. The displacement geometry for this family of cam applications is a result of a desired container spacing, velocity and / or acceleration profile. The designer needs to determine the response characteristics, and then the rotary element of the geometry is constructed to suit. In several instances, formal design principles are not considered during the design, manufacturing and inspection of these variable pitch screws. The result is undesirable motion characteristics.

The design recovery framework is used to capture the timing screw characteristics at the component level. The reverse engineering methodology for rotary components developed by Urbanic et al [2006] is modified to assist with the design recovery. Axiomatic design is used to concisely define and isolate the FRs and DPs.

5.5.2 Design Recovery Assessment for a Velocity Control Timing Screw

Timing screws consist of a threaded form on a cylinder. The container being handled rides in the groove or pocket formed between the threads. Unlike fastening screws or ball screws, which have a constant pitch, timing screws have a variable pitch for container separation or other reasons. Designs have been developed to accelerate, decelerate, halt or position containers for a specified period. The timing screw can be used to divide or combine containers from different sources or discharge containers in a controlled fashion into the appropriate stations of a processing machine. This is not being considered in this analysis; here the focus is on changing the velocity.

The linear velocity of the containers is governed by the rotary speed of the shaft and the pitch distance:

$$Linear\ velocity = RPM*pitch \tag{5.5 a}$$

where RPM is the number of revolutions per minute, and

$pitch$ is the distance travelled per 360° of rotation (mm)

The linear velocity can be changed by varying the pitch in a controlled manner. The RPM is constant; therefore, the linear velocity can be expressed as:

$$Linear\ velocity \propto \frac{\Delta pitch}{\Delta angle} \tag{5.5 b}$$

The timing screws and the containers interface with adjacent machines and other automation. Therefore, there are lead-in and lead-out considerations. The containers must not be damaged during transfer. The changes in velocity must be smooth, and the pockets must enclose the containers in order to reduce perturbations. The high resolution analysis is summarized in Table 5-18.

Table 5-18: High Resolution Timing Screw Summary

Component: Variable Pitch Timing Screw - velocity control				
	What	**How**	**Where**	**Why**
	Data	Function		Motivation
Contextual	High volume motion control	Specialty designed screw mechanism	Material handling line - fluid containers	
Conceptual	Increase or decrease velocity smoothly Enclose container to minimize rattle and shaking Interface with adjacent sections in a controlled fashion	Modify the pitch to control timing for specialty designed pockets for unique container shapes Introduce lead-in/out geometry		
Logical	Channel - transfer - transport	Lead-in / Lead-out chamfer or radial control features in order to interface with adjacent sections without damaging the containers		Provide the smooth flow of containers into or between packaging, labelling, filling, capping or leak detection machines
	Convert - transform motion - rotary to translational	Container enclosed in ball screw pocket with predetermined clearances		
	Control Magnitude - regulate	Utilized a 'modulated' frequency pitch to smoothly change the velocity to the desired requirements		

The timing screw material may be nylon, PTFE (polytetrafluoroethylene or Teflfon®), other similar plastics or steel. The pockets are machined from cylindrical bar stock. The part datum features are the shaft centre line and end faces. The pocket geometry and any tapers (typical lead in geometry) may be reconstructed by analysing the 2D geometry in the top view. The motion characteristics (such as displacement, velocity and acceleration) must be ascertained from the general pocket form. In order to do this, the point cloud data needs to be transformed using an 'unroll/unwind' function, which is described in the next section. The physical and detail viewpoints are summarized in Table 5-19.

Table 5-19: Low Resolution Timing Screw Summary

Component: Variable Pitch Timing Screw - velocity control					
	What		How	Where	Why
	Data		Function	Interconnections (Network)	Motivation
Physical	Material	Nylon, PTFE, Steel			Impact and corrosion resistant, natural lubrication Manufacturability
	Envelope	N/A		Centre shaft Incoming automation Outgoing automation Container Interacting machine	
	Form initial	Cylindrical stock			
	Form final	3D-3D - 'free form' rotary design	Machined		
Detail	Stock	Standard diameter / segment length			
	Shape	Top View: Taper, Pocket		**Set z=0 for all data points to capture profile**	
		Centre hole / shaft		Match interfacing features	
		Variable Pitch: **determine by analysing the velocity profile**		**Unroll/Unwind procedure**	
	Datum	Centreline -A- Front / Rear Faces, -B- & -C- (as labelled)			

5.5.3 Reverse Engineering of Rotary Components

When collecting data for reverse engineering, contact or non-contact scanning techniques are used to collect point cloud data to represent the component of interest. The scanned point cloud data is used as a template or guide to extract wire frame geometry representing the form and shape of the component. Non-contact laser scanning techniques produce data sets with limited order in the data set and there is no organization among the points. The part may also be in a random orientation in space during the data collection process; hence, the first step consists of preparing the data for subsequent analysis. The point cloud data must be aligned, the points sorted, and the data transformed by 'unrolling' and 'unwinding'.

For a component that has a rotary profile, the central axis of the point cloud should be positioned along the x-axis at $y = 0$. The rotational cross section should be in the side view (Figure 5-15).

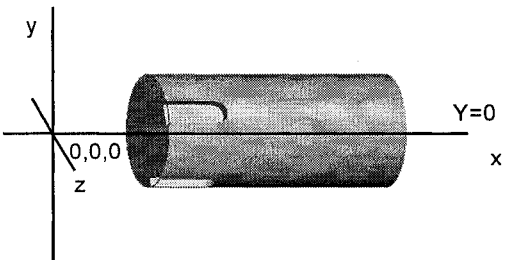

Figure 5-15: Rotary Component Alignment.

Upon completion of the alignment, the data must be sorted (sort order: z first, y second, x third). Then point cloud is 'unrolled' around the x-axis (Figure 5-16) using the following equations. The result is then analysed in the three orthogonal views.

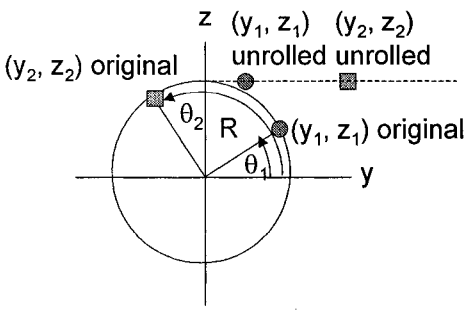

Figure 5-16: Relationship between Rolled to Unrolled Points.

$$x_{unrolled} = x_{rolled} \tag{5.6}$$

$$y_{unrolled} = cal\_rad_{\max} * cal\_angle \tag{5.7}$$

$$z_{unrollled} = cal\_rad \tag{5.8}$$

$$cal\_rad = \sqrt{y^2 + z^2} \tag{5.9}$$

$$cal\_angle = \arctan\left(\frac{y}{z}\right) \tag{5.10}$$

The angle calculated in equation 5.10 is adjusted to fall between 0 and 2π based on the quadrant in which the data points are located. The unroll 'control' radius is usually the maximum calculated radius value. It is the minimum value in very specific applications, such as unrolling a cam with a radial follower. Wire frame geometry is then fit to the transformed points and the model reconstructed as discussed in Urbanic et al [2006].

The 'unroll' function only considers angles between 0 and 2π, which is unsuitable for a variable pitch ball screw that contains more than one full revolution. Hence, an 'unwind' function, which increments the angle and the y distance appropriately, must be introduced for this geometry. For the unwind algorithm, the points are unrolled using equations 5.6 – 5.10 and whenever there is a periodic change from the maximum value of y to 0, (and a positive increment in x) the calculated angle *cal_angle* is incremented by 2π. The unwound value of y increases by discrete increments using a difference expression, as expressed by equation 5.12.

$$cal\_angle = \arctan\left(\frac{y}{z}\right) + n2\pi \tag{5.11}$$

where n is the periodic change count

$$y_{unwound} = \sum_{i=2}^{I} y_{i-1} + abs(y_i - y_{i-1}) \tag{5.12}$$

The difference between the unroll and unwind transformation is illustrated in Figure 5-17 for a constant pitch thread (4mm pitch).

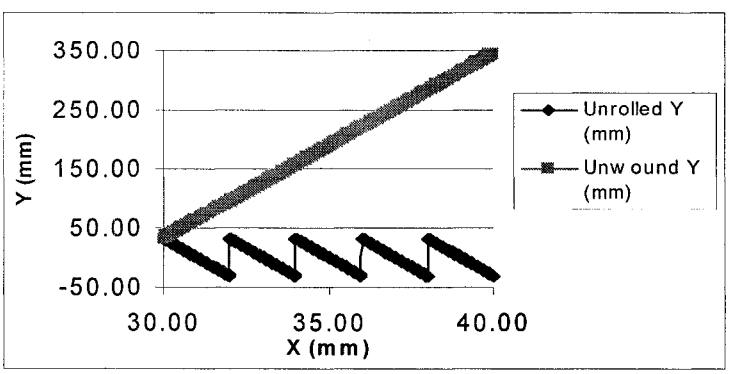

Figure 5-17: A Comparison of the Unrolled to an Unwound Helix Curve.

The variable pitch screw illustrated in Figure 5-14 is now considered. This component could not be used in its designated material handling application due to the damage caused to the containers. The geometry is measured and 'unwound' using the transformation procedure described above, and the velocity is calculated from the 'unwound' displacement data. The control radius (root diameter) is 33 mm. The measurement error is within +/- 0.5 mm.

The unwound displacement for the screw is plotted in Figure 5-18. The calculated the velocity (using equation 5.5b) is illustrated in Figure 5-19. The calculated incoming velocity is approximately 0.2 mm/degree. The velocity is increasing; however, there are significant oscillations. The displacement curve appears to be parabolic between 180° to 1350°. The best fit curve through the relevant points and the resulting correlation coefficient are:

$$y = 9.42E\text{-}05*x^2 + 0.17*x + 45.22,\ R^2 = .9996 \qquad (5.13)$$

where y is the displacement in mm, and

x is the angle, in degrees.

The discrepancies between the measurement data and the best fit model for the inside edge of the pocket are in the order of +/- 3 mm.

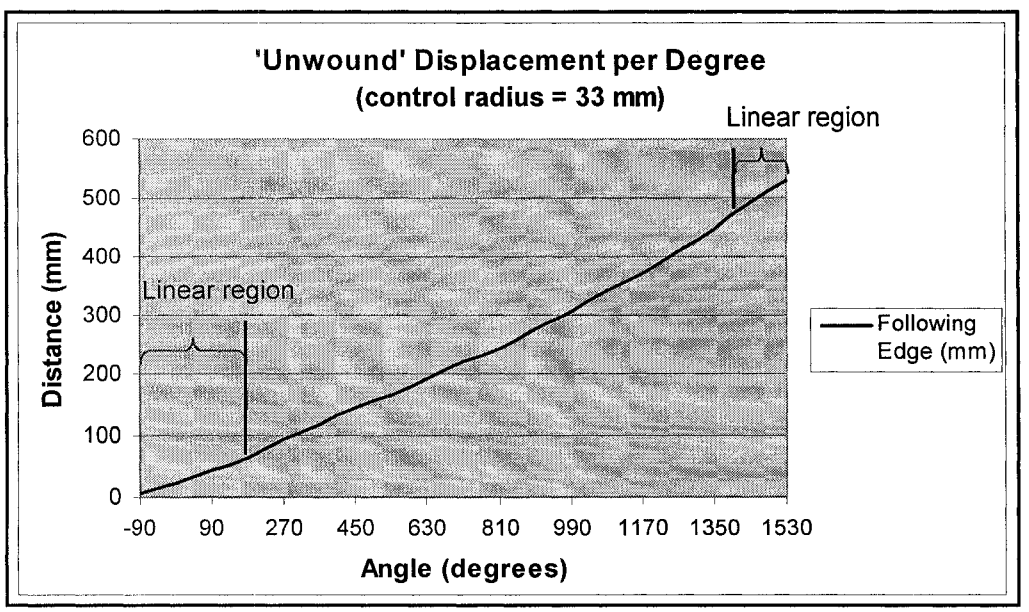

Figure 5-18: Variable Pitch Displacement Diagram.

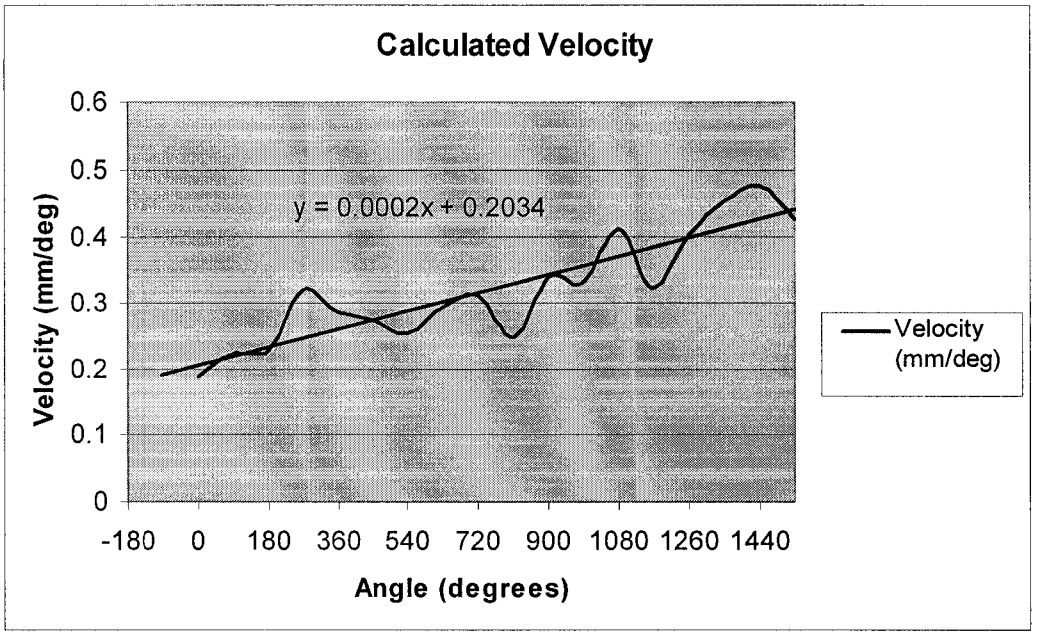

Figure 5-19: Calculated Linear Velocity.

The calculated velocity is not smooth and continuous. Axiomatic Design methods are used to determine the functional requirements for this application and to assist with establishing formal design parameters to address these requirements. A review of common cam profiles is performed in order to determine the cam profile that satisfies the functional requirements. The reverse engineering techniques described above are modified to in order to develop a complete procedure to generate a desired CAD model and inspection method for this type of variable pitch ball screw.

5.5.4 Timing Screw Design Functional Requirements

For this application, the main functional requirement of the variable pitch timing screw is to alter the linear velocity of the item being conveyed. There are several constraints: (i) the change in motion must be transformed smoothly within a given screw length, (ii) the timing screw must interface with the adjacent automation or machinery, (iii) the containers should not be damaged while in motion or at interface junctions, (iv) any the pocket self intersection (i.e. the minimum lead distance is greater than the pocket size) must be controlled, (v) the methodology should be independent of the pocket profile, and (vi) this should be a low cost solution. The component level design characteristics are summarized as:

***FR0**: Mechanism to alter linear velocity*

***DP0**: Variable pitch ball screw system*

C1: Smooth, continuous motion

C2: Contained within a given screw length

C3: No container damage

C4: Controlled pocket self intersection

C5: General solution methodology

C6: Low-cost

For a smooth transition between the ball screw interfaces, the start and finish pitch distances should be designed to match the linear input and output velocities, or the fixture spacing for an interfacing machine. The item being transported should undergo no (or minimal) acceleration at the transition zones (FR1). This is achieved by implementing regions with a constant pitch (DP1). To change the linear velocity smoothly (FR2), the pitch frequency must be modulated in a controlled manner (DP2) to achieve the desired motion characteristics. If the containers are collated in a group at the entrance interface, each package (or cluster) must be transferred into the timing screw pockets (FR3). Lead in geometry is required (DP3). There should be limited motion within the pocket (FR4); consequently, the form of the container (with appropriate clearances) should be used for the pocket design (DP4). The final design needs to be verified (FR5). Reference marks for alignment need to be incorporated in the design to provide reference datum lines for measuring the relevant motion characteristics (DP5). The first level FRs are summarized in Table 5-20. FR2 must be further decomposed to isolate the desired velocity characteristics.

Table 5-20: Decomposition of First Level FRs

		Design Parameters				
		DP1: constant pitch zones	DP2: variable pitch zone	DP3: lead in geometry	DP4: model to proportion pocket	DP5: control markers
Functional Requirements	FR1: No acceleration at transition zones	X				
	FR2: change velocity	X	X			
	FR3: smooth transfer into pockets	X		X	X	X
	FR4: control container perturbations			X	X	X
	FR5: qualify final component design			X		X

To change the velocity smoothly, and have a 'zero' acceleration value at the initial and final velocities (FR2.1), the acceleration curve must undergo a rise-fall type pattern (DP2.1). To reduce the sensitivity to external disturbances (e.g. variations with the rotational velocity) and to prevent container tipping, minimal peak acceleration is desired (FR2.2). Hence, the acceleration curve should have a 'trapezoidal shape', or a curve with a flat plateau (DP2.2). This is presented in Table 5-21.

Table 5-21: Decomposition of FR2

		Design Parameters	
		DP2.1: rise-fall type acceleration curve	DP2.2: acceleration curve with plateau
Functional Requirements	FR2.1: change velocity with no initial or final acceleration	X	
	FR2.2: minimize peak acceleration		X

FR3 and FR4 are coupled and a design contradiction exists between these two functional requirements. Increasing the clearances increases the ease of capturing a container, but also allows the container to shift or tip within the pocket. These FRs must be further decomposed to isolate the controlling design parameters, and resolve the contradiction. The lead in geometry features must occur in a designed transition zones. FR3 decomposed into:

FR3.1 – separate containers, and

FR3.2 – guide container into pocket.

The design parameters for these FRs are:

DP3.1 – incorporate a lead-in taper

DP3.2 – incorporate a chamfer and additional clearance onto the pocket form

Once the container has been captured, the container can be enclosed in a form fitting pocket to reduce any shifting within the pocket (FR4).

When designing cams, the synthesis of the cam profile is dependent on the cam follower type. Here it is assumed that the material being conveyed is equivalent to radial roller follower, and the desired motion characteristics can be designed in the 2D domain and transformed into the desired 3D model using the unroll-unwind methodology.

5.5.5 Standard Cam Profiles

Several standard displacement profiles are used for cam design. Common types are the parabolic curve, modified constant velocity curve, simple harmonic curve, cycloidal curve, the modified trapezoidal curve, and the 3-4-5 polynomial [Erdman and Sandor, 1984]. A relatively unknown displacement curve is the 'third harmonic' curve, which is a modified cycloidal curve [Parmley, 2000]. Each type has its advantages and disadvantages. The primary concerns in this research are the acceleration and jerk characteristics.

The parabolic curve produces the lowest maximum acceleration; however, it produces an abrupt change from the positive to the negative acceleration. This phenomenon is called 'infinite jerk', and can cause transient shock waves due to the high inertial forces that may be destructive [Parmley, 2000]. The modified constant velocity curve avoids the infinite accelerations and the beginning and of the rise; however, there are still undesirable abrupt changes in acceleration at the beginning and end of its cycle. This is also true for the simple harmonic motion. The cycloidal curve has no abrupt changes in acceleration, finite jerk limits, and gives low vibration, noise, and shock; however, the peak acceleration level is the highest of the techniques describes so far. To address this concern, the modified trapezoidal curve has been developed, which is typically a piecewise combination of cycloidal and parabolic motion. Polynomial curves, such as the '3-4-5 polynomial' can be used to generate custom designed motions, but may be cumbersome to implement an analytical solution [Erdman and Sandor, 1984]. The third harmonic curve contains a small third-harmonic component in the cycloidal curve to reduce the peak acceleration to 1.28 times the parabolic peak, essentially flattening the curve. The cycloidal peak acceleration is about 1.57 times that of the parabolic peak [Parmley, 2000]. A comparison of the parabolic, cycloidal and third harmonic acceleration curves illustrated in Figure 5-20, where:

Parabolic acceleration: $\ddot{y} = 2\frac{h}{\beta^2}$ (5.14)

Cycloidal acceleration: $\ddot{y} = \frac{h\pi}{\beta^2}\sin\left(\frac{\pi\theta}{\beta}\right)$ (5.15)

Third harmonic acceleration: $\ddot{y} = \frac{h\pi}{\beta^2}\left[\frac{15}{16}\sin\left(\frac{\pi\theta}{\beta}\right) + \frac{3}{16}\sin\left(\frac{3\pi\theta}{\beta}\right)\right]$ (5.16)

Where h is the rise height,

θ is the rotation angle, and

β is the total rotation angle.

These equations describe the motion characteristics for a 2D cam. However, for a 2D cam, β equals a value between 0 and 2π; whereas for a timing screw, the value of β may be greater than 2π. The total rotation angle is dictated by the length of the screw and the design parameters.

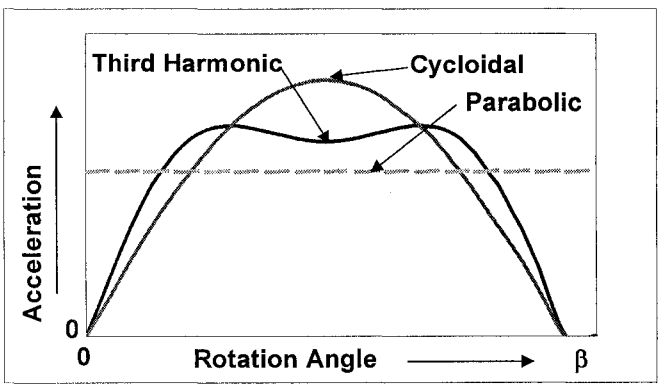

Figure 5-20: Acceleration Curves Used in Cam Design

There should be a constant pitch lead in and lead out zone, which reduces the available variable pitch length (Figure 5-21). Therefore, the parameters to develop a controlled variable pitch timing screw are:

- Input RPM (revolutions per minute)

- Input pitch spacing (distance per 360°), or input velocity (mm/degree), v_{in},
- Output pitch spacing (distance per 360°), or output velocity (mm/degree), v_{out}
- Screw Length (mm), L
- Lead in zone (degrees), l_in
- Lead out zone (degrees), l_out

Given this information, acceleration, velocity and displacement profiles can be generated. From the displacement profile, pocket geometry can be created. This geometry is then modified to satisfy FR3.

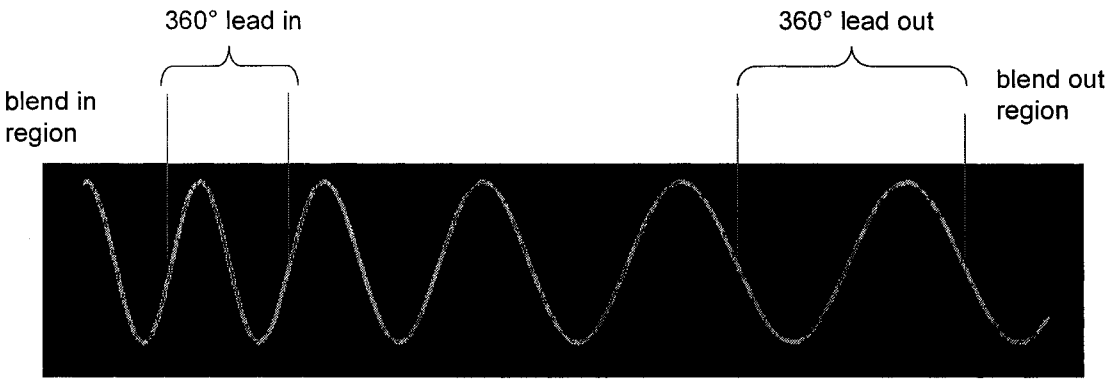

Figure 5-21: Variable Frequency and Transition Zones (Top View)

5.5.6 Timing Screw Pocket Design

The container geometry acts like a template for the pocket geometry. Pocket self intersection occurs if the pocket geometry length is greater than lead in pitch. Controlling the pocket self intersection via a variable pocket chamfer allows a container to be guided into the pocket. The chamfer morphs into the final desired pocket geometry over the length of the lead in transition zone using existing surface modelling tools. An example is shown in Figure 5-22.

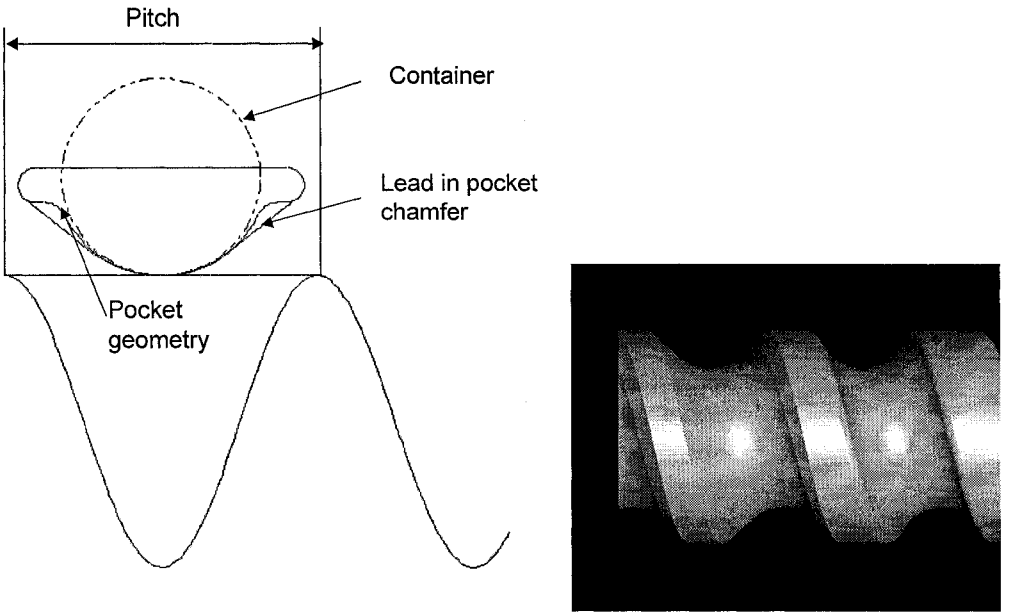

Figure 5-22: Variable Pocket Geometry.

A lead-in taper could also be incorporated in order to extract the containers (Figure 5-23) by trimming the CAD model to a control surface between 0 and 4π radians (typical for cylindrical containers).

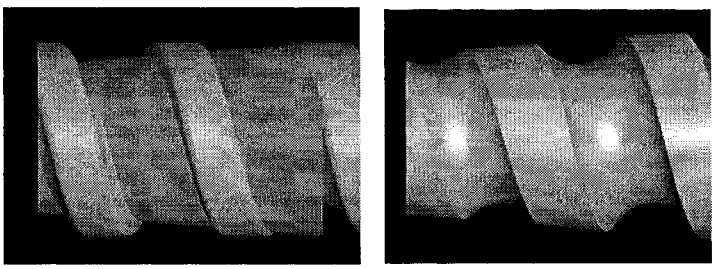

Figure 5-23: Incoming Taper Design and Timing Screw with Lead in Taper

To satisfy FR5 (qualify final component design), linear etch marks, parallel to the central axis, need to be incorporated on outside diameter at 90° intervals. These etch marks are used to orient the timing screw for the data collection and 'unwind' point cloud data transformation.

To summarize, by performing the design recovery tasks in a comprehensive manner, the motion characteristics of these timing screws are determined from the form. The methodology

developed to extract the critical design characteristics for the form-function link has been leveraged to develop formal engineering design guidelines and inspection tools for timing screws. The complete design and inspection process, developed by combining the design recovery framework and the Axiomatic Design methodology, is presented in Appendix F.

5.6 SUMMARY

The developed design recovery framework complements the Axiomatic Design methodology, and the transition between the two approaches is made in a transparent manner. Within the design recovery framework, the product and feature functions and FRs are concisely defined at the 'Logical' viewpoint, and the DPs can be extracted from the 'Physical' and 'Detail' viewpoints. The Axiomatic Design methodology considers features as the physical parameters necessary to realize a specified functional requirement. The necessity of assessing a design with respect to the functional requirements is emphasized with the timing screw example, as the shape of variable pitch form is driven by the desired motion characteristics. Upon generating the Axiomatic Design matrix from the design recovery framework in a rigorous manner, details that may have been over looked in the initial analysis are extracted and included as appropriate. If the design matrix is not square, then further analysis is required to refine the FR and DP relationships. Structuring the design recovery information in this manner allows the designer to determine whether Axiom 1, the independence axiom, has been satisfied in the design, and provides a rational basis to support subsequent design changes. It is challenging to determine whether Axiom 2, the information axiom, is satisfied. One must have a clear understanding of the environment and the context of the component of interest in order to evaluate Axiom 2, as Axiom 2 states that the design with the highest probability of success is the best design. For example, a connecting rod forged or machined from titanium offers the highest strength-to-mass ratio; however, the material cost is prohibitively expensive, and specialized tooling is required for the manufacture. The 'best' design must meet the FRs; however, there may be cost and process limitations that have to be considered.

The DPs that satisfy the FRs may consist of material properties, the feature shape or specific tolerance characteristics. There are various levels of effort which must be applied at the process level in order to produce the DPs that satisfy the FRs. There are several tight tolerances on the connecting rod which are directly associated with the FRs, such as the split

line surface finish and flatness, and the big end bore cylindricity and the surface finish. These issues can be overcome with proper process planning and production control, but independent of the volume, these challenges exist. The volume requirements influence the nature of the solution, but the complexity issues that need to be addressed are inherent with the design of the part. ElMaraghy and Urbanic [2003] developed a framework and heuristic complexity indices in order to assess the complexity of a product in a simple, concise manner. By introducing a standardized coding system, the feature and component complexity can be quickly quantified. The complexity indices and the general attribute analysis can also be used as a basis for a process FMEA, or to highlight areas where feasibility studies and process benchmarking should be performed.

There may be design contradictions that need to be resolved (e.g. the connecting rod neck length, as presented in Table 5-13), or there may be uncertainty with the design relationships between the hypothesized FRs and DPs. For a given set of DPs, contradictions should be indicated with a negative sign within the design matrix, and if there is uncertainty with respect to the design coupling, a small weighting factor should be included in the design matrix [Xue, 2006]. As there may be elements within the design that could not be easily decoupled, other design tools may be required to assist with the design process, such as the Theory of Inventive Problem Solving (TRIZ) [Altschuller, 1997]. TRIZ is a design tool that focuses on resolving design contradictions.

To conclude, the design recovery framework can be leveraged to assess the original design in the physical and logical domains using other design tools in a concise, straightforward manner. Another design method may be required to modify the final design due to other constraints, but as the information is presented in a structured manner within the design recovery framework, these methods can be readily employed. The overall design approach is illustrated in Figure 5-22.

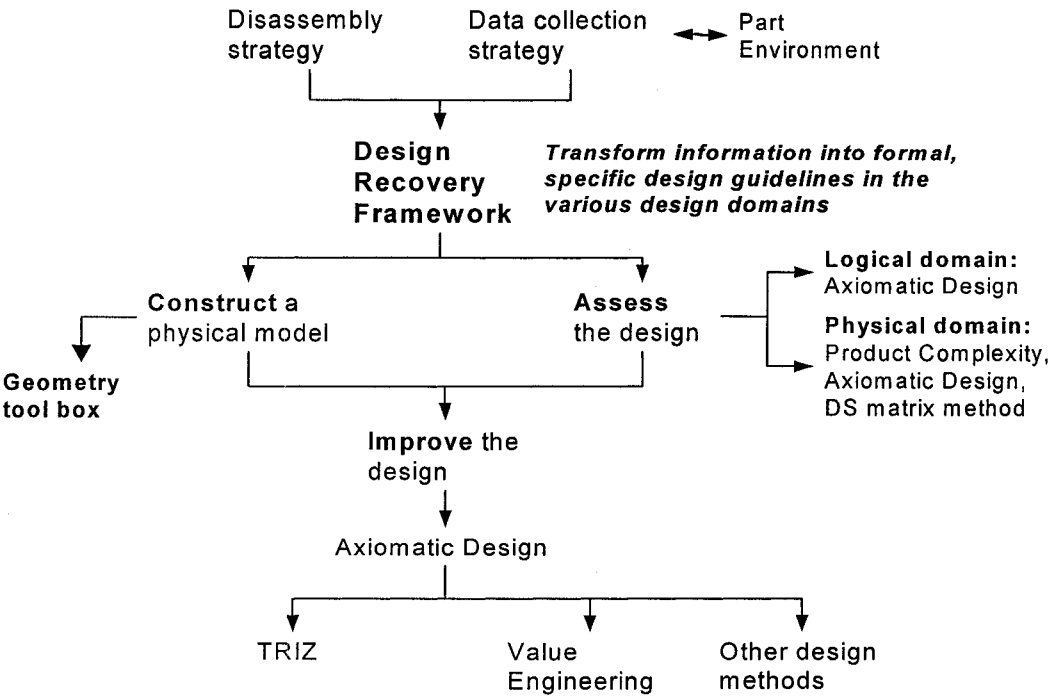

Figure 5-24: Design Flow using the Design Recovery Framework

Chapter 6

SUMMARY AND CONCLUSIONS

6 SUMMARY AND CONCLUSIONS

Formal reverse engineering is analogous to design recovery, and covers many applications. Design recovery goes beyond considering the physical form, or the basic functions of a component/product. The functions must be related to the form in context to the general system, as a product consists of an organized system of components. To understand a design's context, the sub-components and superstructure must be analysed, as well as the operating environment, in order to have confidence in the collected data. There are structural relationships that must be inferred and captured; consequently, there must be a methodology for recognizing design intent. The feature shapes and their patterns of arrangement are not arbitrary. There are identifiable characteristics at the feature level and the system level. Inherent in the reverse engineering process is the fact that one is dealing with incomplete and noisy data. Information sufficiency for accurate reconstruction is critical. An incomplete or inadequate model may be generated by not considering the form, functional requirements and the system as a whole. A framework and tools needed to be developed to address these issues, and to manage the interconnectivity between the different design domains or perspectives. To this end, a unique reverse engineering design recovery framework has been developed, using the Zachman framework as the base model. The design recovery framework was created to systematically capture the relevant design information at differing levels of resolution for the component of interest, and its features. Rules have been developed to define the feature type, their functional requirements, physical characteristics and associations. The product design vocabulary developed by NIST [Hirtz et al, 2002] provides an abstract but concise description of the product functions; hence, this vocabulary is used to describe the functions at the component and feature levels. Component and feature taxonomies have been developed (section 3.3, 3.4 and Appendix C), which serve as the basis for the data gathering activities. A roadmap has been developed to assist the designer in assessing the component and feature

characteristics and associations within context. To illustrate the 'component system network' and its interface, rules for a connectivity diagram have been developed. The goal is to be able to create a relevant, robust model using the gathered information as a set of design guidelines. From these guidelines, an ideal engineering model can be created, independent of the designer. A modified failure modes and effects analysis procedure has been developed to provide insight into recommended testing and verification tasks.

The design recovery framework has a multi-perspective, modular structure. Because of this, the information contained in the different perspectives can be leveraged to assess the original design using other formal design methodologies in a concise, straightforward manner. The transition from the design recovery framework to the Axiomatic Design matrix is made transparently, as illustrated by a detailed example. In the physical domain, the design can be quantified using the Product Complexity Indices. To assist with this, a feature code has been introduced in order to calculate the product complexity in a consistent manner. This code allows one to (i) quickly highlight areas of complexity within a component, (ii) evaluate the influences of changes with respect to the component, and (iii) compare dissimilar components to each other.

Form recovery is a critical element of the design recovery process. Many surface reconstruction techniques have been developed for reverse engineering an object's form. The final surface model may be mathematically exact, but it will contain noise due to manufacturing flaws and measurement errors and the surfaces and edges have no relevant physical meaning. The resulting geometry will not reflect the original design intent, and may not be ideal for subsequent product modifications or remanufacture. Geometry creation tools, which specifically target engineered parts, are essential for aiding in the design recovery process. Typically when designing a component, 2D curves are generated and the 3D features are constructed from these curves. Several CAD systems have geometry creation tools to quickly generate aggregates of features, and feature interrelationships are defined in drafting notation. Corresponding design recovery geometry creation tools/algorithms needed to be developed that reflect the standard design process. Algorithms are developed to reconstruct 'critical 2D curves' from points extracted from a user-defined plane. Once the points are converted into curve primitives, adjustments to these curves are made to capture the design

intent. Modifications to these curves are made based on the premise that common geometry constraints were applied in the original design, i.e. 'almost' parallel, collinear, and tangent means parallel, collinear, and tangent and so forth. For a point cloud slice that contains multiple curves, common shapes and 2D patterns are detected and their parameters stored. The resulting geometry consists of standard curve primitives, and is not difficult to modify if subsequent design changes need to be implemented due to new design or manufacturing constraints. The process flow for the methodologies and tools presented in this research is illustrated in Figure 6-1.

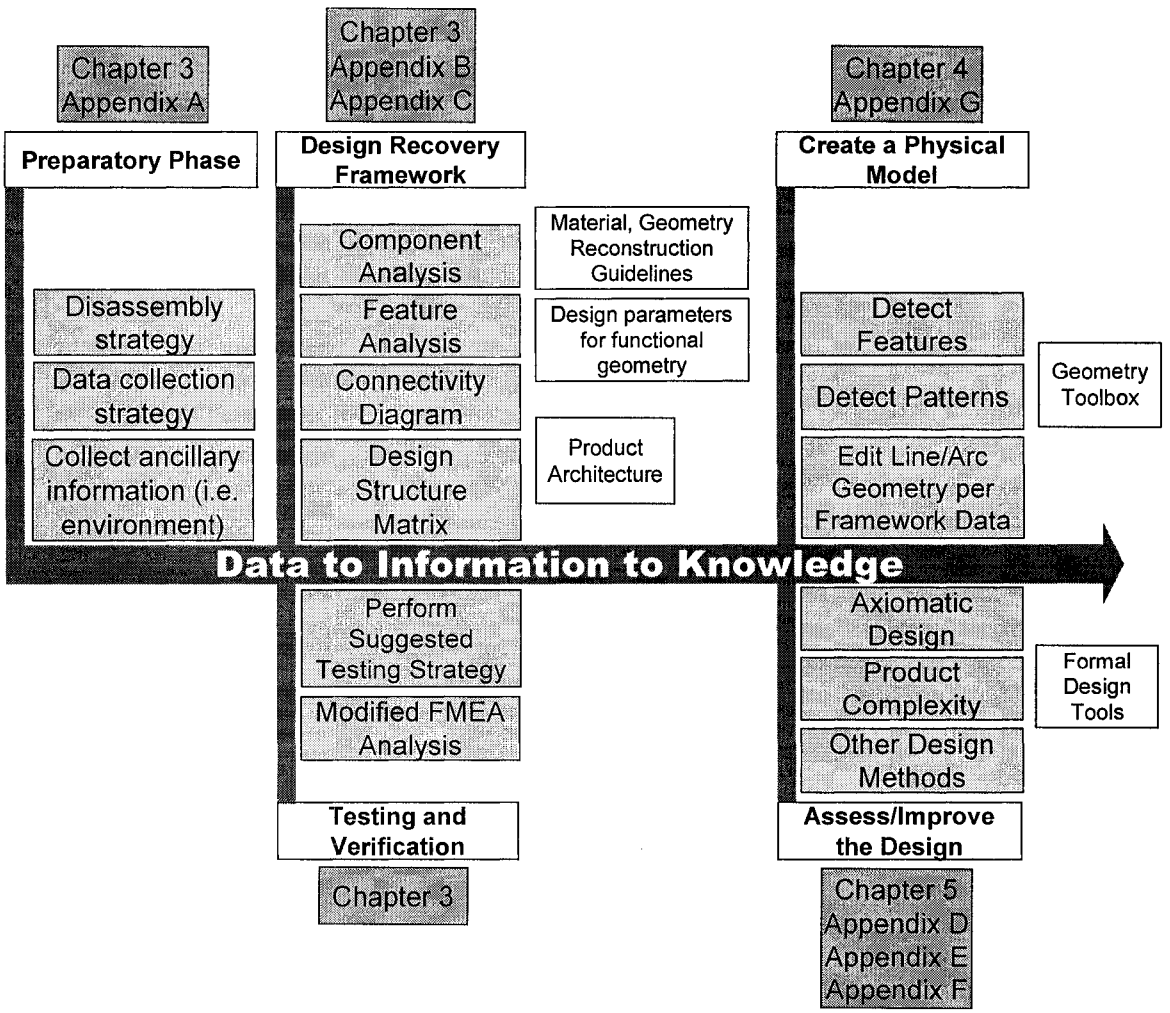

Figure 6-1: Design Recovery Process Flow Summary

To conclude, researchers have focused on processes for extracting general functional or non-specific form data. Effective design recovery consists of merging both elements and refining

them. A form-function link needed to be established at different levels of granularity to infer the designer's intent and to produce pertinent product documentation. To this end, a modular design recovery framework was developed to guide the designer in performing a thorough analysis of the component to be reverse engineered. This framework is an adaptation of the Zachman framework [2002]; however, the perspectives, foci, ontology, and formal reverse engineering tasks and activities have been modified for the design recovery application.

The framework was structured to consider the component in context within the overall system, as well as collect and assess detailed information. The functional requirements of the component and features are determined, as well as explicit physical characteristics and design parameters. Along with the functional requirements and form related information, explicit datum features are assigned to reference dimensions as well as tolerances and geometric inter-relationships between the features. As with forward engineering, these datum points should be used in the design (form reconstruction), manufacturing and inspection processes. All of the relevant engineering specifications at the different perspectives must be defined and linked in an organized manner. This has been done within the design recovery framework.

Using the framework as a guideline, the subjective element of the design recovery process is minimized. The critical form recovery specifications are captured in the framework; therefore, independent of the designer, the characteristics of the component and its features should be captured in a consistent manner when constructing the final CAD model. There may be minor variations with the transition geometry or other non-critical entities, but the core design aspects should be constant. Utilizing the design recovery framework will generate a model which is superior to one created by existing reverse engineering tools.

The framework was employed to recover the design for a damaged cylinder valve cover. The cylinder valve cover had distortion on its sealing surface, variable fillets, and mounting holes that were out of position. Relevant design parameters were determined using the design recovery framework as a roadmap. A realistic ideal CAD model was generated by assessing the environment, mating components, and the functional requirements, in addition to manipulating collected point cloud data.

The framework was also shown to be effective for assisting the designer in improving the recovered design. A case study using a severely damaged power steering pump pulley was used to demonstrate that the information contained in the modular framework can be easily extracted from several related components in order to optimize the design for the present operating environment and address the observed failure mode. Understanding the design based on the various perspectives allows the designer(s) to modify the structure, materials, or manufacturing processes without compromising the basic integrity of the component. The original stamped steel pulley set was replaced with a single multi-sheave machined billet aluminum pulley.

As understanding the interconnectivity of the features within the component and the component to the product architecture is critical, the connectivity diagram and design structure matrices were developed to conceptualize the physical interfaces and determine influence factors. The structural relationships may be much more complicated than those for the cylinder valve cover and power steering pump pulley case studies. The connecting rod case study contained several subtle design couplings that were only evident after constructing the connectivity diagram and the design structure matrix. These tools will help the designer(s) assess the structure of the component and determine the appropriate manufacturing processes.

The framework was extended to facilitate the testing and verification strategies, as they are a vital stage in the reverse engineering process. A modified FMEA procedure was introduced that utilizes a matrix methodology to assess each feature and its attributes contained in the design recovery framework. The results are plotted in a generic, and easy to interpret, 'precision versus complicatedness' chart. Procedures guiding the testing and verification stages through the logical (modified failure modes and effects analysis, tolerance stack up), virtual (simulations, competitive process benchmarking) and physical (prototype) domains were developed based on location of the data within the chart. This technique helps the designer(s) diagnosis potential design issues. It was illustrated using the cylinder valve cover and the power steering pump pulley case studies.

As geometry needs to be created that captures the intended geometric regularities, the point cloud manipulation algorithms have been developed to extract line and arc geometry. Common geometric relationships, shapes and patterns are identified and the parameters are

extracted where appropriate. The detailed point cloud data is transformed into pertinent structural data. The reconstructed geometry can be easily modified using standard design tools, as changes to the form may be required. In addition, surface or solid geometry can be constructed from the wire frame where necessary. Pertinent reference information to 'heal' the geometry and dimensions, and critical cross sections used for constructing the surfaces, is contained in the framework.

The designer may wish to analyse the recovered design using other formal design methodologies. The design recovery framework complements the Axiomatic Design methodology. As the product and feature functions and functional requirements are concisely defined at the logical perspective, and the design parameters are contained in the physical or detail perspectives, assigning a design parameter to a functional requirement per the Axiomatic design theory methodology is straightforward. Upon generating the Axiomatic design matrix from the design recovery framework in a rigorous manner, details that may have been over looked in the original analysis are extracted and refined where appropriate. This will generate a more robust model. Structuring the design recovery information in this manner allows the designer to determine whether Axiom 1, the independence axiom, has been satisfied in the design, and provides a rational basis to support subsequent design changes. It is challenging to determine whether Axiom 2, the information content axiom, is satisfied. Axiom 2 states that the design with the highest probability of success is the best design. One must have a clear understanding of the environment and the context of the component of interest in order to evaluate Axiom 2. The essential information for accomplishing this task is provided in the framework.

The connecting rod and timing screw case studies were presented in detail to illustrate the relationship between the design recovery framework and the Axiomatic design methodology. The necessity of assessing a design with respect to the functional requirements is emphasized with the timing screw case study. The shape of the variable pitch form is based on the desired motion characteristics. It was clearly proven that using these tools allows the designer to establish effective function-form relationships.

It may be necessary to quantify the design. Consequently, the heuristic complexity assessment tools developed by ElMaraghy and Urbanic [2003] have been modified to work with the

design recovery framework. A standard feature code was introduced. The feature complexity is calculated directly from the feature code, and the component complexity is derived by considering all of the features. Areas of complexity are quickly highlighted, allowing the designer to focus on potential areas of concern.

The design recovery framework developed in this research provides a comprehensive basis for effectively constructing a relevant, ideal, robust design. In addition, this framework provides a foundation to enable the designer to assess and make modifications to the original design in a straightforward manner.

Chapter 7

FUTURE RESEARCH DIRECTIONS IN THE DIFFERENT DOMAINS

7 FUTURE WORK

The research work presented here should be extended in several diverse directions, as opportunities exist in both the academic and commercial domains. They are listed as follows:

(i) The design recovery framework, product visualization, and assessment tools should be extended to encompass a full assembly. Spatial relationships and other compatibility concerns between multiple components and their features would need to be identified and linked in a concise manner. System information such as the degrees of freedom, joint interface considerations and precedence data (for assembly) would also need to be considered and represented appropriately.

(ii) A formal methodology should be developed to automatically couple the design recovery framework with some design assessment techniques, such as the modified FMEA procedure, Axiomatic Design or the Product Complexity Indices, for subsequent design analysis.

(iii) From the detailed descriptors for each feature, an IGES (Initial Graphics Exchange Standard) or STEP[1] (STandard Exchange of Product) file could be generated. This would create platform independent geometry that could be used in tandem with the point cloud data. The feature geometry descriptions and the relevant data (constraints, tolerances and associations, etc.) that are captured in the framework would serve as the foundation for subsequent CAD geometry creation. The STEP standard (ISO 10303) has been expanded

[1] STEP is an international referenced as ISO 10303 [ISO 10303-1, 1994]. The STEP standard aims to define a non-ambiguous, computer interpretable representation of the data related to the product throughout its lifecycle. STEP allows the implementation of consistent information systems through multiple applications and materials. This standard also proposes various means for the storage, exchange and archiving of product data in a strategy of long-term re-use. STEP covers a broad range of fields (electronics, mechanical engineering, sheet metal working, composites material design, ship building, architecture & civil engineering, etc.) and lifecycle phases (design, analysis, production planning, manufacturing, etc.). The extent of these application domains continues to grow as new industrial needs come to light [Ducellier et al, [2006].

to include parameterized and constrained data (ISO 10303-108) [Ducellier et al, [2006]. The preliminary application areas for such parameters and constraints in CAD models are 2D sketches or profiles, inter-feature relationships and inter-part relationships in 3D assembly models. The targeted STEP application dovetails into the design recovery framework nicely.

(iv) The geometry creation tools can be extended to automatically detect, recognize and construct 3D features. This automatic geometric reconstruction methodology should be extended to generate a solid model representation of the features. This includes extruded, rotational swept, loft solids and solids created by stitching surfaces. The relevant construction parameters could be contained in the framework in key fields. With complete data (point cloud data for internal and recessed features, or information on recessed features contained in the framework) a solid model with a complete history tree could be constructed from the data. A variation of these techniques could be used to create a solid model with a history tree when importing solid model geometry from another system.

(v) To collect internal, recessed or difficult to measure features without using a CT scan or crude sectioning procedures, destructive methods need to be implemented in an automated way using advanced technology. By cutting and scanning thin layers of a part automatically using a CNC machine and a vision system, a RE data collection system could capture external and internal geometry of complex parts. The part needs to be immersed in material with a contrasting colour, machined to a selected depth, scanned, and the edge contours extracted using the algorithms presented in this research. This process needs to be continuously repeated in order to be able to produce a point cloud or wire frame representation of the complete object. The data collected from this system could be used for either inspection or model reconstruction purposes.

(vi) Commercial application tools should be developed to manipulate the point cloud data in order to generate the relevant wire frame geometry. An interactive reverse engineering system for engineered parts should be developed. This system should be menu driven, incorporate curve primitive creation and pattern detection, design intent healing functions, have libraries based on the process, general feature types, tolerance tables, and links to commercial component libraries.

(vii) A parameter driven timing screw design and inspection software module could be developed directly from the procedures presented in this research. The non-contact data collection systems used in conjunction with the 'unroll'/'unwind' data transformation allows the motion characteristics for a timing screw to be extracted and evaluated.

To conclude, research in the field of reverse engineering is not a mature are of research. There are many exciting opportunities related to this work and significant progress can still be made, especially with engineered components.

BIBLIOGRAPHY

Altshuller, G., 1997, "40 Principles: TRIZ Keys to Technical Innovation", Translated by Lev Shulyak and Steven Rodman, Worchester, Massachusetts: Technical Innovation Center, ISBN 0964074036, USA.

Arunajadai, S., Stone, R., and Tumer, I., A framework for creating a function-based design tool for failure mode identification, Proceedings of DETC2002, DETC2002/DTM-34018, 2002.

Attene, M., Spagnuolo, M., 2000, "Automatic Surface Reconstruction from Point Sets in Space", Computer Graphics Forum, vol. 19, pp. 457 – 465.

Au, C.K., Yuen, M.M.F., 1999, "Feature-Based Reverse Engineering of Mannequin for Garment Design", CAD Computer Aided Design, vol. 31, no. 12, pp. 751 – 759.

Azernikov, S., Fischer, A., 2004, "Efficient Surface Reconstruction Method for Distributed CAD", CAD Computer Aided Design, vol. 36, no. 9, pp. 799 – 808.

Azernikov, S., Fischer, A. 2003, "Surface Reconstruction of Freeform Objects Based on Hierarchical Space Decomposition", International Journal of Shape Modeling, vol. 9, no. 2, pp. 177 – 190.

Bainbridge, A. F., 2002, "Making Things Simpler: Management in Complexity", 2nd International Conference of the Manufacturing Complexity Network, pp. 403 – 410.

Ballinger, R., 2004, "MRI Tutor Web Site and MRI/Radiology Teaching Files", © Ray Ballinger url: http://www.mritutor.org/.

Barhak, J., Fischer, A. 2002, "Adaptive Reconstruction of Freeform Objects with 3D SOM Neural Network Grids", Computers and Graphics, vol. 26, no. 5, pp. 745 – 751.

Barhak, J., Fischer, A., 2001, "Parameterization and Reconstruction from 3D Scattered Points Based on Neural Network and PDE Techniques", IEEE Transactions on Visualization and Computer Graphics, vol. 7, no. 1, pp. 1 – 16.

Barhak, J., Fischer, A., 2001, "Parameterization for Reconstruction of 3D Freeform Objects from Laser-Scanned Data Based on a PDE Method", Visual Computer, vol. 17, no. 6, pp. 353 – 369.

Beckmann, H., Oberg, H., 1988, "Built-up Connecting Rod", US Patent 4,833,939, Volkswagen AG, Wolfsburg, DE.

Behm, R. P., Hahn, J. J., 1999, "Noncontact Inspection Cuts Product Development Time", Plastics Engineering, vol. 55, no. 9, pp. 47 – 49.

Benko, P., Varady, T., 2004, "Segmentation Methods for Smooth Point Regions of Conventional Engineering Objects", CAD Computer Aided Design, vol. 36, no. 6, pp. 511 – 523.

Benko, P., Kos, G., Varady, T., Andor, L., Martin, R., 2002, "Constrained Fitting in Reverse Engineering", Computer Aided Geometric Design, vol. 19, no. 3, pp. 173 – 205.

Benko, P., Martin, R.R., Varady, T. 2001, "Algorithms for Reverse Engineering Boundary Representation Models", CAD Computer Aided Design, vol. 33, no. 11, pp. 839 – 851.

Bernhard, A., Veron, M., 2000, "Visibility Theory Applied to Automatic Control of 3D Complex Parts Using Plane Laser Sensors", Annals of the CIRP, vol. 49, no.1, pp. 113 – 116.

Bernard, A., Davillerd, S., Sidot, B., 1999, "Knowledge-based System for Computer-Aided Process Planning of Laser Sensors 3D Digitizing", Proceedings of SPIE - The International Society for Optical Engineering, vol. 3835, pp. 64 – 71.

Bernardini, F., Bajaj, C., Chen, J., Schikore, D., 1999, "Automatic Reconstruction of 3D CAD Models from Digital Scans", Int. J. on Comp. Geom. and Applications, pp. 327 – 370.

Besl, P.J., McKay, N.D., 1992, "A Method for Registration of 3D Shapes", IEEE Trans. Pattern Analysis. Machine Intelligence, vol. 14, no. 2, pp. 239 – 56.

Boehler W., Heinz G., Marbs A., Siebold M., 2002, "3D Scanning Software: An Introduction" CIPA - ISPRS Workshop Proc., Scanning for Cultural Heritage Recording, pp. 47 – 51, url: http://www.i3mainz.fh-mainz.de/publicat/korfu/p11_Boehler.pdf.

Botsch, M., Kobbelt, L., 2001, "Resampling Feature and Blend Regions in Polygonal Meshes for Surface Anti-Aliasing", Computer Graphics Forum, vol. 20, no. 3, pp. 402 – 410.

Bradley, C., Wei, S., Zhang, Y.F. & Loh, H.T. 1999, "Generation of Polyhedral Models from Machine Vision Data", Proceedings of SPIE - The International Society for Optical Engineering, vol. 3832, pp. 26 – 37.

Bujakiewicz, A., Kowalczyk, M., Podlasiak, P., Zawieska, D., 2004, "Modelling and Visualization of Three Dimensional Objects Using Close Range Imagery", XXth ISPRS Congress, pp. 442 – 446.

Chalermwat, P., 1999, "High Performance Automatic Image Registration for Remote Sensing", PhD. Dissertation, George Mason University, url: http://www.science.gmu.edu/~prachya/thesis/.

Changchien, S.W., Lin, L., 1996, "Knowledge-based Design Critique System for Manufacture and Assembly of Rotational Machined Parts in Concurrent Engineering", Computers in Industry, vol. 32, no. 2, pp. 117 – 140.

Chappuis, C., Rassineux, A., Breitkopf, P., Villon, P., 2004, "Improving Surface Meshing from Discrete Data by Feature Recognition", Engineering with Computers, vol. 20, no. 3, pp. 202 – 209.

Chen, Y., Medioni, G., 1992, "Object Modeling by Registration of Multiple Range Images", Image and Vision Computing, vol. 10, no. 3, pp. 145 – 55.

Chernov, N., Lesort, C., 2003, "Least Squares Fitting of Circles and Lines", Computer Vision and Pattern Recognition, url: http://xxx.arxiv.org/PS_cache/cs/pdf/0301/0301001.pdf.

Chin, K., Zheng, L., Wei, L., 2003, "A Hybrid Rough-Cut Process Planning for Quality", Int. J. Adv. Manufacturing Technology, Vol. 22, pp. 733–743, DOI 10.1007/s00170-003-1618-x.

Chuang, C., Chen, C., Yau, H., 2002, "A Reverse Engineering Approach to Generating Interference-free Tool Paths in Three-Axis Machining from Scanned Data of Physical Models", International Journal of Advanced Manufacturing Technology, vol. 19, no. 1, pp. 23 – 31.

Cicek, A., Gulesin, M., 2004, Reconstruction of 3D Models from 2D Orthographic Views Using Solid Extrusion and Revolution", Journal of Materials Processing Technology, pp. 291 – 298.

Clarke, T.A., Robson S., Chen, J., 1993, "A Comparison of Three Methods for the 3-D Measurement of Turbine Blades", International Symposium on Measurement, Technology and Intelligent Instruments, pp. 12, url: http://www.optical-metrology-centre.com/Downloads/Papers/ISMTII%20Wuhan%201993%20Comparison%20of%20Three%20techniques.pdf.

Cooper, 2005, "Wireframe Projections: Physical Realisability of Curved Objects and Unambiguous Reconstruction of Simple Polyhedra", International Journal of Computer Vision, vol. 64, no. 1, pp.69 – 88.

Corbett, L.M., Brocklesby, J., Campbell-Hunt, C., 2002, "Thinking and Acting: complexity management for a sustainable business", 2nd International Conference of the Manufacturing Complexity Network, pp. 83 – 96.

Davillerd, S., Sidot, B., Bernard, A., Ris, G., 1998, "Definition of the Fundamentals for the Automatic Generation of Digitalization Processes with a 3D-Laser Sensor", Proceedings of the SPIE - The International Society for Optical Engineering, vol., 3520, pp. 214 – 25.

Dey, T. K., Giesen, J., Hudson, J., 2001, "Delaunay Based Shape Reconstruction from Large Data", IEEE Symposium in Parallel and Large Data Visualization and Graphics, pp. 19 – 27.

Dixon, J. R., Poli, C., 1995, "Engineering Design and Design for Manufacturing: A Structured Approach", Field Stone Publishers, Conway, MA, USA.

Dong, X., DeVries, R., Wozny, M., 1991, "Feature-Based Reasoning in Fixture Design", Annals of the CIRP, vol. 41, no.1, pp. 111 – 114.

Ducellier, G., Charles, S., Remy, S., Eynard, B, 2006, " Reverse Engineering Application based on Advanced STEP Parameterized and Constrained Features", Proc. of the 16th CIRP Design Seminar, Calgary, pp. 207 – 216.

Eggert, D.W., Fitzgibbon, A.W, Fisher, R.B., 1998, "Simultaneous Registration of Multiple Range Views for Use in Reverse Engineering of CAD Models", Computer Vision and Image Understanding, vol. 69, no. 3, pp. 253 – 272.

ElMaraghy, H. A., Kuzgunkaya, O., Urbanic, R. J., 2005, "Manufacturing Systems Configuration Complexity", CIRP Annals, vol. 54, no. 1, pp. 445-450.

ElMaraghy, W. H., Urbanic, R. J., 2004, "Assessment of Operational Complexity", CIRP Annals, vol. 53, no. 1, pp. 401 – 406.

ElMaraghy, W. H., Urbanic, R. J., 2003, "Modelling of Manufacturing Systems Complexity", CIRP Annals, vol. 53, no. 1, pp. 363 – 366.

ElMaraghy, W., Rolls, C., 2001, "Design by Quality Product Digitization", CIRP Annals, vol. 50, no. 1, pp. 93 – 96.

ElMaraghy, H. A., ElMaraghy, W. H., 1994, "Computer-Aided Inspection Planning (CAIP)", in Advances in Feature Based Manufacturing, Chap. 16, eds., Shah, J. J, Mantyla, M., Nau, D. S., Elsevier, Amsterdam, Netherlands, pp. 363 – 396.

Erdman, A., Sandor, G., 1984, "Mechanism Design: Analysis and Synthesis, Vol. 1", Prentice Hall, NJ.

Federal Enterprise Architecture, 2006, "E-GOV – Powering America's Future with Technology", U.S. Office of Management and Budget, url: http://www.whitehouse.gov/omb/egov/a-1-fea.html.

Feng, C., 2002, "Internet-Based Reverse Engineering", International Journal of Advanced Manufacturing Technology, vol. 21, no. 2, pp. 138 – 144, url: http://hilltop.bradley.edu/~cfeng/IJAMT03.pdf.

Fischer, A., 2002, "Multi-level of Detail Models for Reverse Engineering in Remote CAD Systems", Engineering with Computers, vol. 18, no. 1, pp. 50 – 58.

Fischer, A., Park, S., 1998, "3D Scanning and Level of Detail Modelling for Design and Manufacturing", Annals of the CIRP, vol. 47, no. 1, pp. 91 – 94.

Fischer, A., Smolin, A., 1997, "Modeling in Reverse Engineering for Injection Molding Analysis of 3D Thin Objects", Annals of the CIRP, vol. 46, no. 1, pp. 96 – 99.

Fisher, R., 2004, "Applying Knowledge to Reverse Engineering Problems", Computer Aided Design, vol. 36, no. 6, pp. 501 – 510.

Fitzgibbon, A., Pilu, M. Fisher, R.B., 1999, "Direct Least Square Fitting of Ellipses", IEEE Trans. Pattern Analysis, Machine Intelligence, vol. 21, no. 5, pp. 476 – 480.

Flisch, A., Wirth, J., Zanini, R., Breitenstein, M., Rudin, A., Wendt, F., Mnich, F., Golz, R., 1999, "Industrial Computed Tomography in Reverse Engineering Applications", Computerized Tomography for Industrial Applications and Image Processing in Radiology, DGZfP-Proceedings BB 67-CD, paper 8.

Francheshini, F., Galetto, M., 2001, "A New Approach for Evaluation of Risk Priorities of Failure Modes in FMEA", Int. J. Prod. Res., vol. 39, no. 13, pp. 2991 – 3002, DOI: 10.1080/00207540110056162.

Gagnon, H., Soucy, M., Bergevin, R., Laurendeau, D., 1994, "Registration of Multiple Range Views for Automatic 3-D Model Building", Proceedings of the 1994 IEEE Computer Society Conference on Computer Vision and Pattern Recognition, Publ by IEEE, pp. 581.

Galantucci, L.M., Percoco, G., Spina, R., 2004, "An Artificial Intelligence Approach to Registration of Free-Form Shapes", CIRP Annals, vol. 53, no. 1, pp. 139 – 142.

Gao, C.H., Langbein, F.C., Marshall, A.D., Martin, R.R., 2004, "Local Topological Beautification of Reverse Engineered Models", CAD Computer Aided Design, vol. 36, no. 13, pp. 1337– 1355.

Groover, M. P., 2001, "Automation, Production Systems, and Computer-Integrated Manufacturing", Prentice Hall, NJ.

Guenov, M., Barker, S., 2004, "Application of Axiomatic Design and Design Structure Matrix to the Decomposition of Engineering Systems", Systems Engineering, vol. 8, no. 1, pp. 29 – 35.

Hausi A. Muller, H. A., Jahnke, J. H., Smith, D. B., Storey, M., Tilley, S. R., Wong, K., 2000, "Reverse Engineering: A Road Map", from "The Future of Software Engineering", Anthony Finkelstein (Ed.), ACM Press 2000, ISBN 1-58113-253-0.

Heisler, H., 1999, "Vehicle and Engine Technology", 2nd ed., SAE International, PA., USA.

Hilton, A, 1997, "Model Building from 3D Surface Measurements", ©University of Surrey, url: http://www.ee.surrey.ac.uk/Research/VSSP/3DVision/model_building/model.html.

Hirania, H.,Suh, N., 2005, "Journal bearing design using multiobjective genetic algorithm and axiomatic design approaches", Tribology International, vol. 38, pp. 481 – 491.

Hirtz, J., Stone, R., McAdams, D, Szykman, S., Wood, K., 2002, "A Functional Basis for Engineering Design: Reconciling and Evolving Previous Efforts" NIST Technical Note 1447.

Hornak, J., 2006, "The Basics of MRI", ©1996-2006, J.P. Hornak, url: http://www.cis.rit.edu/htbooks/mri/index.html.

Hsieh, Y. C., 1993, "Reconstruction of Sculpted Surfaces Using Coordinate Measuring Machines", MASc. Dissertation, University of Utah, url: http://www.cs.utah.edu/techreports/1993/pdf/UUCS-93-010.pdf.

Huang, W., Kong, Z., Ceglarek, D., Brahmst, E., 2003, "The Analysis of Feature-Based Measurement Error in Coordinate Metrology", IIE Transactions, vol. 36, pp. 237 – 251.

Huang, J., and Menq, C. 2001, "Automatic Data Segmentation for Geometric Feature Extraction from Unorganized 3-D Coordinate Points", IEEE Transactions on Robotics and Automation, vol. 17, no. 3, pp. 268 – 279.

Hytech, Anonymous, no date, "Hytec Sensors and Imaging Group: Non Destructive Testing", url: http://www.hytecinc.com/index.html.

Institute for Enterprise Architecture Developments, 2006, "Information Exchange Area of the Institute for Enterprise Architecture Developments", IFEAD, url: http://www.enterprise-architecture.info/.

ISO 10303-1, Anonymous, 1994, "STEP - Part 1: Overview and fundamental principles".

Jain, P.K., 1999, "Extraction of Compound Volumetric Features form a Three-Dimensional Wireframe Model", Proceedings of the I MECH E Part B, Journal of Engineering Manufacture, pp. 597 – 613.

Jordan, Jr., R.L., Van Wie, M., Stone, R.B., Wang, J., Terpenny, J.P., 2005, "A Group Technology Based Representation for Product Portfolios", Proceedings of IDETC/CIE, DETC2005-85313.

Kagan, P., Fischer, A., Shpitalni, M., 1996, "Intuitive Physical-Based CAD System for Designing Sculptured Surfaces", Annals of the CIRP, vol. 45, no. 1, pp. 121 – 124.

Karbacher, S., Laboureux, X., Schön, N., Häusler, G., 2001, "Processing Range Data for Reverse Engineering and Virtual Reality", IEEE Proceedings of Third International Conference on 3-D Digital Imaging and Modeling 2001, pp. 314 – 321.

Karbacher, S., Häusler, G. Schönfeld, H., 1999, "Reverse Engineering Using Optical Range Sensors", Handbook of Computer Vision and Applications, vol. 3, Systems and Applications, 359 – 379.

Karbacher, S., Hausler, G., 1998, "A New Approach for Modeling and Smoothing of Scattered 3D Data", Three-Dimensional Image Capture and Applications, The International Society for Optical Engineering, p. 168.

Knopf, G.K., Sangole, A., 2004, "Interpolating Scattered Data using 2D Self-Organizing Feature Maps", Graphical Models, vol. 66, no. 1, pp. 50 – 69.

Kolmanic, S., Guid, N., 2003, "A New Approach in CAD System for Designing Shoes", Journal of Computing and Information Technology - CIT 11, pp. 319 – 326.

Krause, F. L., Fischer, A., Gross, N., Barhak, J., 2003, "Reconstruction of Freeform Objects with Arbitrary Topology Using Neural Networks and Subdivision Techniques", Annals of the CIRP, vol. 52, no. 1, pp. 125 – 128.

Krause, F. L., Kramer, S., Rieger, E., 1991, "PDGL: A Language for Efficient Feature-Based Product Gestaltung", Annals of the CIRP, vol. 40, no.1, pp. 135 – 138.

Kruth, J. P., Kerstens, A., 1998, "Reverse Engineering Modelling of Free-Form Surfaces from Point Clouds Subject to Boundary Conditions", Journal of Materials Processing Technology, vol. 76, no. 1-3, pp. 120 – 127.

Kumara, S., Kao, C.Y., Gallagher, M., Kasturi, R., 1994, "3D Interacting Manufacturing Feature Recognition", Annals of the CIRP, vol. 43, no. 1, pp. 133 – 136.

Kverh, B., Leonardis, A., 2002, "A New Refinement Method for Registration of Range Images Based on Segmented Data", Computing, vol. 68, no. 1, pp. 81 – 96.

Langbein, F.C., Marshall, A.D., Martin, R.R., 2004, "Choosing Consistent Constraints for Beautification of Reverse Engineered Geometric Models", CAD Computer Aided Design, vol. 36, no. 3, pp. 261 – 278.

Langbein, F. C., 2003, "Beautification of Reverse Engineered Geometric Models", Ph. D. dissertation, Cardiff University.

Langbein, F.C., Mills, B.I., Marshall, A.D., Martin, R.R., 2001, "Finding Approximate Shape Regularities in Reverse Engineered Solid Models Bounded by Simple Surfaces", 6th ACM Symposium on Solid Modeling and Applications, Ann Arbor, MI, pp. 206.

Langrana, N., Chen, Y., Das, A., 1997, "Feature Identification from Vectorized Mechanical Drawings", Computer Vision and Image Understanding, vol. 68, no. 2, pp. 127 – 145.

Lee, K., 1999, "The Principles of CAD/CAM/CAE Systems", Addison Wesley, Toronto, CA.

Levy, G. N., Schindel, R., Kruth, J. P., 2003, "Rapid Manufacturing and Rapid Tooling with Layer Manufacturing (LM) Technologies, State of the Art and Future Perspectives", Annals of the CIRP, vol. 52, no. 2, pp. 589 – 610.

Li, N., Cheng, P., Sutton, M., McNeill, S., Chao J., 2000, "Accurate Integration of Surface Profile Data with Quantitative Error Analysis", Experimental Mechanics, pp. 77 – 83.

Lichti, D. D., Harvey, B. R., 2002, "The Effects of Reflecting Surface Material Properties on Time-of-Flight Laser Scanner Measurements", Symposium on Geospatial Theory, Processing and Applications, url: http://www.isprs.org/commission4/proceedings/pdfpapers/180.pdf.

Limaiem, A., ElMaraghy, H. A., 1999, "Curve and Surface Modeling with Uncertainties Using Dual Kriging", ASME Journal of Mechanical Design, vol. 121, no. 2, pp. 249 – 255.

Limaiem, A. N., A., ElMaraghy, H. A., 1996, "Data Fitting Using Dual Kriging and Genetic Algorithms", Annals of the CIRP, vol. 45, no.1, pp. 129 – 132.

Lipson H., Shpitalni, M., 1996, "Optimization-Based Reconstruction of a 3D Object from a Single Freehand Line Drawing", Computer Aided Design, vol. 28, no. 8, pp. 651– 663.

Liu, S., Ma, W., 2001, "Motif Analysis for Automatic Segmentation of CT Surface Contours into Individual Surface Features", CAD Computer Aided Design, vol. 33, no. 14, pp. 1091 – 1109.

Liwei, Q., Yi, Z., Minghui, L., 2004, "Contour Segments Extraction of 3-D Surfaces from Layer Measurements", International Journal of Advanced Manufacturing Technology, vol. 24, pp. 335 – 344.

Logar, B., Peklenik, J., 1991, "Feature-Based Database Design and Automatic Forming of Part Families for GT", Annals of the CIRP, vol. 40, no. 1, pp. 153 – 156.

Luck, J., Little, C., Hoff, W., 2000, "Registration of Range Data using a Hybrid Simulated Annealing and Iterative Closest Point Algorithm", ICRA 2000: IEEE International Conference on Robotics and Automation, Institute of Electrical and Electronics Engineers Inc., p. 3739.

Machinery's Handbook, 26th Ed., 2003, Industrial Press Inc., NY.

Mantyla, M., Lagus, K., Laakko, T., 1994,"Application of Constraint Propagation in Part Family Modeling", Annals of the CIRP, Submitted by G. Sohlenius, vol. 43, no. 1, pp. 129 – 132.

Miles, L., 1989, "Techniques of Value Analysis and Engineering", 3rd ed, McGraw Hill.

Miller, I., Freund, J., 1977, "Probability and Statistics for Engineers", 2nd Edition, Prentice-Hall, Englewood, NJ, USA.

Metris-Anonymous, 2006, "Products: Focus Reverse Engineering", © Metris, 2006, url: http://www.metris.com/products/point_cloud_software/focus_reverse_engineering/

Mills, B. I., Langbein, F. C., Marshall, A. D., Martin R. R., 2001, "Approximate Symmetry Detection For Reverse Engineering", Sixth ACM Symposium on Solid Modelling and Applications, pdf.

Mills, B. I., Langbein, F. C., Marshall, A. D., Martin R. R., 2001, "Estimate of Frequencies of Geometric Regularities for Use in Reverse Engineering of Simple Mechanical Components", Technical Report GVG 2001-1, Geometry and Vision Group, Department of Computer Science, Cardiff University, 2001.

Motavalli, S. 1998, "Review of Reverse Engineering Approaches", Computers & Industrial Engineering, vol. 35, no. 1-2, pp. 25 – 28.

Mrdjenovich, R., Yeager, D., 1992, "Hollow Connecting Rod", US Patent 5,140,869, Ford Motor Co., Dearborn, MI.

Nassef, A. O., ElMaraghy, H. A., 1997, "Allocation of Geometric Tolerances: New Criterion and Methodology", Annals of CIRP, vol. 46, no. 1, pp. 101 – 104.

NIST – Anonymous, 1993, "Announcing the Standard for Integration Definition for Function Modeling (IDEF0)", Draft Federal Information Processing Standards Publication 183 issued by the National Institute of Standards and Technology.

Otto K, Wood K., 2001, Product Design: Techniques in Reverse Engineering and New Product Development. Prentice Hall, Upper Saddle River, NJ.

Otto, K., Wood, K, 1996, "A Reverse Engineering and Redesign Methodology for Product Evolution", Proc. Of ASME Design Engineering Tech. Conf. and Design Theory and Methodology Conference, DETC96/DTM-1523.

Owodunni, O., Mladenov, D., Hinduja, S. 2002, "Extendible Classification of Design and Manufacturing Features", Annals of the CIRP, vol. 51, no. 1, pp. 103 – 106.

Page, D. L., 2003, "Part Decomposition of 3D Surfaces", PhD dissertation, University of Kentucky, Knoxville.

Page, D., Koshcan, A., Sun, Y., Abidi, M., 2003, "Laser-Based Imaging for Reverse Engineering", Sensor Review, vol. 23, no. 3, pp. 223 – 229.

Pahl, G., Beitz, W., 1988, "Engineering Design: A Systematic Approach", Springer-Verlag, London, UK.

Paraform trainer, 2004, personal conversion.

Parmley, R.O., 2000, "Illustrated Sourcebook of Mechanical Components", McGraw-Hill.

Peng, X., Zhang, Z., Tiziani, H. J., 2002a, "3-D Imaging and Modeling - Part I: Acquisition and Registration", Optik (Jena), vol. 113, no. 10, pp. 44 – 452.

Peng, X., Zhang, Z., Tiziani, H. J., 2002b, "3-D imaging and Modeling - Part II: Integration and Duplication", Optik (Jena), vol. 113, no. 10, pp. 453 – 458.

Philippe, J., Bernard, A., Ris, G., 1998, "Fuzzy Logic Applied to Surface Modelling from Point Clouds", Proceedings of SPIE - The International Society for Optical Engineering, vol. 3520, pp. 182 – 193.

Renishaw, Anonymous, 2004, "Stylus Ball Material Selection", © Renishaw, url: http://www.renishaw.com/client/category/UKEnglish/CAT-1000.shtml.

Ringer, M., Morris, R, 2001, "Robust Automatic Feature Detection and Matching between Multiple Images", Research Institute for Advanced Computer Science, RIACS Technical Report 01.27.

Roland DGA Co., Anonymous, no date, " 3D Laser Scanner, LPX 1200", RDGA-LPX-02, Roland DGA Co., url: http://www.rolanddga.com/pdf/brochure_%20LPX1200%20.pdf.

RSI GmbH, Anonymous, 2000, "HLS Handheld Laser Scanner", Polhemus ©RSI GmbH, url: http://www.rsi.gmbh.de/hls_e.htm.

Rugaber, S., 1994, "White Paper on Reverse Engineering", College of Computing and Software Engineering Res. Center, Georgia Institute of Technology.

Sandia National Laboratories, 2004, "Mechanical Measurements and Calibration", Technologies, url: http://mfgshop.sandia.gov/1400_ext_MechMeasCal.htm.

Schey, J., 1987, "Introduction to Manufacturing Processes", 2nd Edition, McGraw Hill, Toronto, CA, Chap. 6.

Schonfeld, H., Hausler, G., Karbacher, S., 1998, "Reverse Engineering Using Optical 3D Sensors", Three-Dimensional Image Capture and Applications, The International Society for Optical Engineering, San Jose, CA, United States, p. 115.

Shpitalni, M, Lipson, 1997, "Automatic Reasoning for Design under Geometric Constraints", Annals of the CIRP, vol. 46, no. 1, pp. 85 – 88.

Shpitalni, M., Lipson, H., 1996, "Identification of Faces in a 2D Line Drawing Projection of a Wireframe Object", IEEE Transactions on Pattern Analysis and Machine Intelligence", vol. 18, no. 10, pp. 1000 – 1012.

Shum, S., Lau, W., Yuen, M., Yu, K., 1997, "Solid Reconstruction from Orthographic Opaque Views Using Incremental Extrusion", Computer and Graphics, vol. 21, no. 6, pp. 787 – 800.

Smid, P., 2000, "A Comprehensive Guide to Practical CNC Programming: CNC Programming Handbook" 2nd ed., Industrial Press Inc., NY, NY.

Steiner, D., Fischer, A., 2002, "Cutting 3D Freeform Objects with Genus-n into Single Boundary Surfaces Using Topological Graphs", Proceedings Seventh ACM Symposium on Solid Modeling and Applications SM'02, Association for Computing Machinery, p. 336.

Steiner, D., Fischer, A., 2001, "Topology Recognition of 3D Closed Freeform Objects Based on Topological Graphs", 6th ACM Symposium on Solid Modeling and Applications, Ann Arbor, MI, p. 305.

Stone, R., Turner, I., Van Wie, M., 2005, "The Function-Failure Design Method", Journal of Mechanical Design, Vol. 127, pp. 397 – 407, DOI: 10.1115/1.1862678.

StrokeStop Foundation, Anonymous, 2000, "Module 1: Introduction to Stroke and Stroke Prevention", Stroke Curriculum for Medical Students, University of Massachusetts Medical School and the American Stroke Association ©, url: http://www.umassmed.edu/strokestop/graphics/ssmod1.pdf.

Suh, N. P., 2001, "Axiomatic Design: Advances and Applications", Oxford University Press, New York, USA.

Sun, W., Bradley, C., Zhang, Y.F., Loh, H.T., 2001, "Cloud Data Modelling Employing a Unified, Non-Redundant Triangular Mesh", CAD Computer Aided Design, vol. 33, no. 2, pp. 183 – 193.

Tangelder, J., Ermes, P. Vosselman, G., van den Heuvel, F., 2003, "CAD-Based Photogrammetry for Reverse Engineering of Industrial Installations", Computer Aided Civil and Infrastructure Engineering, vol. 18, pp. 264 – 274.

Teutsch, C., Isenberg, T., Trostmann, E., Weber, M., 2004, "Evaluation and Optimization of Laser Scan Data", In Thomas Schulze, Stefan Schlechtweg, and Volkmar Hinz, editors, Simulation und Visualisierung, pp. 311– 322, SCS European Publishing House, url: http://isgwww.cs.uni-magdeburg.de/~isenberg/papers/Teutsch_2004_EAO.pdf.

Teng, S. G., Ho. S. M., Shumar, D., Liu, P., 2006, "Implementing FMEA in a Collaborative Supply Chain Environment", International Journal of Quality & Reliability Management, vol. 23, no. 2, pp. 179 – 196, DOI 10.1108/02656710610640943.

Teoh, P. C., Case, K., 2004, "Failure Modes and Effects Analysis through Knowledge Modeling", Journal of Materials Processing Technology, pp. 253 – 260.

Thompson, W. B., Owen, J. C., De St. Germain, J., Stark, S. R., Henderson T. C., 1999, "Feature Based Reverse Engineering of Mechanical Parts", IEEE Trans. Robotics and Automation, vol. 15, no. 1, pp. 57 – 66.

Tichkiewitch, S., Veron, M., 1998, "Integration of Manufacturing Processes in Design" Annals of the CIRP, vol. 47, no. 1, pp. 99 – 102.

Tilley, S. R., 1998, "A Reverse-Engineering Environment Framework", Software Engineering Institute Technical Report, SEI-98-TR-005, Carnegie Mellon University.

Tonshoff, E., Aurich, J. C., Ehrmann, M., D'Agostino, N., 1996, "A Unified Approach to Free Form and Regular Feature Modeling", Annals of the CIRP, vol. 45, no. 1, pp. 125 – 128.

Towler, K. L., 2003, "Connecting Rod with Increased Effective Length and Engine Using Same", US Patent 6,651,607.

Tsakiri, M., Ioannidis, C., Carty, A., 2003, "Laser Scanning Issues for the Geometrical Recording of a Complex Statue" 11th International Symposium on Deformation Measurements, CD-ROM, url: http://www.archaeoptics.co.uk/downloads/publications/Tsakiri_etal.pdf.

Turk, G., Levoy, M., 1994, "Zippered Polygon Meshes from Range Images", Proc. of ACM SIGGRAPH, pp. 311 – 18.

United States Department of Defense, 2006, "Assistant Secretary of Defense (Networks & Information Integration), DoD CIO", url: http://www.defenselink.mil/nii/global_Info_grid.html.

Urbanic, R. J., ElMaraghy, H. A., ElMaraghy, W. H., 2006, "A Reverse Engineering Methodology for Rotary Components from Point Cloud Data", submitted to International Journal of Advanced Manufacturing Technology.

Urbanic, R. J., ElMaraghy, W. H., 2007, "A Collaborative Design Recovery Framework", International Journal of Computer Integrated Manufacturing, Special Issue, accepted.

Urbanic, R. J., ElMaraghy, W. H., 2006, "A Collaborative Design Recovery Framework", CIRP Digital Technology Enterprises Seminar, CD ROM.

Urbanic, R. J., ElMaraghy, H. A., ElMaraghy, W. H., 2006, "An Integrated Systematic Design Recovery Framework", ASME Journal of Computing and Information Science in Engineering, accepted.

Urbanic, R. J., ElMaraghy, H. A., ElMaraghy, W. H., 2006, "Reverse Engineering Standard Rotary Components from Point Cloud Data Using Data Transformations", Proc. of the 16th CIRP Design Seminar, Calgary, pp. 187–198.

Urbanic, R. J, ElMaraghy, H. A., ElMaraghy, W. H., 2005, "Integrated Reverse and Forward Engineering Design: A Systematic Analysis-Synthesis Approach", Proc. of the 15th CIRP Design Seminar, Shanghai, pp. 451 – 462.

Urbanic, R.J., ElMaraghy W.H., 2004, "Modelling of Manufacturing Process Complexity", Proceedings of the CIRP 2004 Design Seminar, Cairo, Egypt, May 16 – 18, CD ROM.

Urbanic, R.J., ElMaraghy W.H., 2003, "Modelling of Participatory Manufacturing Process", Proceedings of the CIRP 2003 Design Seminar, Grenoble France, pp. 58 – 69.

Vadde, S., Kamarthi, S.V., Gupta, S.M., 2004, "Multi-Scale Registration Algorithm for Alignment of Meshes", Intelligent Manufacturing, The International Society for Optical Engineering, Providence, RI., United States, p. 113.

Vanco, M., and Brunnett, G., 2004, "Direct Segmentation of Algebraic Models for Reverse Engineering", Computing, vol. 72, no. 1-2, pp. 207 – 220.

Van Vliet, J.W., Van Luttervelt, C.A., Kals, H.J.J., 1999, "State-of-the-Art Report on Design for Manufacturing", Proc. ASME Design Engineering Technical Conferences, DETC99/DFM-8970.

Venuvinod, P. K., Yuen, C. F., 1994, "Efficient Automated Geometric Feature Recognition Through Feature Coding", Annals of the CIRP, Submitted by M. Merchant, vol. 43, no. 1, pp. 413 – 416.

Volodine , T., Roose, D., Vanderstraeten, D., 2003, "Efficient Triangulation of Point Clouds Using Floater Parameterization", Proc. of the Eighth SIAM Conference on Geometric Design and Computing, url: http://www.cs.kuleuven.ac.be/~timv/publications/triangulation03.pdf.

Vosniakos, G., 1997, "Conversion of Wireframe to ACIS Solid Models for 2½ D Engineering Components", The International Journal of Advanced Manufacturing Technology, vol. 14, no. 3, pp. 199 – 209.

Wang, C., Vergeest, J., Horvath, I., Dormitrescu, R., Wiegers, T., Song, Y., 2002, "Cross model Shape Reuse: Copying and Pasting of Freeform Features", Proceedings of 2002 ASME Design Engineering Technical Conferences & Computers and Information in Engineering Conferences, pdf. url: http://dutoce.io.tudelft.nl/~chensheng/f-cwang-pub.html.

Weisstein. E., W., 2003, "Circular Segment", From MatthWorld ©2006, A Wolfram Web Resource, url: http://mathworld.wolfram.com/CircularSegment.html.

Werghi, N., Fisher, R., Ashbrook, A., Robertson, C., 2002, "Shape reconstruction incorporating multiple nonlinear geometric constraints", Constraints, vol. 7, no. 2, pp. 117–149.

Werghi, N., Fisher, R., Robertson, C., Ashbrook, A., 1999, "Object Reconstruction by Incorporating Geometric Constraints in Reverse Engineering", CAD Computer Aided Design, vol. 31, no. 6, pp. 363 – 399.

Wiendahl, H.P., and Scholtissek, P., 1994; "Management and Control of Complexity in Manufacturing", CIRP Annals, vol. 43, no. 2, pp. 533 – 540.

Wohlers, T., 2001, "Rapid Prototyping & Tooling State of the Industry", 2001 World Wide Progress Report, Wohlers Associates, Fort Collins, Coronado.

Wohlers, T., 1995, "The Challenge of 3D Digitizing", CGW, vol. 18, no. 11.

Wu, Q., M., Rodd, M., G., 1990, "Boundary Segmentation and Parameter Estimation for Industrial Inspection", IEE PROCEEDINGS, vol. 137, no. 4, pp. 319 – 327.

Xue, D., 2006, "Discussion on Design Matrices in Axiomatic Design", Proc. of the 16th CIRP Design Seminar, Calgary, pp. 266 – 274.

Yau, H., Chen, C., Wilhelm, R.G., 2000, "Registration and integration of multiple laser scanned data for reverse engineering of complex 3D models", International Journal of Production Research, vol. 38, no. 2, pp. 269 – 285.

Yoon, B., Kim, M., 1994, "Reinforced Material for an Automobile Connecting Rod", US Patent 5,523,171, Hyundai Motor Company, Seoul, KR.

Ypsilos, I., 2004, "Capture and Modelling of 3D Face Dynamics", PhD dissertation, University of Surrey. url: http://www.ee.surrey.ac.uk/CVSSP/VMRG/Publications/ypsilos04phd.pdf.

Yuan, X., Zhenrong, X., Haibin, W. 2001, "Research on Integrated Reverse Engineering Technology for Forming Sheet Metal with a Freeform Surface", Journal of Materials Processing Technology, vol. 112, no. 2, pp. 153 – 156

Zachman, J., 2002, "Enterprise Architecture", Zachman International©, url: http://www.zachmaninternational.com/default.htm.

Zhang, Z., Zhang, D., Peng, X., 2004, "Performance Analysis of a 3D Full-Field Sensor Based on Fringe Projection", Optics and Lasers in Engineering, pp. 341 – 353.

Zhang, L. Y., Zhou, R. R., Zhu, J. Y., Wu, X., 2002, "Piecewise B-Spline Surfaces Fitting to Arbitrary Triangle Meshes", Annals of the CIRP, vol. 51, no. 1, pp. 131 – 134.

Zhongwei. Y., Shouwei, J., 2003, "Automatic Segmentation and Approximation of Digitized Data for Reverse Engineering", International Journal of Production Research, pp. 3045 – 3058.

Zimmermann, J. U., Haasis, S., van Houten, F. J. A. M., 2002, "ULEO- Universal Linking of Engineering Objects", Annals of the CIRP, vol. 51, no. 1, pp. 99 – 102.

APPENDIX A: IDEF0 MODELLING OF FORWARD AND REVERSE ENGINEERING

A.1 BACKGROUND

Forward Engineering (FE) design is the process of creating an end product that meets a specific need. The final product can be a component, an assembly, a process or system. A logical thought process is utilized to migrate from 'WHAT' needs to be achieved to satisfy the need to 'HOW' to satisfy the need within the given constraints (Figure A-1). Engineering design is an open – ended process. There is no correct solution: engineers strive for an optimal solution based on the available information and a given set of constraints. To this end several engineering design methodologies have been developed, which are based on generalized systematic procedures to transform the abstract 'WHAT' into a physical 'HOW'.

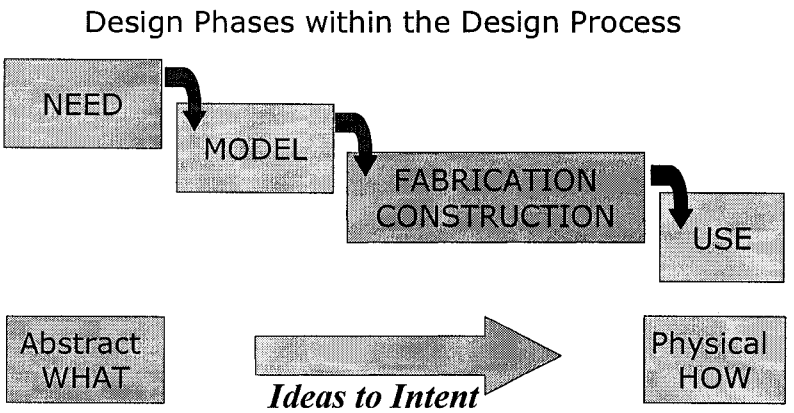

Figure A-1: Engineering Design

With reverse engineering, a deductive process is combined with data gathering techniques to migrate from a physical 'WHAT' to the hypothetical 'WHY' and a conjectured model. The fabrication techniques are essentially out of the "design loop" (Figure A-2).

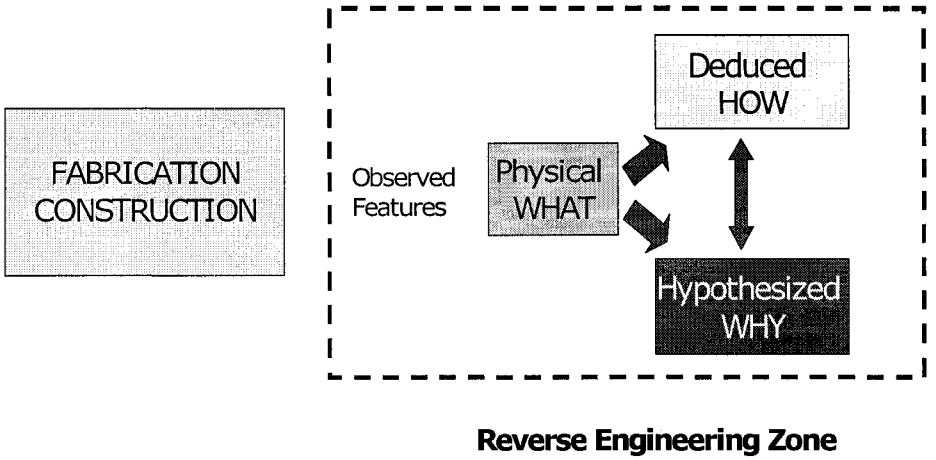

Figure A-2: Reverse Engineering Design

A.2 FORWARD ENGINEERING IDEF0 MODEL

The generic product development activities as illustrated in Figures A-3 (a) and (b) are: (i) define the need, (ii) design the product, (iii) plan the manufacturing process, (iv) establish the production process, (v) plan the product production, (vi) operate the production process and (vii) maintain and improve the production process.

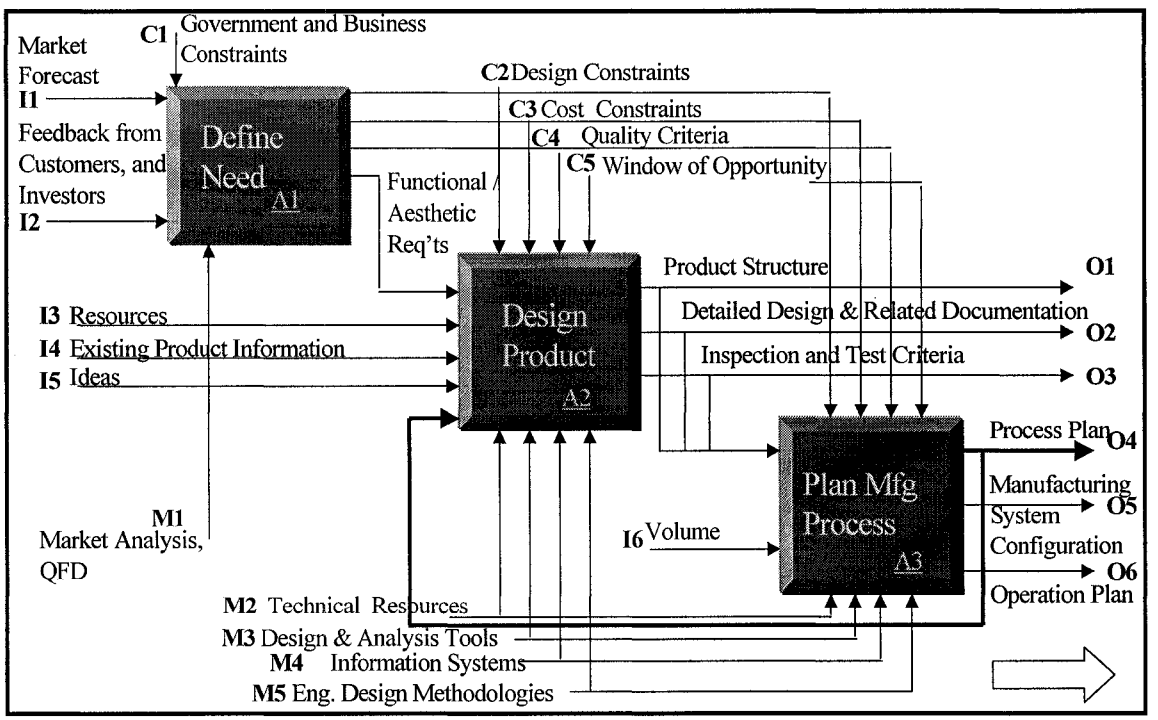

Figure A-3 (a): A0 Node for Product Development, Elements A1 – A3

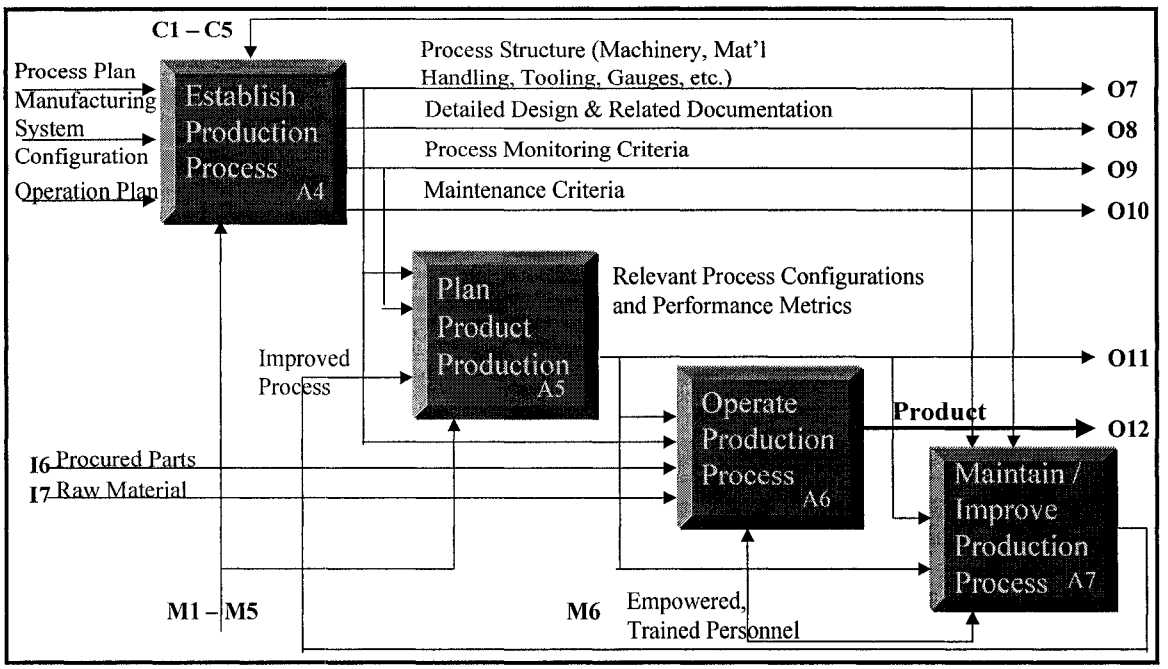

Figure A-3 (b): A0 Node for Product Development, Elements A4 – A7

Modern consumers demand innovative products that are low cost, convenient, flexible and robust. Based on market forecasts and other customer or stakeholder feedback, the abstract "what is needed" and "what must it do" is translated into functional and aesthetic requirements. A complete "customer description" or review of the environment is required. This includes specific, quantitative information such as all relevant dimensions, weights, capacity requirements, operating temperatures, loading, hardware, software, timing issues, available resources, legal requirements and any other relevant information not contained in this list. The problem must be specified in detail before it can be properly solved. A complete problem statement outlines the main goals and constraints. This defines the envisioned outcome and establishes a baseline for the subsequent design tasks. Conflicting or ambiguous inputs must be clarified at this stage. Market analysis techniques such as surveys and the Quality Function Deployment (QFD) and benchmarking techniques (Figure A-4) are used to highlight issues and clarify the design problem.

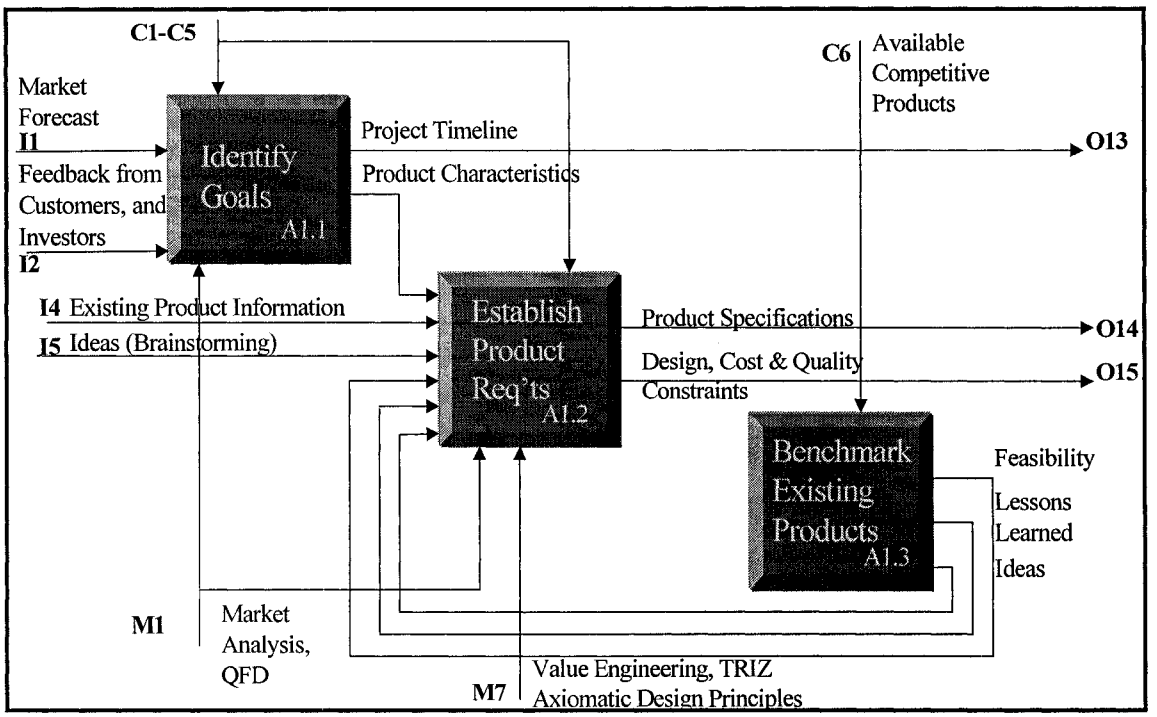

Figure A-4: A1 Node – Define Need

Based on the requirements, resources, design ideas and constraints, the high level abstract concepts are developed into concrete detailed designs (Figure A-5). The final output of the design process is the product structure, the detailed design criteria and inspection and test criteria for critical characteristics. The product structure includes items such as physical features, information flow, embedded software, man/machine interfaces (hardware/software) and the system integration. The detailed design criteria include items such as the tolerances and ancillary specifications such as cleanliness, porosity, hardness, torque levels and so forth. Inspection and test criteria for critical characteristics are generated not only manufacturing purposes, but for usage and maintenance in the field.

The specific design features (functional, structural, assembly, interface, and form), the manufacturability, the physical characteristics, quality, testing and validation criteria are analysed and refined to produce a detailed design of the product components, tolerances, specifications and a bill of material (BOM), as illustrated in Figure A-6.

Several engineering design methodologies such as Value Engineering (VE), Axiomatic Design, and the Theory of Inventive Problem Solving (TRIZ) assist the designer in creating a robust

design based on logical and rational thought processes. Parameter analysis and optimization tools enable designers to rapidly assess alternatives. Simulations and physical tests are performed to provide insight into the design robustness. Knowledge gained throughout the design cycle is used to refine and finalize the design details.

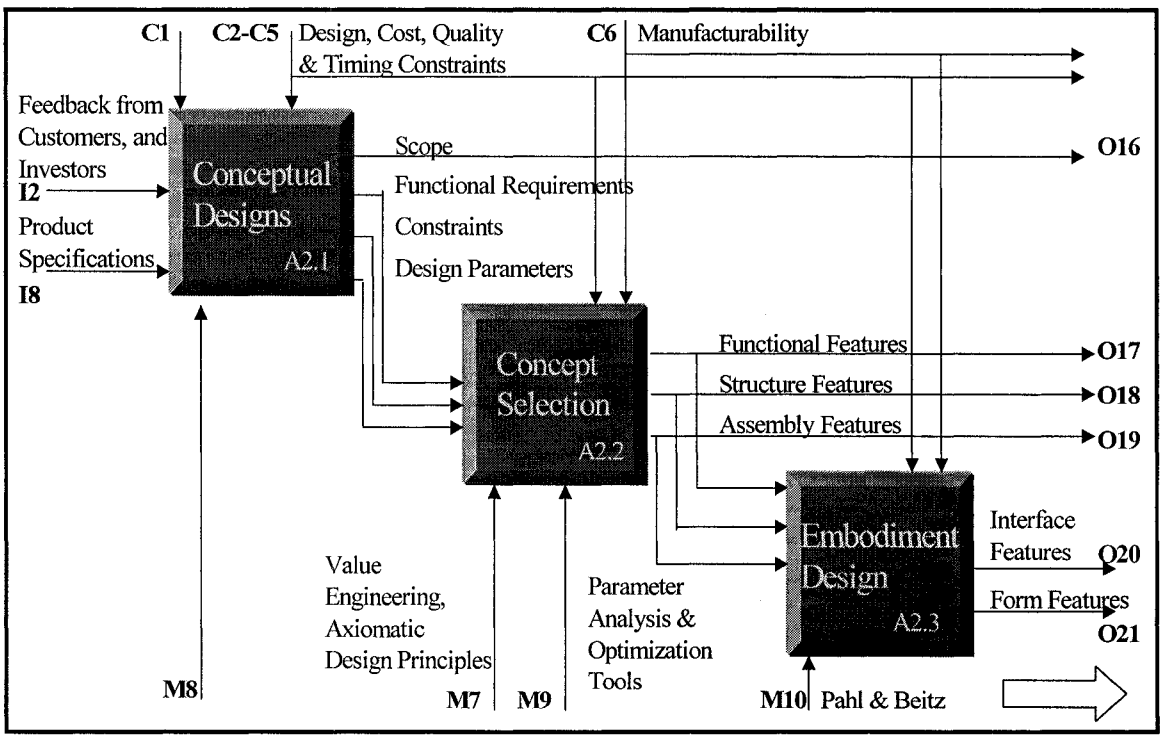

Figure A-5: A2 Node – Design the Product, Elements A2.1 – A2.3

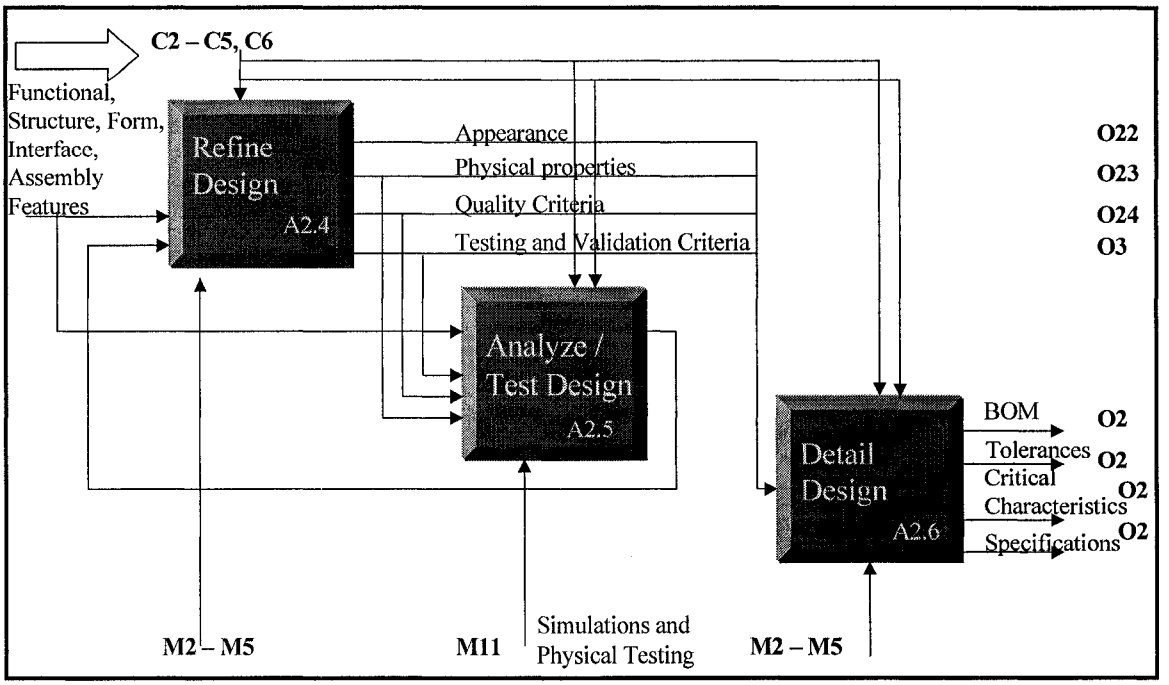

Figure A-6: A2 Node – Design the Product, Elements A2.4 – A2.6

However, today's designers cannot work in a vacuum. To meet the challenges in today's aggressive, volatile, global market, innovative processes are as much of a strategic weapon as innovative products. Design for "X" and concurrent product and process engineering are common practice. New product and process design philosophies such as life cycle considerations and reconfigurable manufacturing systems are on the horizon; consequently, the manufacturability of the product / product elements is a constraint that cannot be ignored (constraint C6 in these illustrations). New product development is intertwined with the planning, implementation, and operation of the process (Figure A-3). The final quality of the product is based on two main aspects: the quality of design and the conformance to specification or the quality of the process; hence, the maintenance and improvement of the process is also vital. The information on the final design requirements combined with the projected volumes is used to generate a manufacturing strategy. Design strategies that incorporate horizontal or vertical leveraging, or family of parts enables the use of group technologies, cellular manufacturing techniques, etc. Once the process and operating plan and a manufacturing system configuration have been determined, the complete manufacturing process can be designed and implemented. The design loop for the manufacturing process complements that of the product to be fabricated (Figure A-7).

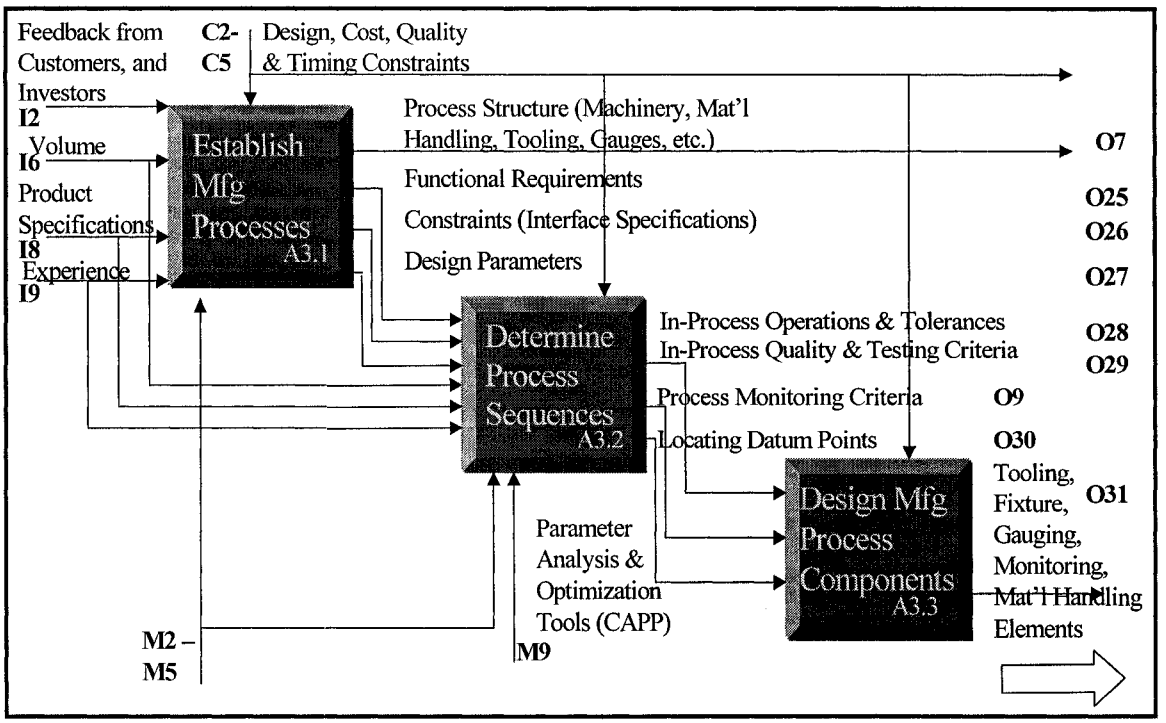

Figure A-7: A3 Node – Plan the Manufacturing Process, Elements A3.1 – A3.3

The functional requirements for the machines, tooling, fixturing, material handling, storage, layout, process capability, testing and validation equipment must developed, analysed and refined, and a final product (the process components) fabricated from the resulting criteria (Figure A-8).

The performance metrics (such as the quality, reliability, efficiency and usability) of the resulting process strongly influence the process's production planning, operation and maintenance, which have a direct influence on the availability, cost and quality of the final product.

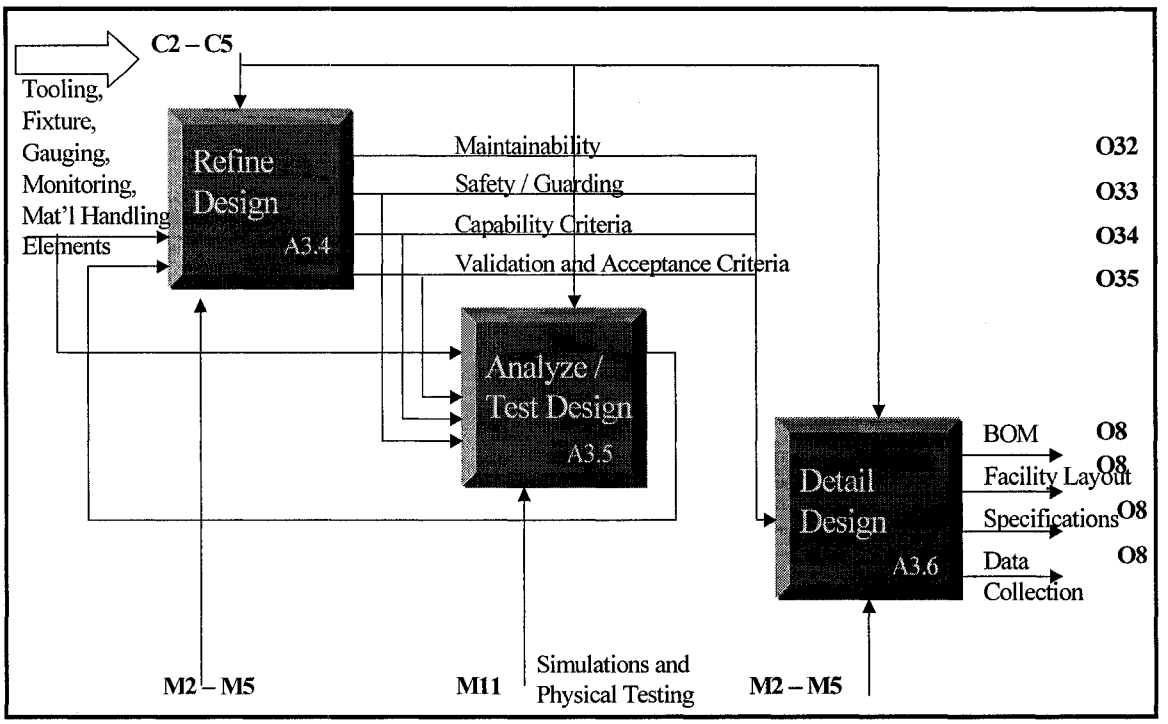

Figure A-8: A3 Node – Plan the Manufacturing Process,
Elements A3.4 – A3.6

A.3 REVERSE ENGINEERING IDEF0 MODEL

The generic reverse engineering activities as illustrated in Figures A-9 are: (i) define the functions, (ii) gather data, and (iii) deduce the "detailed" functional model. When reverse engineering you are interpreting 'WHAT' has been accomplished into a 'WHY' has this been accomplished. The "HOW was this accomplished" related questions focus on linking form-feature relationships, not establishing the fabrication / manufacturability information. The relevance of the final model is contingent on the available knowledge associated with the product. Without an understanding of the environment, super structure or sub-system components, information with respect to the device functionality and the design parameters may be misinterpreted. A thorough analysis of the system of parts must be conducted in order determine the overall and individual functional requirements and to infer the original needs and produce pertinent product documentation.

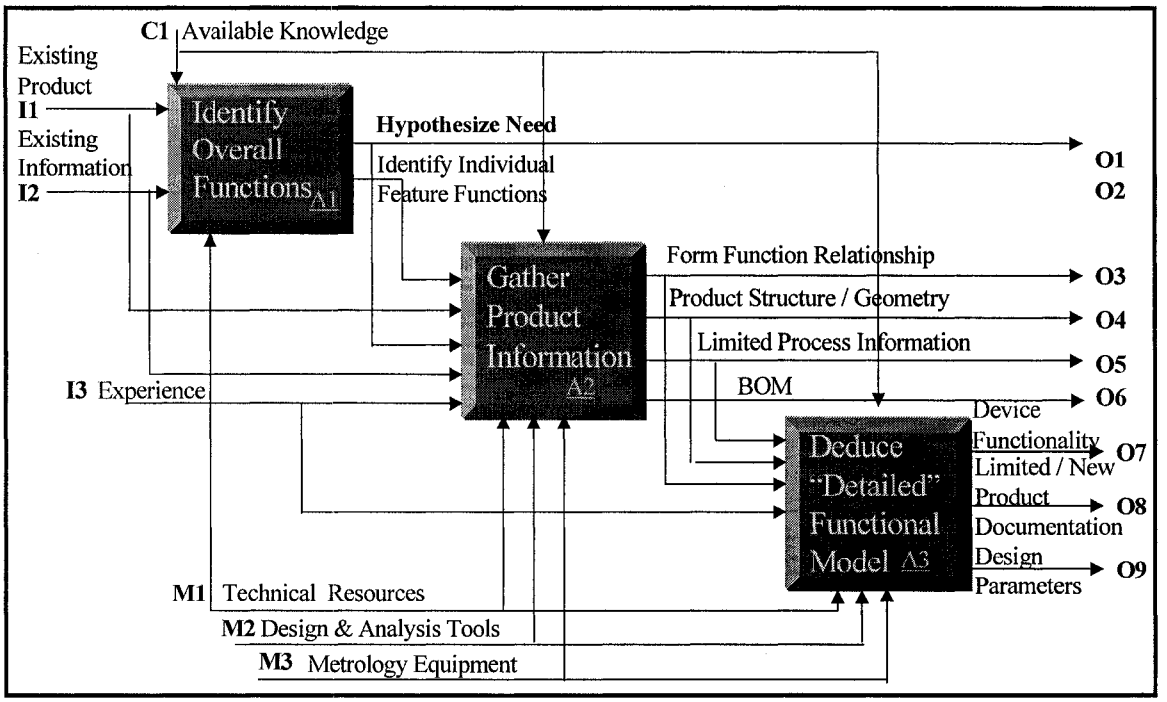

Figure A-9: A0 Node – Reverse Engineering

With forward engineering, the desired goals drive the specific product requirements, while the opposite is true with reverse engineering. By assessing existing products or a competitor's products (benchmarking), the product requirements and goals are inferred (Figure A-10). The benchmarking aspect of reverse engineering is a powerful design tool: observing how a product has been designed provides insights (feasibility, new ideas) for designing a new product; hence, the negative connotations associated with reverse engineering.

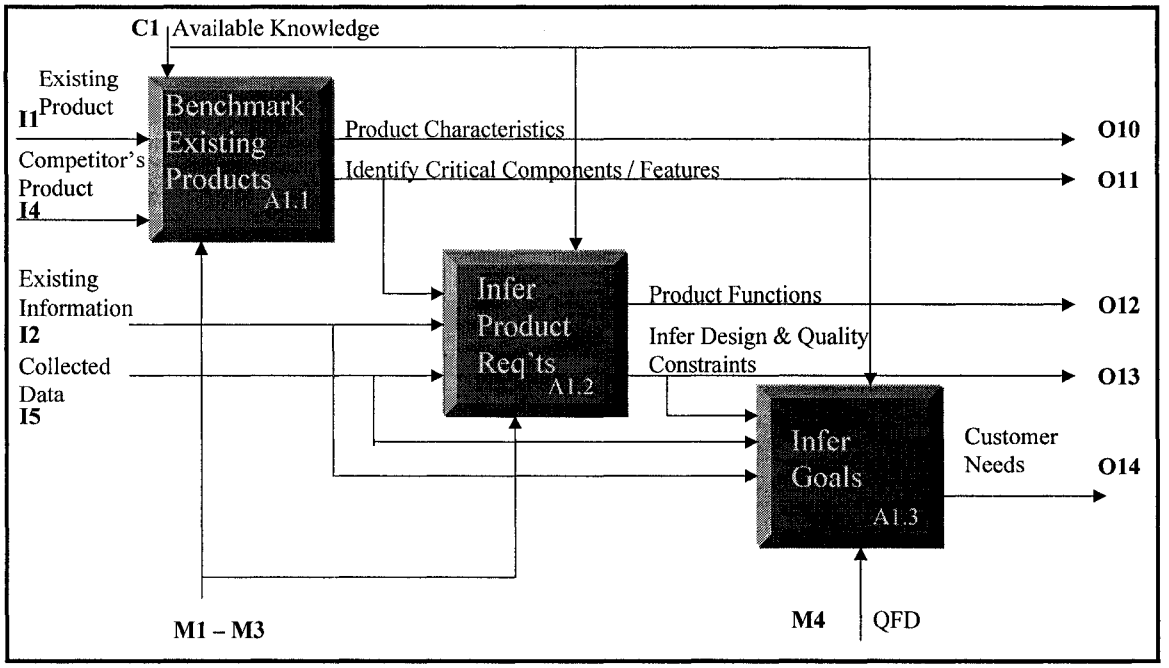

Figure A-10: A1 Node – Hypothesize Need

When gathering data (Figure A-11), the relationship between all components must be carefully documented during the disassembly phase. The commercial products must be identified in tandem with the custom designed components to generate a complete bill of materials (BOM). The selection of the commercial products provides insight into the build tolerances of the product. Characteristics such as the material and metallurgical properties, physical geometry, surface finishes, etc. all provide critical information. As much knowledge with respect to the environment, applied stresses and loading, and so forth must be captured in order to be able to link the form and functional properties and to deduce the device functionality, the design parameters and generate relevant product documentation. Physical and virtual experimentation tools such as finite element modelling (FEM) can be used to test and validate the recreated reverse engineering model.

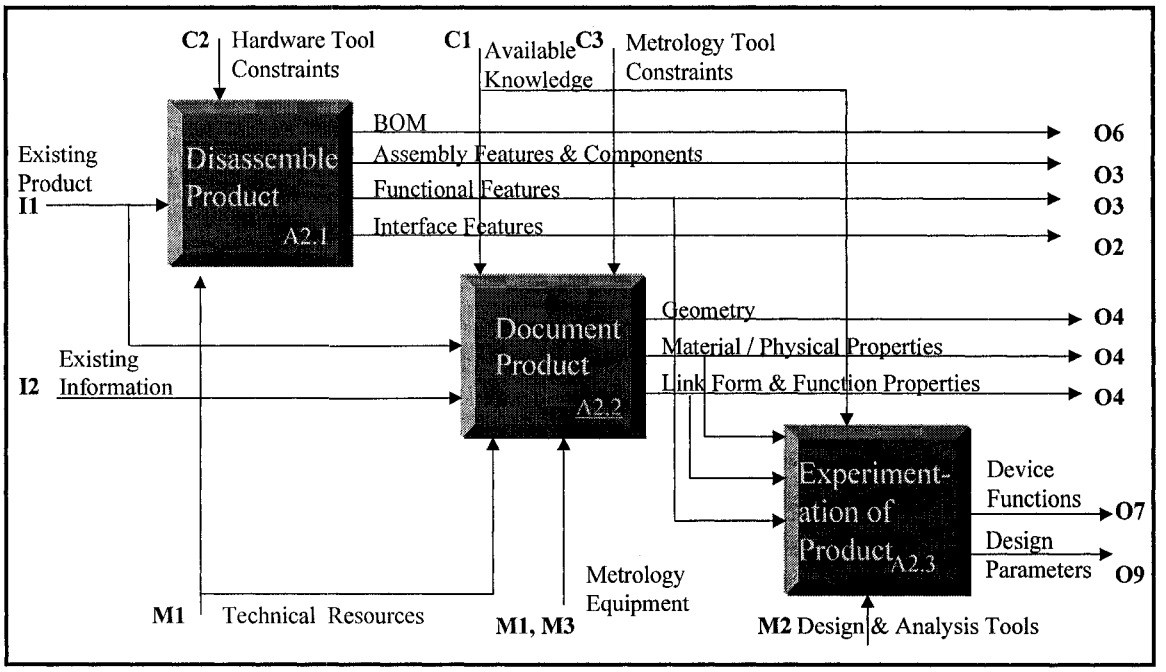

Figure A-11: A2 Node – Gather Data

Engineering design methodologies in combination with assessing the collected data can be used to determine the design parameters and infer the final product documentation (such as tolerances and specification). This is speculative in nature, and highly dependent on the quality of the available data and existing information (Figure A-12).

Morphological analysis (MA) is a structured methodology for identifying and investigating the total set of possible "solution configurations" for a problem. The problem must be restructured to a set of parameters or required functions, and an array of alternative means for achieving each individual requirement (Figure A-12). Solutions for the overall design problem are found by determining the optimal combination of sub-function alternatives. MA is a tool that can provide insight to the function – form link; however, for reverse engineering analysis the physical objects are used to determine the solution principle. It must be remembered that the particular method used for a given situation depends not only on the purpose, but also on the available means and resources. Therefore, TRIZ and VE techniques can help provide insights into the solution principles, functions and constraints.

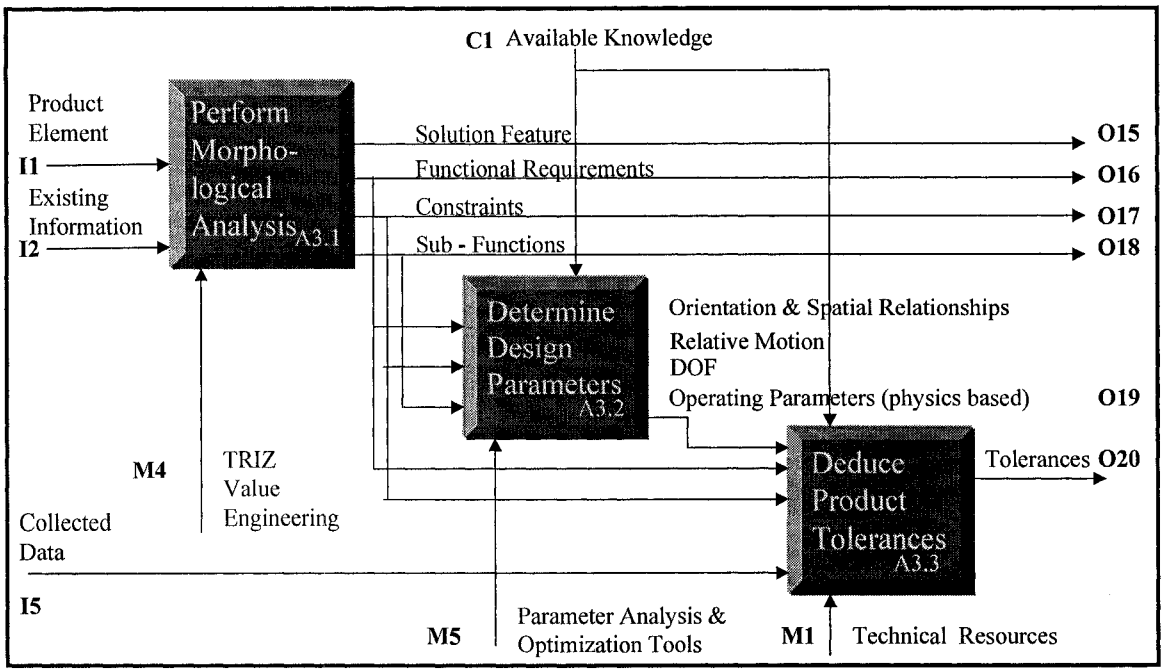

Figure A-12: A3 Node – Deduce "Detailed" Functional Model

A two-pronged measurement strategy must be developed to collect form and feature data and the physical properties (mechanical, metallurgical, electrical, chemical) of the product (Figures A-13 and A-14). The appropriate type of micrometers and gages can be used to measure hole diameters and depths, fillets, threads, etc. A CMM with a touch probe or scanning head can be used to generate the (x, y, z) coordinates of the features and surfaces and assist in evaluating geometric relationships (straightness, flatness, cylindricity, perpendicularity, angularity, etc.). A profilometer that provides surface finish parameters over and above Ra and Rq (such as Rp, Rv,) will provide information with respect to specialized surface finish requirements.

Scanned data must be filtered to reduce noise and the decrease the number of data points to improve processing times. From the filtered data, sophisticated algorithms are utilized to generate a surface model. Beautification techniques are used to identify primitives, detection of similarities and symmetry, edges, curvature estimation and so forth. The quality of the reconstruction not only depends on the number and density of the sample points but also on their alignment to sharp and rounded features of the original geometry. Bad alignment can lead to severe alias artefacts [Botch and Kobbelt, 2001].

Geometric data should be collected before investigating the physical characteristics because destructive techniques are required to collect the requisite data. Mass, volume, and hardness (at the surface level) can be determined non-destructively, but the tensile and impact strengths and metallurgical properties cannot. The product must be tested for surface treatments, coatings, and heat treatments. Wear patterns, warping and distortion, cracks and tears, porosity and other phenomena must be assessed to provide design, manufacturing and usability information.

When collecting data, any available documentation such as service manuals, sub component or "super structure" documentation, non-proprietary related drawings and so forth could also be beneficial.

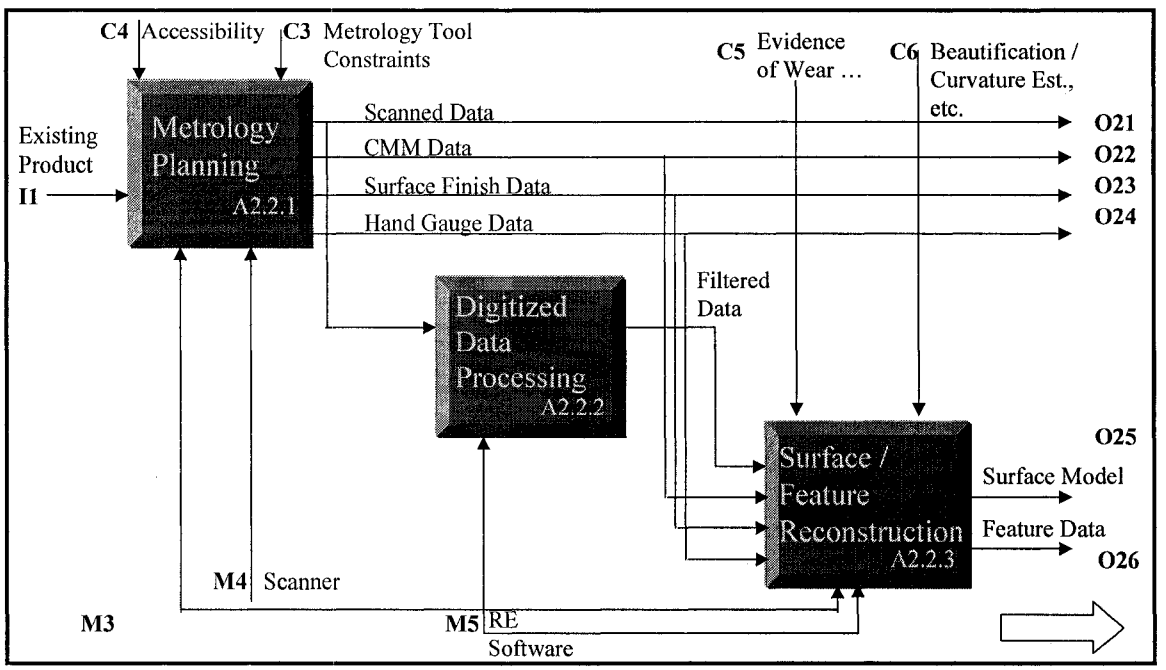

Figure A-13: A2.2 Node – Document Product, Elements A2.2.1 – A2.2.3

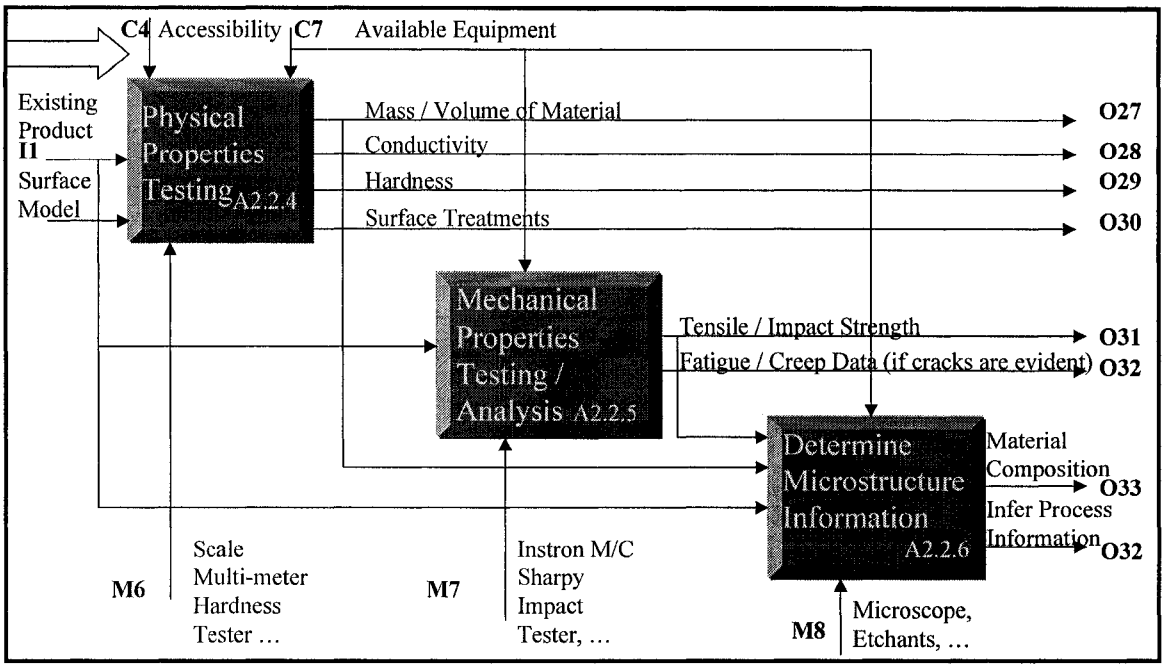

Figure A-14: A2.2 Node – Document Product,
Elements A2.2.4 – A2.2.6

APPENDIX B: DESIGN FOR X TABLES

Table B-1: Process Comparison Overview: Material, Volume and Size

Process Type	Material											Production Volume (pcs / unit time)			Size (kg)							
	Aluminum	Copper	Iron	Magnesium	Steel	Stainless Steel	Titanium	Zinc	Superalloys	Thermoplastic	Thermoset	Low	Medium	High	0.001 - 0.01	0.01 - 1	1 - 10	10 - 50	50 - 100	100 - 500	500 - 1000	> 1000
Investment Casting	x	x		x	x	x		x				x	x			x	x	(x)	(x)			
Permanent Casting	x	x	x	x	x	x		x					x	x			x	x	x			
Sand Casting	x	x	x	x	x	x		x	x			x	x	x		x	x	x	x	x	x	x
Shell Casting	x	x	x		x	x		x	x				x			x	x	x	x			
Die Casting	x	x		x				x						x		x	x	x	x			
Cold Extrusion	x	x	x	x	x	x	x	x	x				x	x	x	x	x	x				
Hot Extrusion	x	x	x	x	x	x	x	x	x								x	x	x	x		
Cold Forging	x	x	x	x	x	x	x	x	x				x	x	x		x	x				
Stamping / Stretching	x	x	x	x	x	x	x	x	x					x								
Deep Drawing	x	x	x	x	x	x	x	x	x					x								
Injection Moulding										x	x		x	x								
Compression Moulding										x	x		x	x								
Transfer Moulding										x	x		x	x								
Thermoplastic Extrusion										x				x								
Machining	x	x	x	x	x	x	x	x	x	(x)	(x)	x	x	x								

Adapted from Schey [1987], and Dixon and Poli [1995]

x – applicable, (x) – restricted applications, shaded areas – irrelevant

Table B-2: Process Comparison Overview: Characteristics, Costs and Design Considerations

Process Type	Characteristics												Costs			
	Porosity	Non-Uniform Hardness	Inclusions	Variable Strength	Surface Discontinuity	Shrinkage	Distortion	Achievable Tolerance Range (mm)	Lower Limit Surface Finish (μm)	Minimum Section (mm)	Maximum Section (mm)	Surface Detail	Die	Equipment	Labour	Finishing
Investment Casting	L	x		x	x	x		0.08-0.3	0.6			H	MH	LM	H	LM
Permanent Casting	H	x		x	x	x	x	0.4-2.0	0.8			M	M	MH	LM	MH
Sand Casting	M	x	x	x	x	x		0.9-2.1	6.3			L	L	L	MH	H
Shell Casting	L	x	x	x	x	x		0.5-1.0	3.2			M	LM	MH	LM	MH
Die Casting	H	x	x	x	x	x	x	0.1-0.4	0.4			M	H	H	LM	LM
Cold Extrusion								0.06-0.2	0.4				H	H	LM	L
Hot Extrusion								0.15-1.5	1.6				H	H	LM	M
Cold Forging								0.25-.04	0.4			M	H	H	LM	L
Stamping / Stretching							x	0.015-0.3	0.1		2	M	MH	M	LM	LM
Deep Drawing							x	0.3-0.7	0.2		10		H	H	LM	L
Injection Molding					x	x	x	0.7-0.35	0.18	0.4(a) 1.0(b)		H	MH	MH	L	LM
Compression Molding					x	x		0.7-0.35	0.18	1.5		H	MH	M	L	LM
Transfer Molding					x	x		0.7-0.35	0.18	1.5		H	MH	M	L	LM
Thermoplastic Extrusion								0.7-0.35	0.18	0.4			M	MH	L	L
Machining							L	0.0002-0.5	< 0.025	(c)						

Adapted from Schey [1987], and Dixon and Poli [1995]

(a) thermoplastic, (b) thermoset, (c) varies with process

x – relevant, L – low, M – medium, H – high, shaded areas – irrelevant

Table B-3: Process Design Considerations

Process Type	DFX															
	No Internal Geometry	No External Undercuts	No Internal Undercuts	Constant Cross Section	Smooth transitions	Large radii	Draft Angle	Parting Plane	Uniform Thickness	Minimize no. of distinct features	Avoid closely spaced features	Avoid narrow cutouts/ projections	Minimize bend axes	Avoid bends greater than 90 deg.	Avoid long, thin sections	Minimize semi-hollow features
Investment Mold Casting					x		x		x							
Permanent Mold Casting	x	x	(l)		x		x	x	x							
Sand Casting		(l)			x	x	x		x							
Shell Casting					x		x		x							
Die Casting	x	x	(l)		x		x	x	x							
Cold Extrusion	x	x	x	x			x		x			x			x	x
Hot Extrusion	x	x	x	x			x		x			x			x	x
Cold Forging	x	(l)	x				(x)	x				x				
Stamping / Stretching	x	x	x							x	x	x	x	x		
Deep Drawing	x	x	x													
Injection Molding	x	(l)	(l)		x		x	x	x							
Compression Molding	x	(l)	(l)		x		x	x	x							
Transfer Molding	x	x	x		x		x	x	x							
Thermoplastic Extrusion	x	x	x	x	x				x						x	x
Machining	(l)	(l)	(l)													

Adapted from Schey [1987], and Dixon and Poli [1995]

x – applicable, (l) – limited applications, shaded areas – irrelevant

APPENDIX C: SUPPLEMENTARY DESIGN INFORMATION

C.1 ONTOLOGY

Ontology is defined here as containing a set of taxonomies related to the design recovery process domain. A taxonomy is a collection of controlled vocabulary terms organized into a hierarchical structure. A controlled vocabulary is a list of terms that have been enumerated explicitly. The controlled vocabulary focuses on the function and form aspects of the component and feature designs. The function related taxonomy is illustrated in Figure C-1, and the controlled vocabulary follows.

Generic Function Information: The NIST terminology [Hirtz et al, 2002] is used to describe the general functions for the component and features.

Feature Function Family: The features are used to satisfy product, process or assembly related functional requirements.

Product function: A form that assists with meeting the product related FRs.

Process function: A feature that assists with meeting process related FRs.

Assembly function: Assembly features that allow the product to be assembled.

Feature Function Type: A general function-form description used to classify the features. These function-form types are applicable for each member of the feature function family.

Clearance feature: A feature that clears another component in its vicinity, and has a loose tolerance associated with it.

Complex feature: A feature consisting of intricate edges, multiple edges, and tight tolerances (i.e. multiple step bearing pocket bore).

Enclosure feature: A feature that closes in the surrounding environment.

External protrusion: A feature that juts out from the surrounding surface to meet its FRs (i.e. boss, tab, cooling fin).

Fastening feature: A feature that assists with making the mating component fast and secure.

Free-form feature: An intricate feature used for aesthetic purposes that has loose tolerances.

Fillet feature: A 'radial' form that blends surrounding features.

Locating feature: A feature that assists with setting or establishing a particular reference.

Planar feature: A feature with a flat surface.

Power transmission feature: A feature that used in transmitting power, torque or other motion characteristics (i.e. gear or spline tooth).

Precision bore feature: A cylinder (subtractive feature) with a precision shape and / or surface finish.

Precision shaft feature: A cylinder (additive feature) with a precision shape and / or surface finish.

Seating feature: A feature that assists with position and orientation for a mating component.

Support feature: A feature that assists with supporting the structure of the component or mating features (i.e. gusset).

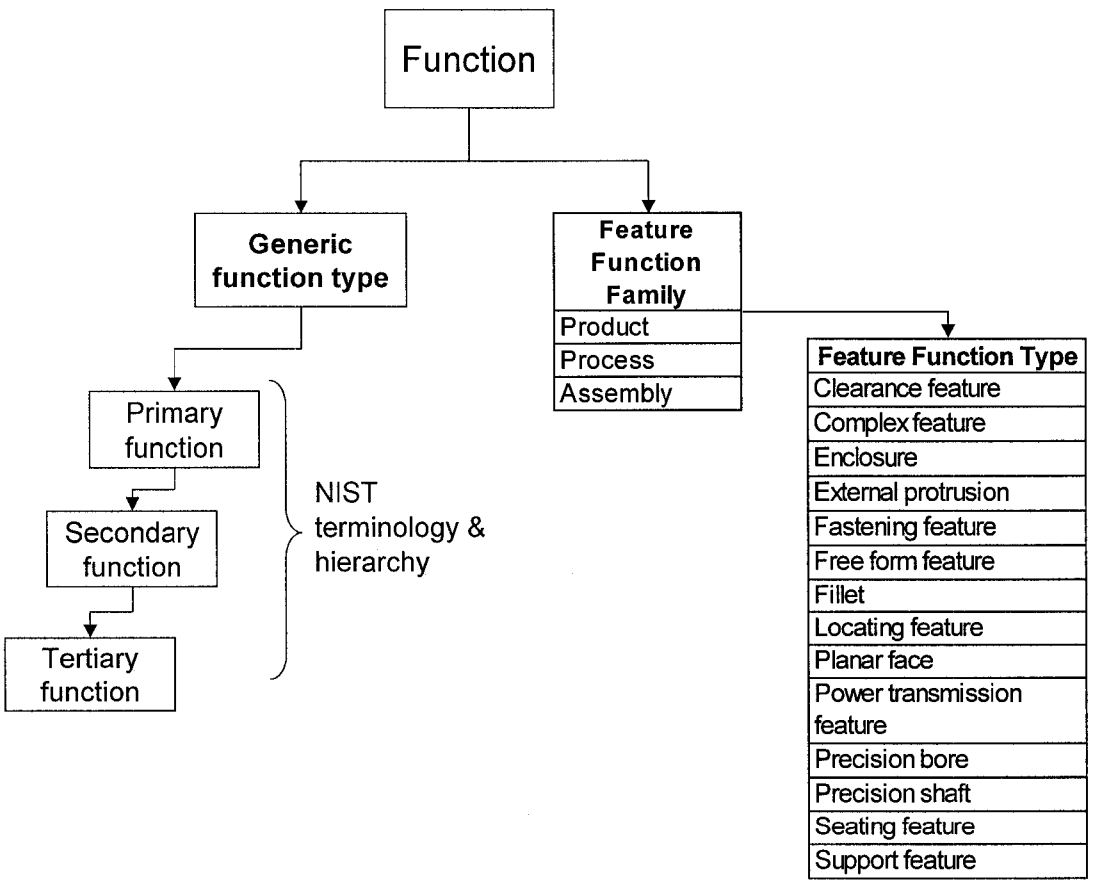

Figure C-1: Function Taxonomy

The form taxonomy is illustrated in Figure C-2, and the controlled vocabulary is listed below. The component is composed of a set of features. The form for each feature has a structure consisting of a set of design parameters, and a set of relationships to other features or external mating components.

Generic Feature Geometry Type: Each feature consists of specific design parameters or by blending certain wire frame geometry. The feature type is defined by nature of the feature's parameters.

Feature Construction Methods: The procedure used in CAD surface or solid modelling systems to create the feature from specific wire frame data and parameters [Lee, 1999].

Boolean: The method used to combine design parameters from multiple features to create the final part.

Internal feature: A feature created by a subtractive operation

External feature: A feature created by an additive operation

Pattern Type: The family of common patterns or characteristic arrangements of features that are typically used in fabrication processes. The pattern types illustrated in Figure 4-34 and identified in Figure C-2 can be easily generated using specific CNC G codes [Smid, 2000].

GDT/Ancillary Feature Relationships: The GD&T terms are defined in the ASME-Y14.5M Standard. The ancillary relationships are used to convey other descriptive information during the design recovery process that complement the GD and T terms.

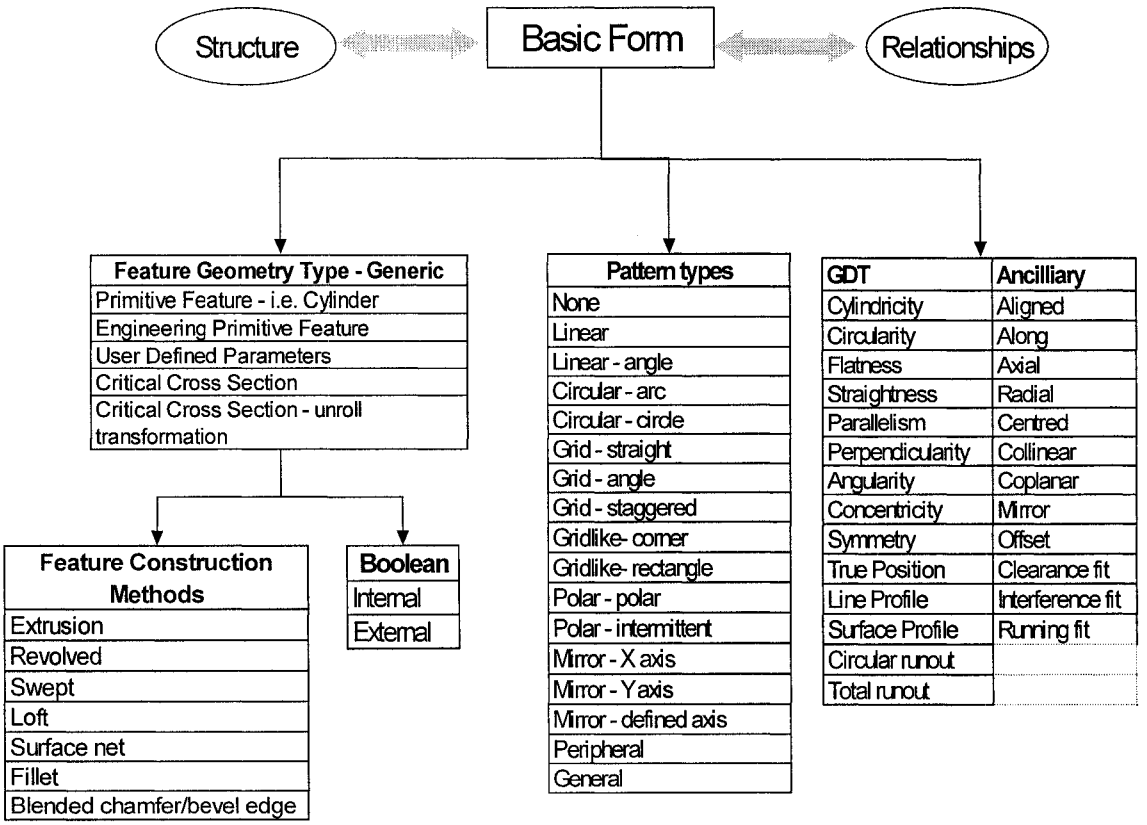

Figure C-2: Form Taxonomy

C.2 SUPPLEMENTARY DESIGN INFORMATION FOR THE POWER STEERING PUMP PULLEY

The features contained in the power steering pump pulley are the:

- Crankshaft mounting bolt hole, A1 (datum -A-)
- Threaded fastener clearance holes, B1 – B3, pattern B_C1
- Threaded fastener clearance holes, C1 – C4, pattern C_C2
- Locating dowel holes D1 and D2, pattern D_C2

The connectivity diagram is illustrated in Figure C-3

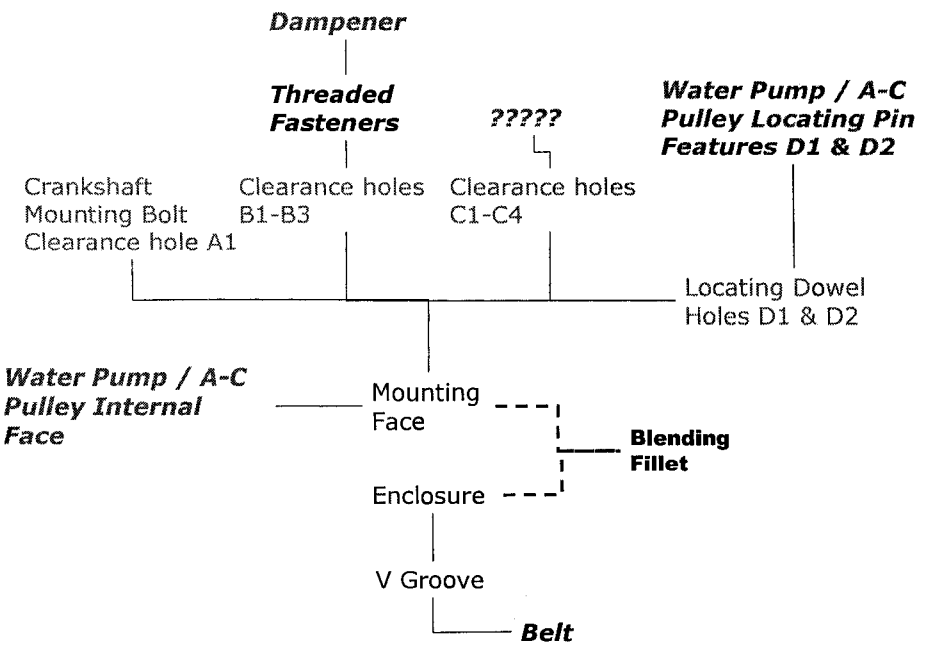

Figure C-3: Power Steering Pump Pulley Connectiviety Diagram

The context of these features is identical to the pulley component, but the feature design concepts vary: these features are specifically used for the assembly, location or power transmission functions. The clearance holes are assembly features. Hence, the logical function is "couple-join". The ideal holes are cylindrical, although up to 0.010 inches of ovality is observed. The crankshaft mounting bolt is a ½-13 threaded fastener; therefore, the crankshaft mounting bolt clearance hole diameter is not critical, and is rounded to an easily understood

nominal value. 3/8-24 inch threaded fasteners (with washers) are used to mount the pulley system onto the dampener through clearance holes B1-B3. Typically, 1/32 inch clearance is used for holes under ½ inch; therefore, this rule of thumb is utilized for the diameter of the B fastener pattern. For the 'C' fastener set, the power steering pump pulley and the water pump/air-conditioning pulley diameters are analysed statistically to determine an acceptable nominal value. The 'C' pattern clearance holes are determined to be ½ inch. However, these holes are not utilized in this system.

The bolt circles are analysed for the power steering pump pulley, water pump/air-conditioning pulley and the dampener. For the B_C1 pattern, there are three holes at 120° intervals. The bolt circle diameter for both pulleys is approximately 3.20 inches, and there is angular variation of approximately +/-0.75°. Whereas the bolt circle for the dampener is 3.156 inches (or 3 5/32 inch), and there is no measurable angular variation. The dampener bolt circle is an 'even' number within the imperial measurement system; hence, this value is chosen. For the C_C2 pattern, the bolt circle is approximately 3.5 inches, and the holes are offset 30° from the B_C1 hole pattern; hence, these values are used. All holes should be concentric to datum -A-, and have limited diameter and angular position variations. This information is summarized in Table C-1.

Table C-1: Summary for the Clearance Holes

Features: Mounting hole A and patterns B & C				
	What	**How**	**Where**	**Why**
	Data	Function	Interconnections (Network)	Motivation
Contextual	Power & rotary motion transmission	Flexible belt drive - pulley system	Crankshaft to power steering pump	
Conceptual	Assembly features	Clearance holes	Pulley face	
Logical	Couple - join.	Connection for joining several components using threaded fasteners	internal feature to external feature	Standard assembly features - ease of assembly, disassembly (common parts)
Physical	Cylinder	Punched	*Bolts & Washers* *Air conditioning pulley* *Crankshaft mounting bolt - dampener*	
Detail	Diameter A: 1 1/4 in Diameter B: 13/32 in Diameter C: 1/2 in		Tolerance: '+/- 0.025 in	Clearance for crankshaft (-A- datum) Clearance for 3/8-24 bolts (B pattern) & Clearance for **xx-xx** bolts (C pattern)
	Depth: through		No burr	Planar mounting face
	Position B: 120° intervals Position C: +/-30° from centreline B pattern		Angularity to -A- -B- -C- 0.015 in	Mating geometry
	Position B: 3.156 inch bolt circle (3 5/32") Position C: 3.500 inch bolt circle		Concentric to centre -A- 0.015 in	Mating geometry

The locating dowel holes D1 and D2 are used to locate and align the power steering pump features with respect to the water pump/air-conditioning pulley. The D1 and D2 hole centres lie on the C2 bolt pattern circle. The dowel hole diameters are approximately 0.015 inches larger than the locating 'pin' features (raised lip on the water pump); hence, it is determined that the clearance should be 1/64 inch. The locating dowel hole centre line is 90° from the -A- to -B- datum line. These holes must be concentric to -A-, and have a relatively tight limit on the diameter and angular variations. This is summarized in Table C-2.

Table C-2: Locating Hole Pattern D Summary

Features: Locating hole pattern D				
	What	**How**	**Where**	**Why**
	Data	Function	Interconnections (Network)	Motivation
Contextual	Power & rotary motion transmission	Flexible belt drive - pulley system	Crankshaft to power steering pump	
Conceptual	Location features	Hole - 'pin' strategy	Pulley face	
Logical	Support - position	Dowel holes that fit over lip on mating pulley features	internal feature to internal feature	Ease of assembly & disassembly, and easily manufactured
Physical	Cylinder	Punched	*Water pump / A-C pulley*	
Detail	Diameter D: 41/64 in		Tolerance: '+/- 0.010 in	Clearance for 5/8 in. flanged locating features (D1, D2) on mating pulley
	Depth: through		No burr	Planar mounting face
	Position D: +/-90° from centreline A-B		Angularity to -A- -B- -C- 0.010 in	Mating geometry
	Position D: 3.500 inch bolt circle		Concentric to centre -A- 0.010 in	Mating geometry

There are significant amounts of damage observed on the power steering pump pulley. The cracking and damage appeared to originate from the blending fillet between the mounting face and pulley enclosure. The diameter of the fillet is approximately 1/8 inch (an average of 9 measurements taken at relatively even intervals between damaged areas). This feature must be altered to prevent a future failure, but there must be clearance for the washers (0.675 in. diameter) and the socket used to assemble/disassemble the fasteners. This information is summarized in Table C-3.

Table C-3: Blending Fillet Summary

Features: Mounting face blending fillet				
	What	**How**	**Where**	**Why**
	Data	Function	Interconnections (Network)	Motivation
Contextual	Power & rotary motion transmission	Flexible belt drive - pulley system	Crankshaft to power steering pump	
Conceptual	Assembly features	Clearance holes	Pulley face	
Logical	Couple - join	Connection for joining several components using threaded fasteners	internal feature to internal feature	Manufacturing feature - cannot fabricate sharp corners
Physical	Partial torus	Rolled	Mounting face Enclosure	
Detail	Diameter fillet: 1/8 (0.125) in		Tolerance: '+/- 0.030 in	Clearance for bolt head, 0.675 inch washers and socket wrench - **must be modified - failure point**

The V groove geometry is designed to optimize the power/motion characteristics from one shaft to another. The V groove geometry is established by measuring both the belt and the groove in order to determine the appropriate design standard. As expected, the pulley geometry conforms to an SAE standard: based on the pulley geometry, the groove is a SAE standard 440. The pulley outside diameter is 6.75 inches, the nominal diameter minus D (minimum groove depth, as illustrated in Figure C-4) is 5.75 inches, and the groove height from datum -C- is 1.750 inches. The centre of the pulley groove should align with the corresponding driven pulley. This information is summarized in Table C-4.

It is evident that the original groove was not designed or manufactured to ideal conditions when comparing the measured results to the SAE standard. This pulley has a tendency to 'throw belts' during usage. This is problem is probably caused by the lack of belt engagement; therefore, the depth in the final model is increase to meet the SAE standard.

Table C-4: V Groove Summary

Features: V groove				
	What	**How**	**Where**	**Why**
	Data	Function	Interconnections (Network)	Motivation
Contextual	Power & rotary motion transmission	Flexible belt drive - pulley system	Crankshaft to power steering pump	
Conceptual	Power transmission feature	Standard belt-groove geometry	Pulley face	
Logical	Channel - transfer	Standard belt-groove system used to transfer rotary motion and power from one device to another	internal feature to external feature	Simple, efficient, cost effective and low maintenance method of transmitting power and motion between widely spaced shafts
Physical	See standards: OD = 6.75 in	Rolled	*SAE Standard V belt - 440*	Standard geometry for effective power / motion transmission
Detail	See standards - Nominal Diameter – D= 5.75 in **Increase depth to min 0.512 in** Groove Height: 1.75 in from -C-		Concentric to centre -A- 0.010 in	Align with the driven power steering pump pulley

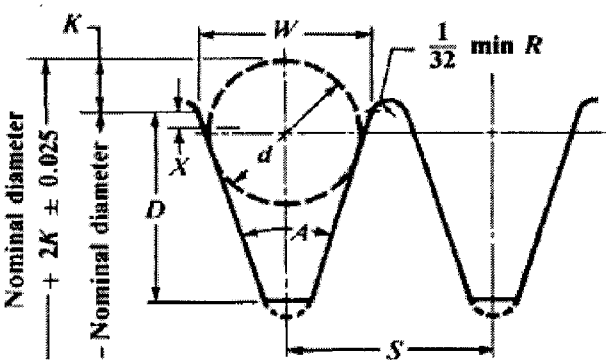

SAE Size	Recommended Min. Eff Dia[a]	A Groove Angle (deg) ±0.5	W Eff. Groove Width	D Groove Depth Min	d Ball or Rod Dia (±0.0005)	2K 2 × Ball Extension	2X[b]	S Groove[c] Spacing (±0.015)
0.250	2.25	36	0.248	0.276	0.2188	0.164	0.04	0.315
0.315	2.25	36	0.315	0.354	0.2812	0.222	0.05	0.413
0.380	2.40	36	0.380	0.433	0.3125	0.154	0.06	0.541
0.440	2.75	36	0.441	0.512	0.3750	0.231	0.07	0.591

Figure C-4: SAE Standard Groove Data

For the redesigned pulley, the mounting hole features for pattern B_C1 remain constant, but the information pertaining to the other features is eliminated. The crankshaft mounting bolt clearance feature A1 must be redesigned to include a tapered protrusion that acts as an assembly guide; however, there must be clearance with the dampener hole diameter. This information, which is captured in the water pump/air-conditioning pulley analysis (Table C-6), is utilized in the new pulley design.

The groove diameter and height information is also gathered for the complete pulley system. All the belts and grooves correspond to the SAE standard 440. The mounting face datum -C- has shifted to the system mounting face; hence, there is approximately 0.100 offset for the power steering pump pulley height, which corresponds to the average material thickness of the water pump/air-conditioning pulley mounting face. The V groove system information is presented in Table C-7 and Figure C-5. The critical information is extracted and utilized in the new pulley design.

Table C-5: Redesign Pulley Mounting Hole Summary

Features: Mounting hole pattern B				
	What	**How**	**Where**	**Why**
	Data	Function	Interconnections (Network)	Motivation
Contextual	Power & rotary motion transmission	Flexible belt drive - pulley system	Crankshaft to power steering pump	
Conceptual	Assembly features	Clearance holes	Pulley face	
Logical	Couple - join	Connection for joining several components using threaded fasteners	internal feature to external feature	Standard assembly features - ease of assembly, disassembly (common parts)
Physical	Cylinder	Drilled	*Bolts & Washers* *Air conditioning pulley* *Crankshaft mounting bolt - dampener*	
Detail	Diameter B: 13/32 in		Tolerance: '+/- 0.025 in	Clearance for 3/8-24 bolts (B pattern)
	Depth: through		No burr	Planar mounting face
	Position B: 120° intervals		Angularity to -A- -B- -C- 0.015 in	Mating geometry
	Position B: 3.156 inch bolt circle		Concentric to centre -A- 0.015 in	Mating geometry

Table C-6: Locating Hole A1 Summary for the Water Pump/Air-Conditioning Pulley

Features: Locating hole A				
	What	**How**	**Where**	**Why**
	Data	Function	Interconnections (Network)	Motivation
Contextual	Power & rotary motion transmission	Flexible belt drive - pulley system	Crankshaft to power steering pump	
Conceptual	Location features	Hole - 'pin' strategy	Pulley face	
Logical	Support - position	Locating hole with lead chamfer to locate on crankshaft, in dampener	internal feature to internal feature	Ease of assembly & disassembly, and easily manufactured
Physical	Cone, protrusion	Turned	*Dampener & Crankshaft mounting bolt*	
Detail	Internal Dia. A: 1.050 in (minimum) External Dia. bottom A: 1 7/32 (1.219) in (ref) External Dia. top A: 1 5/32 (1.156) in		Tolerance: '+/- 0.010 in	Clearance for crankshaft mounting bolt (1/2-13) and dampener (1 1/8 inch)
	Depth: through Lip 0.125 in (max)		Tolerance: '+/- 0.010 in	Lead in geometry
	Fillet 1/64 inch radius		General tolerance	Manufacturing feature

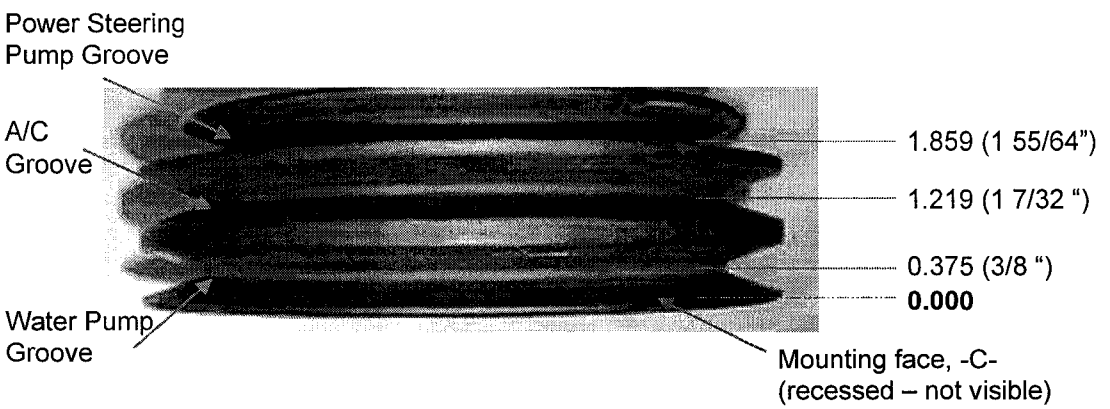

Figure C-5: Pulley System Height Measurements

Table C-7: Summary for the V Groove Geometry when Analysing the Pulley System.

Features: Dual V grooves				
	What	**How**	**Where**	**Why**
	Data	Function	Interconnections (Network)	Motivation
Contextual	Power & rotary motion transmission	Flexible belt drive - pulley system	Crankshaft to power steering pump	
Conceptual	Power transmission feature	Standard belt-groove geometry	Pulley face	
Logical	Channel - transfer	Standard belt-groove system used to transfer rotary motion and power from one device to another	internal feature to external feature	Simple, efficient, cost effective and low maintenance method of transmitting power and motion between widely spaced shafts
Physical	See standards using: Power steering pump OD = 6.75 in Water pump OD = 7.625 in	Rolled	*SAE Standard V belt - 440*	Standard geometry for effective power / motion transmission
Detail	**Power steering pump** Groove depth: 0.512 in (new) Groove Height: 1.859 (1 55/64) in from -C- (new) **Water steering pump** Nominal Diameter - Groove depth: 6.469 (6 15/32) in Groove Height: 0.375 (3/8) in from -C-		Concentric to centre -A- 0.010 in	Align with the corresponding driven pulleys

Table C-8 (a): GD and T Information for the Pulley

	Feature	Primary Datum	Secondary Datum	Tertiary Datum	Tolerance Value	Comment
Flatness	Mounting face				0.010	Flat, smooth surface
Angularity	Mounting holes	-A-	-B-	-C-	0.015	
Angularity	Grooves	-A-	-B-	-C-	0.010	Per side of groove
Line Profile	General body	-A-	-B-	-C-	0.030	Profile
Total run out	Grooves	-A-	-B-	-C-	0.015	Use 0.3750 ball per SAE guidelines

Table C-8 (b): Ancillary Geometry Information for the Pulley

	Datum	Feature	Comment
Location			
Radial	-A-	Mounting holes B1-B3	
Centred	-A-	Locating hole	
Fit			
Clearance		Mounting holes	1/32 inch
Clearance		Crankshaft	1/8 inch
Clearance		Dampener	1/32 inch

Table C-9: Geometry Failure Model Analysis for FMEA

			Feature (Geometry)								Feature and Pattern Inter-relationships															
	Fit		Size		Depth		Form (1 of 4)				Orientation (max 2)			Location (max 2)			Run out (1)		Profile (1)		Other		Surface			
Feature Name	Description	Standard Table	Size +	Size -	Depth +	Depth -	roundness	cylindricity	straightness	flatness	perpendicularity	parallelism	angularity	position	concentricity	symmetry	circular	total	linear	surface	Radial	Centred	Finish	Characteristics	No. of Factors	SUM
V groove	power trans-mission	SAE Standard V groove	7	7	3	5							7					7					5		**7**	**41**
Mounting faces	planar face	N/A	3	3	3					5															**4**	**14.0**
Mounting holes	clearance	N/A	1	1										5							3	3			**5**	**13.0**
Support body	support	N/A	1	1	1	1													3						**5**	**7.0**

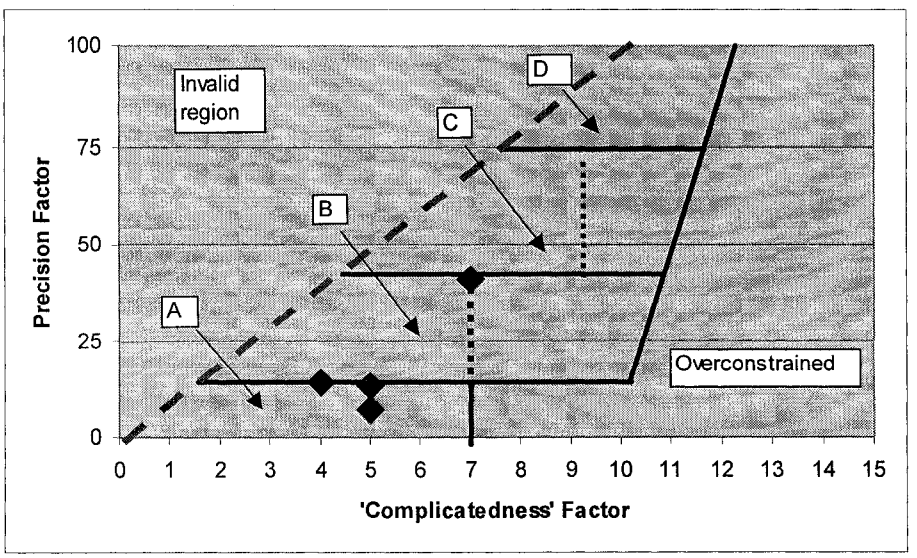

Figure C-6: FMEA Results Chart

C.3 RETOOL SOFTWARE APPLICATION PROTOTYPE

A prototype software application was developed using the framework presented in Chapter 3 as the guideline. The application was developed in Excel™. The data fields are partially filled using the power steering pump pulley as an example. Incomplete fields have the design reference notes that are contained in the template. A combination of information is presented in order to illustrate different aspects of the prototype software (Figure C-7 to C-14).

For each component to be reverse engineered, the designer creates an new file using the prototype file as a template. There is a general menu form, a set of component forms, and one general feature form. Additional feature forms may be created as necessary using the sample form as a base template. This application can serve as a front end for search engines that link into specific design databases (materials, machine design components and ISO standards).

New Project Set up:

The set up sheet is used to provide general, informal information with respect to the component being reverse engineered. In the set up sheet, the designer provides:

- a concise name for the component,
- a brief general description, and
- notes on wear, damage and/or potential redesign issues.

The designer rates the environmental factors using a 0, 0.5, 1 rating (minimal, moderate or extreme concern), and provides any essential information with respect to the operating conditions that would influence any design changes (Figure C-7).

Generate Formal Abstract General Information:

The designer then formalizes the general abstract information with respect to the context of the design and the utilized concepts. "What, How, Where and Why" questions are answered in the appropriate fields. Links to other relevant documents should be included in the description. The component functions (primary, secondary and tertiary) are defined using the

NIST terminology. The user selects the appropriate functions from a drop down list. The methods used to achieve the functions and the hypothesized functional requirements are defined in the logical layer (Figure C-8).

Generate Formal Abstract Physical Information:

The abstract physical data is formalized in the physical layer, such as the material, material treatments, the work envelope, general shape information and a feature list. Drop down lists help with selecting the material family, sub family and type, and the reasons 'why' this material is appropriate (Figure C-9).

The designer is to provide specific design information for the peripheral components that mate with the component of interest and specific general feature data. A peripheral component drop down list is created from this external component information (Figure C-10). The peripheral components are used to define the envelope. The clearance relationship between the peripheral components and the component of interest is explicitly defined qualitatively (drop down list) and quantitatively. Any feature may be associated with a set of peripheral components. These relationships must also be determined formally.

Each peripheral component/ feature is given a name, pattern type and pattern label as appropriate, and explicit (but generic) functions are identified (Figure C-10 and C-11). The feature list is created from the identified features in the physical data sheet. General process related information is captured on a per feature basis, as well as the feature type, general functions and the motivation for including this feature within the component structure.

Generate Formal Abstract Detail Information:

General shape information must be provided for each feature within the component. Drop down lists control the generic feature geometry and function type selection. General reconstruction guidelines for individual feature are identified. This includes point cloud data manipulation instructions, references to design tables or a reference to the specific feature assessment within this project.

The reference datum features for the component must be clearly defined in order to develop appropriate feature inter-relationships and tolerance associations. A pictorial representation of the datum features should be included to clearly illustrate the reference datum features. These datum points are to be used for the design recovery process as well as the manufacturing and inspection stages (Figure C-12).

New Feature Set up:

For each defined feature, a specific feature data sheet must be generated. The general abstract context and concepts may be a subset of the component, or there may be unique details to be presented when performing the feature analysis. This is also true for the logical or function based information. The individual characteristics of the feature are provided in the system related fields.

The physical characteristics (number of features, the type, characteristics, the internal and external connections) are defined. Drop down lists with a controlled vocabulary are used to determine the feature type and characteristics. The peripheral and feature lists created from the component domain are used to assist the designer with the internal feature and external component selection.

The detailed design parameters for the feature are identified and numerical values defined. This includes the feature and pattern data, as well as any relationships and tolerance values (Figure C-13 and C-14 illustrates the feature specific data for the crankshaft mounting bolt clearance hole).

The general design domains for this application are illustrated in Figure C-15, and the data flows are illustrated in Figure C-16. The interactions between the design domains are illustrated in Figures C-17 and C-18.

Figure C-7: Set up Sheet Information

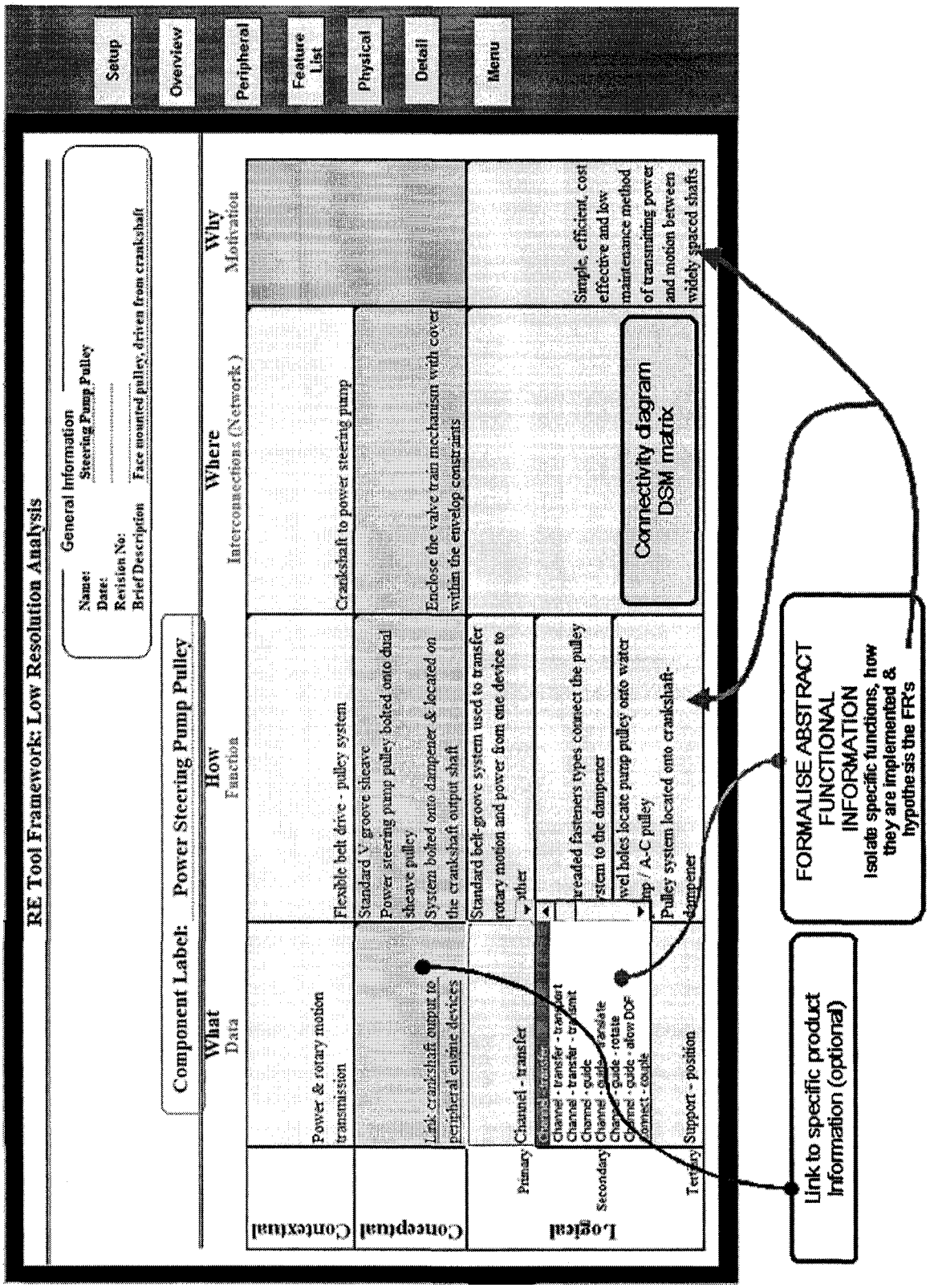

Figure C-8: Formal System Related Information

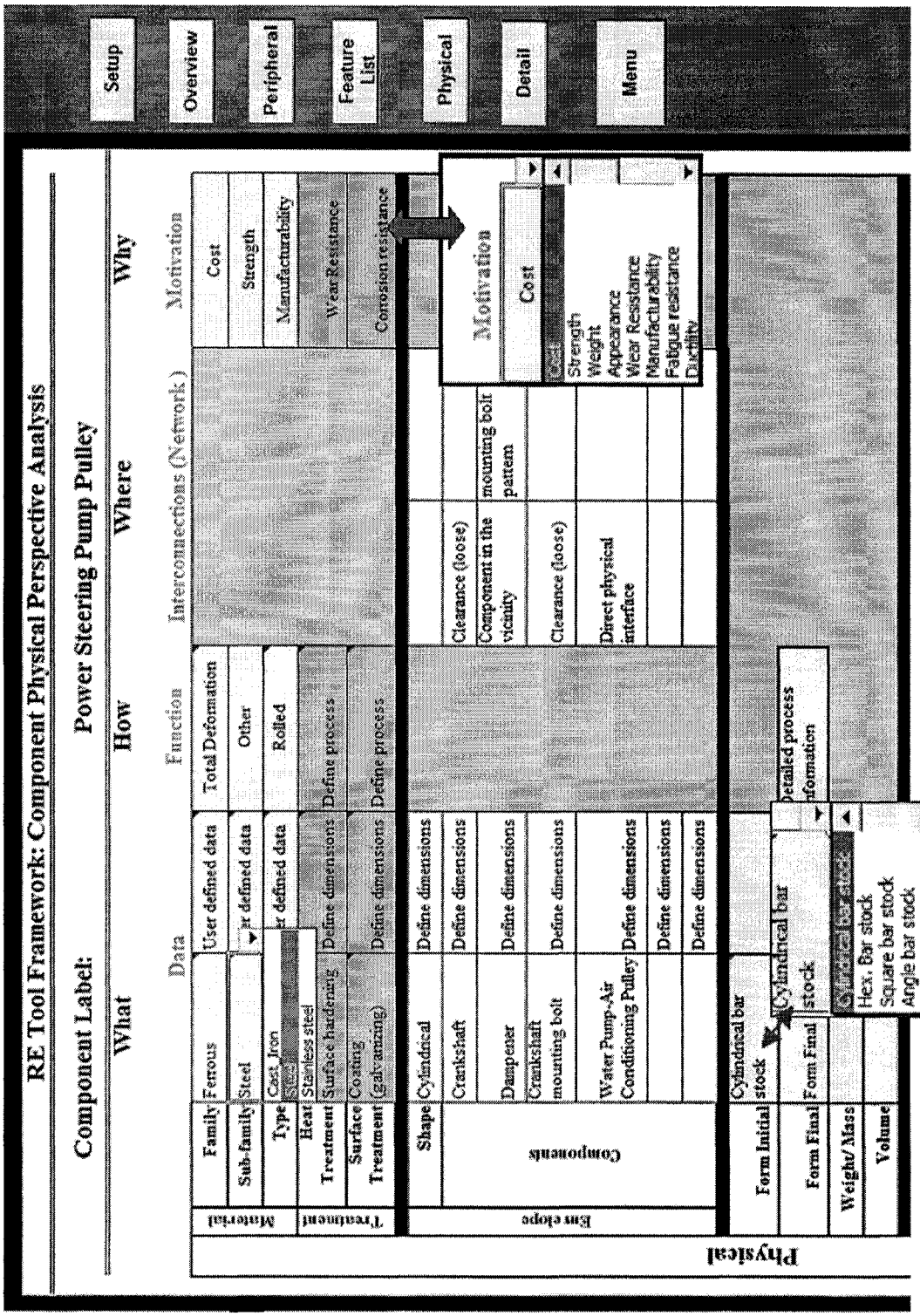

Figure C-9: Formal Physical Information (part 1)

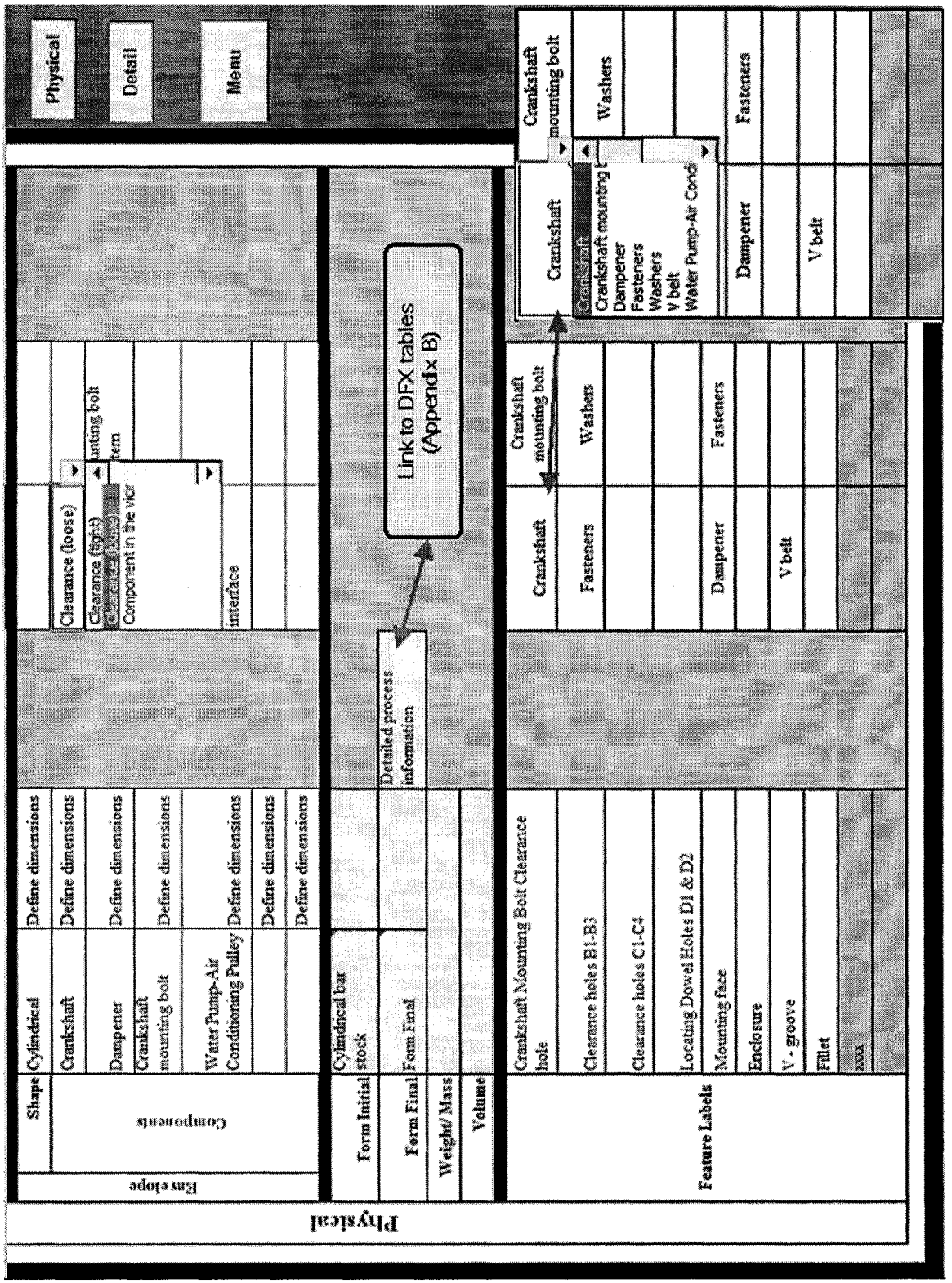

Figure C-9: Formal Physical Information (part 2)

Figure C-10: Peripheral Component Information and Data

Figure C-11: Formal Feature Information for the Component

Figure C-12: Formal Detail Component Information

Figure C-13: Formal Specific Feature Related Information for the Crankshaft Mounting Bolt Clearance Hole (part 1)

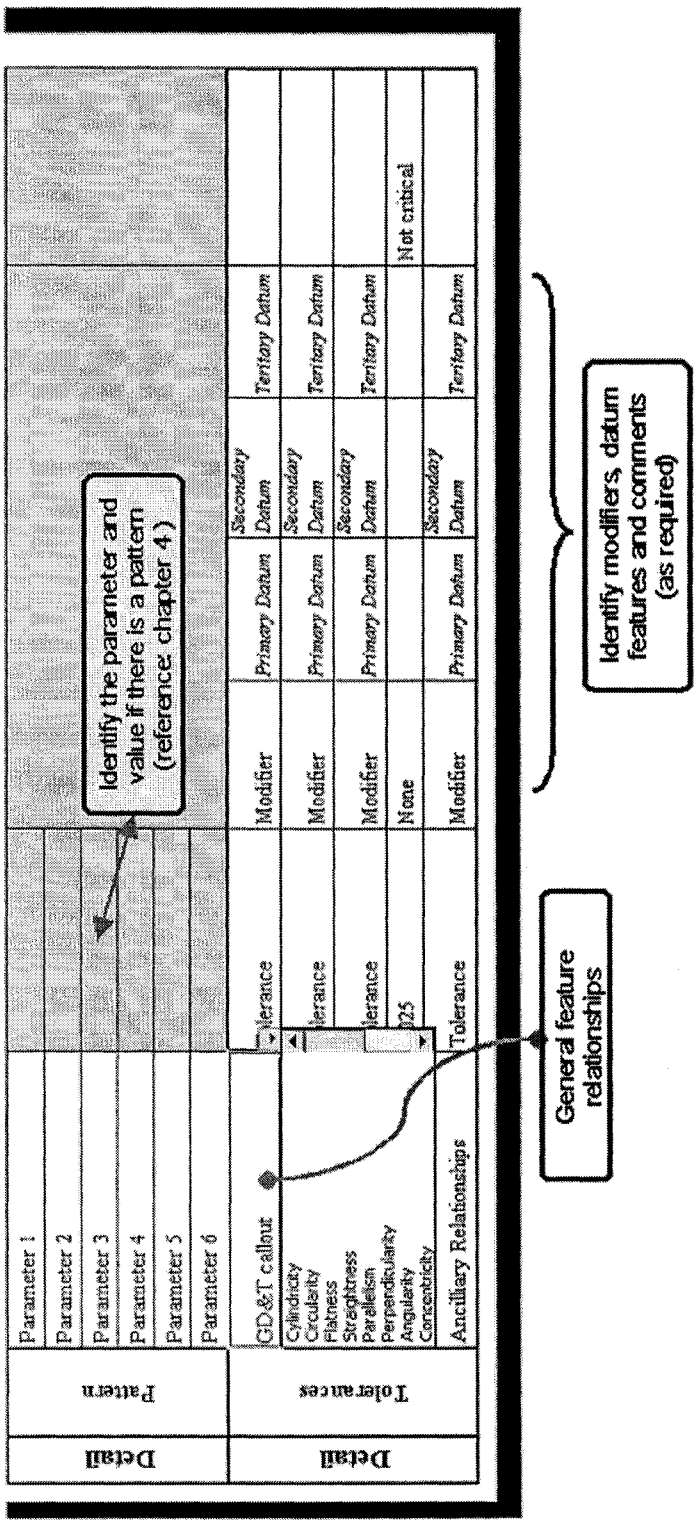

Figure C-14: Formal Specific Feature Related Information for the Crankshaft Mounting Bolt Clearance Hole (part 2)

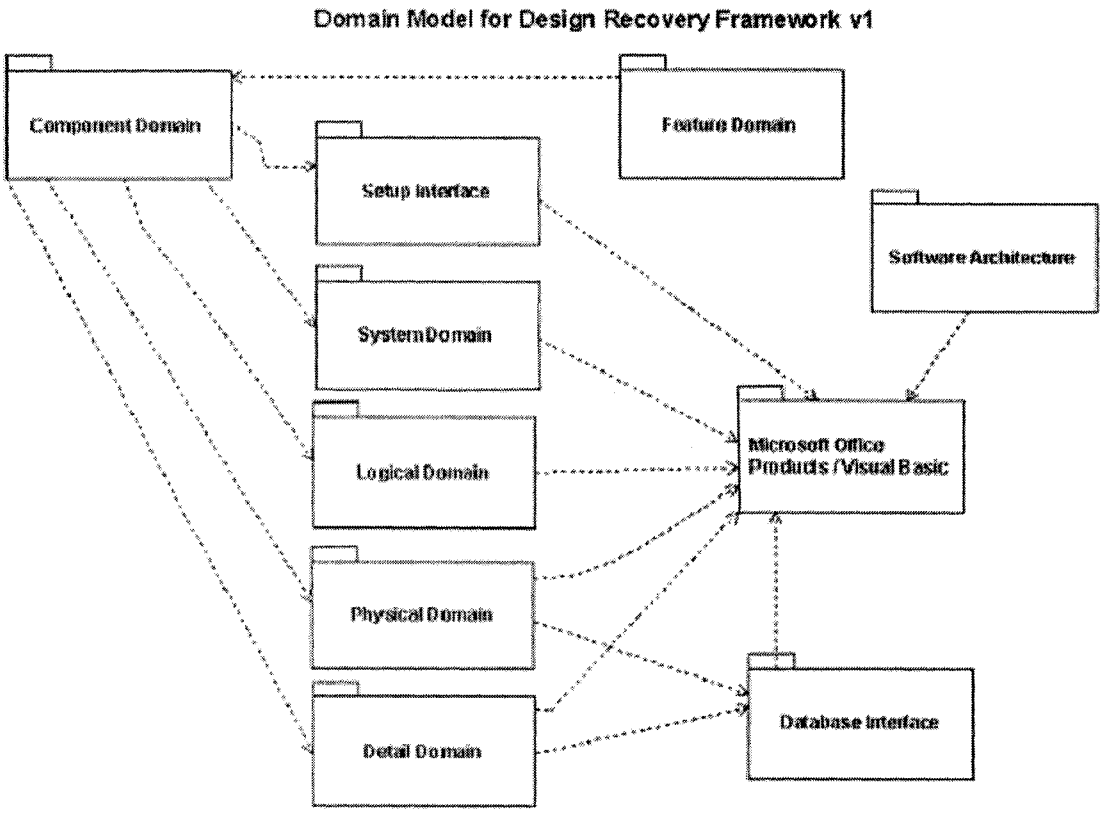

Figure C-15: Domain Model

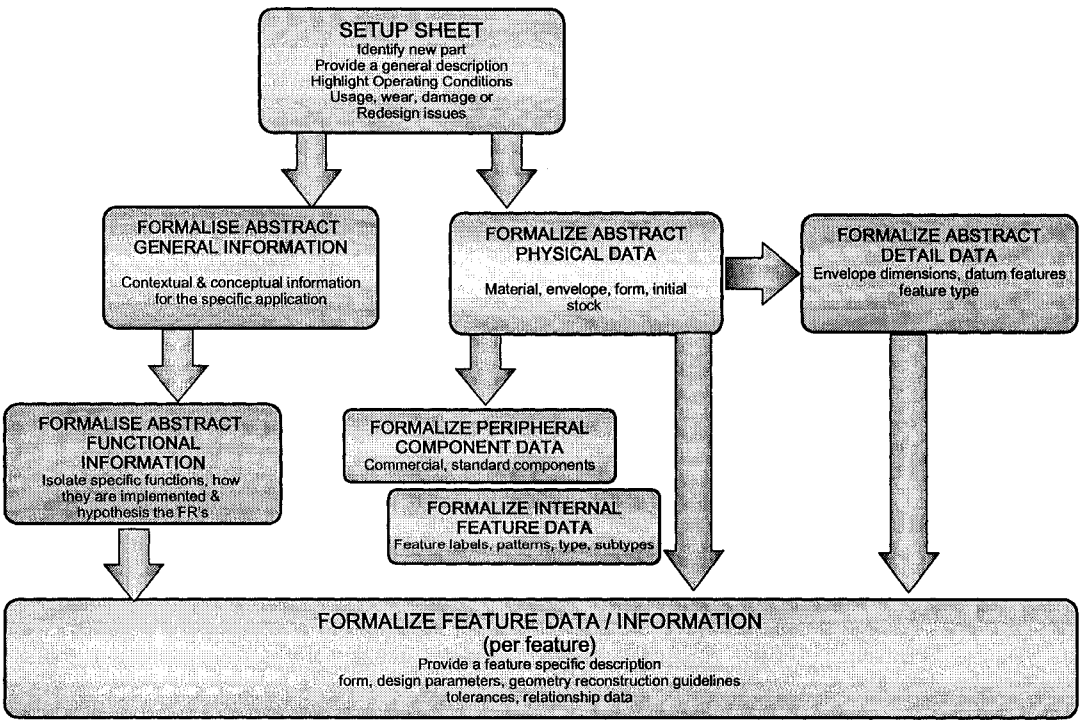

Figure C-16: Design Recovery Framework Flow

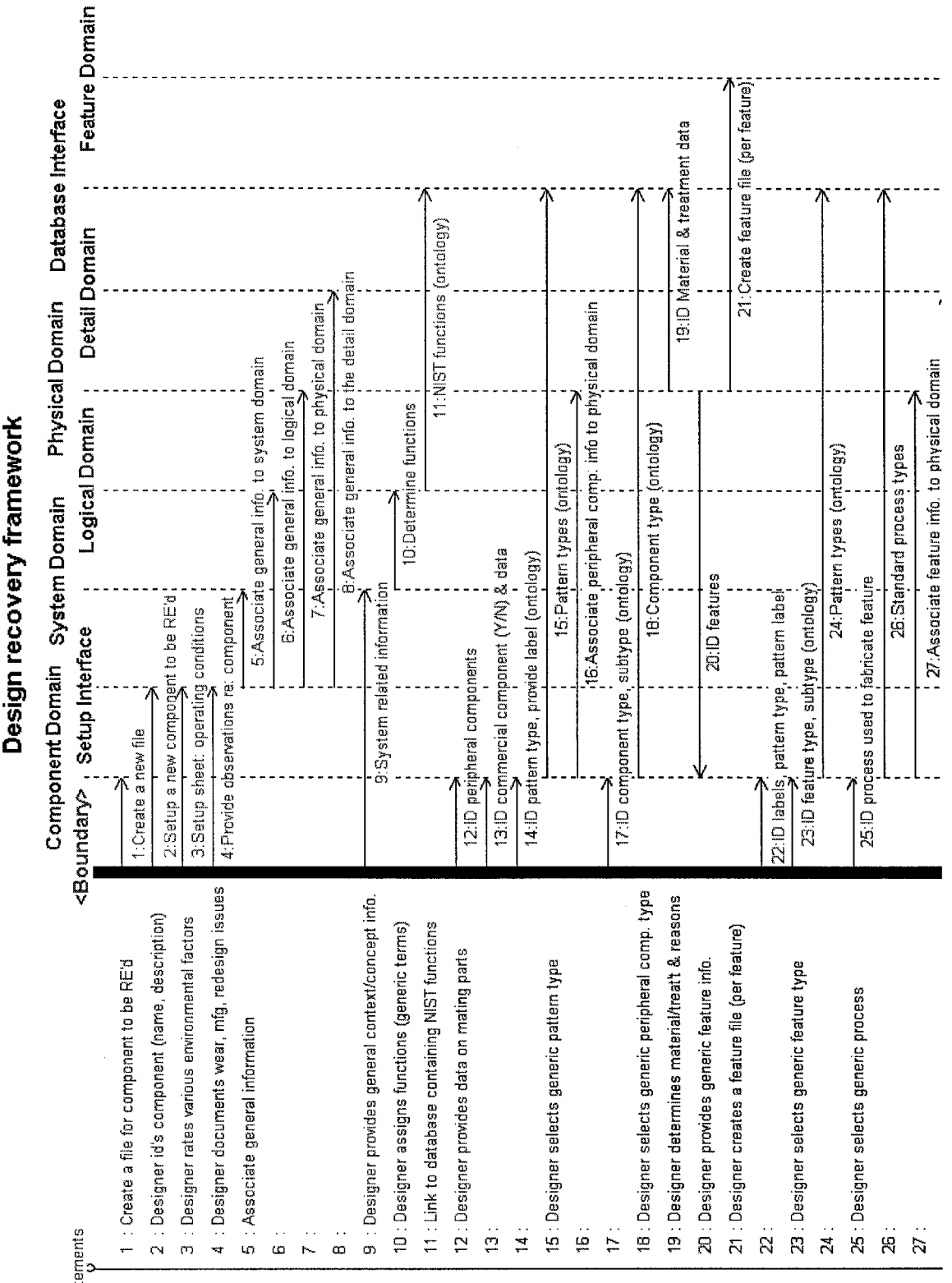

Figure C-17: Domain Interactions (part 1)

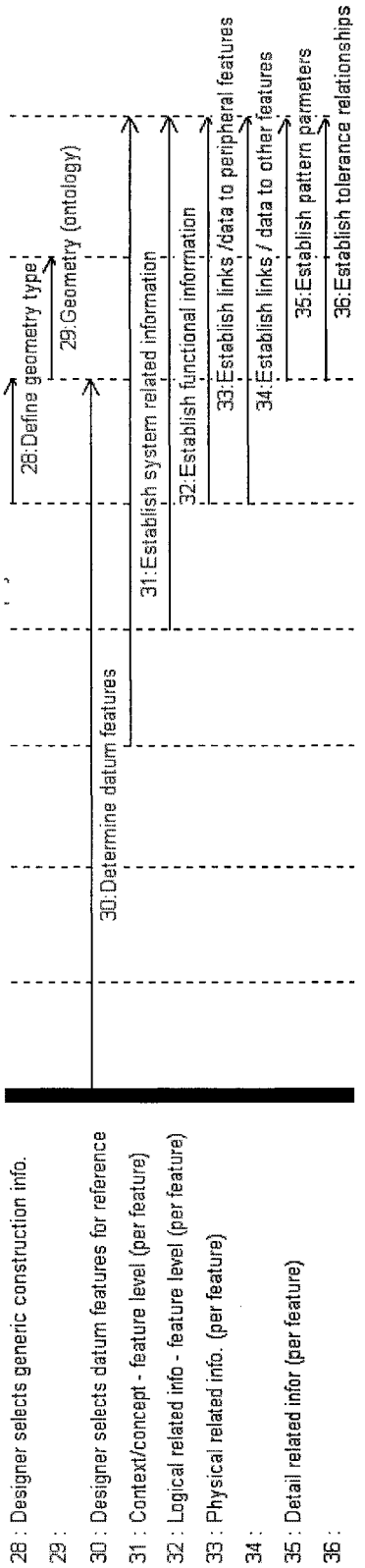

Figure C-18: Domain Interactions (part 2)

APPENDIX D: COMPLEXITY INDEX

The product manufacturing relative complexity coefficient $c_{j,product}$ is defined as:

$$c_{j,product} = \sum_{f=1}^{F} x_f * c_{f,feature} \tag{D.1}$$

where c_f is the relative feature complexity coefficient

x_f is the percentage of the x^{th} dissimilar feature

The relative complexity coefficient is a weighted average associated with the relative complexity of the various aspects and specifications of a given feature, and is represented by:

$$c_{f,feature} = \frac{F_N * F_{CF} + S_N * S_{CF}}{F_N + S_N} \tag{D.2}$$

where: F_N is the quantity of features,

F_{CF} is the feature complexity factor,

S_N is the quantity of specification checks, and S_{CF} is the specification complexity factor (note: in general F_N equals S_N; therefore, the value of $c_{f,feature}$ is an average)

$$F_{CF} = \frac{\sum_{j=1}^{J} factor\_level_j}{J} \tag{D.3}$$

where: F_{CF} is the feature complexity factor,

J the number of categories,

Factor level$_j$ is the factor for the j^{th} category

$$S_{CF} = \frac{\sum_{k=1}^{K} factor\_level_k}{K} \tag{D.4}$$

where S_{CF} is the specification complexity factor

K is the number of specifications

$factor\_level_k$ is the factor for the k^{th} specification

The factor level corresponds to the level of "effort" to produce the feature or perform the task. A multi tier ranking system is used where low, medium, and high effort levels correspond to factor levels 0, 0.5 and 1 respectively. Alternatively, a 1-10 scale could be used, with the final "difficulty factor" value normalized by the maximum value of the scale.

The methodology to generate the product complexity index $CI_{product}$ is developed below:

1. Define the multi-tier ranking system to be used.
2. Determine the total number N of all the individual feature information, components, sub-components, etc. and from equation 5.2, calculate $H_{product}$.
3. Determine the specific quantity n of each diverse feature defined in step 2, and from equations 5.2 and 5.3, calculate the product diversity ratio $D_{R_{product}}$.
4. Define the number and type of diverse "aspects" for evaluating the features *(J)* and the specifications *(K)* associated with manufacturing the product (Table D-1).
5. Generate the *FxJ* feature matrix and the *FxK* specification matrix and assign the appropriate complexity levels into each cell.
6. Calculate the product complexity coefficient $c_{j,product}$ as defined by equations, D.1 – D.4.
7. Calculate the product complexity index $CI_{product}$ as defined by equation 5.4.

D.1 PRODUCT COMPLEXITY EXAMPLE [ELMARAGHY AND URBANIC, 2003]

Consider the machined features of a Mass Air Flow Body (MAFB). The MAFB is made from 10% Si Die Cast Aluminum. There are two casting sizes, but the machining and assembly features are constant for both products. The actual assembled product and the main features are illustrated in Figure D-1.

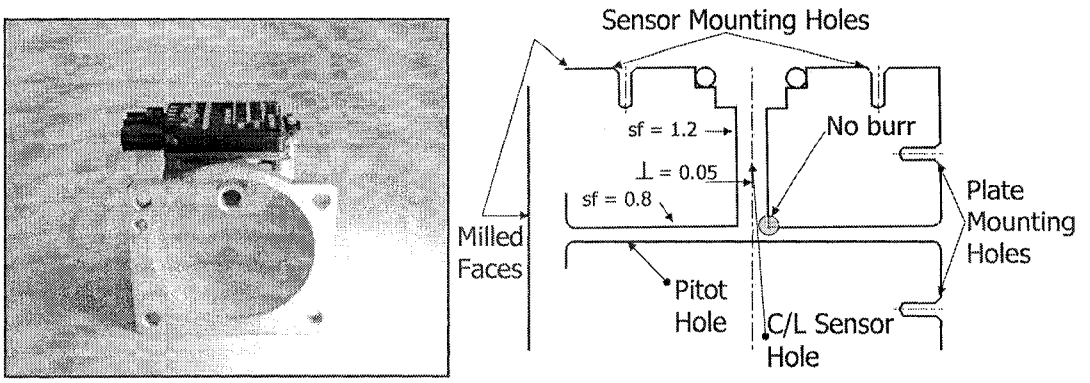

Figure D-1: Mass Air Flow Body Features

Upon analysing the product features, tolerances and specifications, N = 123 and n = 66; consequently, $H_{product}$ = 6.95 and $D_{Rproduct}$ = 0.54. Table D-1 lists the features, specifications and the critical aspects for this product, and the resulting relative product complexity coefficient $c_{jproduct.}$ In this example, the product complexity index $CI_{product}$ is:

$$CI_{product} = (0.54 + 0.20) * 6.95;\ CI_{product} = 5.14$$

Using the rules listed in Chapter 5, complexity analysis is performed on the MAFB (Tables D-2 and D-3) and compared to the detailed analysis in Table D-1. The feature and component complexity values are illustrated in Figure D-2.

Table D-1: Calculation of c_j for the MAFB

Description	J = 4						
	Number	Aspects					
		Shape	Geometry	Tolerances	Tolerance Stack Up	SUM	Sum/J
Sensor Hole	1	0.5	0.5	0.5	0	1.5	0.38
Pitot Hole	1	0.5	0.5	1	0	2	0.50
Sensor Mounting Holes	2	0.5	0	0	0.5	1	0.25
Plate Mounting Holes	2	0	0	0	0	0	0.00
Milled Surfaces	2	0	0	0	0.5	0.5	0.13

Description	K = variable						
	Number	Aspects					
		General Surface Finish	6H Thread Fit	No Sharp Edges or Burrs	No Surface Discontinuities	SUM	Sum/K
Sensor Hole	1	0		1	0.5	1.5	0.50
Pitot Hole	1	0		1	0.5	1.5	0.50
Sensor Mounting Holes	2		0			0	0.00
Plate Mounting Holes	2		0			0	0.00
Milled Surfaces	2	0		0.5		0.5	0.25

	Feature Complexity	Weighted Feature Complexity
Sensor hole(s)	0.44	0.05
Pitot holes	0.50	0.06
Sensor Mounting holes	0.13	0.03
Plate Mounting holes	0.00	0.00
Milled surfaces	0.19	0.05
Relative Product Complexity Co. c_j		0.20

Table D-2: Individual Feature Complexity Aspects Analysis for the Mass Air Flow Body

Mass Air Flow Body												
	Feature Description	# of Features	Basic	Type	Material	Shape	Pattern	Tolerance	Surface Finish	Spatial Relations	Sum of Fields 5 - 10	Average of Fields 5 - 10
	1	2	3	4	5	6	7	8	9	10		
Sensor hole(s)	Precision internal feature	1	2	10	0	0.5	0	1	0.5	0	2	0.333
Pitot holes	Precision internal feature	1	2	10	0	0.5	0	0.5	0.5	0.5	2	0.333
Sensor Mounting holes	Fastening features	2	1	5	0	0	0	0.5	0	0	0.5	0.083
Plate Mounting holes	Fastening features	2	1	5	0	0	0	0	0	0	0	0.000
Milled surfaces	Planar surfaces	2	1	8	0	0	0	0.5	0	0	0.5	0.083

Table D-3 (a): 'Feature Type' Analysis for the Mass Air Flow Body

	N	n	Basic	Type	Material	Shape	Pattern	Tolerance	Surface Finish	Spatial Relations		
	1	**2**	**3**	**4**	**5**	**6**	**7**	**8**	**9**	**10**		
Precision internal feature	2	2	2	10	0	0.5	0	1	0.5	0.5	**Sum: Field 5**	**Average: Field 5**
Fastening features	4	2	1	5	0	0	0	0.5	0	0	0.5	0.083
Planar surfaces	2	2	1	8	0	0	0	0.5	0	0	0.5	0.083
Sum	**8**	**6**										

Table D-3 (b): 'Feature Type' Analysis for the Mass Air Flow Body

	$H_{j\ feature}$	$c_{j\ feature}$	$CI_{feature}$
Precision internal feature	4.392	0.417	1.830
Fastening features	5.358	0.083	0.446
Planar surfaces	3.907	0.083	0.326

Table D-3 (c): 'Feature Type' Analysis for the Mass Air Flow Body

	$c_{j\ feature}$	***Weighted*** $c_{j\ feature}$
Precision internal feature	0.417	0.104
Fastening features	0.083	0.042
Planar surfaces	0.083	0.021
Relative Product Complexity Co. c_j		0.167

The *N*factors* summation for the information quantity is 74; therefore, H = 6.23. $N_{detailed}$ is 123. The diversity ratio D_R is 0.75. $D_{Rdetailed}$ is 0.54. From Table D-3(c), the relative product complexity coefficient is ≈ 0.17. Using equation 5.4, this generates a CI_{MAFB} = 5.71, as opposed to 5.14.

Using this systematic assessment technique, the relative product complexity coefficient c_j is similar to the example presented in the detailed analysis (0.17 versus 0.20). This value is less as there are more aspects being considered, effectively attenuating the result slightly. H is ≈ 12% less and the diversity ratio D_R is ≈ 39%greater, generating a slightly higher complexity index (≈11%) for the part. However, assessing the complexity indices using this more generalized, structured methodology allows one to quickly assess the relative complexities for disparate components and features. A more thorough analysis targeting specific concerns and including design specifications can be done if necessary.

This complexity analysis technique is applied to a regulator gear for driver's side power window. The results for the regulator gear and then compared to the MAFB.

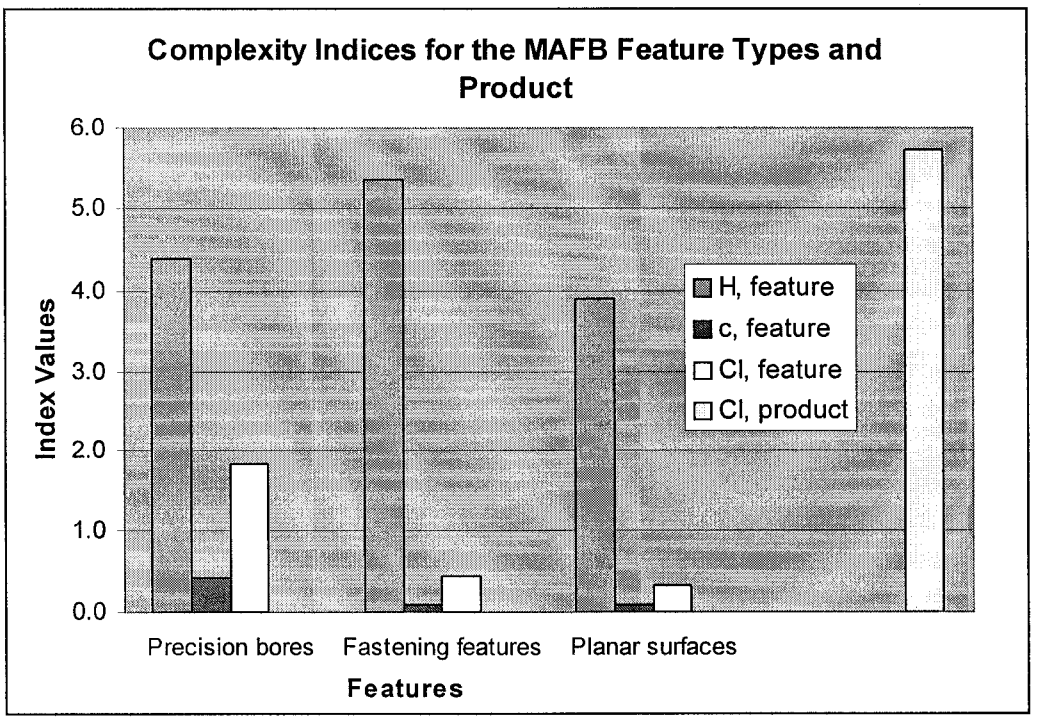

Figure D-2: Complexity Analysis for the MAFB

D.2 COMPLEXITY ANALYSIS FOR THE REGULATOR GEAR

The complexity analysis is performed for the regulator gear (Figure D-3), which is presented in Chapter 4. The primary datum is the surface of the part, the secondary datum is hole C4, and the tertiary datum is hole C1 (Figure D-5). Table D-4-shows the nominal values and associated positional tolerances. The reconstructed geometry is illustrated in Figure D-5. The holes are punched, and the peripheral shape it is cut out from plate stock. The gear teeth were probably broached, as this process is commonly used for manufacturing gear and spline teeth. The detailed design recovery analysis is presented in Urbanic et al [2005].

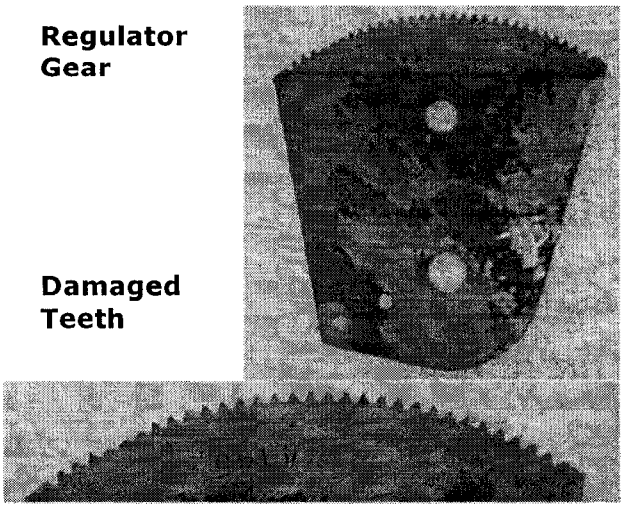

Figure D-3: Regulator Gear with Damaged and Worn Teeth

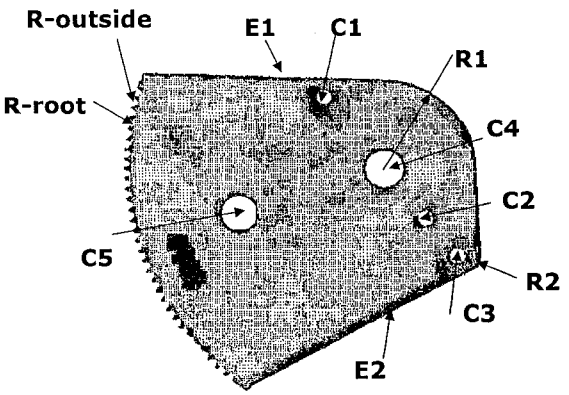

Figure D-4: Scanned Data and Feature Labels for the Power Window Regulator Gear

Table D-4: Positional Nominal Values and Tolerances

Feature Relationship	Nominal Value (in)			Tolerance			
E1-C1	0.375		+/-	0.010	-C-		
C1-C5	1.750	⊕	Ø	0.010	-A-	-B-	-C-
C1-C2	2.980	⊕	Ø	0.010	-A-	-B-	-C-
C1-C3	3.875	⊕	Ø	0.010	-A-	-B-	-C-
C5-C4	2.800	⊕	Ø	0.025	-A-	-B-	-C-
R1	0.000	⊕	Ø	0.025	-A-	-B-	-C-
R-pitch circle	0.000	⊕	Ø	0.015	-A-	-B-	-C-

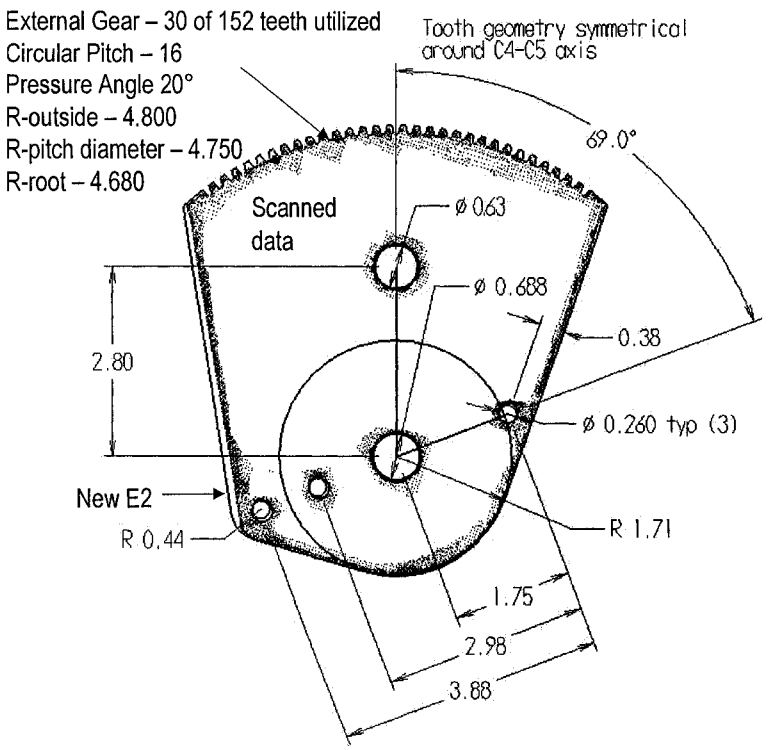

Figure D-5: Final Part Geometry

The complexity analysis for the regulator gear is presented in Tables D-5 and D-6. For the regulator gear, the sum of $N^{*}factors$= 56; therefore, H = 5.83. D_R is 0.57 and the CI_{Gear} = 3.96. As expected, the gear teeth have the highest features complexity value, and the planar surface has the lowest, (0.0). The results for the MAFB and regulator gear are compared in Figure D-6. The gear features have noticeably smaller complexity values than the MAFB features.

Table D-5: Individual Feature Complexity Aspects Analysis for the Regulator Gear

Regulator Gear												
	Feature Description	# of Features	Basic	Type	Material	Shape	Pattern	Tolerance	Surface Finish	Spatial Relations	**Sum of Fields 5 - 10**	**Average of Fields 5 - 10**
	1	**2**	**3**	**4**	**5**	**6**	**7**	**8**	**9**	**10**		
Rivet Holes, C1-C3	Fastening features	3	2	1	0	0	0	0.5	0	0	0.5	0.083
Bracket Locating Hole, C4	Locating feature	1	2	7	0	0	0.5	0	0	0.5	1	0.167
Assembly Guide, C5	Locating feature	1	2	7	0	0	0	0	0	0	0	0.000
Gear Teeth	Complex feature	1	2	2	0	0.5	0.5	0.5	0	0	1.5	0.250
External Profile	Planar surfaces	1	2	8	0	0	0	0	0	0	0	0.000

Table D-6 (a): Feature Type Analysis for the Regulator Gear

	N	n	Basic	Type	Material	Shape	Pattern	Tolerance	Surface Finish	Spatial Relations	**Sum of Fields 5 - 10**	**Average of Fields 5 - 10**
	1	**2**	**3**	**4**	**5**	**6**	**7**	**8**	**9**	**10**		
Clearance features	3	1	2	1	0	0	0	0.5	0	0	0.5	0.083
Locating feature	2	1	2	7	0	0	0.5	0.5	0	0	1	0.167
Complex feature	1	1	2	2	0	0.5	0.5	0.5	0	0	1.5	0.250
Planar surfaces	1	1	2	8	0	0	0	0	0	0	0	0.000

Table D-6 (b): Feature Type Analysis for the Regulator Gear

	$H_{feature}$	$c_{feature}$	$CI_{feature}$
Clearance features	4.459	0.083	0.372
Locating feature	4.087	0.167	0.681
Complex feature	3.700	0.167	0.925
Planar surfaces	3.000	0.000	**0.000**

Table D-6 (c): Feature Type Analysis for the Regulator Gear

	$c_{feature}$	***Weighted*** $c_{feature}$
Clearance features	0.083	0.036
Locating feature	0.167	0.048
Complex feature	0.250	0.036
Planar surfaces	0.000	0.000
Relative Product Complexity Co. c_j		0.119

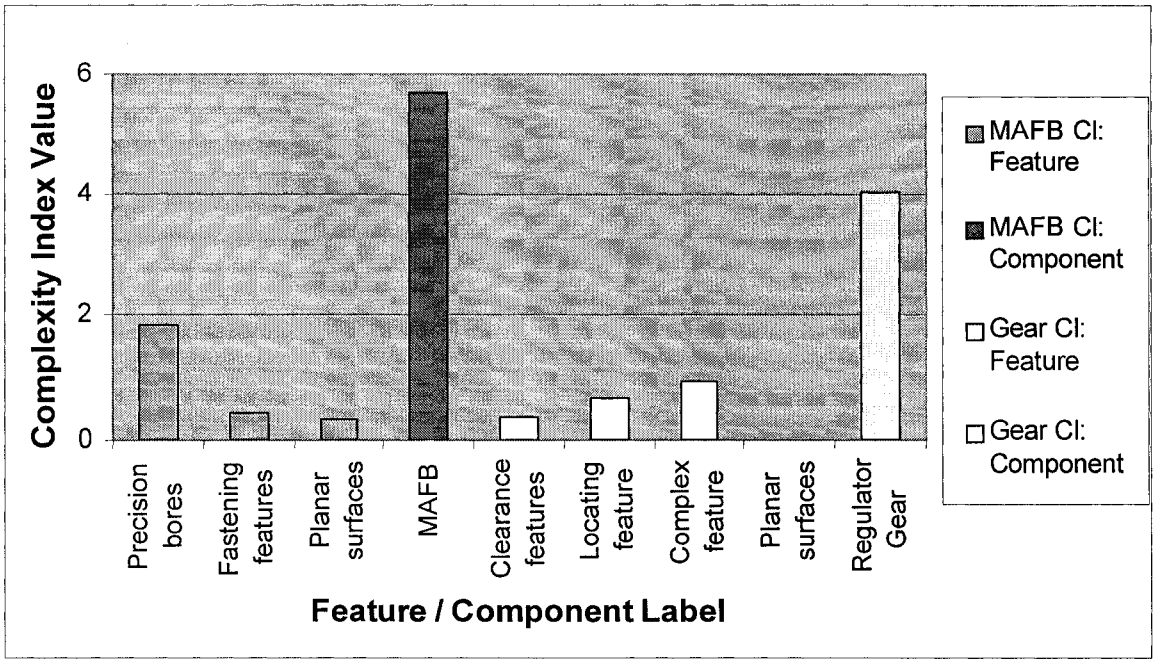

Figure D-6: A Comparison of the Complexity Index Values for the MAFB and the Regulator Gear

APPENDIX E: FEATURE AND COMPONENT CODE STRUCTURE

Table E-1: Form Related Fields for the Component Code

Component Code: Form		
Shape		
Initial Shape	**Parameters**	**Final Shape**
1 - Round bar stock	D, L	0 - Uniform cross section 1 - Change at one end 2 - Change at centre 3 - Spatial curvature 4 - Transverse element 5 - Spline or gear teeth 6 – Complex shape
2 - Rectangular bar stock	H, W, L	
3 - Plate bar stock	H, W, L	
4 - Extrusion	1 - Angle 2 - Channel 3 - Square Tube 4 - Rectangular Tube 5 - Round Tube 6 - Beam 7 - Tee 8 - User Defined	
5 - Casting	0 - External features only 1 - Internal features	0 - No additional processing 1 - Planar surface machining 2 - Hole machining 3 - Planar and hole machining 9 - 100% machined
6 - Forging		
7 - Sheet Metal	Thickness	0 - Blanking/punching 1 - Bending + blanking /punching 2 - Drawing + blanking / punching
8 - User Defined		

Table E-2: Material Related Fields for the Component Code

Component Code: Material			
Material		**Treatment**	
Material Family	**Sub-family**	**Treatment Family**	**Type**
1 - Ferrous	1 - Cast iron 2 - Mild Steel 3 - Stainless Steel	0 - No treatment 1 - Heat treatment 2 - Surface Finishing treatments 3 - Heat and Surface treatments	y - surface treatment 0y - No hardening 1y - Surface hardening 2y - Through hardening 3y - Annealing
2 - Non-Ferrous	1 - Aluminum 2 - Brass 3 - Bronze 4 - Copper 5 - Magnesium 6 - Titanium 7 - Zinc		
3 - Superalloy			x - heat treatment x0 - No surface treatment x1 - Coating (galvanizing) x2 - Texture Modification x3 - Deburring
4 - Polymers	1 - Thermoplastic 2 - Thermoset		
5 - Ceramics	1 - Porcelain		
6 - Composite Materials	1 - Carbon Fibre 2 - Kevlar 3 - Fibreglass		
7 - Glass			
8 - Wood	1 - Hardwood 2 - Softwood 3 - Fibre board		
9 - Other			

Table E-3: Envelope Related Fields for the Component Code

	Envelope	
	Shape	**(Values 0, 0.5, 1)**
1	Cylindrical	No clearance concerns
2	Prismatic	Moderate clearance concerns
3	Spherical	
4	Specific	Tight clearance concerns

Table E-4: Operating Conditions Related Fields for the Component Code

Operating Conditions (Values 0, 0.5, 1)						
Heat / Cold	**Vibration**	**Corrosive Environment**	**Pressure / Vacuum**	**Humidity**	**Dirt Levels**	**Force / Stress Levels**
No issue	No issue	No issue	No issue	No issue	No issue	No issue
Moderate	Moderate	Moderate	Moderate	Moderate	Moderate	Moderate
Extreme	Extreme	Extreme	Extreme	Extreme	Extreme	Extreme

APPENDIX F

F.1 CONNECTING ROD SUPPLEMENTARY INFORMATION

Table F-1: Contextual, Conceptual and Logical Layers for the Connecting Rod

Connecting Rod				
	What	**How**	**Where**	**Why**
	Data	Function	Inter-connections (Network)	Motivation
Contextual	Part of the system to convert translational motion to rotary motion	Linkage between moving components	Air cooled, overhead valve single cylinder engine	
Conceptual	Part of lubricated, slider-crank joint	Precision, static beam, link between two rotary joints	Connect the piston (through the pin) to the crankshaft journal through precision bores at a specific distance	
Logical	Couple - link	Couple external components through precision bores		Transmit the piston linear reciprocating motion into the crank shaft rotary motion with minimum side motion or bending
	Support - position	Position the piston with respect to the crank		
	Channel - transport	Provide lubricating oil to the bearing surfaces via holes and grooves	External feature to component	Hydrostatic bearing between the crank and connecting rod

Table F-2: Physical and Detail Layers for the Connecting Rod

Connecting Rod				
	What	**How**	**Where**	**Why**
	Data	Function	Inter-connections (Network)	Motivation
Physical	**Material:** Aluminium	Die cast component with finish machining and assembly		Lightweight Cost effective Manufacturability Corrosion resistant
	Envelope: piston, pin, crank shaft journal, crankshaft cheeks		Collect interface component data in order to determine relevant tolerances	
	Operating environment: Function between -40°C and 200°C (oil temperatures) Dynamic component - interface conditions critical			
	Shape: Axially symmetric shape (in general), I cross section + 2 bores		*Crankshaft* *Piston Pin*	
Detail	93 Brinell hardness	Alloying, porosity control, heat treatment	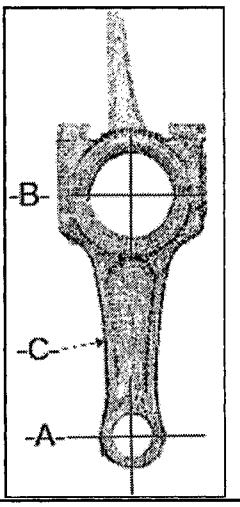	Strong and tough
	Part datum features: -A- small bore centre -B- large bore centre -C- centre plane perpendicular to line drawn though -A- & -B-, as shown			

The small end bore interfaces with the reciprocating features. It has a 15.018 mm diameter, with a surface finish of 80 Ra. The piston pin has a diameter of 15.000 mm; hence, there is a 0.018 mm clearance. The big end bore interfaces with the rotary component. It has a diameter of 30.010 mm, and has a surface finish of 74 Ra. The crankshaft journal has a 29.978 mm

diameter. There is a 0.032 mm clearance for this feature. These bores must be cylindrical, and parallel to each other. This information is summarized in Tables F-3 andF-4.

Table F-3: Small End Bore Summary

Small End Bore (Product Feature)			
	What	**How**	**Where**
	Data	Function	Interconnections (Network)
Contextual	Link the reciprocating component	Part of hinged joint: slider crank mechanism	Between the piston and the connecting rod
Conceptual	Link feature - Precision	Clearance hole	Connection to piston pin
Logical	Couple - link	Precision bore in which the piston pin is located	External feature to component
Physical	Cylinder	Machined	Small End Boss (Internal) *Piston Pin* (External)
Detail	Diameter: 15.018 mm Depth: Through Position: Bore center at (0,0,0) Datum -B-		Dia.: 15.020 +/- 0.005 mm Cylindricity: 0.008 mm Parallelism to Big End Bore: 0.008 Surface finish: 80 Ra

Table F-4: Big End Bore Summary

Big End Bore (Product Feature)			
	What	**How**	**Where**
	Data	Function	Interconnections (Network)
Contextual	Link the rotary component	Part of rotary joint: slider crank mechanism	Between the crankshaft and the connecting rod
Conceptual	Link feature - Precision	Clearance hole	Connection to crank journal
Logical	Couple - link	Precision bore in which the crank journal is located	External feature to component
Physical	Cylinder	machined	Large End Boss Split Clearance Chamfer Oil Channels Oil Holes (Internal) *Crank Journal* (External)
Detail	Diameter: 30.010 mm Depth: Through Position: Bore center at (0,86,0) Datum -A-		Dia.: 30.010 +/- 0.005 mm Cylindricity: 0.008 mm Parallelism to Small End Bore: 0.008 Surface finish: 74 Ra

The weight savers are incorporated to reduce the mass of the rod. The pockets must be symmetric around the parting line and the central axis to reduce balancing concerns. The pocket geometry is defined by analysing the point cloud data. The outer profile is determined at specific heights (z +/- 12.0 mm), and the cross section is defined at y = 40 mm. There are variable fillets; hence, the fillet geometry is defined at selected intervals. This is presented in Table F-5.

Table F-5: Weight Saver Summary

Weight Savers (Product Feature)			
	What	**How**	**Where**
	Data	Function	Interconnections (Network)
Contextual	Rod feature of the connecting rod		Between the piston and the crankshaft linkages
Conceptual	Material reduction feature	Pockets to reduce weight	Connection to neck
Logical	Reduce Inertia	Pockets that result in an I beam type cross section	Internal feature to internal feature
Physical	Profile symmetric around the central axis Pockets symmetric around the parting line	Cast in place	Neck Oil Lubrication Holes
Detail	Point cloud profile as template @ z = 12.0 mm and z = -12.0 mm, with the cross section @ y = 40 mm Draft: 3 ° Variable Fillet: measure at 0, 180 & 270 °		Symmetric to central axis and parting plane Profile offset from neck outline 3 mm

The critical measurements for this connecting rod and its mating components are summarized in Table F-6.

Table F-6: Connecting Rod and Mating Component Measurements

Description	Measurement (mm)	Comments
Wrist pin O.D. (piston)	15.000	
Connecting rod small end bore diameter	15.018	
Clearance between wrist pin and the connecting rod	0.018	
Crank journal O.D.	29.978	
Connecting rod big end bore	30.010	Ovality: 0.004 mm
Clearance between crank journal and big end bore	0.032	
Centre distance from small end bore to big end bore	86.00	
Crank side clearance	0.4 mm	
Surface finish – small bore	80 Ra	
Surface finish – big bore	74 Ra	
Surface finish – break line	77 Ra	
Tightening torque for the cap bolts	Approximately 16.2 N.m	
Bolt thread	M7x1.0	
Bolt shank diameter	7.193	Average of two bolts, two measurements – top and bottom
Bolt hole diameter in the rod cap	7.255	Average of two bolt holes
Bolt hole depth	23.24	Average of two bolt holes
Bolt hole centre distance	40.03	
Angle oil lubrication hole	25 °	
Oil lubrication hole diameter	3.08	
Chamfer angle	45 °	
Chamfer depth	3.6	
Material hardness	93 HB (average)	

F.2 THE TIMING SCREW DESIGN AND INSPECTION METHODOLOGY

F.2.1 Design Process

This section in the appendix is divided into two sub-sections: the first sub-section focuses on the design process; the second sub-section focuses on the inspection process. The design process flow is shown in Figure F-1. Excel® and Mastercam® software packages are used to design the timing screws and manipulate the inspection data. The input parameters consist of the motion characteristics, the container geometry and the initial stock conditions or bounding parameters of the stock. The cam characteristics are determined from this information, and a point cloud data file, representing the pocket centreline, is generated and imported into the CAD/CAM system. A spline curve is fitted through the points, and used as the basis for the final surface model.

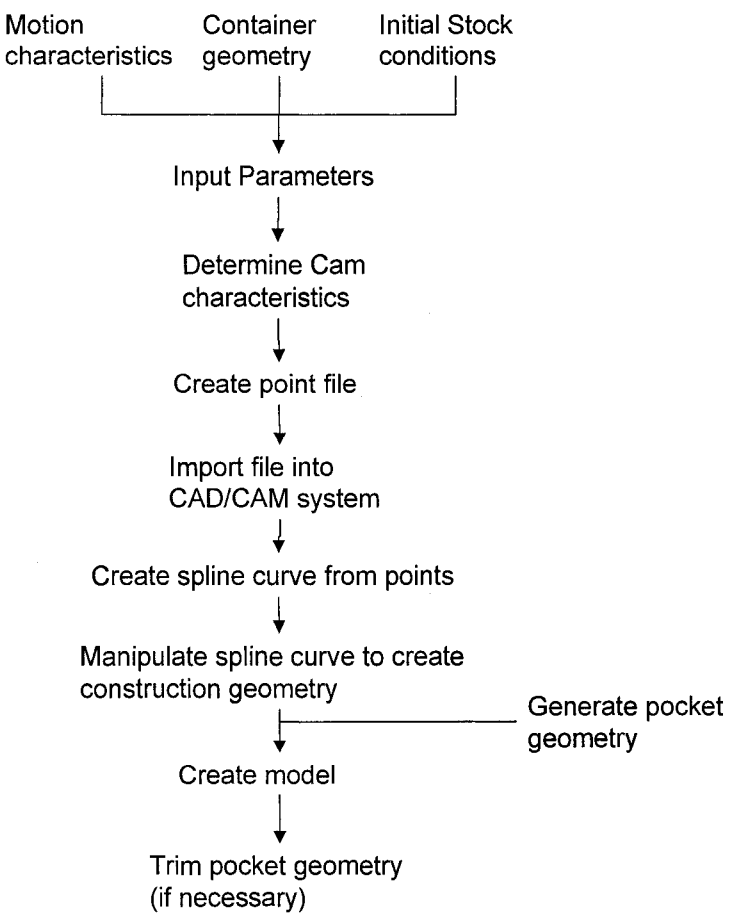

Figure F-1: Timing Screw Design Process Flow

The parameters to develop a controlled variable pitch timing screw are:

- Input RPM (revolutions per minute)
- Input pitch spacing (distance per 360°), or input velocity (mm/degree), v_{in},
- Output pitch spacing (distance per 360°), or output velocity (mm/degree), v_{out}
- Screw Length (mm), L
- Lead in zone (degrees), l_in
- Lead out zone (degrees), l_out

For the parabolic, cycloidal and third harmonic curves, the maximum velocity and acceleration is expressed as:

Maximum velocity: $\dot{y}_{\max} = 2\frac{h}{\beta}$ (F.1)

Maximum parabolic acceleration: $\ddot{y}_{\max} = \frac{\Delta V}{2\beta}$ (F.2)

Maximum cycloidal acceleration: $\ddot{y}_{\max} = \frac{\Delta V \pi}{2\beta}$ (F.3)

Maximum third harmonic acceleration: $\ddot{y}_{\max} \approx 0.815 * \frac{\Delta V \pi}{2\beta}$ (F.4)

Determining the maximum acceptable total rotation angle β is essential for reducing the peak acceleration. The value is dependent on the shaft length, L, input pitch or velocity, v_{in}, output pitch or velocity, v_{out} lead in zone, l_in and lead out zone l_out lengths (in degrees). The working length is defined as:

$$Lworking = L - v_{in} * l\_in - v_{out} * l\_out \quad \text{(F.5)}$$

where $v_{in} = \frac{RPM}{v_{in}\_linear}$ or $v_{in} = \frac{Pitch\ Distance}{360°}$ (F.6)

$$v_{out} = \frac{RPM}{v_{out}\_linear} \ or \ v_{out} = \frac{Pitch\ Distance}{360°} \quad \text{(F.7)}$$

Therefore:

$$\beta \max = \frac{2 * L\_working}{(v_{out} + v_{in})} \tag{F.8}$$

For ease of measurement for subsequent inspection processes, this value is rounded to the closest 90° increment less than βmax.

$$\beta \max\_90 = \text{int}\left(\frac{\beta \max}{90}\right) * 90 \tag{F.9}$$

The rise height h is defined as:

$$h = \frac{\beta \max\_90 * \Delta V}{2} \tag{F.10}$$

From these parameters, a variable pitch screw can be designed. The rise height points per degree increment are generated using the desired acceleration profile. In the example presented here, the third harmonic profile is used. Once this curve is generated, these points are transformed into Cartesian coordinates, and then 'wrapped' using an appropriate control radius to generate a helix type curve. These points are used to create the final CAD design.

$$Xcoor = \left\{\frac{h}{\beta \max\_90}\left[1 - \frac{15}{16} * \cos\left(\frac{\pi\theta}{\beta \max\_90}\right) - \frac{1}{16} * \cos\left(\frac{3\pi\theta}{\beta \max\_90}\right)\right] + v_{in}\right\} * \Delta\theta \tag{F.11}$$
$$+ x\_prev$$

$$Ycoor = Rad * \cos\left(\frac{2\pi * \theta}{\beta \max\_90}\right) \tag{F.12}$$

$$Zcoor = Rad * \sin\left(\frac{2\pi * \theta}{\beta \max\_90}\right) \tag{F.13}$$

A timing screw is designed for a 45 mm diameter container. The screw rotates at 1000 rpm. input velocity is 200 mm/min (72 mm pitch) and the output pitch spacing is 142 mm. The root diameter is 66 mm, and the stock diameter is 100 mm. The screw length is 600 mm.

There is a constant lead in and lead out zone of 360°. The design parameters for the acceleration curve are (Table F-7):

Table F-7: Input Parameters for a Timing Screw

Input velocity (mm/degree)	0.200 mm/degree	Equation F.6
Output velocity (mm/degree)	0.394 mm/degree	Equation F.7
Working Length	386 mm	Equation F.5
βmax (degrees)	1300	Equation F.8
βmax_90 (degrees)	1260	Equation F.9
Rise height (cam displacement) h (mm)	122.2 mm	Equation F.10

The peak acceleration for the cycloidal curve is **2.42×10^{-4}** mm/degree^2 (equation F.3) and the peak third harmonic acceleration is **1.97×10^{-4}** mm/degree^2 (equation F.4). The resulting acceleration curves for cycloidal and the third harmonic profiles are illustrated in Figure F-2.

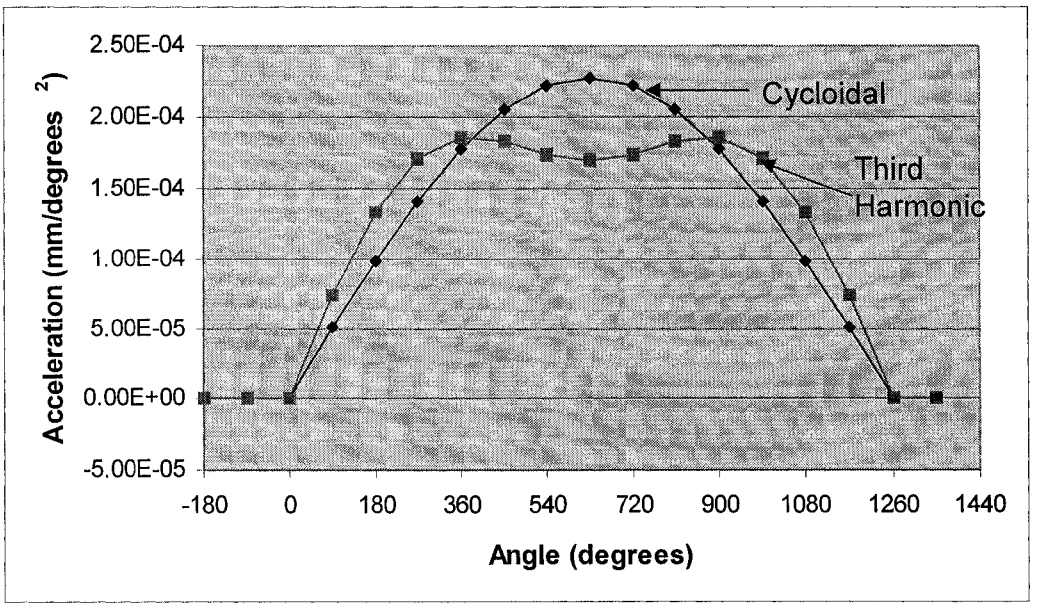

Figure F-2: Cycloidal and Third Harmonic Accelration Curves

Data points are generated at 0.5 degree intervals using the third harmonic equations of motion, and imported into Mastercam®. To eliminate lead in and lead out blending problems, 360° of data is appended onto the angular bounds. A modified helix spline curve is generated from the points. This curve represents the following edge. It is translated by the input pitch distance to create the lead edge. The pocket geometry is developed at the mid point of these curves. A 50

mm diameter pocket with 5 mm radius blend fillets is used to enclose the container in the variable frequency and lead out zones. Standard surface creation tools are used to create the CAD model. A taper is used that extends over two pitch intervals is included in the in-feeding zone, as the container are round and require no special separation geometry. A solid model of the timing screw is constructed from this information. This screw is illustrated in Figure F-3, with the lead in taper and the pocket geometry included. The model is completed when inspection lines are engraved at 90° intervals on the outside diameter surfaces.

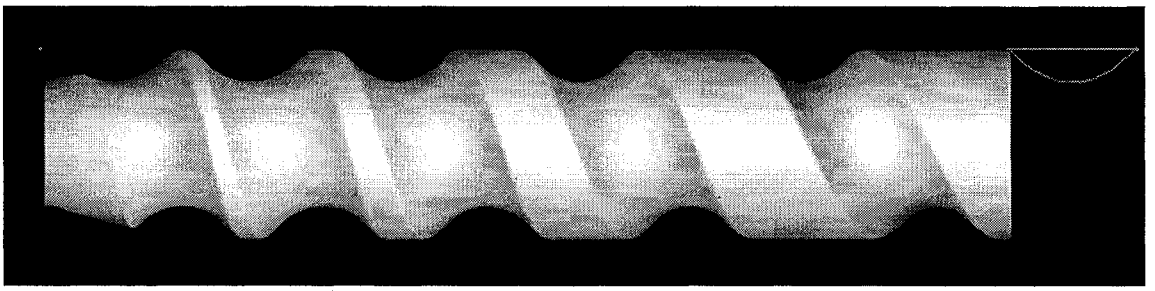

Figure F-3: Final Trimmed Model (Lead out End Partially Hidden to Show Pocket Geometry)

Using the CAD model tool paths are created. It is assumed that a 4-axis lathe is used for machining the timing screw. The tool paths are verified in order to analyse whether any tool collisions or gouges would occur during machining, and to determine whether the tool step over and other set up parameters are acceptable. The model generated by the verification process is a good virtual representation of a product manufactured using the machining parameters. The verification geometry for the pocketing tool paths is illustrated in Figure F-4. The darker colour represents the initial stock material.

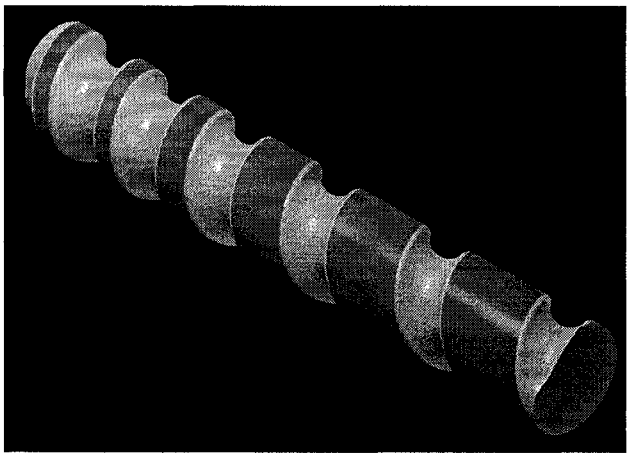

Figure F-4: Tool Path Verification Model

F.2.2 Inspection Process

In order to determine the validity of this design and manufacturing process, an inspection procedure using point cloud data is developed to quantify the motion characteristics for these timing screws. The procedure is corroborated using several Mastercam® 'verified' models, as this model contains surface scallops caused by the selection of the tool geometry and step over characteristics. The 'verification' model is an STL (Standard Triangulation Language) file. Points are generated at the tips of each vertex (duplicates removed), and the generated point cloud data is imported into the analysis module. The general inspection process is illustrated in Figure F-5. Once the point cloud data has been generated, it has to be transformed into usable information. Within the CAD/CAM system, the points are oriented via the inspection datum lines, and the critical points selected by applying a bounding filter to the geometry. These points are transformed using the 'unroll'/'unwind' procedure described in Chapter 5. The boundary points are selected using the scanning process described in Chapter 4. From this data, the velocity and acceleration motion characteristics can be calculated, as describe below.

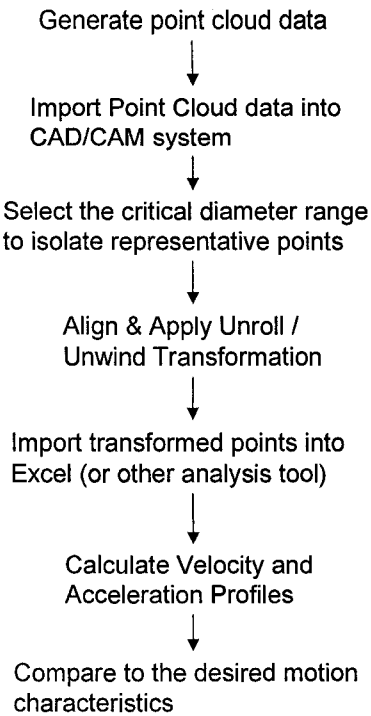

Figure F-5: Inspection Process Flow

The edge boundaries must be extracted from the point cloud data. This is done by selecting a range of acceptable points. The data presented in Figure F-6 is for a ball screw with a 50 mm diameter. For illustration purposes, the points less than 49.8 mm are displayed. Although at the lead out end the boundaries are clear, they are not at the lead in end. Consequently, a filter is applied. For the points illustrated in Figure F-7, all points greater than 40 mm are discarded. The filter should be applied to extract the desired point cloud data. The boundary edges are clearly distinguishable along the length of the screw.

Figure F-6: Point cloud Data (without Outside Diameter Points)

Figure F-7: Critical Points (Diameter less than 40 mm)

These points are unrolled, (Figure F-8), the edge points determined, and transformed using the 'unwind' transformation (Figure F-9).

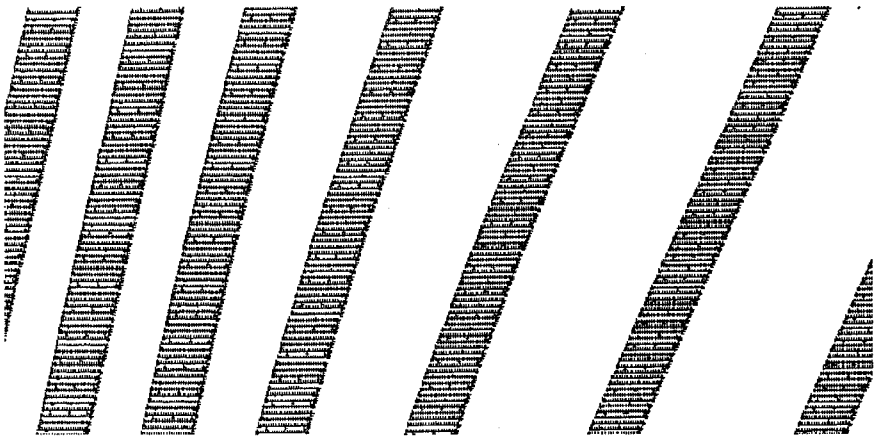

Figure F-8: Unwound Critical Points

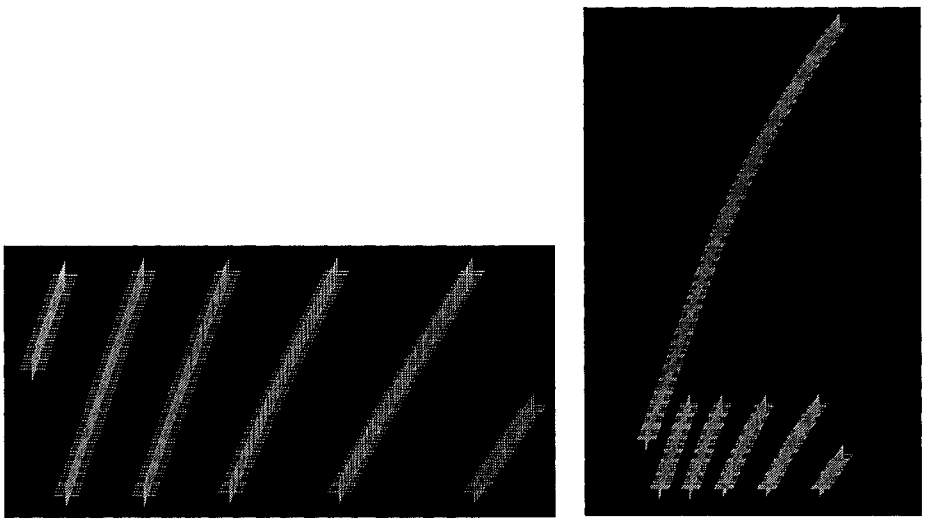

Figure F-9: Unrolled and Unwound Edge Points

The x-axis data remains constant, as it represents the distance traveled for an interval; however, the y-axis data must be converted to an equivalent angle. As the edge points were placed on a circle (in the side view) prior to unrolling, the angle is calculated by:

$$Angle = \frac{Yvalue * 360}{\pi * Diameter} \tag{F.11}$$

The velocity is calculated from the data points using:

$$Velocity = \frac{\Delta x}{\Delta Angle} \tag{F.12}$$

The velocity profile for the sample part is illustrated in Figure F-10. It shows a smooth and continuous flow from the initial velocity to the final velocity. The average initial velocity between 300 – 810° is 0.200 mm/degree +/- 0.005, and the final velocity is 0.394 mm/degree +/- 0.005. The variations (order of magnitude is 5%) are caused by the tool scallops. To reduce the effects of the noise, data points are selected at 30° intervals, as shown in Figure F-11. The acceleration profile is calculated from this data using:

$$Acceleration = \frac{\Delta Velocity}{\Delta Angle} \tag{F.13}$$

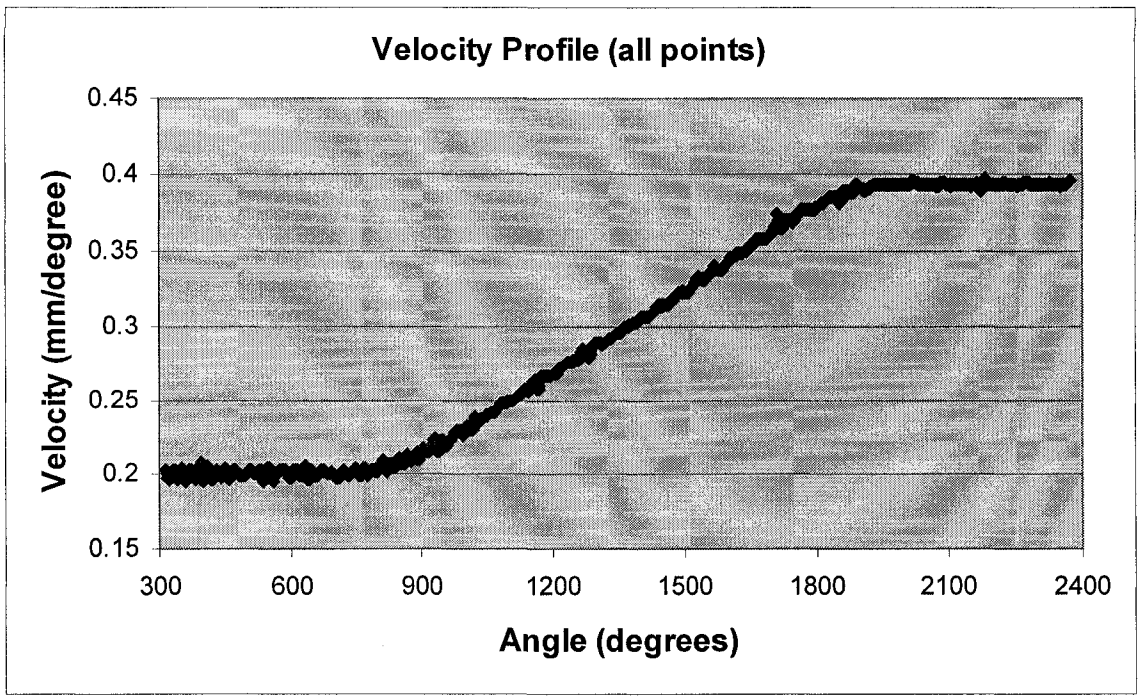

Figure F-10: Velocity Profile for the Sample Part

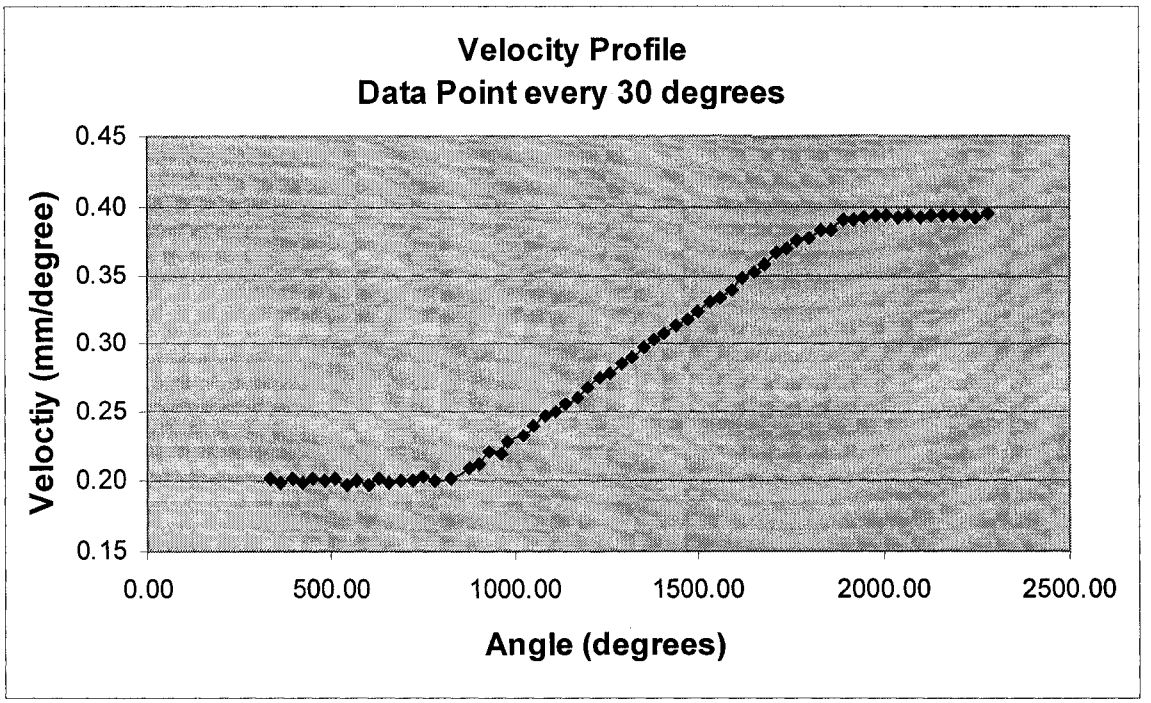

Figure F-11: Velocity Profile for Sample Part Using Selected Points

The calculated acceleration profile is shown in Figure F-12. Although there some is noise evident, the third harmonic curve is apparent, as well as the fact that there is minimal acceleration at the beginning and end of the timing screw.

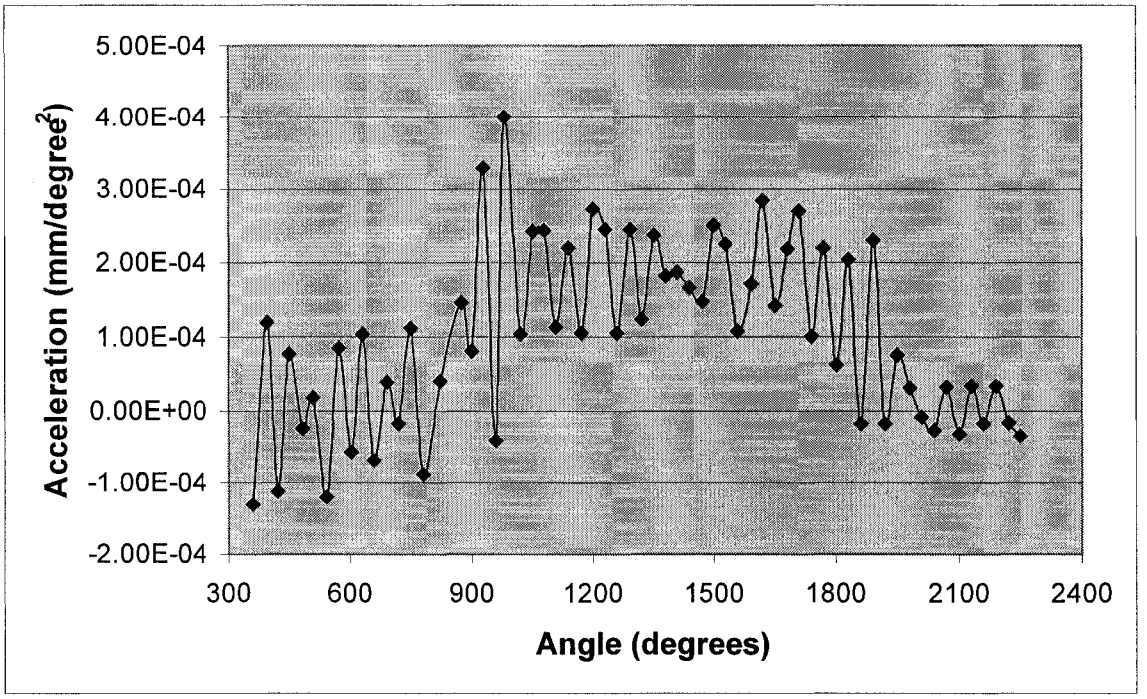

Figure F-12: Acceleration Profile

The angular data points are offset from the design references. An appropriate shift can be made using the inspection datum lines as guidelines to fix the angular position.

In summary, a comprehensive design and inspection strategy has been developed for variable pitch timing screws. This methodology is a result of associating the form with a function when performing the design recovery. Tools needed to be created in order to determine whether the functional requirements are met (or not) in the design. Using the Axiomatic Design methodology refined the FR and DP relationships, and established a platform for the detailed design and inspection process flows presented here.

APPENDIX G: INVESTIGATION OF NON-ITERATIVE CURVE PRIMITIVE GENERATION TECHNIQUES TO CREATE THE CURVE PRIMITIVES

G.1 INTRODUCTION

Iterative techniques are computationally expensive, and result in "mathematically" accurate curves, but an exact solution may not be a correct solution. Therefore, non-iterative techniques are investigated and the appropriate ones are utilized to create the applicable curve primitives. The basic primitives under consideration are the line, circle and circular arc, ellipse and elliptical arc. These are illustrated in Figure G-1 along with their associated data records. For each primitive the relevant parameters must be extracted. The parameters consist of the start and end points for each curve segment, and any other relevant curve properties (i.e. radius and the radius centre of an arc).

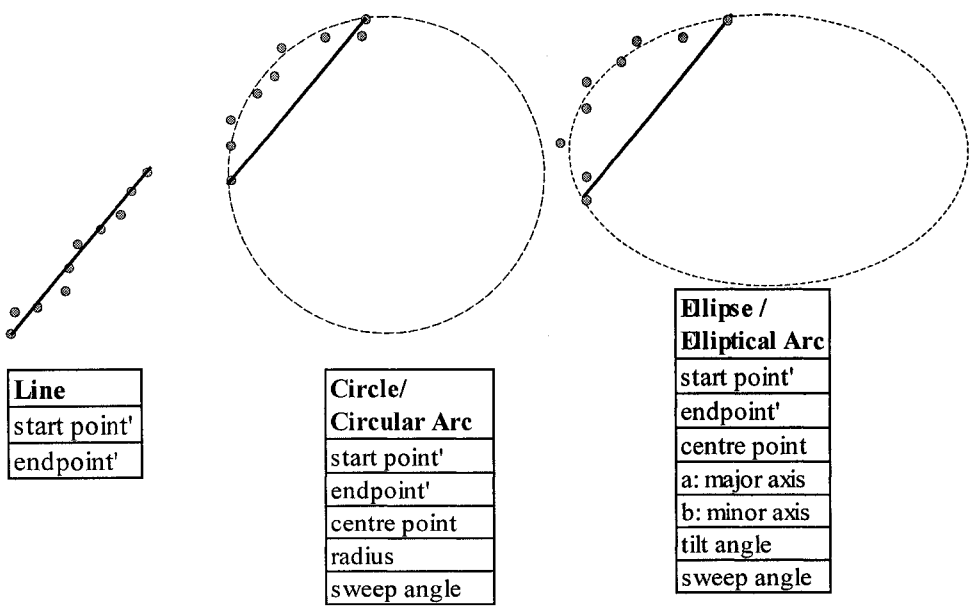

Figure G-1: Basic 2-D Primitive Curves and Data Records

The least squares method (LSM) is used to calculate the slope of the line. Degenerate conditions, caused by Δx or Δy approximately equalling 0, are accommodated. The error for each point is calculated. If the error is greater than 0.5 mm, that point is discarded. Once the points have been filtered, the slope again is calculated and updated endpoints stored in the database. The start and end points are recalculated based on the LSM slope using the original x coordinates as a reference.

G.2 ARC CREATION

The minimization of an arc/circle (equation G.1) is a non-linear problem that has no closed form solution.

$$F(x_0, y_0, R) = \sum_{i=1}^{n} \left[(x_i - x_0)^2 + \left(y_i - y_0\right)^2 - R^2 \right]^2 \tag{G.1}$$

A solution can be found using iterative least squares techniques, but iterative algorithms for minimizing non-linear functions like equation G.1 are sensitive to the choice of the initial guess, computationally expensive and for rapid convergence, an initial guess needs to be provided that is close enough to the minimum. A comparison of non-iterative techniques that use geometric, algebraic, and statistical approaches is presented for a hole within a hole template used for drafting (Figure G-2). Although clearly a circular hole, there is distortion due to the plate flex, and noise along the edges of the hole. Raw data points along the distorted region of the template were chosen to in order to assess each method's sensitivity to noise.

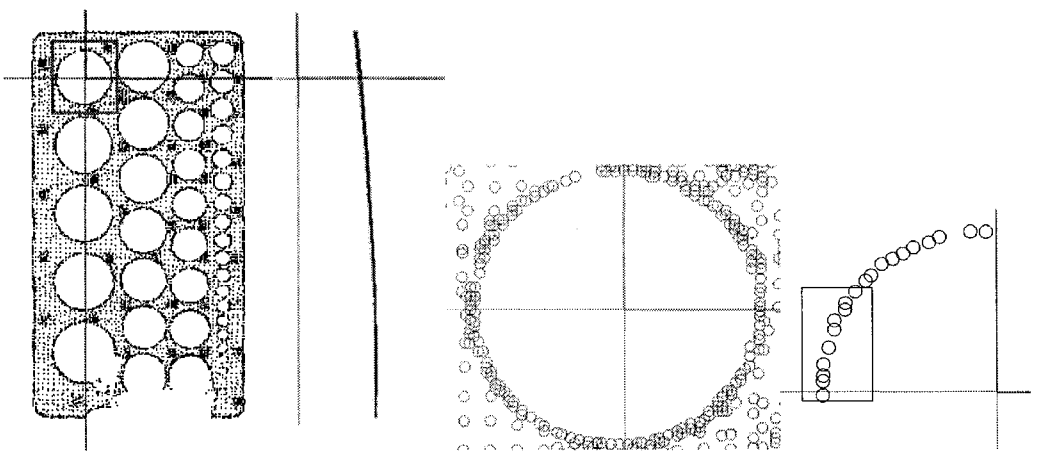

Figure G-2: Front and Side View of Hole Template, and
Points on Arc used for Data Analysis

The parameters of interest for an arc or circle are the radius, R, sweep angle, θ, the circle centre (x_0, y_0), and the arc sweep start and finish coordinates, (x_s, y_s) and (x_f, y_f) respectively. Using two sample sets, one of 10 points (enclosed region in Figure G-3), the other of 20 points, the following methods were investigated for generating the required parameters:

- Circumcircle,

- Arc segment to circle relationships, and
- Algebraic Fit (AF).

A circumcircle is a unique circle that passes through the three vertex points of a triangle, as shown in Figure G-3. Theoretically, selecting any three points from a set of points along an arc will generate the same radius, and rotation centre. Practically, this is not the case due to the noise variations. As shown in Figure G-4, selecting three points randomly within the first sample of ten points on the circle of interest produces widely varying results (circles 1 – 3). However, if points are spread out, and the data is averaged within a sample, a more realistic (and consistent) result occurs (circle 4). With the twenty point sample, the results are more consistent between selecting the first, middle and last points, and creating a circle from averaged values (Table G-1).

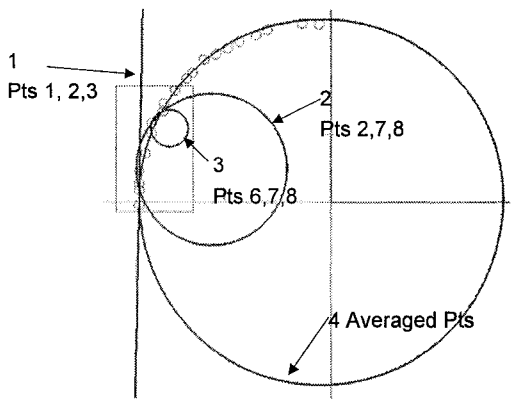

1 Radius: 12905.39 mm, Center: X: -12919.54 Y: 259.97
2 Radius: 6.61 mm Center: X: -10.41 Y: 2.91
3 Radius: 1.63 mm, Center: X: -14.09 Y: 6.45
4 Radius: 15.90mm, Center: X: -0.86 Y: 0.28

Figure G-3: Three Points Circles from First 10 Data Points

Table G-1: Summary of Circles Created Using 3 Points

Circumcircle Points	R (mm)	x_0 (mm)	y_0 (mm)	θ (°)
Points 1, 2, 3	12905.39	-12919.54	259.97	-
Points 1, 5, 10	16.52	-0.26	0.06	37.5
Ave.: 1-3, 4-7, 8 -10	15.90	-0.86	0.28	39.0
Points 1, 11, 20	15.34	-1.46	0.43	94.4
Ave.: 1-3, 8 -11, 18-20	15.27	-1.50	0.42	95.0

Another analytical geometric method used to generate the radius and circle centre information is based on manipulating the properties of a chord within a circle. Upon subtending perpendicular lines from the midpoints of two non-parallel chords, the intersection point of those lines represents the circle centre (Figure G-4). The radius is the distance between the end points of a chord and the circle centre.

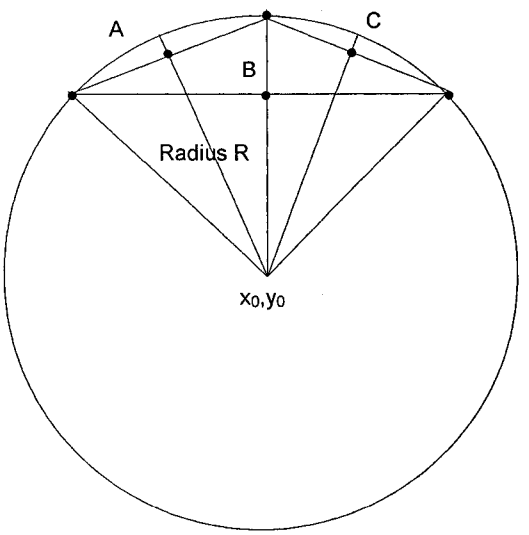

Figure G-4: Circle Centre by Intersecting Two Lines Perpendicular to Two Non-Parallel Chords

The following method is used to calculate the circle parameters:

The slope of the chord is:

$$m_{chord} = \frac{\Delta y_{endpo\,int\,s}}{\Delta x_{endpo\,int\,s}} \tag{G.2}$$

The slope of a line perpendicular to the chord is:

$$m\perp = \frac{-1}{m_{chord}} \tag{G.3}$$

The equations of the two intersecting lines are:

$$y_1 = m_{\perp 1} x_1 + b_1$$
$$y_2 = m_{\perp 2} x_2 + b_2 \tag{G.4}$$

The b intercept for each line is calculated by using the pertinent chordal midpoint coordinate (x_m, y_m). Upon equating the two lines, the circle centre coordinates are:

$$x_c = \frac{m_{\perp 1} - m_{\perp 2}}{b_2 - b_1} \tag{G.5}$$

$$y_c = m_{\perp 1} x_c + b_1 \quad or$$
$$y_c = m_{\perp 2} x_c + b_2 \tag{G.6}$$

To minimize the effects of noise for I points, the chord endpoints, shown in Figure G-5, are selected as:

- Chord 1 Endpoints: $(x_1, y_1) - (x_{I-1}, y_{I-1})$
- Chord 2 Endpoints: $(x_2, y_2) - (x_I, y_I)$.

The chordal analysis method is computationally simple and relatively consistent results are obtained between the two data sets as shown in Table G-2.

Table G-2: Radius and Centre Points Using Chordal Analysis

Chordal Analysis	R (mm)	x_c (mm)	y_c (mm)	θ (°)
10 points	15.37	-1.42	0.48	40.4
20 points	15.08	-1.57	0.59	96.6

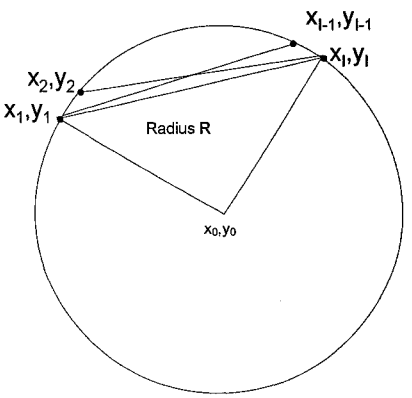

Figure G-5: Chords used for Circle Analysis

All lines perpendicular to the midpoint of non-parallel chords have a common intersection point for a circle or arc as shown in Figure G-4. Taking advantage of this property of a circle, a modification of the standard least squares solution for a line can be utilized as a method to solve for the parameters of interest for an arc, essentially linearizing the problem. Typically, given the expression:

$$y = mx + b \tag{G.7}$$

For a given set of (x, y) points, a best-fit estimate is generated for m and b. In lieu of solving for the slope and intercept, which is known for each line perpendicular to the chord, we solve for the circle centre point (x_0, y_0). To minimize the influence of noise and horizontal chords (which result in m = ∞), the chords used for the analysis are:

- first point to each of the last five points
- last point to the second to fifth points
- second, third and fourth point to the second, third and fourth to last point

Once the centre is estimated, the radius is determined by evaluating the average distance between the points along the arc and the centre. A summary of the least squares chordal analysis estimate is presented in Table G-3. This method is fast, stable and relatively insensitive to noise.

Table G-3: Radius and Centre Points Using the Least Squares Chordal Analysis

Least Squares Chordal Analysis	R (mm)	x_0 (mm)	y_0 (mm)	θ (°)
10 points	14.91	-1.87	0.63	41.7
20 points	15.60	-1.23	0.21	92.4

A fast and non-iterative approximation to the least squares methods is provided by the algebraic fit (AF) method [Chernov and Lesort, 2003]. AF is an older, straightforward method where the sum of squares of algebraic distances is minimized:

$$F(x_0, y_0, R) = \sum_{i=1}^{n} \left[(x_i - x_0)^2 + (y_i - y_0)^2 - R^2 \right]^2 \tag{G.1}$$

$$F(x_0, y_0, R) = \sum_{i=1}^{n} (z_i + Bx_i + Cy_i + D)^2 \qquad \text{(G.9)}$$

where

$$z_i = x_i + y_i$$
$$B = -2x_0$$
$$B = -2y_0$$
$$D = x_0^2 + y_0^2 - R^2$$

Differentiating F with respect to B, C, and D yields a system of linear equations:

$$\begin{aligned} M_{xx}B + M_{xy}C + M_x D &= -M_{xz} \\ M_{xy}B + M_{yy}C + M_y D &= -M_{yz} \\ M_x B + M_y C + nD &= -M_z \end{aligned} \qquad \text{(G.10)}$$

where $M_{xx} = \Sigma x_i^2$, $M_{yy} = \Sigma y_i^2$, $M_{xy} = \Sigma x_i y_i$.

$M_x = \Sigma x_i$, $M_y = \Sigma y_i$, $M_{xz} = \Sigma x_i z_i$, $M_{yz} = \Sigma y_i z_i$, $M_z = \Sigma z_i$.

Solving this system of equations gives B, C, and D from which x_0, y_0 and R can be computed. If the data points are sampled along a small circular arc, this method is biased and tends to return small circles [Chernov and Lesort, 2005]. The results generated from the 10 point and 20 point samples are presented in Table G-4.

Table G-4: Radius and Centre Points Using the Algebraic Fit Method

AF	R (mm)	x_0 (mm)	y_0 (mm)	θ (°)
10 points	13.45	-3.31	1.09	46.5
20 points	15.31	-1.49	0.42	94.7

G.3 ERROR ANALYSIS

The linear standard coefficient of correlation cannot be used for non-linear curves. It may be close to zero (or negative) when there is a strong relationship [Miller and Freund, 1977]; therefore, an analysis of the total error and the standard deviation of the error between the estimated and the actual values is performed for the circular arcs. For the various parameter estimation techniques two methods of analysing the error are performed: (i) the error is

calculated using equation G.1a, and (ii) the standard deviation of the error is calculated using equation G.1b.

$$Error = \sum_{i=1}^{n}\left[(x_i - x_0)^2 + (y_i - y_0)^2 - R^2\right]^2 \quad \text{(G.1a)}$$

$$Error = \sum_{i=1}^{n}\left[\sqrt{(x_i - x_0)^2 + (y_i - y_0)^2} - R\right] \quad \text{(G.1b)}$$

The estimate of R varies approximately 15% for the 10 point sample, and 3% for the 20 point sample. Although the AF method results in the smallest cumulative error for both sets of data, for the 10 point sample the AF method has the smallest radius estimate and the largest standard deviation. For the 10 point sample, the chordal analysis methods provided the smallest standard deviations (highlighted), while for the larger sample that encompassed a larger sweep angle, the circumcircle and AF methods had the smallest standard deviations (highlighted). With the increased amount of points, the standard deviations are reduced, indicating a better overall fit. Except for the two chord method, the cumulative error has increased by a factor of two. Performing the chordal analysis with only two chords provided inconsistent error results, although the standard deviation indicates that the estimated parameters are close. The results are shown in Table G-5.

Table G-5: Summary of Circle Analysis Results

	10 points					20 points				
	R (mm)	x_0 (mm)	y_0 (mm)	Standard Deviation (mm)	Error	R (mm)	x_0 (mm)	y_0 (mm)	Standard Deviation (mm)	Error
Circumcircle	15.90	-0.86	0.28	0.1284	179	15.27	-1.50	0.42	0.1116	245
Chordal Analysis	15.37	-1.42	0.48	0.1271	138	15.08	-1.57	0.59	0.1163	1008
Least Squares Chordal Analysis	14.91	-1.87	0.63	0.1270	131	15.60	-1.23	0.21	0.1161	249
AF	13.45	-3.31	1.09	0.1353	119	15.31	-1.49	0.42	0.1115	223

G.4 ELLIPTICAL ARCS

The 20 points used for the above analysis where rotated 30° around the x-axis, generating an ellipse (Figure G-6). The above analysis repeated in order to determine whether an ellipse could be detected.

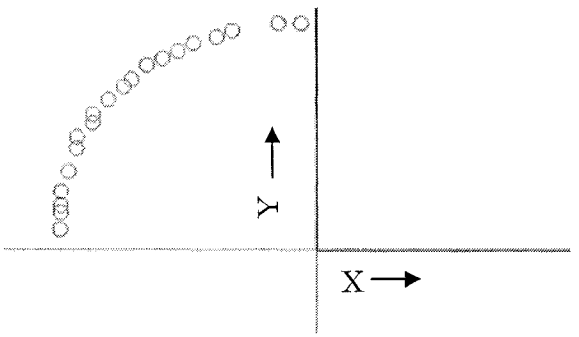

Figure G-6: Points Representing an Ellipse

For each 10 point segment, the radius was estimated, as well as for 15 points and 20 points. As shown by Figure G-7, the radius values were relatively consistent for each circle estimation technique, but varied greatly between point sets. This is in contrast to the data sets representing a circular arc (Figure G-8).

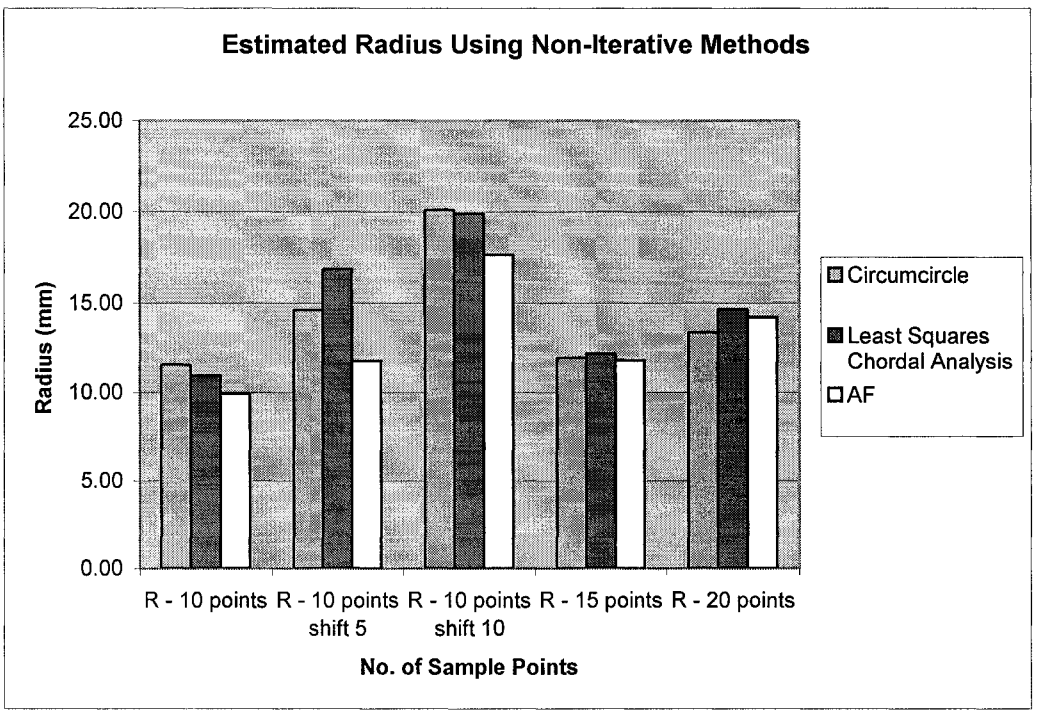

Figure G-7: Estimates of the Arc Radius

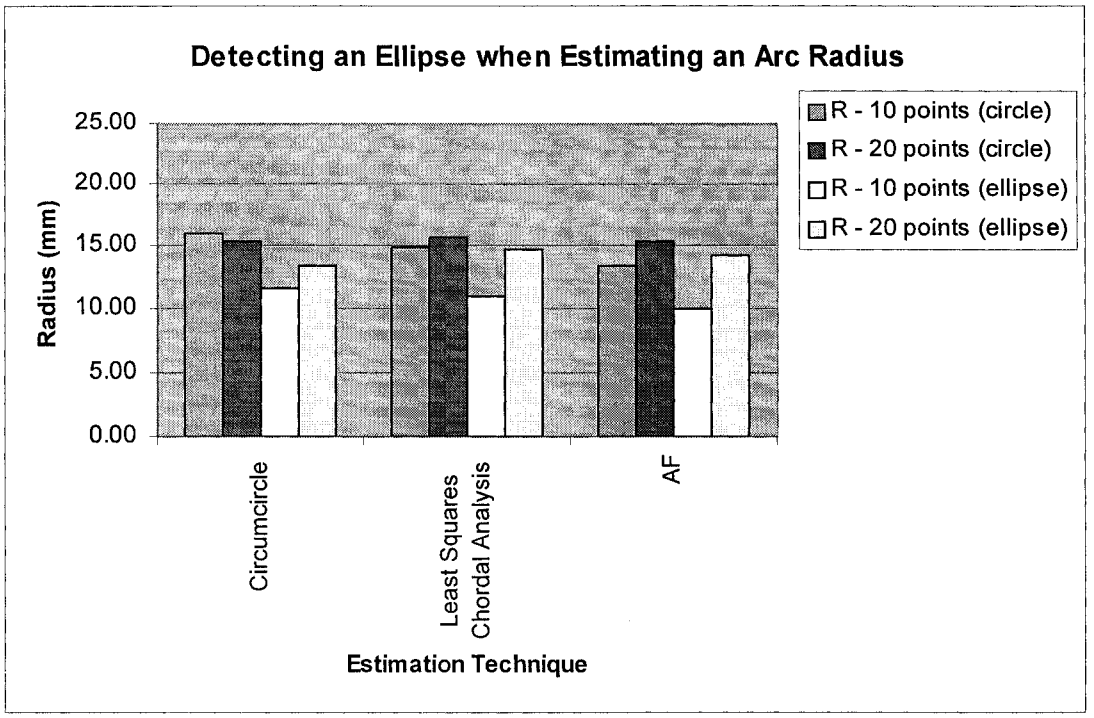

Figure G-8: Comparison of a Circular Arc Estimates to an Elliptical Arc

The cumulative error also increased significantly. As seen with the prior example of the circular arc, the cumulative error increased by a factor of two when the amount of points increased by the same amount. Here the error increased by approximately by a factor of 10 for a doubling of point quantity (Table G-6). Hence, an elliptical arc exists when the individual cluster sample has a low cumulative error, but the cumulative error increases disproportionably to the sample size or when the radius value changes significantly between the data sets.

Table G-6: Summary of Ellipse Analysis

	10 points					20 points				
	R (mm)	x_0 (mm)	y_0 (mm)	Standard Deviation (mm)	Error	R (mm)	x_0 (mm)	y_0 (mm)	Standard Deviation (mm)	Error
Circumcircle	11.58	-5.19	1.62	0.1209	83	13.38	-3.40	1.09	0.2303	766
Least Squares Chordal Analysis	10.97	-5.81	1.91	0.1196	62	14.66	-2.36	0.00	0.1972	639
AF	9.95	-6.80	2.28	0.1267	57	14.21	-2.89	0.25	0.1806	536

When an ellipse is detected, its parameters need to be estimated. The general conic equation is:

$$Ax^2 + By^2 + Cxy + Dx + Ey + F = 0 \tag{G.11}$$

For an ellipse, A > B, A and B are positive and satisfy the constraint:

$$4AB > C^2 \tag{G.11a}$$

Similar to estimating a circle with three points, an ellipse whose axes are parallel to the coordinate axes can be uniquely determined by any four non-concyclic points on it. Note: for an ellipse parallel to the coordinate axes, $C = 0$. An ellipse passing through the four points (x_i,y_i), $i = 1-4$ has equation:

$$\begin{vmatrix} x^2 & y^2 & x & y & 1 \\ x_1^2 & y_1^2 & x_1 & y_1 & 1 \\ x_2^2 & y_2^2 & x_1 & y_1 & 1 \\ x_3^2 & y_3^2 & x_1 & y_1 & 1 \\ x_4^2 & y_4^2 & x_1 & y_1 & 1 \end{vmatrix} = 0 \tag{G.12}$$

As with the circumcircle method, the data points are averaged to reduce the effects of noise. Upon solving for the coefficients A, B, D, E, and F, they must be transformed into the form shown by equation G.13 in order to determine the major axis a, minor axis b and the centre point of the ellipse:

$$\left(\frac{x - x_0}{a}\right)^2 + \left(\frac{y - y_0}{b}\right)^2 = 1 \tag{G.13}$$

The ellipses fitted from the samples of 10 and 20 points are shown in Figure G-9.

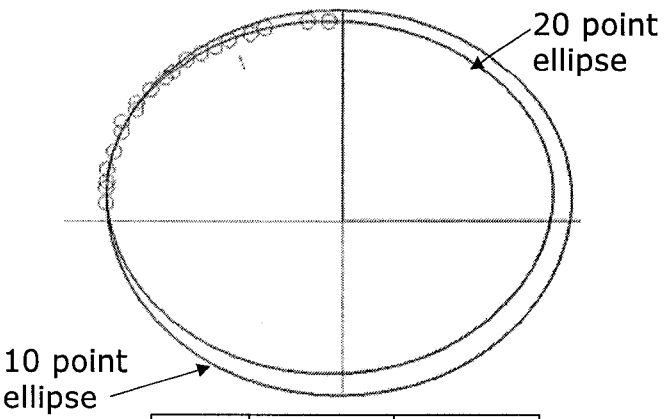

	10 point	20 point
a (mm)	16.47	15.81
b (mm)	13.76	12.61
x_0 (mm)	-0.30	-0.94
y_0 (mm)	1.64	2.02

Figure G-9: Ellipse Fitted by Using Four Points

The AF method was extended to encompass an ellipse, and the best-fit statistical method developed by Fitzgibbon et al [1999] was tested. For the 10 point sample, the coefficients did not satisfy the constraint stated in equation G.11a, therefore both the extended AF and Fitzgibbon methods failed. However, for the 20 point sample, the estimated parameters are in line with those from the 4 point method. This is summarized in Table G-7.

Similar to the circle fit analysis, the absolute error and the standard deviation of the error is assessed for the fitted ellipse. The error function used to assess the ellipse fit is presented in equation G.14a. The magnitude of the error for the ellipse is to the power of four compared to that of the circle. Therefore, the error calculations are normalized by raising the error at each point to the power of *0.25* (equation G.14b) for the standard deviation assessment.

$$Error = \sum_{i=1}^{I} \sqrt{\left[b^2(x-x_0)^2 + a^2(y-y_0)^2 - b^2a^2\right]^2} \qquad \text{(G.14a)}$$

$$Normalized\_Error_i = \sqrt[4]{Error_i} \qquad \text{(G.14b)}$$

Table G-7: Fitted Ellipses

	10 points						20 points					
	a (mm)	b (mm)	x_0 (mm)	y_0 (mm)	Standard Deviation (mm)	Error	a (mm)	b (mm)	x_0 (mm)	y_0 (mm)	Standard Deviation (mm)	Error
4 Point Method	16.47	13.76	-0.30	1.64	1.39	24174	15.81	12.61	-0.94	2.02	1.64	31578
AF	-	-	-	-	-	-	16.16	12.53	-0.62	2.13	1.97	60598
Fitzgibbon et al [1999]	-	-	-	-	-	-	15.70	12.45	-0.87	2.17	1.58	57711

If the ellipse is tilted, i.e. $C \neq 0$, and there is no simple method using analytical geometry in order to estimate the parameters. The estimated ellipse parameters for one point set do not remain constant around the elliptical curve when the ellipse has a tilt angle. The points used for the previous example were rotated around the z-axis by 15°, and ellipse curves fitted from the 10 and 20 point sample. As illustrated in Figure G-10, there is a significant difference in the estimated parameters. The standard deviation increases accordingly. This inconsistency indicates that the ellipse is at an angle. The extended AF and Fitzgibbon et al [1999] methods can be used to detect a tilt. However, as there are sensitivities with these methods for a small set of points that could be represented as a circular arc, a set of arcs is used to represent a tilted ellipse or elliptical arc. An example of a tilted elliptical arc fitted with a set of best-fit arcs is shown in Figure G-11.

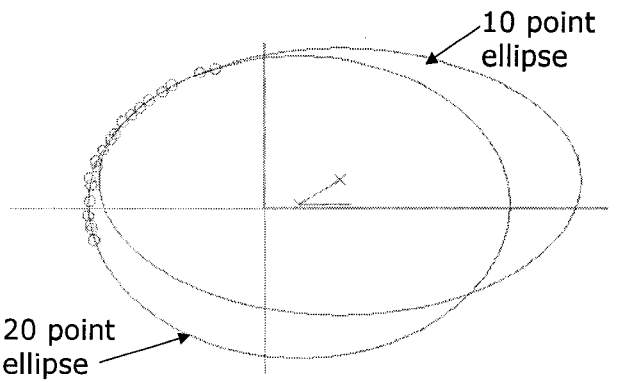

	10 point	20 point
a (mm)	23.35	20.45
b (mm)	13.02	14.64
x_0 (mm)	7.30	3.36
y_0 (mm)	2.77	0.41

Figure G-10: Fitting an Ellipse to Points on a Tilted Elliptical Arc

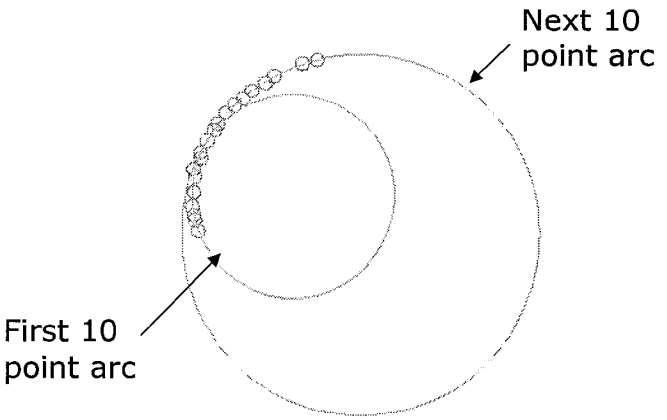

1 Radius: 9.95 mm, Center: X: -7.17 Y: 0.44

2 Radius: 17.63 mm Center: X: -0.51 Y: -3.26

Figure G-11: Tilted Ellipse Fitted with Circular Arcs

G.5 SUMMARY

Using analytical geometry methods in combination with statistical analyses, lines, circular and elliptical arcs and ellipses can be detected. The parameters for the curve primitives are estimated directly from the points and stored without incorporating any iterative analysis. Three points can be used to detect a circle but, but this method is susceptible to noise if the

points are closely spaced. For multiple points, the AF method is used to generate the estimated parameters, and verified with the circumcircle method. If an ellipse is detected, the 4 point method using averaged points is used to generate an estimate for the ellipse parameters. If the ellipse is tilted, a set of circular arcs trimmed by the procedure described in Chapter 4 is used to represent the curve.

VITA AUCTORIS

NAME: R. Jill Urbanic

PLACE OF BIRTH: St. Catharines, Ontario, Canada

EDUCATION: University of Windsor, Windsor, Ontario

2002 – 2006 Ph.D.

2001 – 2002 M. A. Sc.

University of Waterloo, Waterloo, Ontario

1980 – 1985 Hons. B. A. Sc.